UNIVERSIDADE FEDERAL DE MINAS GERAIS
INSTITUTO DE CIÊNCIAS BIOLÓGICAS
PÓS-GRADUAÇÃO EM ZOOLOGIA

FILOGENIA, TAXONOMIA E MACROEVOLUÇÃO DE ESTRUTURAS COPULATÓRIAS DOS GÊNEROS DE GNAPHOSIDAE (ARANEAE: GNAPHOSOIDEA)

GUILHERME HENRIQUE FERNANDES DE AZEVEDO

BELO HORIZONTE – MINAS GERAIS
2016

GUILHERME HENRIQUE FERNANDES DE AZEVEDO

FILOGENIA, TAXONOMIA E MACROEVOLUÇÃO DE ESTRUTURAS COPULATÓRIAS DOS GÊNEROS DE GNAPHOSIDAE (ARANEAE: GNAPHOSOIDEA)

Tese apresentada à Pós-Graduação em Zoologia do Instituto de Ciências Biológicas da Universidade Federal de Minas Gerais, como requisito parcial para a obtenção do titulo de doutor em Zoologia.

Orientador: Adalberto J. Santos
Coorientador: Charles E. Griswold

BELO HORIZONTE – MINAS GERAIS
2016

Sumário

Agradecimentos

Ao olhar pra trás, percebo que, durante essa longa jornada, várias pessoas cruzaram meu caminho e deixaram, direta ou indiretamente, sua contribuição para a realização da tese através de ensinamentos profissionais ou pessoais. Mencionarei aqui algumas dessas pessoas até onde o espaço e a memória cansada de final de doutorado permitirem.

Agradeço imensamente ao Adal, que há oito anos transmite seus conhecimentos de forma única e inspiradora. Sua didática impressionante ao ensinar, sua maneira de estimular o pensamento científico e de incentivar que busquemos o melhor, mas sem nunca esquecer o lado pessoal dos alunos, faz com que a relação entre orientador e orientado seja fácil e maximiza o aprendizado. Sem dúvida alguma, grande parte do que eu sou e serei como profissional deve-se à oportunidade de ter convivido com ele durante minha formação.

No início desse projeto eu e Adalberto pensamos em uma parceria para o desenvolvimento da pesquisa e o nome do Charles Griswold pareceu bem interessante como coorientador. Charles foi muito receptivo nos primeiros contatos e respondeu muito entusiasmado com a ideia. Sua contribuição para esta tese foi, no entanto, muito maior do que o esperado. O seu enorme conhecimento sobre biologia de aranhas, sua disposição em ensinar e discutir, seu relacionamento profissional com outros cientistas tiveram grande influência na minha formação como doutor. Além disso, Charles se tornou um grande amigo, juntamente com a Teresa, sua esposa. Eles me receberam com grande carinho em São Francisco e fizeram com que minha estadia no exterior fosse muito mais agradável. Por tanto, agradeço imensamente ao Charles e a Teresa, pelos quais tenho grande estima e carinho.

Agradeço aos membros da banca examinadora pela disposição em dedicar parte do seu tempo e conhecimento para avaliação desta tese: Antonio Domingos Brescovit (Instituto Butantan), Lina Maria Almeida Silva (Instituto Butantan), Fernando Amaral da Silveira (UFMG), Almir Rogério Pepato (UFMG), Mario Alberto Cozzuol (UFMG) e Ubirajara de Oliveira (UFMG).

Agradeço à CAPES pela bolsa de doutorado no país e pela bolsa de doutorado sanduíche que possibilitou a realização de parte dessa pesquisa no exterior, possibilitando aquisição de experiência internacional e contribuindo para minha formação profissional. Agradeço à California Academy of Sciences e ao Charles Griswold que me receberam durante o estágio no exterior. Ao CNPq pelo financiamento

concedido ao projeto coordenado pelo Adalberto J. Santos no qual a pesquisa desta tese está inserida.

Para o desenvolvimento deste trabalho foi necessário fazer visitas às coleções científicas para obtenção de material. Sem a ajuda de algumas pessoas essas viagens seriam muito mais difíceis ou impossíveis. Portanto, gostaria de agradecer aos curadores (listados no material e métodos dos capítulos) e assistentes de curadoria coleções, aos pesquisadores e amigos que possibilitaram essas viagens, seja na logística, permitindo acesso à coleção, recebendo em casa ou saindo para um momento relaxante na cidade da visita. Cito aqui o nome de algumas dessas pessoas: Ricardo Ott, Stenio e família, Vit, Toti, Antonio Brescovit, João Victor, Ana Lúcia Tourinho, Willians Porto, Bruno "Chimbinha" Rodrigues, Regiane, Laura, Alexandre Bonaldo, Adriano Kury, Carla Barros, Oswaldo Manzanilla, Thiago "Menudo" Moreira, Gustavo Hormiga e pessoal de seu laboratório na The George Washington University, Dana De Roche, Rafael "Pomarola", Sabrina, Trota, Laura Leibensperger, Gonzalo Giribet e pessoal de seu laboratório em Harvard University, Louis Sorkin, Vladimir Ovtsharenko e Norman Platnick. Agradeço também ao Martín Ramírez por disponibilizar o manuscrito da filogenia de Dionycha, o que ajudou muito na elaboração da matriz.

Agradeço ao pessoal do laboratório de aracnologia da UFMG por todos esses anos de discussões sobre ciência ou qualquer assunto inútil e divertido, coletas, almoços, viagens, seminários e etc. Essas pessoas se tornaram grandes amigos e deixaram um ambiente de trabalho agradável, amigável e engraçado: Bárbara, Bira, Leo, Graci, Vinícius, Pedro, Philip, Mayara, Marcia, Vivi, Ivan e todos que já passaram por lá. Sempre serei grato também ao Professor Mário de Maria pelo grande exemplo de professor e pessoa, e por abrir as portas da aracnologia para mim quando eu estava na graduação. Agradeço também ao pessoal do departamento de Zoologia, professores e colegas, pelos momentos de distração na Meire comendo torresmo e pelas discussões científicas ou sobre "Master Chef" no "Whatsapp". E obrigado à Meire, pelo belo torresmo.

Uma parte desse doutorado foi realizada no exterior. Viver durante um ano em um país distante com culturas diferentes pode ser desafiador. Algumas pessoas contribuíram para que essa experiência fosse proveitosa, tanto pessoalmente como profissionalmente, e gostaria de agradecer aqui: Charles, Teresa, Lina, Rachel, Marina, Darrell, Facundo, Dani, Liz, Erika, Norm, Vic Smith, Jere, Scott Serata, Jay, Jef, Darko, Susan, Rachael, Ed, Charlotte, Nicole, Tamas, Aislan, Nadia, Camila, Carla, Aline,

Rosemary Gillespie e pessoal do Evolab em Berkeley. Um agradecimento especial à Lina pela amizade, apoio, conselhos, conversas, passeios, dicas, desabafos, risadas e alegria durante esse tempo.

Muitos amigos também apoiaram essa jornada e foram importantes durante o doutorado, não só de perto, mas também no momento em que eu estava longe. Gostaria de agradecer imensamente à galera do Bonde do Padreco, ao pessoal da bio e das bandas Old Skull e R4: Tigrão, Gli, Parmalat, Monique, Leandro, Ju, Gael, Vit, Adinam, MT, Tintim, Claudinho, Carmem, Iza, Toti, Didi, Naty, Aninha, Pedro, Fernanda, Alan, Callithrix, Prezzuntinho, Empada, Pedrão, Rafael Magalhães, Xexéu, Lelis, Véia, Pomarola, Russo, Cajuru, Fabito, Caio, Manguaça, Goiás, Rafael Frade, Leleo, Pedro, Léo...

Nem se eu procurasse as mais rebuscadas palavras do dicionário, os mais belos poemas ou as mais bregas letras do Roberto eu seria capaz de expressar toda minha gratidão pela Júlia. Sua presença, sempre ao meu lado, me apoiando, me deu forças para continuar, mesmo quando o cansaço parecia ter consumido todo meu corpo e mente. Obrigado pelo carinho, pelo sorriso, pelas palavras, pelos cantos, pelas rimas, pelo abraço, pelo olhar, pela inspiração, pela companhia, pela alegria, por "fazer de cada instante um infinito". Obrigado por me suportar e entender momentos que o estresse me deixou chato. Obrigado também por ajudar com a preparação das pranchas que ilustram essa tese. Gostaria de agradecer também a Eliane e ao Paulo César por me receberem tão bem, sempre muito alegres.

O apoio da minha família também foi essencial para que eu pudesse realizar esse doutorado. Também não acho palavras para agradecer todo o amor que me fez superar os momentos mais difíceis nesses quatro anos. Obrigado Xande, Laya, Déia, Gustavo, Helena, Rafa, Lucas, Francisco. Agradeço também à Tia Fátima pelo carinho e atenção quando precisei. Claro que não deixaria de agradecer minha mãe, Magdala. Seu amor, carinho e presença foram os fatores mais importantes que me deram força e estímulo para seguir sempre em frente, buscando pelos sonhos. Serei eternamente grato ao meu pai, Vicente, por toda a luta, dedicação e carinho que me permitiram chegar até aqui. Suas poucas e simples palavras me ensinaram muito e contribuíram bastante para o que eu sou hoje. Com ele aprendi a aplicar a parcimônia na vida, não apenas para inferências filogenéticas.

Por fim agradeço a todos que de alguma forma contribuíram para esse trabalho, mesmo que o nome não esteja mencionado aqui.

Introdução Geral

Gnaphosidae é a sexta maior família de aranhas, com 2183 espécies agrupadas em 124 gêneros, e pode ser encontrada em todos continentes, exceto na Antártida (embora seja provável que ocorra em ilhas subantárticas). Na América do Sul a família é representada por 26 gêneros e 173 espécies, sendo que 17 gêneros e 69 espécies ocorrem no Brasil. Essa diversidade sul-americana representa apenas 0,08% do número de espécies conhecidas de Gnaphosidae. Com as informações a respeito da família que temos no momento, é difícil explicar essa baixa diversidade. Ela pode estar relacionada a deficiências de esforço de coleta e estudo taxonômico focado na fauna sul-americana. Por outro lado, é possível que as condições ambientais na região Neotropical não sejam favoráveis à diversificação da família, ou talvez a explicação seja uma combinação de vários desses fatores.

Os gnaphosídeos são aranhas de pequeno a médio porte (2 a 15 mm), que não usam a seda para construção de teias e forrageiam no solo, sob pedras e troncos caídos. Os órgãos produtores do fio de seda, as fiandeiras, apresentam características muito peculiares nessa família: as fiandeiras laterais anteriores são longas, com um único segmento tubular esclerotinizado, e as fúsulas (estrutura pele qual a seda é secretada) das glândulas piriformes são grandes, com uma base membranosa. Exemplares de Gnaphosidae apresentam aparência geral que pode não atrair tanto a atenção de pesquisadores e do público leigo, ao contrário de famílias como Araneidae, Thomisidae e de alguns theraphosídeos, por exemplo. Gnaphosídeos são aranhas, na sua maioria, de cores pálidas ou escuras com morfologia não muito diferenciada de uma aranha genérica de solo. Muitas delas podem lembrar superficialmente formigas, passando despercebidas a olhares pouco atentos. Entretanto, apesar do *habitus* aparentemente pouco diferenciado, uma observação mais cuidadosa da morfologia dessas aranhas revela uma diversidade enorme nas estruturas que compõe o corpo desses animais. Cerdas de cobertura corporal, espinhos, fiandeiras, olhos, quelíceras, órgãos sensoriais, garras tarsais, tufos de cerdas subungueais e genitálias são algumas das estruturas que apresentam grande variação entre os gêneros da família e indicam que Gnaphosidae apresenta grande potencial para estudos evolutivos e de morfologia comparada e funcional. A diversidade morfológica de genitália de Gnaphosidae, por exemplo, é algo notável entre essas aranhas por apresentarem tanto órgãos complexos, com várias estruturas, até órgãos simples, com poucas partes. Exemplares dessa família podem

servir de modelo para estudos de evolução sexual ajudando a compreender melhor os processos envolvidos na evolução de órgãos copulatórios.

Gnaphosidae é um grupo muito antigo de aranhas, globalmente distribuído, mas que apresenta certo endemismo, ou seja, alguns grupos de espécies são restritos a regiões específicas do planeta. Isso indica que essas aranhas podem ser modelos interessantes para estudos biogeográficos em grande e média escala. Entender como e onde as espécies de aranhas estão distribuídas e quais os fatores limitam essa distribuição pode fornecer informações importantes de como a história do planeta influenciou na história dos organismos. Assim, é possível desvendar os processos macroecológicos e geológicos que geraram a biodiversidade na Terra.

Para utilizar gnaphosídeos como modelo de estudos de processos geradores da biodiversidade é necessária uma boa compreensão da composição da fauna e das relações evolutivas entre as espécies. Trabalhos taxonômicos são importantes para descrever e conhecer adequadamente os organismos de determinada região. A taxonomia de Gnaphosidae vem sendo bem explorada nos últimos anos, principalmente no hemisfério norte, o que permitiu um grande avanço no conhecimento da família. Entretanto, muitas regiões, como na África, Ásia e América do Sul, continuam pouco exploradas com relação à fauna de Gnaphosidae, sendo que muitos gêneros necessitam revisões taxonômicas detalhadas.

Para melhor entender processos evolutivos envolvidos na diversificação das espécies é necessário ter hipóteses de relações filogenéticas entre os organismos. O uso de filogenias para estudos comparativos permite isolar o efeito filogenético ao testar hipóteses evolutivas. Uma vez que espécies proximamente relacionadas tendem a ter traços semelhantes, resultados espúrios podem ser obtidos em análises de correlação entre variáveis de interesse, e a filogenia é necessária para remover o efeito indesejado da autocorrelação filogenética. Embora Gnaphosidae tenha grande potencial como modelo para estudo de processos evolutivos, a falta de hipóteses filogenéticas impede esse tipo de investigação.

Esta tese pretende contribuir para o avanço na compreensão dos padrões e processos que podem explicar a biodiversidade de aranhas da família Gnaphosidae através da proposição de uma hipótese filogenética para a família, de testes de hipóteses de diversificação da genitália e de uma revisão taxonômica de um gênero neotropical. Esses objetivos são abordados aqui em três capítulos na forma de manuscritos para submissão em revistas científicas. O primeiro capítulo, a ser submetido ao periódico

Cladistics, apresenta uma análise cladística baseada em dados morfológicos para Gnaphosidae. O segundo capítulo trata da evolução da complexidade do aparelho copulatório na família e será submetido à revista *Biological Journal of Linnean Society*. Por fim, o terceiro capítulo apresenta uma revisão taxonômica do gênero *Apopyllus* aceita para publicação na revista *Zootaxa*.

CAPÍTULO I

CLADISTIC ANALYSIS OF THE WORLDWIDE SPIDERS OF THE FAMILY GNAPHOSIDAE (ARANEAE, DIONYCHA)

Cladistic analysis of the worldwide spiders of the family Gnaphosidae (Araneae, Dionycha)

GUILHERME H.F. AZEVEDO[1,2], CHARLES E. GRISWOLD[3] & ADALBERTO J. SANTOS[1]

[1]*Departamento de Zoologia, Instituto de Ciências Biológicas, Universidade Federal de Minas Gerais. Av. Antônio Carlos 6627, 31270-901, Belo Horizonte, MG, Brasil. E-mail: ghfazevedo@gmail.com*

[2]*Pós-graduação em Zoologia, Universidade Federal de Minas Gerais.*

[3]*California Academy of Sciences, 55 Music Concourse Drive, San Francisco, CA 94118, United States.*

Abstract

Gnaphosidae Pocock is a very diverse spider family with remarkable spinning organs morphology. Although the family has received intense taxonomical attention in latest years, its inter-generic relationships remain obscure. A cladistic analysis of Gnaphosidae genera was performed to untangle the evolutionary history of the family. A matrix of 336 morphological characters, scored for 70 gnaphosids and 29 outgroups, was analyzed through parsimony. Gnaphosidae is not recovered as a monophyletic group, neither were most previously proposed intrafamiliar groupings. *Vectius* Simon and *Hemicloea* Thorell are transferred to Trochanteriidae Karsch, and *Xenoplectus* Schiapelli & Gerschman to Liocranidae. *Micaria* Westring, *Nauhea* Forster and *Verita* Ramírez & Grismado (and probably some related genera) are most likely not gnaphosids, though their phylogenetic placement is uncertain. Gnaphosidae *Sensu Stricto* is defined as spiders with enlarged piriform spigots, longer and wider than major ampullate pigots. Within Gnaphosidae *S.S.*, well-supported clades allow the definition, on quantitative phylogenetics bases, of Gnaphosinae Pocock, Zelotinae Platnick, Herpyllinae Platnick, Prodidominae Simon **Rank Res** and the newly proposed Leptodrassinae **New Subfamily**. Many genera are not assigned to subfamily given low supported relationships. The homology and evolution of some structures like the claw tuft clasper, the elongated base of piriform spigots and the modification of chelicera promargin are discussed. This work points some directions towards a better understanding of the generic relationships of Gnaphosidae and related taxa.

Introduction

Recent efforts to elucidate inter-familiar and deeper relationships of spiders have improved significantly the knowledge about systematics and evolution of higher level lineages within the order (Silva Davila, 2003; Griswold et al., 2005; Bond et al., 2014; Fernández et al., 2014; Ramírez, 2014; Polotow et al., 2015; Garrison et al., 2016). However, there are still many taxa whose the intra-familiar and lower levels relationships are poorly know (Coddington, 2005). Gnaphosidae Pocock, 1898, for example, is a diverse family that needs formal phylogenetic analysis to unravel the evolutionary history of its genera.

Gnaphosidae, as nowadays delimited, comprises 2183 species (the sixth richer spider family) arranged in 124 genera with worldwide distribution (World Spider Catalog, 2016). The family has been traditionally placed in the superfamily Gnaphosoidea (Lehtinen, 1967; Platnick, 1990; Coddington, 2005) together with Prodidomidae Simon, 1884, Lamponidae Simon, 1893, Gallieniellidae Millot, 1947, Trochanteriidae Karsch, 1879, Ammoxenidae Simon, 1893 and Cithaeronidae Simon, 1893; based on the following shared characters: (1) presence of minor ampullate gland spigots (MiAm) on the posterior lateral spinnerets (PLS) and on the posterior median spinnerets (PMS), (2) oblique and flattened posterior median yes (PME) and (3) oblique, depressed endites (Platnick, 1990, 2000, 2002; Coddington, 2005). The limits and relationships of those families were explored in several important studies (Platnick, 1985, 1990, 1991, 2000, 2002; Platnick & Baehr, 2006) but, regardless of the putative synapomorphies mentioned above, the Gnaphosoidea monophyly was recently challenged in a recent investigation of Dionycha spiders, where the superfamily appeared to be paraphyletic (Ramírez, 2014). Although the relationships of gnaphosoid families are not clear, it seems that Gnaphosidae is closely related to Prodidomidae, being the enlarged piriform gland spigots a candidate synapomorphy for this sister group relationship.

The monophyly of Gnaphosidae have never been systematically tested in a formal phylogenetic analysis and the position of some genera inside the family is still discussed (e.g.: *Micaria* Westring, 1851, *Vectius* Simon, 1897, *Xenoplectus* Schiapelli & Gerschman, 1958, *Anagraphis* Simon, 1893; Murphy, 2007; Ramírez, 2014). It is acknowledged, nevertheless, that most members of the family share some peculiar characteristics of the ALS and piriform gland spigots (Pi). Platnick (1990) redefined the family to include genera with Pi "enormously enlarged", with a widened base and shaft

and a slit-like opening. Murphy (2007) diagnosed Gnaphosidae as having the ALS with a single sclerotized tubular segment and having enlarged Pi emerging from a distensible membranous tip. Ramírez (2014) proposed the widened Pi with the shaft-base transition superficially marked (fused) as a synapomorphy of a more narrowly defined Gnaphosidae. However it is known that some gnaphosid genera have the Pi with a defined shaft-base transition and the fusion could be an apomorphic condition inside the family (Platnick, 1990). The study carried out by Ramírez (2014) sampled only eight Gnaphosidae genera and, as stated therein, the inclusion of more representatives could challenge the results. The morphology of spinnerets and spigots of Gnaphosidae are remarkable and uncommon within Araneae (Platnick, 1990) and deserve more evolutionary investigation.

Several works have brought substantial contributions to solve the taxonomy of Gnaphosidae, especially regarding the New World fauna (Platnick & Shadab, 1976a, 1979, 1984; Platnick, 1983; Zambonato & Lise, 2004; Ott, 2012, 2014; Ott et al., 2012; Jorge et al., 2013) and, therefore, many genera are well delimited. However, the phylogenetic relationships among gnaphosid genera are still obscure. The family is traditionally divided into eight, loosely delimited, subfamilies: Drassodinae, Echeminae, Gnaphosinae, Hemicloeninae, Laroniinae, Micariinae, Herpyliinae and Zelotinae (Platnick 1990). These subfamily names refer basically to some groupings proposed by Simon (1893) and some recent proposals (e.g. Platnick & Shadab, 1977, 1982a) but they were never formally described. Although some subfamilies have putative synapomorphies, they have never been put into test of character congruence in a cladistics analysis. A more recent alternative internal classification of Gnaphosidae divides the family in 14 groups of genera (Murphy, 2007). However, these groups were proposed to facilitate identification and were not intended to reflect any phylogenetic relationship.

A phylogenetic hypothesis for Gnaphosidae could help to understand the evolution of some remarkable characters in the family, like the spinnerets and spigots morphology, and contribute to a systematic classification that reflects the evolutionary history of the group. Also, it could be the base for biogeographical and macroecological studies, since it is a globally distributed family with some endemic groups (e.g. Platnick, 1976). In this study, a cladistics analysis using morphological characters is performed to elucidate the relationship of the Gnaphosidae genera, testing the family

monophyly, the monophyly of internal groupings and subfamilies, as well as the relationship of the family with other spider families.

Material and Methods

Taxon sampling

The outgroup was selected to sample at least one exemplar of all the main lineages of the Oblique Median Tapetum (OMT) clade (Ramírez, 2014), which includes all the former Gnaphosoidea families (Prodidomidae, Lamponidae, Gallieniellidae, Trochanteriidae, Ammoxenidae and Cithaeronidae), plus Trachelidae Simon, 1897, Phrurolithidae Banks, 1892 and Liocranidae Simon, 1897. More than one genus was sampled from the families that appeared to be paraphyletic in Ramírez (2014) analysis. The families Trochanteriidae and Prodidomidae were sampled more extensively, since they dispute with Gnaphosidae the taxonomic position of some species (Platnick & Shadab, 1976b; Platnick, 1985, 1986a, 1990; Platnick & Baehr, 2006) and the three families seem to be closely related (Ramírez, 2014). This outgroup composition allows a good testing of Gnaphosidae monophyly and inter-familiar relationship. *Anyphaena accentuata* (Walckenaer, 1802), a member of Anyphaenidae, were chosen to root the tree.

The ingroup was chosen in a way that all subfamilies and Murphy's (2007) groups were represented, whenever possible, by a sufficient number of genera to test their monophyly. Since it was not the objective to test the monophyly of genera, only one species of each genus were used as terminals, except for a few cases in which only one female and one male from different closely related species were available. Thus, the following species were composed to represent their genera as a single chimera taxon: *Aphantaulax cincta* (L. Koch, 1866) and *Aphantaulax* sp.; *Asemesthes albovittatus* Purcell, 1908 and *A. montanus* Tucker, 1923; *Gertschosa amphiloga* (Chamberlin, 1936) and *G. concinna* (Simon, 1895); *Oltacloea beltraoe* Brescovit & Ramos, 2003 and *Oltacloea* sp.*; Plator indicus* Simon, 1897 and *Plator* sp.; *Zelanda erebus* (L. Koch, 1873) and *Z. kaituna* (Forster, 1979).

Species were selected to represent each genus based on nomenclatural importance and material availability. Whenever possible, type species of families, subfamilies and genera were included in the matrix, to guide nomenclatural decisions. Additionally, since it is important to have both sexes sampled and Scanning Electronic Microscopy (SEM) images to code many of the characters, it was selected species with

sufficient well preserved material of both sexes. Notwithstanding, a few taxa (31) could not be examined through SEM due to shortage of collection material. For at least part of these species, when SEM images were missing or the specimens available were not in good conditions, the character scoring was complemented by observations of other species and/or SEM images from literature for the same or closely related species. These cases are noted in the character list (Appendix 1). Two taxa were scored based only on images (from published studies and from unpublished Assembling the Tree of Life Spiders database), since specimens were not available at the time of the study: *Verita williamsi* Ramírez & Grismado, 2015 and *Trachycosmus sculptilis* Simon, 1893. The former was included because it could be important to explore the relationship of some Gnaphosidae taxa (like *Micaria* and *Nauhea* Forster, 1979), the latter was included in order to provide clues about the relationship and monophyly of Trochanteriidae.

A total of 99 terminal taxa were used in the analysis, being 29 from outgroups and 70 Gnaphosidae. Twenty one taxa were scored only from one sex. The material examined for this study is listed in the Appendix 2 and are deposited in the following collections (abbreviations and curators in parenthesis): American Museum of Natural History, New York, USA (AMNH, Lorenzo Prendini); California Academy of Sciences, San Francisco, USA (CASENT, Lauren Esposito and Darrell Ubick); Canterbury Museum, Christchurch, New Zeland (CMNZ, Cor Vink); Centro de Coleções Taxonômicas, Universidade Federal de Minas Gerais, Belo Horizonte, Brazil (UFMG, Adalberto J. Santos); Coleção de História Natural da Universidade Federal do Piauí, Floriano, Brazil (CHNUFPI, Leonardo S. Carvalho); Democritus University of Thrace, Alexandroupolis, Greece (DUT, Maria Chatzaki); Instituto Nacional de Pesquisas da Amazônia, Manaus, Brazil (INPA, A.L. Henriques); Laboratório Especial de Coleções Zoológicas, Instituto Butantan, São Paulo, Brazil (IBSP, Antonio D. Brescovit); Museo Argentino de Ciencias Naturales 'Bernadino Rivadavia', Buenos Aires, Argentina (MACN, Martín J. Ramirez); Museo de Historia Natural, Universidad Nacional Mayor de San Marcos, Lima, Peru (MUSM, Diana S. Dávila); Museo de La Plata, La Plata, Argentina (MLP, Luís A. Pereira); Museo Zoologico de "La Specola", Florence, Italy (MZLS, Luca Bartolozzi); Museu de Ciências e Tecnologia, Pontifícia Universidade Católica do Rio Grande do Sul, Porto Alegre, Brazil (MCTP, Arno A. Lise); Museu de Ciências Naturais, Fundação Zoobotânica do Rio Grande do Sul, Porto Alegre, Brazil (MCN, Ricardo Ott); Museu de Zoologia da Universidade de São Paulo, São Paulo,

Brazil (MZSP, Ricardo Pinto-da-Rocha); Museu Nacional, Rio de Janeiro, Brazil (MNRJ, Adriano B. Kury); Museu Paraense Emílio Goeldi, Belém, Brazil (MPEG, Alexandre B. Bonaldo); Museum of Comparative Zoology, Harvard University, Cambridge, USA (MCZ, Gonzalo Giribet); Museum of Zoology of the Invertebrates, Perm State University, Russia (PSU, Sergey L. Esyunin); National Collection of Arachnida, Pretoria, South Africa (NCA, A.S. Dippenaar-Schoeman); National Museum of Natural History, Smithsonian Institution, Washington D.C., USA (USNM, Jonathan A. Coddington); Queensland Museum, Brisbane, Australia (QSM, Robert Raven); Western Australian Museum, Perth, Australia (WAM, Mark Havey).

Character sampling and specimen preparation

Many of the characters used in this study were obtained or adapted from previous phylogenetic works on Entelegynae, especially when it included dionychans and gnaphosoid spiders (Griswold, 1993; Platnick, 2000, 2002; Bosselaers & Jocqué, 2002; Griswold et al., 2005; Platnick & Baehr, 2006; Haddad et al., 2009; Ramírez, 2014) as well from diagnoses and description of genera. Adaptation of characters involved reinterpretation of homology statements, separation of sexually dimorphic characters or separation of one mixed character into two or more neomorfic and transformational characters (sensu Sereno, 2007). Additionally, a search for new characters were done during specimen examination and added to the matrix. Autapomorphies were kept in the analysis since they can be useful for genus diagnosis or for possible future intrageneric phylogenetic research. When the state of a character (especially of multistate characters) could not be seen clearly, due to bad preparation or specimen condition, or when it looked like an intermediate condition between two states, it was coded as polymorphic (0&1 codding in Mesquite) and noted.

Shapes of structures are frequently used as discrete characters to reconstruct spider phylogeny or to diagnose taxa (e.g. Ramírez 2014: char. 9). The reliability of such separation into discrete states are rarely discussed, even though it has been show that the use of carapace shape as discrete character might not be adequate for estimating Mygalomorphae phylogeny (Bond & Beamer, 2006). Here, Geometric Morphometrics (Rohlf, 1990; Adams et al., 2004; Zelditch et al., 2004; Slice, 2007) techniques were applied to evaluate if the shape of some structures could be used as discrete character states in the phylogeny. Standardized images (photographs or SEM) were taken for the following structures: cephalothorax in dorsal view, labium in ventral view, sternum in

ventral view, anterior eye row in frontal view and posterior eye row in dorsal view. Landmarks and semi-landmarks were established for each structure, aligned and submitted to a Relative Warp Analysis (RWA; Adams et al., 2004; Zelditch et al., 2004). The tps series software (Rohlf, 2015) were used for the Geometric Morphometrics analysis, as detailed in the Supplemantary Material.

Specimens were examined immersed in 75% ethanol under a Motic K series, Leica M205C and a Leica MZ12 stereoscopic microscopes. Female genitalia were dissected and soft tissues were cleaned using a pancreatin solution (Álvarez-Padilla & Hormiga, 2007), digested with contact lens cleaner and/or temporarily cleared using clove oil or methyl salicylate solution (Levi, 1965; Holm, 1979). Male palpi and spinnerets were expanded using lactic acid heated in double boiler for a few minutes (Levi, 1965; Murphy, 2007). Photographs were made using Leica M205C equipped with a Leica DFC295 digital camera. Multifocal images were mounted using the softwares Leica Application Suite and Helicon Focus (Helicon Soft Ltd).

For SEM, specimens were submitted to critical-point drying after an overnight period in 100% ethanol, mounted in aluminum stubs with adhesive copper tape and sputter coated with gold. For each species, about eight stubs were prepared for SEM (male palp and abdomen, female abdomen, epigynum, legs I and IV, chelicerae and cephalothorax with palp). Images were taken with a Quanta 2000 SEM at the Centro de Microscopia da UFMG and with a LEO 1450vp SEM at the Entomology Department of California Academy of Sciences.

Mesquite v.3.04 (Maddison & Maddison, 2015) was used to construct and edit the matrix with 336 morphological characters. All characters were treated as non-additive. The character list with descriptions and argumentation can be found in the Appendix 1.

Phylogenetic analysis

The optimal trees under the parsimony criterion were searched using the new technologies (Goloboff, 1999) on TNT v.1.5-beta (Goloboff et al., 2008a). It was performed Random Sectorial Searches (S=45; X=30; N=43) + Consensus Sectorial Searches (S=10; Y=30) + Ratchet (C=12; 30 iterations) + Drift (C=12; D=30) + Tree Fusing (30 rounds) with 15 random addition sequences. Additionally, a round of tree bisection-and-reconnection (TBR) and sub-tree-pruning-and-regrafting (SPR) were performed on the trees found with new technologies search. Searches were done using

Equal Weights (EW) and Implied Weights (IW; Goloboff, 1993; Goloboff et al., 2008b) with 10 different values of the concavity constant (k= 3, 5, 7, 9, 11, 15, 17, 19, 21 and 23). The best trees under different weight regimes were compared using SPR distances (Goloboff, 2008) and the tree with the highest mean similarity with the others were chosen as working hypothesis. Character optimization to explore the evolution of some features was done with WinClada (Nixon, 2002). Clade support was estimated through jackknifing under symmetrical resampling (Goloboff et al., 2003), with 1000 pseudoreplications, and with bremer support (BS) values (Bremer, 1994). A preliminary run indicate a maximum BS value of 0.85 in fit difference. After an initial run retaining 3000 trees with fit difference of 0.01, other nine cycles were run, increasing the fit difference in ten units and the trees in memories in 3000 each cycle. This way, a universe of suboptimal trees up to 0.90 units of difference of fit was explored to estimate BS values. Search parameters were the same mentioned above. The support of clades is shown in the preferred tree.

Results

Matrix and Character Statistics

The final dataset resulted in a matrix with 336 active characters scored for 99 taxa, in which 21% of entries are missing data and 13% are inapplicable. The great proportion of missing data was due to the high number of taxa without SEM preparation (31 taxa) and with only one sex available (21 taxa). There are 35 characters from female genitalia, 57 from male genitalia, 52 from spinnerets and 222 from other body parts.

The Geometric Morphometrics contributed to the codding of four characters. The cephalothorax analysis yielded two independent binary characters: the overall shape (Char. 278, Supplementary Material Figure S2A) and the shape of the anterior margin (Char. 279, Supplementary Material Figure S2A). The sternum ordination shows the presence of one character with two states (Char. 280, Supplementary Material Figure S2B). The posterior eye row could be coded in two states: a procurved closely spaced eye row, and a straight to recurved row (Char. 281, Supplementary Material Figure S3A). The analysis of the anterior eye row and labium reveals a continuum of shape variation, so those structures could not be coded as binary character states, although some of them were tentatively scored qualitatively, but kept as inactive characters (see Appendix 1: chars. 336–345 and the Supplementary Material).

Phylogeny

The equal weights analysis resulted in 2088 most parsimonious trees with 2016 steps (CI= 17, RI=51). The strict consensus of these trees is highly unresolved for the Gnaphosidae genera relationships, with only few clades consistently recovered among all trees, although the outgroup shows good resolution (Fig. 1).

The tree obtained in the implied weights analysis with k=15 was the one with the highest mean similarity with the other trees (Table 1). Therefore, this tree was used as working hypothesis for the Gnaphosidae genera phylogeny (Fig. 2, fit= 69.32592). The trees found under other concavity values and under equal weights are, nevertheless, used to discuss robustness of clades. Most of the clades are weakly supported by the resampling analysis and bremer support values (Fig. 2). The sensitivity analysis (sensu Giribet, 2003) to weighting regime as well as the supports are summarized in the working hypothesis tree (Fig. 2).

Gnaphosoidea is not recovered here as a monophyletic group, since Gallieniellidae is closer to Phrurolithidae and some Liocranidae than to the other gnaphosoid families (Fig. 2). The Claw Tuft Clasper (CTC) clade, recently proposed (Ramírez 2014), also appears paraphyletic in this analysis. Among the former Gnaphosoidea families, Ammoxenidae, Gallieniellidae and Prodidomidae are monophyletic (Lamponidae and Cithaeronidae monophyly could not be tested since only one terminal was used from each family). Ammoxenidae is sister to Cithaeronidae and prodidomids are closely related to gnaphosids (Fig. 2).

Gnaphosidae as currently delimited is not monophyletic, neither are most of the subfamilies or Murphy's groups. Only Zelotinae (equivalent to Murphy's *Zelotes* group) and Herpyllinae are recovered as natural groups. The Hemicloeinae (*Hemicloea* group) are grouped with the flattened trochanteriids. *Micaria*, *Verita* and *Nauhea* are related to Ammoxenidae+Cithaeronidae clade, Lamponidae and Trochantheriidae, respectively. *Xenoplectus* is related to trochanteriids in the IW analysis and to *Liocranum* L. Koch, 1866 under EW. Some gnaphosids are more closely related to prodidomids than to other gnaphosids (e.g. *Anagraphis* Simon, 1893 and *Anzacia* Dalmas, 1919).

Discussion

Gnaphosoidea

In the past few years, Gnaphosoidea received substantial attention on its systematics and taxonomy (Platnick, 1990, 2000, 2002; Platnick & Baehr, 2006). A recent analysis,

nevertheless, revealed that many of the characters thought to be synapomorphies of the superfamily are, in fact, shared derived characters of a more inclusive clade named OMT (Ramírez, 2014). This clade includes all the Gnaphosoidea families plus Liocranidae, Phrurolithidae and Trachelidae. The findings here also suggest a paraphyletic Gnaphosoidea, and the classic gnaphosoid median eyes, with oblique tapetum, and the obliquely depressed endites emerge as synapomorphies of the OMT clade. In the dataset herein, the oblique tapetum is present in all taxa except for *Anyphaena* Sundevall, 1833, *Meedo* Main, 1987, *Oltacloea* Mello-Leitão, 1940 and *Tricongius* Simon, 1893. The oblique depressed endites might be, in some cases, hard to recognize, and the interpretation might disagree between authors (e.g. *Trachycosmus* Simon, 1893; Platnick, 2002; Ramírez, 2014). Here it was considered primitively absent only in *Anyphaena* and secondarily lost in *Notiodrassus* Bryant, 1935.

The CTC clade

The CTC clade was recently proposed to include Trachelidae, Ammoxenidae, Cithaeronidae, Phrurolithidae, Prodidomidae, Gnaphosidae, some gallieniellids, some trochantheriids, and some liocranids (Ramírez, 2014). The main synapomorphy of the clade, the claw tuft clasper, is a structure located on base of the tarsal claw that probably is used to move the tenent setae of the claw tuft (Fig. 8). The homology of the claw tuft clasper was interpreted in a different manner herein, what probably led to finding the CTC clade paraphyletic. The structure was divided in three independent characters, a classic clasper (char. 134; Fig. 8 B, C, G), a folded clasper (char. 135; Fig. 8 A, E) and a solid pointed clasper (char. 136; Fig. 8 C, F), since they do not seem to be homologous.

The classic clasper was originally discovered by Platnick et al. (2005) who called it specialized proximal claw teeth. This clasper is a digitiform structure that looks like several teeth closely spaced and it is located just above a basal claw fold (Fig. 8B, C, G). This fold seems to be present (in different degrees of development) in all taxa examined through SEM (Fig. 9). In some genera, like *Eilica* Keyserling, 1891, the basal fold is very developed and might be used to clasp the claw tuft seta (Fig. 8A, E), serving the same function as the classic clasper. The classic clasper differs from the folded clasper regarding their position and structural composition. In other cases, as in *Ammoxenus* Simon, 1893 and *Micaria*, the basal fold is not very developed, but it has a solid pointed projection towards claw tuft and also might be used to clasp tenant setae (Fig. 8F). The pointed clasper, although in the same position as the folded clasper,

differs in structural composition and seems independent modifications of the same structure, the basal fold. Both pointed clasper and classic clasper can be found in *Chilongius* Platnick, Shadab & Sorkin, 2005 (Fig. 8C). All these evidences suggest that the three described structures might not be homologous, although they serve the same function, and should be treated as different independent characters.

Ramirez (2014) stated that, even with the uncertain taxonomic composition of the CTC clade, the evolution of the clasping mechanism with one single origin is well established. This single origin would be consistent with the transition from articulate to fixed claw tuft insertion and possibly related to the appearance of the ribs of the basal section of claw tuft tenant setae (Ramírez, 2014). This suggests that the spider would be able to move the claw tuft even without an articulated claw tuft insertion, clasping the basal ribs of tenent setae. The homology reinterpretation and the results presented here imply, however, an alternative explanation to clasper evolution. It might be that those taxa with a clasping mechanism evolved independent ways to control the movement of tenant setae and overcome the problem of the unarticulated claw tuft insertion. The classic clasper evolved once in the working hypothesis herein (Fig. 10) as a synapomorphy of the Neotropical tricongiine prodidomids (in agreement with Platnick et al., 2005). The folded clasper is a synapomorphy of a small group of laroniines and some gnaphosines (Fig. 10). The pointed clasper is more homoplasic, evolving at least four times in the OMT clade (Fig. 10). The clasping mechanism evolution does not seems directly related to the evolution of basal section of the tenant setae with ribs, thought it could be a pre-adaptation to evolution of clasper, facilitating the coupling of these structures and allowing better movement of the claw tuft. However, it is still a puzzle the mechanism in which the taxa with fixed claw tuft insertion would suppress the problem (if it is really a problem) of reduced movability of tenant seta, since many taxa with claw tuft do not have a clasper. Detailed comparative studies of morphology and mechanics of these structures could help to understand better de homology, function and evolution of the claw tuft clasping mechanisms.

Gallieniellidae

Gallieniellidae is supported here by the elongated, tubular, semi-paraxial chelicerae (chars. 61, 96, 97; Figs 3, 21D, G), absence of claw tuft, loss of conductor, absence of aciniform gland spigots (Ac) on PLS, among others. This result agrees with Platnick (2002) and Haddad et al. (2009). A disputed member of the family, *Austrachelas*

Lawrence, 1938; was not included in the analysis. Haddad et al. (2009) transferred this genus from Liocranidae since it was found, in a phylogenetic analysis, embeded in Gallieniellidae clade. However, in the Dionycha phylogeny (Ramírez, 2014) *Austrachelas* was found to be closer to *Liocranum*. In fact, Gallieniellidae appeared paraphyletic, with taxa scattered through OMT clade. *Austrachelas* do not have clearly semi-paraxial chelicerae, have Ac on PLS and have claw tuft, and, therefore, the inclusion of this taxa might change the Gallieniellidae monophyly obtained herein. On the other hand, a constrained analysis with Gallieniellidae monophyletic shown to be slightly suboptimal, recovering a possible secondary signal (Ramírez, 2014). Therefore, it might be interesting more studies on this family to elucidate its relationships.

Ammoxenidae and Cithaeronidae

Ammoxenidae (at least *Ammoxenus*) and Cithaeronidae are often recovered as weakly supported sister clades (Platnick 2002, Ramirez 2014). Although Ramírez (2014) did not find a monophyletic Ammoxenidae, a constrained analyses shown to perform almost as better, resulting in Ammoxenidae sister to Cithaeronidae. Herein, this sister group relationship is weakly supported by characters related to tarsi pseudosgmentation (althoug with reversion in *Rastellus* Platnick & Griffin, 1990; Figs 2, 4) and the loss of palpal conductor. Ammoxenidae monophyly, on the other hand, is very well supported, and the main synapomorphies are strong spines on chelicerae, PMS anteriorly displaced, terminal apophysis on embolus, absence of piriform gland spigots in females and procurved posterior eye row (Fig. 3).

Trochanteriidae and Flattened Gnaphosoids

The taxonomic position and relationships of the flattened gnaphosoid genera has always been confusing (see Platnick, 1985, 1986a, 1986b, 1990, 2002). *Vectius* and *Hemicloea* Thorell, 1870 are, until nowadays, accepted to be members of the subfamily Hemicloeinae (or *Hemicloea* group in Murphy 2007) and placed in Gnaphosidae (World Spider Catalog, 2016). This placement was justified based on the presence of enlarged piriform gland spigots and the lack of a distal sclerotized ring on PLS (Platnick, 1990). However, in those taxa the piriform spigots are not considerably longer nor wider than the major ampullate spigots, as in the true gnaphosids (Fig. 13) and most trochanteriid genera studied here (except for *Trachycosmus*) have an inflatable membrane and incomplete distal ring on ALS (Fig. 13). Herein, the extremely flattened trochanteriids

(*Trochanteria* Karsch, 1878, *Doliomalus* Simon, 1897, *Platyoides* O. Pickard-Cambridge, 1890 and *Plator* Simon, 1880) group with the hemicloeinae gnaphosids in a strongly supported clade, which is phylogeneticaly distant from *Trachycosmus* (Fig. 2). Many of the synapomorphies of this clade are related to the body flatness (Fig. 4B).

The support of flattened gnaphosoid group as a natural one could be questioned based on the argument that many shared characters recovered as synapomorphies would be a convergence resulting from the same way of life under tree bark and cracks. Notwithstanding, deactivating those characters during tree search recovered the same grouping. Beside the flatness related characters, those taxa also shares remarkable similarities in male genitalia, with a detached, laminar embolus with some projections, a rounded conductor, and a cymbium with a short apex (Figs 22E, F; 23G–L). The results herein suggest, therefore, that the flattened gnaphosoid group, composed of *Platyoides*, *Trochanteria*, *Hemicloea*, *Vectius*, *Doliomalus* and *Plator*, might be monophyletic and that lifestyle under tree bark or cracks could had be present on their most recent common ancestor.

As a taxonomic implication for these findings, *Hemicloea* and *Vectius* should be transferred to Trochantheriidae, but a careful study is needed to redelimit the family, regarding the Trachycosminae, Morebilinae and, maybe, some members of Trochanteriinae (Platnick, 2002). These taxa are not extremely flattened, have the complete distal article of ALS, and, at least some of them, does not have the oblique median tapetum characteristics of OMT clade (Platnick, 2002; Ramírez, 2014). In the Dionycha phylogeny (Ramírez, 2014) *Fissarena* Henschel, Davies & Dickman, 1995, *Desognaphosa* Platnick, 2002 and *Trachycosmus* appeared as sister to all the OMT clade. Herein, only *Trachycosmus* were included and, since this genus have an oblique median tapetum, they emerged inside the OMT, but far apart from the remaining Trochantheriidae. An analysis with a broader sampling of trochanteriids would help elucidate if the family, as nowadays delimited, is actually an artificial assembling of two distinct, not closely related lineages.

Other flattened (but not extremely) taxa historically associated with Trochanteridae are *Oltacloea* and *Xenoplectus* (Schiapelli & Pikelin, 1957; Platnick, 1985, 1986a, 1986b). *Oltacloea* are clearly a Prodidomidae and is recovered nested in the prodidominae clade. The position of *Xenoplectus*, currently placed in Gnaphosidae, is more uncertain. In the working hypothesis it is sister to the flattened trochanteriids, but the relationship is sensitive to weighting schemes, being sister to *Liocranum* in

analyses with some values of k, and closely related to Phrurolithidae in another. Besides, when deactivating the flatness related characters, *Xenoplectus* fall sister to *Liocranum*. *Xenoplectus* spinnerets and spigots are not the gnaphosids kind and it is most certain that this genus should not be placed in Gnaphosidae. Considering that the deactivation of flatness related characters changes *Xenoplectus* position regarding the trochanteriids, it is likely that this genus should not be allocated in Trochanteriidae. As suggested before (per Brescovit, in Murphy, 2007), a better taxonomic position for *Xenoplectus* should be in Liocranidae, until more liocranid genera are included in a phylogenetic analysis and the family is more clearly delimited.

Gnaphosidae

The monophyly of Gnaphosidae, as nowadays delimited, is challenged here by the position of prodidomids as derived gnaphosids and by few "problematic" taxa. The close relationship of Prodidomidae and Gnaphosidae has been suggested in many previous studies (Platnick, 1990, 2000, 2002; Platnick & Baehr, 2006; Ramírez, 2014). Both taxa have an enlarged piriform gland spigot, compared to the major ampullate spigots. This is the main synapomorphy of a clade recovered herein that involve the two families. Although some "problematic" genera, like *Vectius* (as discussed in Trochanteriidae section) and *Micaria*, *Nauhea and Verita* (discussed below), might have questionable coding for this character and might not be real gnaphosids, the prodidomid genera and the real Gnaphosidae have the Pi clearly longer and wider than MaAm. This enlarged piriform spigot clade have negligible support, probably due to its few synapomorphies, but it is stable through weighting schemes, and these two shared derived characters are remarkable and uncommon in spiders. A similar analogous enlargement is found only on males of Clubionidae Wagner, 1887. Within the OMT clade, the enlargement of the piriform spigots might have evolved only once without reversions (Fig. 17). Therefore, the close relationship of prodidomids and gnaphosids are reasonable.

Platnick & Shadab (1976b) argued that prodidomids would be a branch of derived gnaphosids and it should be given a subfamilial taxonomic status inside Gnaphosidae. This hypothesis was abandoned later in subsequent works on Gnaphosoidea (Platnick, 1990). Herein, we found evidence suggesting that a monophyletic group of prodidomid spiders could really be a derived branch of gnaphosids (Fig. 2) and none of the weighting schemes recovered prodidomids as sister

group of gnaphosids. Therefore, the Prodidominae taxonomical rank should be resurrected and the subfamily should be placed in Gnaphosidae.

The Micariines and the Anzacia G*roup*

It has been suggested that *Micaria* could be related to some Phrurolithidae taxa (Lehtinen, 1967) and also that the genus should be placed in its own family (Mikhailov & Fet, 1986). The inclusion of *Micaria* in Gnaphosidae has been justified on the presence of enlarged piriform gland spigots (Platnick, 1990; Murphy, 2007). However, although *Micaria*'s piriform spigots have broad openings, they are not wider or longer than the major ampullates, as it is found in true Gnaphosidae (Fig. 12E). In fact, males of *Micaria* have no piriform spigots at all (Fig. 16C) and females have only one. Ramírez (2014) found *Micaria* to be sister to a clade formed by Gnaphosidae plus Prodidomidae. Herein, *Micaria* is sister to the Cithaeronidae plus Ammoxenidae clade, but the relationship is not well supported. The most notable synapomorphies are the solid pointed claw-tuft clasper (unknown state in Cithaeronidae and with homoplasy in the dataset) and the pseudosegmentation on legs III and IV (lost in *Rastellus* and homoplastic). *Arboricaria* Bosmans, 2000 was not included in this analysis but it might be closely related to *Micaria* since they are very similar in genitalia and general morphology (Mikhailov, 2016).

The *Anzacia* group includes genera that resemble *Micaria* (except *Hypodrassodes* Dalmas, 1919 and *Anzacia* Dalmas, 1919) in many aspects, including genital and spinnerets morphology (Murphy, 2007; Ramírez & Grismado, 2015). The recently described *Verita* Ramírez & Grismado, 2015 also was supposed to be related with *Micaria* and some genera of the *Anzacia* group, like *Homoeothele* Simon, 1908 and *Matua* Forster, 1979. Herein, the *Anzacia* group (represented by *Anzacia*, *Nauhea*, *Verita* and *Hypodrassodes*) was found to be polyphyletic and was not closely related to *Micaria*.

Anzacia and *Hypodrassodes* are the most different genera among the *Anzacia* group. Both have piriform spigots clearly longer and wider than the major ampullates, and both genera most certainly belong to the Gnaphosidae *S.S.* clade. They also have quite complex palp morphology (Fig. 23A–C; Zakharov & Ovtcharenko, 2011). *Anzacia* is quite unstable through different weighting schemes, and it is recovered as sister to *Hypodrassodes* only under two concavity values (k=19, 21). *Hypodrassodes* have many piriform spigots with long base and short shaft and the genital morphology

is quite elaborate. It is possible that *Hypodrassodes* is really not closely related to the *Anzacia* group, but rather to some gnaphosids with the same spigot morphology (*Zelanda*, *Drassodex* and *Notiodrassus*). Howsoever, it is most likely that both *Anzacia* and *Hypodrassodes* are not related to the remaining genera in *Anzacia* group.

Nauhea has unstable position, probably due to many missing data, since there was only one male available and it was not possible to obtain SEM images. *Verita* is always recovered as sister to *Lampona* Thorell, 1869 based on the absence of squamose setae, presence of plumose seta, post epigastric sclerites, male dorsal scutum and absence of separated cylindrical spigot field on PMS. *Micaria*, *Nahuea* and *Verita* do not have the enlarged piriform spigots and, therefore, most likely do not belong to the Gnaphosidae. However, their positions in the OMT clade are not clear. The inclusion of *Homoeothele* and *Matua*, as well as more species of *Micaria* and *Arboricaria*, could help elucidate if the similarities between those taxa are convergences resulting from a reduced size, convergences related to ant mimicking or even if the taxa are indeed closely related. Given the uncertain position of these taxa, they should be kept in Gnaphosidae until more data is available to establish a better placement. The name Gnaphosidae *Sensu Stricto* is used here, however, to refer to the monophyletic group that includes taxa that have the piriform spigots longer and wider than the major ampullate gland spigots (Fig. 2), excluding, therefore, those uncertain taxa.

Prodidomines

Prodidomidae has been recovered as monophyletic in every analysis so far, with good support and clear synapomorphies, although it was never rigorously tested in previous studies, since few representatives of the family and outgroups were used (Platnick & Baehr, 2006; Ramírez, 2014). Herein, a third of the described genera were used and the family is well supported by an incomplete distal article of the ALS with patches of long setae around spinnerets (Fig. 11A–D, G), by a piriform spigot with base longer than shaft (Fig. 11A–D, G), by the absence of epiandrous spigots, by primary spermathecae absent (lumen indistinct from ducts; Fig. 26G, H), and dorsal chemosensory patch on male palp and dorsal triangular scales on tarsal claw (Figs 5, 8D, G, H). Among those, the patches of long setae on ALS and the long base of piriform spigots are traditionally accepted as the most distinctive and noticeable diagnostic characters for the family. An elongated base of Pi, but not associated to patches of long setae, is also found at least in *Hypodrassodes*, *Zelanda* Özdikmen, 2009, *Drassodex* Murphy, 2007 and *Notiodrassus*,

evolving independently in two clades on the working hypothesis (Fig. 17). In some weighting regimes those taxa are found closely related to Prodidominae, but without compromising the monophyly of the subfamily. Therefore, even with some uncertainties related to the evolution of the long base Pi spigots, the prodidomids are most likely a natural group. Although most of the prodidomid terminals are Neotropical, the inclusion of exemplars from the recently revised Australian fauna (Platnick & Baehr, 2006) is not likely to challenge the subfamily monophyly, since they seem to have the main synapomorphies of the family. It might be of interest, nevertheless, the careful examination and revision of the less known and relatively diverse African prodidomine fauna.

The Gnaphosines

Simon (1893) defined the groups Gnaphoseae and Laronieae basically based on the modifications of the chelicerae retromargin. These groups were subsequently referred to as Gnaphosinae and Laroninae subfamilies (Platnick, 1975a, 1975b; Platnick & Shadab, 1975; Ovtsharenko et al., 1992), or *Gnaphosa* and *Laronius* group (Murphy, 2007). The former would be defined by the presence of a serrated keel on the chelicerae (Fig. 28D), while the latter would be diagnosed by the presence of translucent laminas on retromargin (Fig. 28B). Platnick & Shadab (1975) argued that the lumping of both groups in one would be extremely artificial, and that it is most likely that chelicerae modification arose independently, not being homologous. Herein, all types of cuticular projections of retromargin – teeth, lamina and serrated keel – were considered homologous, given their position, and were represented as a neomorphic character. However, the morphological variation of these projections suggests distinct modifications of same structure and a transformational unordered character was created to accommodate these differences. This way, the data allows the congruence test to reveal if these cheliceral modifications arose independently or if one has originated from the other. The results show support for a possible single origin of the chelicerae retromargin serrated keel and that the lamina in laroniines (represented by *Eilica* and *Callilepis* Westring, 1874) could be a derived modification of the former structure (Figs 2; 6, 28B, D, F), appearing two times (or three, depending on the interpretation of the character state in *Pterotricha* Kulczyński, 1903). Anyway, such a kind of promargin projection as laminas would have arisen independently, and not from a serrated keel, in *Leptodrassus* Simon, 1878.

Although Laroniinae might be monophyletic, as suggested by some weighting regimes, its position as sister group to a monophyletic Gnaphosinae is quite unlikely. The clade formed by gnaphosines and laroniines are, nevertheless, very well supported by the absence of promarginal and retromarginal escort seta on the chelicerae, a subtegulum that covers part of the proximal part of the tegulum, and that can be seen on ventral view (Fig. 24A, D, G), and the serrated keel on retromargin of the chelicerae (modified into translucent lamina in *Eilica* and *Callilepis*). Even though *Laronius* Platnick & Deeleman-Reinhold, 2001 were not examined here, it is expected to be nested in this clade, since the taxa have the retromargin translucent lamina. Therefore, the Gnaphosinae should be redelimited to include *Laronius*, *Eilica* and *Callilepis*.

The Zelotines

Berland (1919) proposed a small group of gnaphosid genera based on the presence of a preening comb on metatarsi III and IV, and the generic limits and composition of this group were subsequently clarified through a series of revisionary papers (Platnick & Shadab, 1982a, 1982b, 1983; Platnick & Murphy, 1984, 1987; Platnick & Song, 1986; Snazell, 1997; Levy, 1998; Russell-Smith & Murphy, 2005; FitzPatrick, 2007; Chatzaki, 2010; Murphy & Russell-Smith, 2010; Senglet, 2012). This group, commonly referred to as *Zelotes* complex, Zelotinae (Platnick, 1990) or *Zelotes* group (Murphy, 2007), was recovered herein with good support, being the preening comb the main synapomorphy, with no convergence or reversion through Gnaphosidae evolution. The group is also united by the presence of post epigastric sclerites (convergent in Lamponidae and other genera) and a teardrop shaped tarsal organ opening.

Most of the zelotines have remarkable male palp and also share some characters in female genitalia, which have been target of recent studies about the copulatory mechanism and homology (Senglet, 2004). All genera but *Berinda* Roewer, 1928 and *Zelotibia* Russell-Smith & Murphy, 2005 have a detached embolar division with a terminal apophysis and a terminal membrane on a laminar embolus. The male palp also has a characteristically shaped median apophysis and has no conductor (Fig. 25A, E, F). The position of *Berinda* and *Zelotibia* arising from the two most basal dichotomies suggest that this characteristic palp evolved once, with no reversion (Fig. 5C).

The Herpyllines

Platnick & Shadab (1977) proposed the *Herpyllus* complex (Herpyllinae in Platnick, 1990) to comprise a few genera with simple but similar genitalia. This grouping included genera with black and white coloration patterns on the abdomen, like *Herpyllus* Hentz, 1832 and *Sergiolus* Simon, 1891, and with plain-colored abdomen, like *Nodocion* Chamberlin, 1922, *Litopyllus* Chamberlin, 1922 and *Scotophaeus* Simon, 1893. Murphy (2007) included in *Herpyllus* group, for identification purposes, only the black-and-white species. Herein, we found support for a clade of black-and-white herpyllines, which is sister to *Nodocion* plus *Litopyllus*. This relationship is supported by the loss of epiandrous spigots and the presence of a keel on chelicerae promargin (Fig. 28E, G), in addition to the remarkable genitalia similarities (Fig. 24B, E, F, H). Even though the *Nodocion/Litopyllus* clade might be nested inside the black and white clade, as appeared in some weighting regimes, the single origin of the colored abdomen is well established.

Scotophaeus, although originally included in Herpyllinae, seems to be distantly related to the herpylline clade found here. *Scotophaeus* have a simple palp, but with detached embolus, rather than fused to tegulum, and the median apohysis and conductor are not twisted around the embolus. Though the genus is most likely not a Herpyllinae, the relationships of *Scotophaeus* are still uncertain, being probably related to A*podrassodes* Vellard, 1924 and *Drassodes* Westring, 1851.

Leptodrassus *and Relatives*

The *Leptodrassus*, *Leptodrassex* and *Cryptodrassus* groups were delimited based on eye disposition, presence/absence of male dorsal scutum and presence/absence of chelicera lamina (Murphy, 2007). Although they differ in these characters, the genera included in *Cryptodrassus, Leptodrassus* and *Leptodrassex* groups have considerably similar genital morphology and they were found to be closely related in this study. They all belong to a well-supported clade in which some synapomorphies are an epigynal plate without an atrium, a posteriorly direct fertilization duct, an accessory secondary median apophysis on male palp, a thin filiform embolus (sometimes hidden on the unexpanded bulb; Fig. 23D–F).

The species of *Cryptodrassus* Miller, 1943 examined herein, *C. creticus* Chatzaki, 2002, might not be congeneric with the type species of the genus, *C. hungaricus* (Balogh, 1935) (Murphy, 2007). *C. creticus* have the genitalia

morphological pattern as in the genera of the *Leptodrassus* and *Leptodrassex* groups, while *C. hungaricus* might be slightly different. The females do not have a posteriorly directed fertilization duct (Murphy, 2007; Kovblyuk & Nadolny, 2010), and only one tegular sclerite, possibly the secondary median apophysis (the apical tegular sclerite in Kovblyuk & Nadolny, 2010), is found in males. Even with those differences, the general morphology of the body and genitalia suggest that *C. hungaricus* could still be closer to the clade mentioned here than to other gnaphosid genera. Unfortunately, there was no *C. hungaricus* specimens available for this study, and a closer examination of this species might be of interest.

The "Echemines" and "Drassodines"

The Echeminae were defined to include genera with strongly procurved posterior eye row, dentate tarsal claw, unadvanced ALS and a long embolus inserted on the prolateral side of the tegulum (Platnick & Shadab, 1976a, 1976b, 1976c, 1979). Murphy (2007) defined the *Echemus* group as having plain colored abdomen and a dorsal scutum. Many of the characters used by those authors seem to be plesiomorfic, or at least shared by a great number of genera, and it is not surprising that those groupings were not recovered here as monophyletic. The only derived and more restrict character is the procurved posterior eye row, although it is homoplasic.

The group Drassodeae, as proposed by Simon (1893), was delimited based on the robust chelicerae armed with strong teeth. After the relimitation of the other gnaphosid subfamilies mentioned above, many genera in that group were transferred, and the limits of Drassodinae remained obscured. As said by Platnick (1990), this subfamily was used as "wastebasket" of gnaphosids, grouping genera that do not belong to the other subfamilies. Murphy (2007) defined the *Drassodes* group as having plain colored abdomen, a notched trochanter and lacking dorsal scutum. Again, many characters are plesiomorphic and the only derived homoplasic character, the notched trochanter, was not enough to recover the monophyly of the group. The relationships of drassodines (and *Drassodes* group) genera are still unstable and more study is necessary to establish their phylogenetic placement.

The Anagraphidines

Anagraphidinae was redelimited to include two genera with sclerotized tip on anterior lateral spinnerets: *Anagraphis* Simon, 1893 and *Talanites* Simon, 1893 (Platnick &

Baehr, 2006). Murphy (2007) described a new genus, *Drassodex* and placed it on his *Anagraphis* group. Here, the annular crescent with fringe thin seta (as the sclerotized tip was called in Murphy, 2007) was tentatively included in the matrix, but not used, because the annular crescent might be a reminiscent of spinneret distal article. This sign of a distal article is found in gnaphosids and prodidomids in many levels. There might be just some few setae near the MaAm spinning field, or there might be many setae on patches associated to the piriform spigots (Platnick & Baehr, 2006; Ramírez, 2014). The sclerotization is hardly seen, but rather inferred through the presence of setae. Although in the mentioned genera the sclerotized tip can be more easily seen, it was considered as the same state as the other gnaphosids, since levels of sclerotization might be hard to delimit. Given that almost none of the derived characters present in *Anagraphis* are shared with *Drassodex*, it is quite unlikely that both genera are closely related, even if this state of character is included. Howsoever, regardless of the position of *Drassodex*, it seems that *Anagraphis* and *Talanites* might constitute a natural group. However, most of their synapomorphies are ambiguous or highly homoplastic.

The taxonomic position of anagraphidines has been floating between Gnaphosidae and Prodidomidae (Platnick, 1990; Platnick & Ovtsharenko, 1991; Levy, 1999; Chatzaki et al., 2002a, 2002b; Platnick & Baehr, 2006). Herein, anagraphidines and prodidomines were found to be sister groups supported by a secondary spermatheca with long duct (Fig. 26G, H), a fingerprint cuticle texture and the major ampullate spigots field touching distal article border (Fig. 14A). The sister group relationship found here is stable through weighting regimes, but it has low support regarding Bremer and jackknife values. The close relationship of anagraphidines and prodidomids was also hypothetized by Platnick & Shadab (1976c) and recovered in the cladistics analysis of Ramírez (2014). Ramírez (2014) showed that a constrained analysis with *Anagraphis* closer to Gnaphosidae resulted in a slightly suboptimal tree with *Anagraphis* sister to the remaining gnaphosids, but with no synapomorphy. Therefore, all these evidence suggest that is quite plausible that anagraphidines might be closely related to prodidomids than to remaining gnaphosids.

Conclusions

The position of *Xenoplectus* is uncertain but it is clearly that it does not belong to Gnaphosidae. Therefore, *Xenoplectus* should be transferred to Liocranidae until more data are available for untangling its evolutionary relationships. Regarding the

hemicloeine genera, *Vectius* and *Hemicloea*, they should be transferred to Trochanteriidae. This family might be composed by two distinct, distant related lineages and needs a careful investigation.

The most problematic taxa in Gnaphosidae are *Micaria*, *Nauhea*, *Verita* and, probably, also *Arboricaria*, *Homoeothele* and *Matua*. These genera do not have the characteristic spigots morphology and are not nested within the true gnaphosids, but also, do not clearly fit to any other well established clade. For the lack of a better place, *Micaria*, *Arboricaria*, *Nauhea*, *Verita*, *Homoeothele* and *Matua* should be kept in Gnaphosidae.

The position of prodidomids as an offshoot of Gnaphosidae suggests that the former should be ranked as a subfamily of the latter. A Gnaphosidae *Sensu Stricto* could be defined as the spiders that belong to OMT clade that have widened piriform spigots (clearly wider and longer than the major ampullate spigots). In a broader sense, Gnaphosidae would also include *Micaria*, *Arboricaria*, *Nauhea*, *Verita*, *Homoeothele* and *Matua*. Gnaphosidae *sensu lato* would be more loosely defined including small spiders (2–5mm) with few (1–8) piriform spigots about the same size as the major ampullate, and with shaft as wide as base with broad opening. Although loosely defined, this definition still allow the identification, with some confidence, of members of this paraphyletic family.

Within the Gnaphosidae *S.S.* the well-established monophyletic groups are noteworthy. Among the traditional groups, there are the Gnaphosinae (relimited to include "laroniines"), Prodidominae **Rank Res.,** Herpyllinae and Zelotinae. There is also the newly grouping Leptodrassinae **New Subfamily,** which is proposed here to include *Leptodrassus*¸ *Leptodrassex, Leptopilos* Levy, 2009 and *Cryptodrassus*. The remaining Gnaphosidae that do not belong to any of the well supported subfamily, although they could be informally grouped in the paraphyletic "drassodinae", should rather not be placed in any formal taxonomic rank until more evidence is available to organize them in monophyletic groups. The present work show some interesting results regarding the evolution of gnaphosids and, although it does not solve many of the previous systematic problems, this work points some directions towards a better understanding of the genus-level relationships of Gnaphosidae and closely related taxa.

Taxonomy

The taxonomic decisions were made to avoid changes based on weakly supported evidence and that would imply unstable taxonomical names. All decisions are justified on the bases of evidence found here and explained above in the text.

Family Gnaphosidae Pocock, 1898

Drassides Sundevall, 1833: 17 (type genus *Drassus* Walckenaer, 1805 = *Gnaphosa* Latreille, 1804).

Drassidae Simon, 1893: 339 (type genus *Drassodes* Westring, 1851)

Gnaphosidae Pocock, 1898: 219 (type genus *Gnaphosa* Latreille, 1804).

Drassodidae Berland, 1932: 343 (Type genus *Drassodes* Westring, 1851).

Diagnosis: The spiders that belong to Gnaphosidae have piriform gland spigots homogeneous in morphology and clearly longer and wider than the major ampullate spigots in males and females (Figs 11, 12 A–D, F–G). Sometimes, in small (2–5mm), non-flattened spiders (*Micaria*, *Nauhea*, *Verita*, *Homoeothele* and *Matua*) the piriform spigots might be about as long as wide, but they are few in number (1–8) and their shafts are tubular, with broad opening (Fig. 12E). Usually, the base of piriform spigots is shorter or about the same size as the shaft, but in some cases (*Hypodrassodes*, *Zelanda*, *Drassodex*, *Notiodrassus* and Prodidominae) the base might be longer than the shaft (Fig. 11).

Composition: The family includes five well established monophyletic subfamilies, but given the low support of relationships, many genera could not be assigned to a formal subfamiliar rank. The doubtful used subfamilial groups Drassodinae, Echeminae, Anagraphidinae, and Micariinae do not have any clearly unambiguous diagnosis and might not form monophyletic groups. Therefore, they are not formally defined herein, but their composition is mentioned below for historical purpose. The following genera are transferred to other families: *Xenoplectus* is transferred to Liocranidae; *Vectius* and *Henmicloea* (together with the subfamily Hemicloeinae) are transferred to Trochanteriidae.

Subfamily Gnaphosinae Pocock, 1898

Gnaphoseae Simon, 1893: 379. (type genus *Gnaphosa* Latreille, 1804)

Laronieae Simon, 1893: 378. (Type genus *Laronia* Simon, 1893 = *Eilica* Keyserling, 1891). **New synonymy**
Gnaphosinae: Roewer 1944, Platnick 1990: 4
Laroniinae: Platnick 1990: 4

Diagnosis: Gnaphosidae spiders that have a modified projection on chelicerae retromargin, which could be a serrated keel or a rounded lamina (Fig. 28B, D, F).

Included genera: *Amusia* Tullgren, 1910; *Aneplasa* Tucker, 1923; *Asemesthes* Simon, 1887; *Berlandina* Dalmas, 1922; *Callilepis; Echemella* Strand, 1906; *Eilica; Fedotovia* Charitonov, 1946; *Gnaphosa; Laronius; Microsa* Platnick & Shadab, 1976; *Minosia* Dalmas, 1921; *Minosiella* Dalmas, 1921; *Nomisia* Dalmas, 1921; *Pterotricha* Kulczyński, 1903; *Pterotrichina* Dalmas, 1921; *Scotognapha* Dalmas, 1920; *Shiragaia* Paik, 1992; *Smionia* Dalmas, 1920; *Trephopoda* Tucker, 1923.

Subfamily Zelotinae Platnick, 1990
Zelotes complex Platnick & Shadab, 1982a: 3
Zelotine Platnick & Murphy, 1987: 2
Zelotinae Platnick, 1990: .4 (Type genus *Zelotes* Gistel, 1848)

Remarks: Berland (1919) proposed a small group of gnaphosid genera based on the presence of a preening comb on metatarsi III and IV, which was later called *Zelotes* complex (Platnick & Shadab, 1982a) or zelotine (Platnick & Murphy, 1987). Only more recently the name Zelotinae was used to rank this group as subfamily (Platnick, 1990). Although there is no formal description of the taxa, it is implicit that *Zelotes* should be the type genus and that the preening comb should be the diagnostic character.

Diagnosis: Gnaphosidae spiders that have a preening comb on metatarsi III and IV (Fig. 30H).

Included genera: *Allozelotes* Yin & Peng, 1998; *Berinda* Roewer, 1928; *Camillina* Berland, 1919; *Canariognapha* Wunderlich, 2011; *Civizelotes* Senglet, 2012; *Drassyllus* Chamberlin, 1922; *Echemographis* Caporiacco, 1955; *Heser* Tuneva, 2004;

Ibala Fitzparick, 2009; *Setaphis* Simon, 1893; *Trachyzelotes* Lohmander, 1944; *Turkozelotes* Kovblyuk & Seyyar, 2009; *Urozelotes* Mello-Leitão, 1938; *Zelominor* Snazell & Murphy, 1997; *Zelotes; Zelotibia* Russell-Smith & Murphy, 2005; *Zelowan* Murphy & Russell-Smith, 2010.

Subfamily Herpyllinae Platnick, 1990
Herpyllus complex Platnick & Shadab, 1977: 3
Herpyllinae Platnick, 1990: 4 (Type genus *Herpyllus* Hentz, 1832)

Remarks: The *Herpyllus* complex was proposed to comprise a few genera with simple but similar genitalia (Platnick & Shadab, 1977). Later, this group was treated as the subfamily Herpyllinae (Platnick, 1990) implicitly assuming *Herpyllus* as the type genus.

Diagnosis: Gnaphosidae spiders that have a keel on chelicerae promargin, does not have epiandrous spigots, have the embolus fused to tegulum and involved by an elongated, membranous conductor, and that the female genitalia have an elongated primary spermathecae, frequently reniform in shape. The keel might be a subtle projection or might be teeth with fused bases. The median apophysis might be present as a small enlongated sclerite, apical in not-expanded bulbus, and closely associated to conductor and embolus. The majority of the spiders in this group have a distinct black and white pattern on abdomen, which is not found outside the subfamily.

Included genera: *Aphantaulax* Simon, 1878; *Cabanadrassus* Mello-Leitão, 1941; *Ceryerda* Simon, 1909; *Cesonia* Simon, 1893; *Cladothela* Kishida, 1928; *Epicharitus* Rainbow, 1916; *Gertschosa* Platnick & Shadab, 1981; *Herpyllus; Hitobia* Kamura, 1992; *Kishidaia* Yaginuma, 1960; *Ladissa* Simon, 1907; *Latonigena* Simon, 1893; *Litopyllus* Chamberlin, 1922; *Macarophaeus* Wunderlich, 2011; *Nodocion* Chamberlin, 1922; *Phaeocedus* Simon, 1893; *Poecilochroa* Westring, 1874; *Scotocesonia* Caporiacco, 1947; *Sergiolus* Simon, 1891; *Sernokorba* Kamura, 1992; *Symphanodes* Rainbow, 1916; *Trichothyse* Tucker, 1923; *Xizangia* Song, Zhu & Zhang, 2004.

Subfamily Leptodrassinae ***New Subfamily***
Type genus *Leptodrassus* Simon, 1878

Diagnosis: Gnaphosidae spiders that have an epigynal plate without an atrium, a posteriorly direct fertilization duct, an accessory secondary median apophysis on male palp that involve a thin filiform embolus (sometimes hidden on not expanded bulb; Figs. 23D–F).

Included genera: *Cryptodrassus* Miller, 1943; *Leptodrassex* Murphy, 2007; *Leptodrassus; Leptopilos* Levy, 2009; *Neodrassex* Ott, 2012.

Subfamily Prodidominae Simon, 1884 *Rank Resurrected*

Prodidomides Simon, 1884: 302 (Type genus *Prodidomus* Hentz, 1847)

Prodidominae Platnick & Shadab, 1976b: 3

Prodidomidae Platnick, 1990: 36

Molycriinae Platnick, 1990: 4 (Type genus *Molycria* Simon, 1887) **New synonymy**

Theuminae Platnick & Baher, 2006: 5 (Type genus *Theuma* Simon, 1893) **New synonymy**

Diagnosis: Gnaphosidae spiders that have the distal incomplete article of the anterior lateral spinnerets composed of patches of setae closely associated piriform spigot, which have base longer than shaft (Fig. 11A–D, G).

Included genera: *Anagrina* Berland, 1920; *Austrodomus* Lawrence, 1947; *Brasilomma* Brescovit, Ferreira & Rheims, 2012; *Caudalia* Alayón, 1980; *Chileomma* Platnick, Shadab & Sorkin, 2005; *Chileuma* Platnick, Shadab & Sorkin, 2005; *Chilongius* Platnick, Shadab & Sorkin, 2005; *Cryptoerithus* Rainbow, 1915; *Eleleis* Simon, 1893; *Katumbea* Cooke, 1964; *Lygromma* Simon, 1893; *Lygrommatoides* Strand, 1918; *Molycria* Simon, 1887; *Moreno* Mello-Leitão, 1940; *Myandra* Simon, 1887; *Namundra* Platnick & Bird, 2007; *Neozimiris* Simon, 1903; *Nomindra* Platnick & Baehr, 2006; *Oltacloea; Plutonodomus* Cooke, 1964; *Prodida* Dalmas, 1919; *Prodidomus; Purcelliana* Cooke, 1964; *Theuma* Simon, 1893; *Theumella* Strand, 1906; *Tivodrassus* Chamberlin & Ivie, 1936; *Tricongius* Simon, 1893; *Wesmaldra* Platnick & Baehr, 2006; *Wydundra* Platnick & Baehr, 2006; *Zimirina* Dalmas, 1919; *Zimiris* Simon, 1882.

Doubtful subfamilies

“Echeminae”

Composition: *Amazoromus* Brescovit & Höfer, 1994; *Arauchemus* Ott & Brescovit, 2012; *Echemoides* Mello-Leitão, 1938; *Echemus* Simon, 1878; *Scopoides* Platnick, 1989; *Megamyrmaekion* Reuss, 1834; *Zimiromus* Banks, 1914.

"Drassodinae"

Composition: *Apodrassodes* Vellard, 1924; *Apopyllus* Platnick & Shadab, 1984; *Drassodes; Haplodrassus; Hypodrassodes* Dalmas, 1919; *Nopyllus; Odontodrassus* Jézéquel, 1965; *Orodrassus* Chamberlin, 1922; *Synaphosus* Platnick & Shadab, 1980.

Anagraphidinae

Composition: *Anagraphis; Talanites* Simon, 1893; *Talanitoides* Levy, 2009.

Micariinae

Composition: *Arboricaria; Micaria*.

Genera with no subfamiliar placement

Allomicythus Ono, 2009; *Anzacia* Dalmas, 1919; *Apodrassus* Chamberlin, 1916; *Aracus* Thorell, 1887; *Asiabadus* Roewer, 1961; *Australoechemus* Schmidt & Piepho, 1994; *Benoitodes* Platnick, 1993; *Coillina* Yin & Peng, 1998; *Coreodrassus* Paik, 1984; *Cubanopyllus* Alayón & Platnick, 1993; *Diaphractus* Purcell, 1907; *Drassodex; Encoptarthria* Main, 1954; *Homoeothele; Hongkongia* Song & Zhu, 1998; *Intruda* Forster, 1979; *Kaitawa* Forster, 1979; *Matua* Forster, 1979; *Microdrassus* Dalmas, 1919; *Micythus* Thorell, 1897; *Montebello* Hogg, 1914; *Nauhea; Notiodrassus* Bryant, 1935; *Parabonna* Mello-Leitão, 1947; *Parasyrisca* Schenkel, 1963; *Pseudodrassus* Caporiacco, 1935; *Sanitubius* Kamura, 2001; *Scotophaeus* Simon, 1893; *Shaitan* Kovblyuk, Kastrygina & Marusik, 2013; *Sidydrassus* Esyunin & Tuneva, 2002; *Sosticus* Chamberlin, 1922; *Symphanodes* Rainbow, 1916; *Titus* O. Pickard-Cambridge, 1901; *Verita; Xerophaeus* Purcell, 1907; *Zelanda* Özdikmen,2009.

References

Adams D., Rohlf F. & Slice D.E. (2004) Geometric morphometrics: ten years of progress following the "revolution." *Italian Journal of Zoology*, **71**, 5–16.

Álvarez-Padilla F. & Hormiga G. (2007) A protocol for digesting internal soft tissues and mounting spiders for scanning electron microscopy. *Journal of Arachnology*, **35**, 538–542.

Berland L. (1919) Note sur le peigne métatarsal que possèdent certaines Araignées de la famille des Drassidae. *Bulletin du Musée d'Histoire Naturelle de Marseille*, **1919**, 458–463.

Berland L. (1932) Les Arachnides (Scorpions, Araignées, etc.). *Encyclopédie entomologique*, **Paris 16**, 1–485.

Bond J.E. & Beamer D.A. (2006) A morphometric analysis of mygalomorph spider carapace shape and its efficacy as a phylogenetic character (Araneae). *Invertebrate Systematics*, **20**, 1–7.

Bond J.E., Garrison N.L., Hamilton C.A., Godwin R.L., Hedin M. & Agnarsson I. (2014) Phylogenomics resolves a spider backbone phylogeny and rejects a prevailing paradigm for orb web evolution. *Current Biology*, **24**, 1765–1771.

Bosselaers J. & Jocqué R. (2002) Studies in Corinnidae: Cladistic analysis of 38 corinnid and liocranid genera, and transfer of Phrurolithinae. *Zoologica Scripta*, **31**, 241–270.

Bremer K. (1994) Branch support and tree stability. *Cladistics*, **10**, 295–304.

Chatzaki M. (2010) New data on the least known zelotines (Araneae, Gnaphosidae) of Greece and adjacent regions. *Zootaxa*, **61**, 43–61.

Chatzaki M., Thaler K. & Mylonas M. (2002a) Ground spiders (Gnaphosidae; Araneae) of Crete (Greece). taxonomy and distribution. I. *Revue Suisse de Zoologie*, **109**, 559–601.

Chatzaki M., Thaler K. & Mylonas M. (2002b) Ground spiders (Gnaphosidae; Araneae) of Crete (Greece). Taxonomy and distribution. II. *Revue Suisse de Zoologie*, **109**, 603–633.

Coddington J.A. (2005) Phylogeny and Classification of Spiders. *Spiders of North America: an identification manual.* (ed. by D. Ubick and P. Cushing), pp. 18–24. American Arachnological Society.

Fernández R., Hormiga G. & Giribet G. (2014) Phylogenomic analysis of spiders reveals nonmonophyly of orb weavers. *Current Biology*, **24**, 1772–1777.

FitzPatrick M.J. (2007) A taxonomic revision of the Afrotropical species of *Zelotes* (Arachnida: Araneae: Gnaphosidae). *Bulletin of the British Arachnological Society*, **14**, 97–172.

Garrison N.L., Rodriguez J., Agnarsson I., Coddington J.A., Griswold C.E., Hamilton C.A., Hedin M., Kocot K.M., Ledford J.M. & Bond J.E. (2016) Spider phylogenomics: untangling the Spider Tree of Life. *PeerJ*, **4**, e1719 https://doi.org/10.7717/peerj.1719

Giribet G. (2003) Stability in phylogenetic formulations and its relationship to nodal support. *Systematic Biology*, **52**, 554.

Goloboff P.A. (1993) Estimating character weights during tree search. *Cladistics*, **9**, 83–91.

Goloboff P.A. (1999) Analyzing large data sets in reasonable times: solutions for composite optima. *Cladistics*, **15**, 415–428.

Goloboff P.A. (2008) Calculating SPR distances between trees. *Cladistics*, **24**, 591–597.

Goloboff P.A., Farris J.S., Källersjö M., Oxelman B., Ramírez M.J. & Szumik C.A. (2003) Improvements to resampling measures of group support. *Cladistics*, **19**, 324–332.

Goloboff P.A., Farris S. & Nixon K. (2008a) TNT, a free programm for phylogenetic analysis. *Cladistics*, **24**, 774–786.

Goloboff P.A., Carpenter J.M., Arias J.S. & Esquivel D.R.M. (2008b) Weighting against homoplasy improves phylogenetic analysis of morphological data sets. *Cladistics*, **24**, 758–773.

Griswold C.E. (1993) Investigations into the phylogeny of the Lycosoid spiders and their kin (Arachnida: Araneae: Lycosoidea). *Smithsonian Contributions to Zoology*, **539**, 1–39.

Griswold C.E., Ramírez M.J., Coddington J.A. & Platnick N.I. (2005) Atlas of phylogenetic data for entelegyne spiders (Araneae: Araneomorphae: Entelegynae) with comments on their phylogeny. *Proceedings of the California Academy of Sciences*, **56**, 1–324.

Haddad C.R., Lyle R., Bosselaers J. & Ramirez M.J. (2009) A revision of the endemic South African spider genus *Austrachelas*, with its transfer to the Gallieniellidae (Arachnida: Araneae). *Zootaxa*, **2296**, 1–38.

Holm A. (1979) A taxonomic study of European and East African species of the genera *Pelecopsis* and *Trichopterna* (Araneae, Linyphiidae) with descriptions of a new genus and two new species of *Pelecopsis* from Kenya. *Zoologica Scripta*, **8**, 255–278.

Jorge C., Carrión N.L., Grismado C. & Simó M. (2013) On the taxonomy of *Latonigena auricomis* (Araneae, Gnaphosidae), with notes of geographical distribution and natural history. *Iheringia. Série Zoologia*, **103**, 66–71.

Kovblyuk M. & Nadolny A. (2010) *Cryptodrassus hungaricus* and *Leptodrassex memorialis* from Crimea (Aranei: Gnaphosidae). *Arthropoda Selecta*, **19**, 189–197.

Lehtinen P.T. (1967) Classification of the Cribellate spiders and some allied families , with notes on the evolution of the suborder Araneomorpha. *Annales Zoologici Fennici*, **4**, 199–468.

Levi H.W. (1965) Techniques for the study of spider genitalia. *Psyche*, **72**, 152–158.

Levy G. (1998) The ground-spider genera *Setaphis*, *Trachyzelotes*, *Zelotes*, and *Drassyllus* (Araneae: Gnaphosidae) in Israel. *Israel Journal of Zoology*, **44**, 93–158.

Levy G. (1999) Spiders of the genera *Anagraphis* and *Talanites* (Araneae, Gnaphosidae) from Israel. *Israel Journal of Zoology*, **45**, 215–223.

Maddison W.P. & Maddison D.R. (2015) *Mesquite: a modular system for evolutionary analysis.* Version 3.04. Available at: mesquiteproject.org/mesquite/download/download. html.

Mikhailov K. (2016) On the spider genus *Arboricaria* with the description of a new species (Araneae, Gnaphosidae). *ZooKeys*, **558**, 153–169.

Mikhailov K.G. & Fet V.Y. (1986) Contribution to the spider fauna (Aranei) of Turkmenia. I. Families Anyphaenidae, Sparassidae, Zoridae, Clubionidae, Micariidae, Oxyopidae. *Sbornik Trudov Zoologicheskogo Muzeya*, **24**, 168–186.

Murphy J.A. & Russell-Smith A. (2010) *Zelowan*, a new genus of African zelotine ground spiders (Araneae; Gnaphosidae). *Journal of Afrotropical Zoology*, **6**, 59–82.

Murphy J.A. (2007) *Gnaphosid Genera of the World.* British Arachnological Society.

Nixon K.C. (2002) *WinClada, version 1.00. 08.* Published by the author, Ithaca, New York.

Nzigidahera B. & Jocqué R. (2009) An update of *Zelotibia* (Araneae, Gnaphosidae), a spider genus with a species swarm in the Albertine Rift. *ZooKeys*, **13**, 1–28.

Ott R. (2012) *Neodrassex* , a new genus of the *Leptodrassex* group (Araneae , Gnaphosidae) from South America. *Iheringia. Série Zoologia*, **102**, 343–350.

Ott R. (2014) *Nopyllus*, um novo gênero de Drassodinae sul-americano (Araneae, Gnaphosidae). *Iheringia. Série Zoologia*, **104**, 252–261.

Ott R., Nei E., Rodrigues L. & Brescovit A.D. (2012) Seven new species of *Latonigena* (Araneae , Gnaphosidae) from South America. *Iheringia. Série Zoologia*, **102**, 227–238.

Ovtsharenko V.I. & Platnick N.I. (1995) On the australasian ground spider genera *Anzacia* and *Adelphodrassus* (Araneae, Gnaphosidae). *American Museum Novitates*, **3154**, 1–16.

Ovtsharenko V.I., Platnick N.I. & Song D.X. (1992) A review of the North Asian ground spiders of the genus *Gnaphosa* (Araneae, Gnaphosidae). *Bulletin of the American Museum of Natural History*, **212**, 1–88.

Platnick N.I. (1975a) A revision of the spider genus *Eilica* (Araneae, Gnaphosidae). *American Museum Novitates*, **2578**, 1–19.

Platnick N.I. (1975b) A revision of the Holarctic spider genus *Callilepis* (Araneae, Gnaposidae). *American Museum Novitates*, **2573**, 1–32.

Platnick N.I. (1976) Drifting spiders or continents?: Vicariance biogeography of the spider subfamily Laroniinae (Araneae: Gnaphosidae). *Systematic Zoology*, **25**, 101–109.

Platnick N.I. (1983) A revision of the neotropical spider genus *Apodrassodes* (Araneae, Gnaphosidae). *American Museum Novitates*, **2763**, 1–14.

Platnick N.I. (1985) Study on Malagasy spiders, 2. The family Trochanteriidae (Araneae, Gnaphosoidea), with a revision of the genus *Platyoides*. *American Museum Novitates*, **2808**, 1–17.

Platnick N.I. (1986a) A revision of the spider genus *Trochanteria* (Araneae Gnaphosoidea). *Bulletin of the British Arachnological Society*, **7**, 29–33.

Platnick N.I. (1986b) On the spider genus *Oltacloea* (Araneae Gnaphosidae). *Revue Arachnologique*, **7**, 9–14.

Platnick N.I. (1990) Spinneret morphology and the phylogeny of ground spiders (Araneae, Gnaphosoidea). *American Museum Novitates*, **2978**, 1–42.

Platnick N.I. (1991) A Revision of the Ground Spider Family Cithaeronidae (Araneae, Gnaphosoidea). *American Museum Novitates*, **3018**, 1–13.

Platnick N.I. (2000) A Relimitation and Revision of the Australasian Ground Spider Family Lamponidae (Araneae: Gnaphosoidea). *Bulletin of the American Museum of Natural History*, **245**, 1–328.

Platnick N.I. (2002) A revision of the Australasian ground spiders of the families Ammoxenidae, Cithaeronidae, Gallieniellidae, and Trochanteriidae (Araneae: Gnaphosoidea). *Bulletin of the American Museum of Natural History*, **271**, 1–244.

Platnick N.I. & Baehr B. (2006) A revision of the Australasian ground spiders of the family Prodidomidae (Araneae: Gnaphosoidea). *Bulletin of the American Museum of Natural History*, **298**, 1–287.

Platnick N.I. & Murphy J.A. (1984) A revision of the spider genera *Trachyzelotes* and *Urozelotes* (Araneae, Gnaphosidae). *American Museum Novitates*, **2792**, 1–30.

Platnick N.I. & Murphy J.A. (1987) Studies on Malagasy spiders. 3, The zelotine Gnaphosidae (Araneae, Gnaphosoidea), with a review of the genus *Camillina*. *American Museum Novitates*, **2874**, 1–33.

Platnick N.I. & Ovtsharenko V.I. (1991) On Eurasian and American *Talanites* (Araneae, Gnaphosidae). *Journal of Arachnology*, **19**, 115–121.

Platnick N.I. & Shadab M.U. (1975) A revision of the spider genus *Gnaphosa* (Araneae, Gnaphosidae) in America. *Bulletin of the American Museum of Natural History*, **155**, 1–66.

Platnick N.I. & Shadab M.U. (1976a) A revision of the Neotropical spider genus *Zimiromus*, with notes on *Echemus* (Araneae, Gnaphosidae). *American Museum Novitates*, **2609**, 1–24.

Platnick N.I. & Shadab M.U. (1976b) A revision of the spider genera *Lygromma* and *Neozimiris* (Araneae, Gnaphosidae). *American Museum Novitates*, **2598**, 1–23.

Platnick N.I. & Shadab M.U. (1976c) A revision of the spider genera *Rachodrassus*, *Sosticus* and *Scopodes* (Araneae, Gnaphosidae) in North America. *American Museum Novitates*, **2594**, 1–33.

Platnick N.I. & Shadab M.U. (1977) A revision of the spider genera *Herpyllus* and *Scotophaeus* (Araneae, Gnaphosidae) in North America. *Bulletin of the American Museum of Natural History*, **159**, 1–44.

Platnick N.I. & Shadab M.U. (1979) A revision of the Neotropical spider genus *Echemoides*, with notes on other echemines (Araneae, Gnaphosidae). *American Museum Novitates*, **2669**, 1–22.

Platnick N.I. & Shadab M.U. (1982a) A revision of the American spiders of the genus *Camillina* (Araneae, Gnaphosidae). *American Museum Novitates*, **2748**, 1–38.

Platnick N.I. & Shadab M.U. (1982b) A revision of the American spiders of the genus *Drassyllus* (Araneae, Gnaphosidae). *Bulletin of the American Museum of Natural History*, **173**, 1–96.

Platnick N.I. & Shadab M.U. (1983) A revision of the American spiders of the genus *Zelotes* (Araneae, Gnaphosidae). *Bulletin of the American Museum of Natural History*, **174**, 99–191.

Platnick N.I. & Shadab M.U. (1984) A revision of the neotropical spiders of the genus *Apopyllus* (Araneae, Gnaphosidae). *American Museum Novitates*, **2788**, 1–9.

Platnick N.I., Shadab M.U. & Sorkin L. (2005) On the Chilean spiders of the family Prodidomidae (Araneae, Gnaphosoidea), with a revision of the genus *Moreno* Mello-Leitão. *American Museum Novitates*, **3499**, 1–31.

Platnick N.I. & Song D.X. (1986) A review of the zelotine spiders (Araneae, Gnaphosidae) of China. *American Museum Novitates*, **2848**, 1–22.

Pocock R.I. (1898) The arachnida from the province of Natal, South Africa, contained in the collection of the British Museum. *Annals and Magazine of natural History*, **2**, 197–226.

Polotow D., Carmichael A. & Griswold C.E. (2015) Total evidence analysis of the phylogenetic relationships of Lycosoidea spiders (Araneae, Entelegynae). *Invertebrate Systematics*, **29**, 124–163.

Ramírez M.J. (1995) A phylogenetic analysis of the subfamilies of Anyphaenidae (Arachnida, Araneae). *Insect Systematics & Evolution*, **26**, 361–384.

Ramírez M.J. (2014) The morphology and phylogeny of dionychan spiders (Araneae: Araneomorphae). *Bulletin of the American Museum of Natural History*, **390**, 1–374.

Ramírez M.J. & Grismado C.J. (2015) Description of the spider *Verita williamsi*, a new genus and species from Santa Fe, Argentina (Araneae, Gnaphosidae). *Revista del Museo Argentino de Ciencias Naturales "Bernardino Rivadadvia,"* **17**, 173–182.

Roewer C.F. (1944) *Katalog der Araneae 1758-1940.* Bremen 2(1), 1–160.

Rohlf F.J. (1990) Morphometrics. *Annual Review of Ecology and Systematics*, **21**, 299–316.

Rohlf F.J. (2015) The tps series of software. *Hystrix, the Italian Journal of Mammalogy*, **26**, 1–4.

Russell-Smith A. & Murphy J.A. (2005) *Zelotibia*, a new zelotine spider genus from Central Africa (Araneae, Gnaphosidae). *Journal of Afrotropical Zoology*, **2**, 103–122.

Schiapelli R.D. & Pikelin B.S.G. de (1957) Arañas argentinas III Arañas de Misiones. *Revista del Museo Argentino de Ciencias Naturales "Bernardino Rivadadvia"*, **3**, 187–217.

Senglet A. (2012) *Civizelotes* new genus, and other new or little known Zelotinae (Araneae, Gnaphosidae). *Revue Suisse de Zoologie*, **119**, 501–528.

Senglet A. (2004) Copulatory mechanisms in *Zelotes*, *Drasillus* and *Trachyzelotes* (Araneae, Gnaphosidae) with additional faunistic and taxonomy data on species from Southwest Europe. *Bulletin de la Société entomologique Suisse*, **77**, 87–119.

Sereno P.C. (2007) Logical basis for morphological characters in phylogenetics. *Cladistics*, **23**, 565–587.

Sierwald P. (1989) Morphology and ontogeny of female copulatory organs in American Pisauridae, with special reference to homologous features (Arachnida, Araneae). *Smithsonian Contributions to Zoology*, 484, 1–24.

Silva Davila D. (2003) Higher-Level Relationships of the Spider Family Ctenidae (Araneae: Ctenoidea). *Bulletin of the American Museum of Natural History*, **274**, 1–86.

Simon E. (1884) Note synonomique sur les genres *Prodidomus* Hentz et Miltia E. S. *Annales de la Société Entomologique de Belgique*, **28**, 302.

Simon E. (1893) *Histoire naturelle des araignées.* Paris 1, 257–488.

Slice D.E. (2007) Geometric Morphometrics. *Annual Review of Anthropology*, **36**, 261–281.

Snazell R. (1997) *Zelominor* (Araneae, Gnaphosidae), a new genus of zelotine spider from the Western Mediterranean region. *Genus*, **10**, 260–264.

Sundevall J.C. (1833) Conspectus Arachnidum. *Londini Gothorum*, **1833**, 1–39.

Tuneva T.K. (2004) A contribution on the gnaphosid spider fauna (Araneae: Gnaphosidae) of east Kazakhstan. 319–332.

World Spider Catalog (2016) *World Spider Catalog*. Natural History Museum Bern, online at http://wsc.nmbe.ch, version 17.0, accessed on 27.V.2016.

Zakharov B.P. & Ovtcharenko V.I. (2011) Morphological organization of the male palpal organ in Australian ground spiders of the genera *Anzacia*, *Intruda*,

Zelanda, and *Encoptarthria* (Araneae: Gnaphosidae). *Journal of Arachnology*, **39**, 327–336.

Zakharov B.P. & Ovtcharenko V.I. (2013) Male palp organ morphology of three species of ground spiders (Araneae, Gnaphosidae). *Arachnologische Mitteilungen*, **45**, 15–20.

Zambonato B.P. & Lise A.A. (2004) New data on *Camillina major* with the description of the male and the proposition of a new name (*Camillina ventana*) for a male described by Platnick & Murphy , 1987 from Argentina (Araneae , Gnaphosidae). *Biociências*, **12**, 43–50.

Zelditch M.L., Swiderski D.L., Sheets H.D. & Fink W.L. (2004) *Geometric morphometrics for biologists: a primer*. Elsevier Academic Press, London.

Tables

Table 1: Mean similarity between trees generated with each k value and the remaining trees obtained with implied weighting, calculated through SPR distances. The tree with the highest mean similarity with the remaining trees is in bold.

Weighting Regime	Mean Similarity
k=3	0.5530
k=5	0.6695
k=7	0.7178
k=7'	0.7112
k=9	0.7671
k=11	0.7689
k=15	**0.7784**
k=17	0.6828
k=19	0.6818
k=21	0.7169
k=23	0.6913

Figures

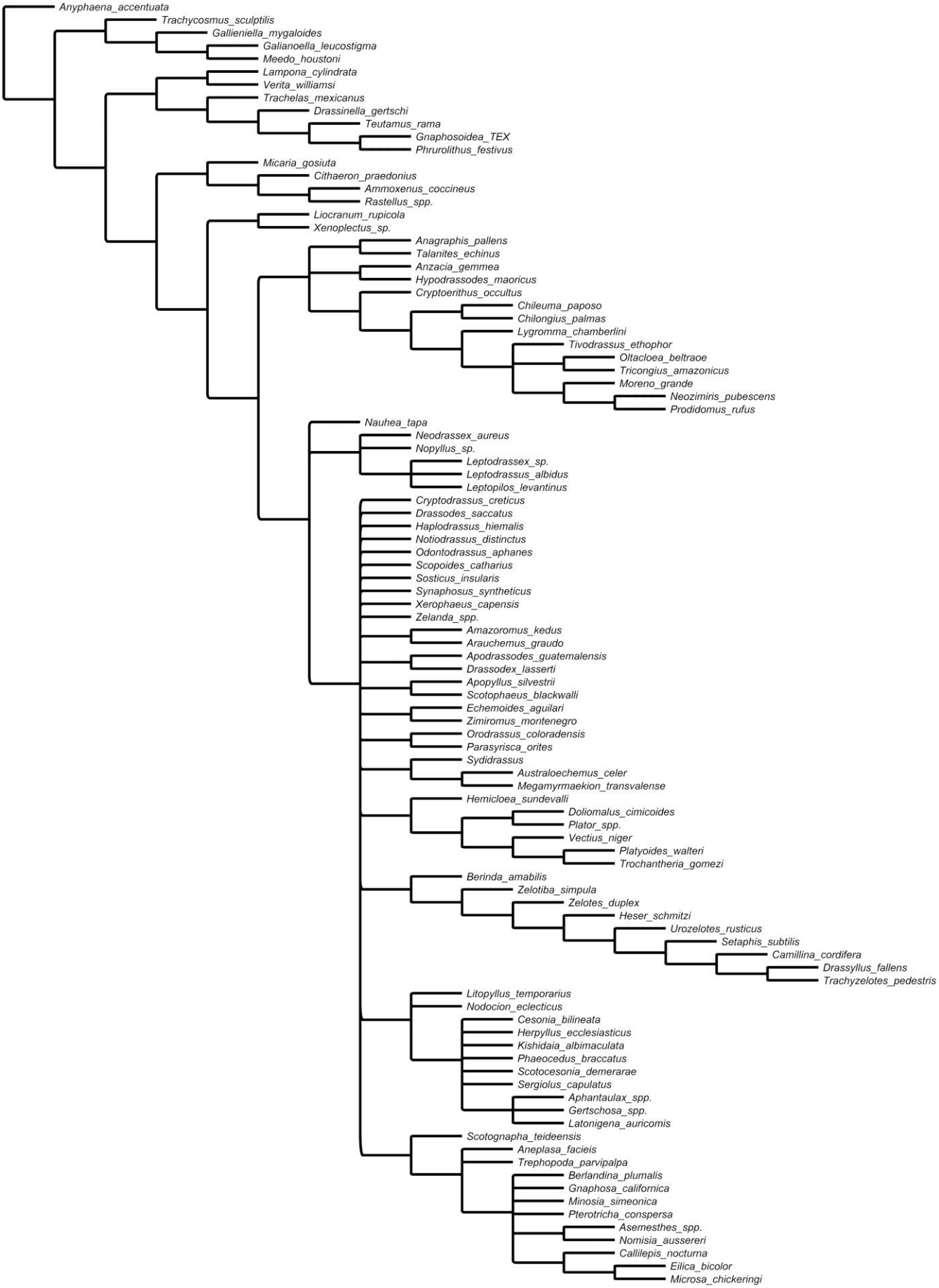

Fig. 1: Strict consensus of the 2098 most parsimonious trees obtained under equal character weights analysis.

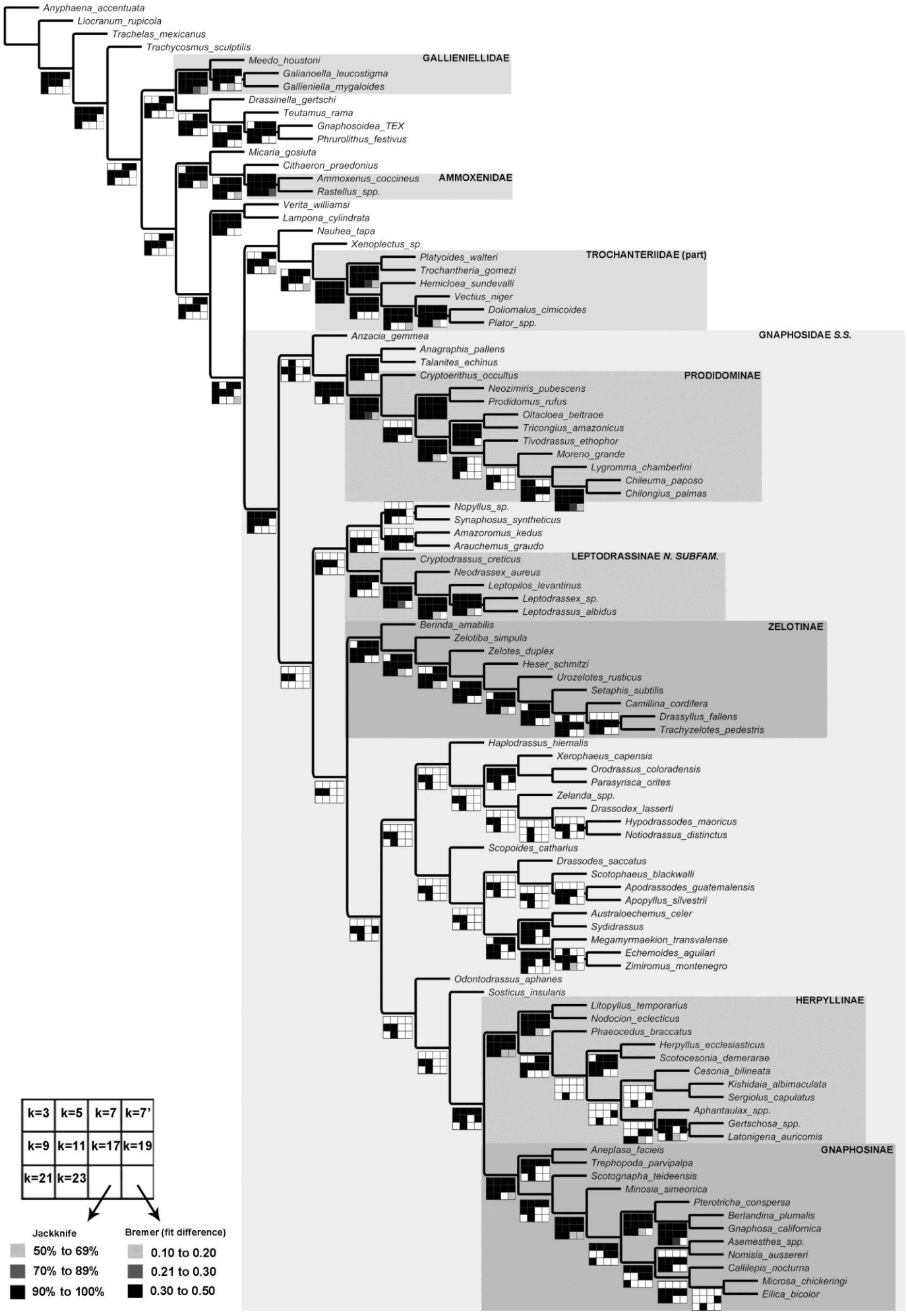

Fig. 2: Working phylogenetic hypothesis of gnaphosid spiders, with clade support and sensitivity to weighting regimes. The well supported clades discussed in text are highlighted.

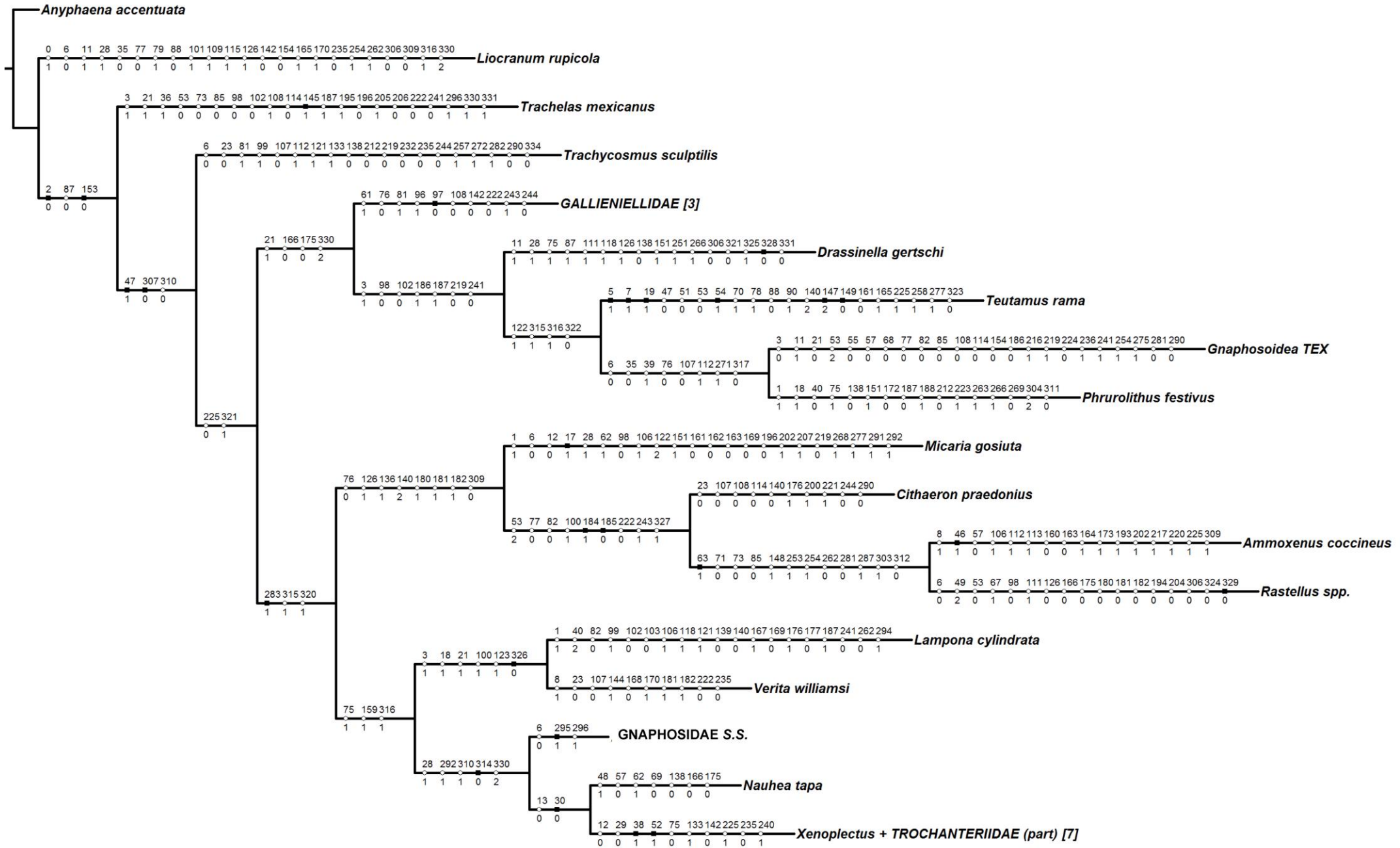

Fig. 3: Character optimization outgroup taxa on the working hypothesis, according to accelerated transformation series (ACTRAN) criteria. Some nodes are collapsed and are represented in other figures. Numbers in brackets show terminals in collapsed clades.

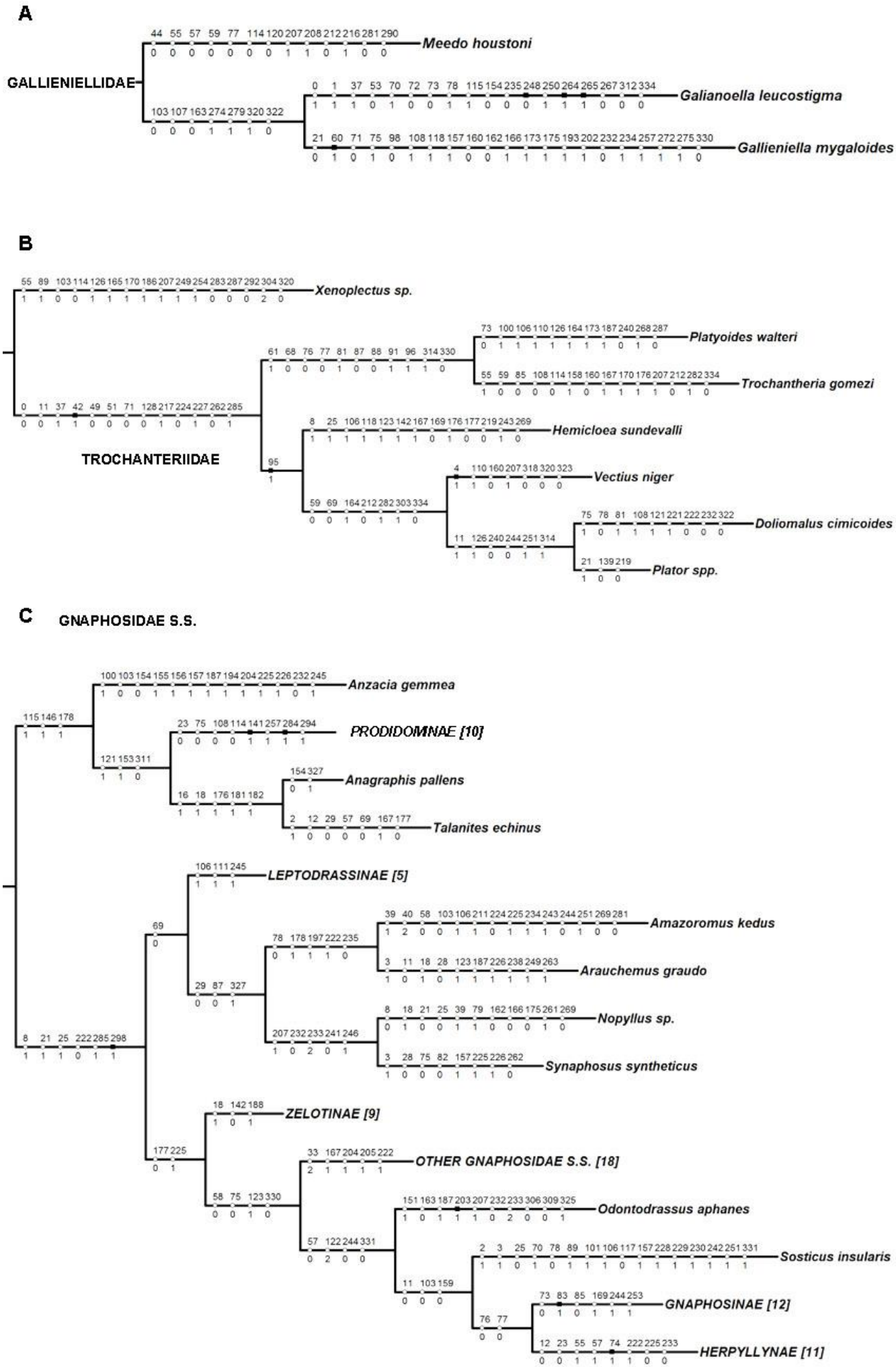

Fig. 4: Character optimization on the Gallienielidae (A), *Xenoplectus*+Trochanteriidae (B) and Gnaphosidae S.S. (C) clades, according to accelerated transformation series (ACTRAN) criteria.

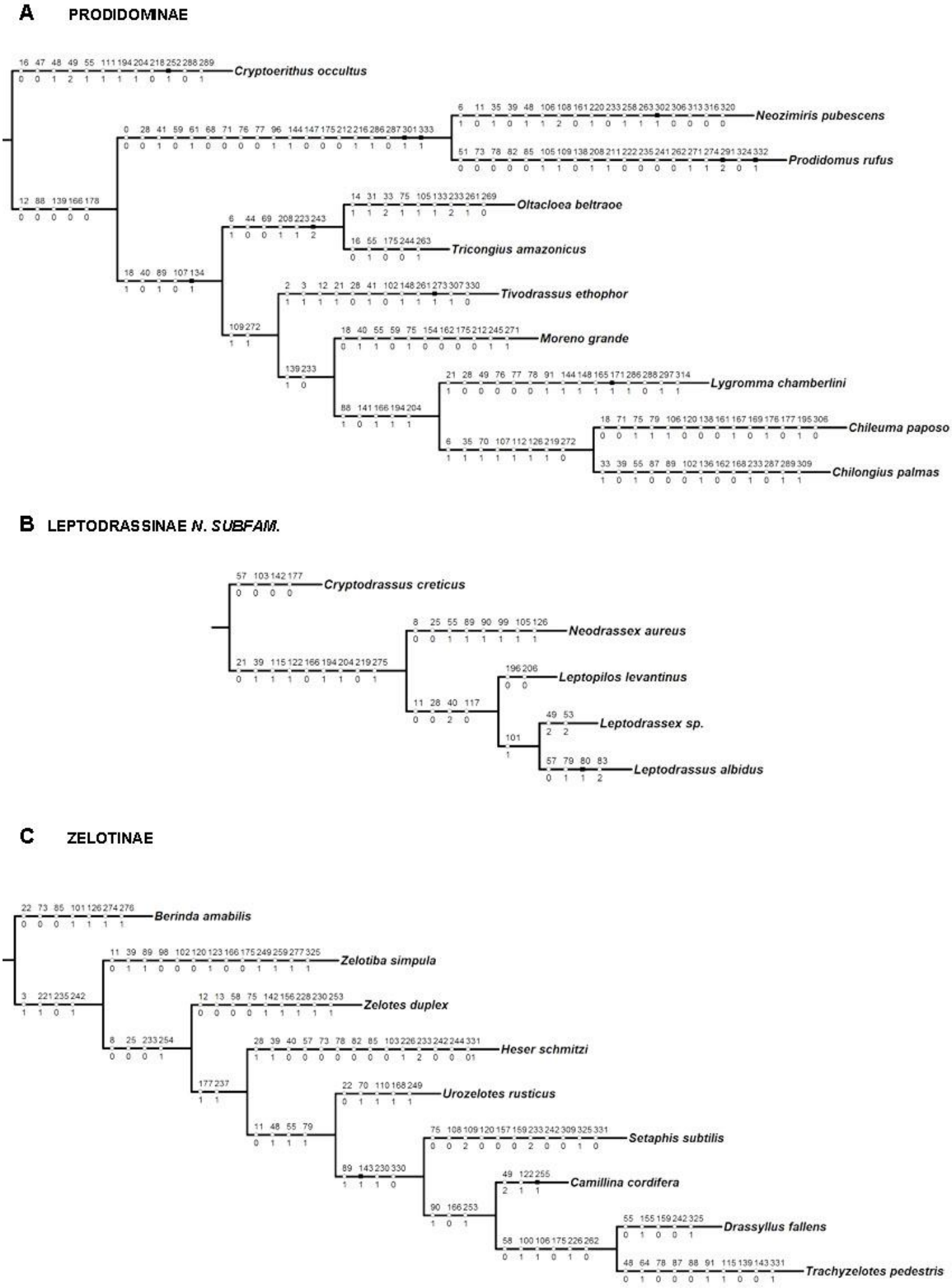

Fig. 5: Character optimization on the Prodidominae (A), Leptodrassinae (B) and Zelotinae (C) clades, according to accelerated transformation series (ACTRAN) criteria.

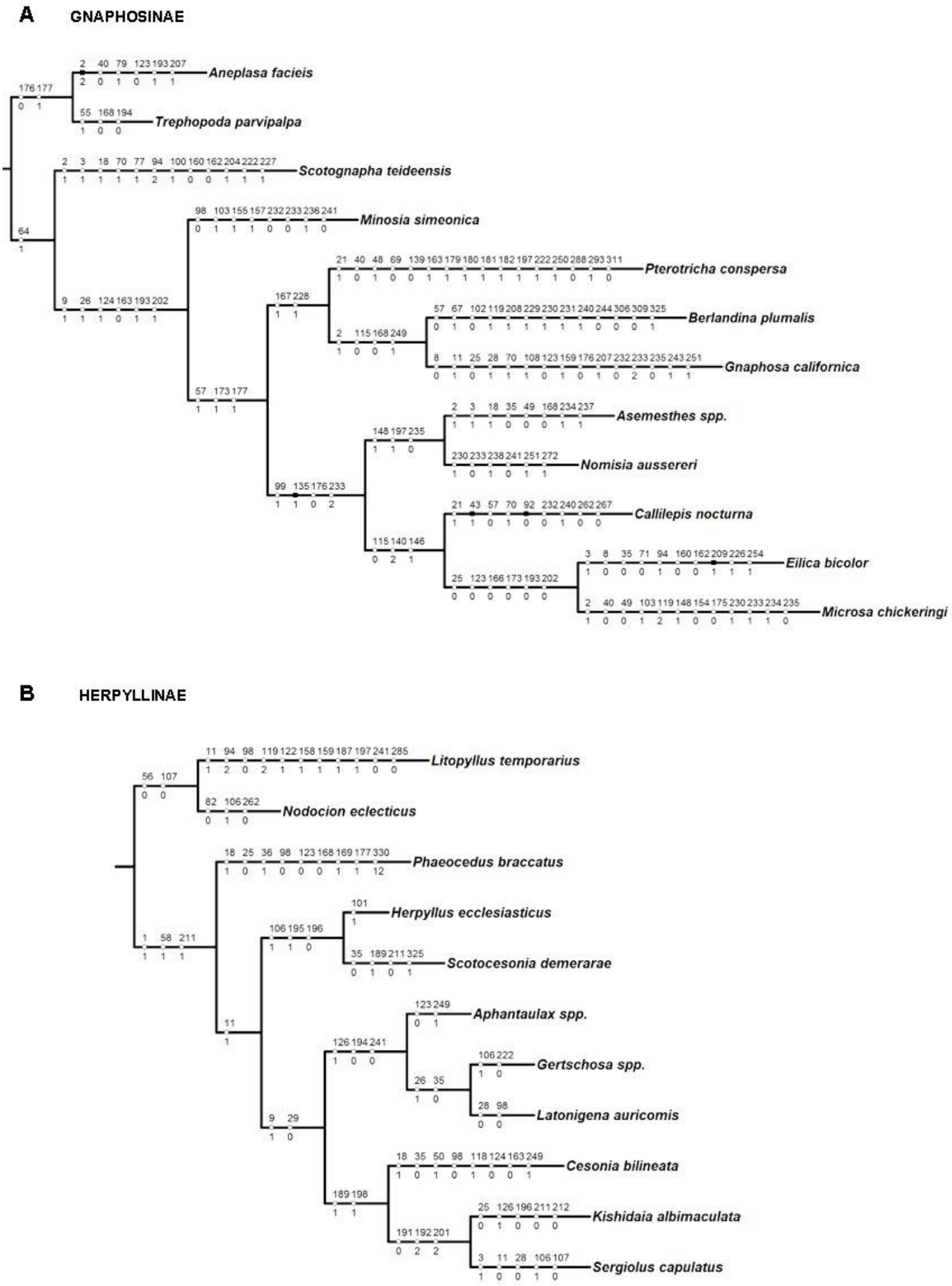

Fig. 6: Character optimization on the Gnaphosinae (A) and Herpyllinae (B) clades, according to accelerated transformation series (ACTRAN) criteria.

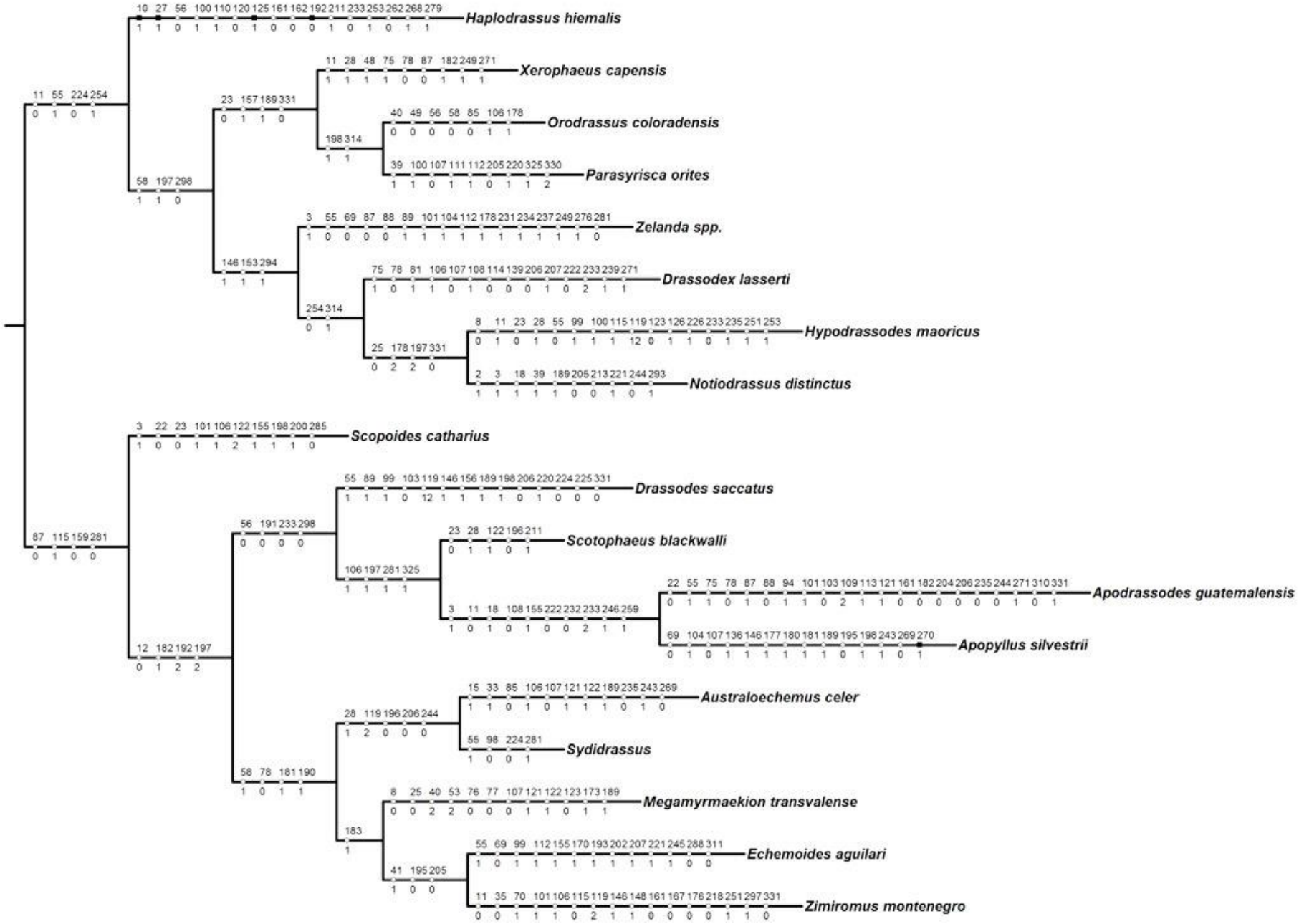

Fig. 7: Character optimization on the Other Gnaphosidae S.S. branch, according to accelerated transformation series (ACTRAN) criteria.

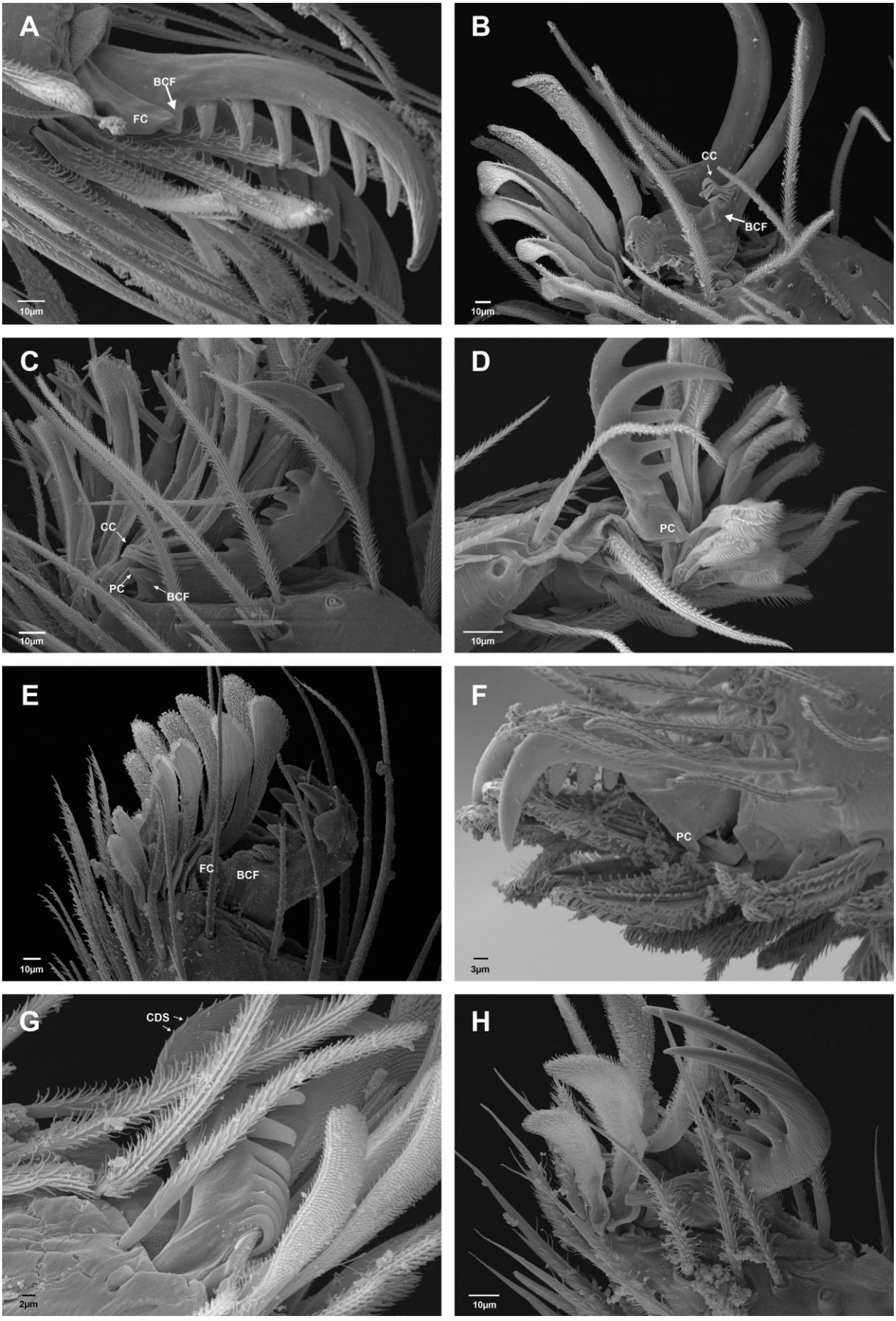

Fig. 8: Types of claw tuft claspers. A) *Callilepis gosoga*, leg IV. B) *Chileuma paposo*, leg IV. C) *Chilongius palmas*, leg IV. D) *Cryptoerytus occultus*, leg IV. E) *Eilica bicolor*, leg IV. F) *Micaria gosiuta*, leg I. G) *Moreno grande*, leg I. H) *Tivodrassus etaphor*, leg IV. BCF: Basal claw fold; CC: Classic clasper; CDS: Claw dorsal scales; FC: Folded clasper; PC: Pointed solid clasper.

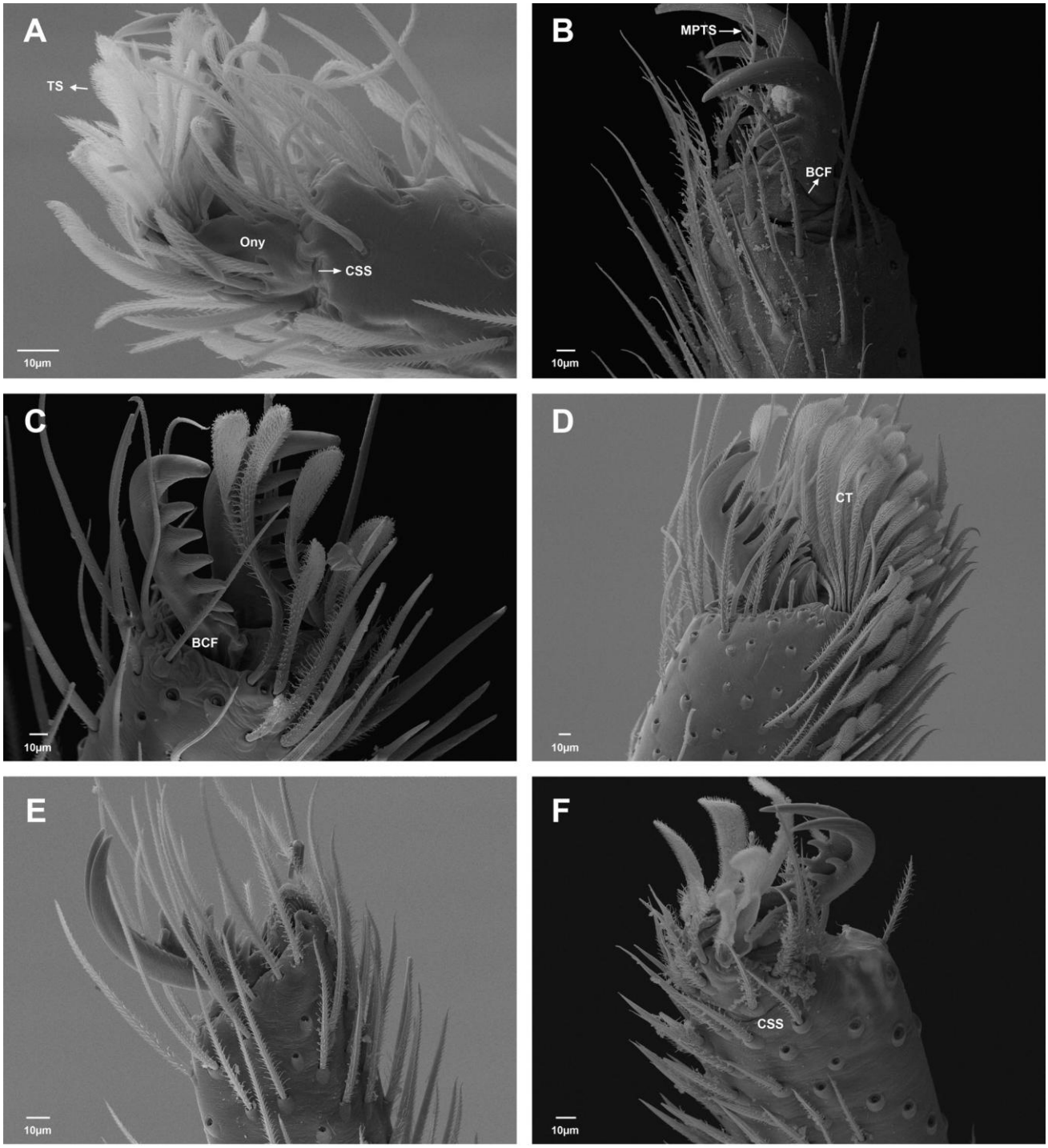

Fig. 9: Tarsi. A) *Cryptoeritus occultus*, female leg I, retrolateral. B) *Drassyllus fallens*, female leg IV, retrolateral. C) *Minosia simeonica*, female leg IV, prolateral. D) *Nodocion eclecticus*, female leg IV, prolateral. E) *Synaphosus syntheticus*, female leg IV, prolateral. F) *Tivodrassus etaphor*, male leg IV, retrolateral. BCF: Basal claw fold; CSS: Claw slit suture; CT: Claw tuft; MPTS: Modified pseudotenent setae; Ony: Onychium; TS: Tenent setae.

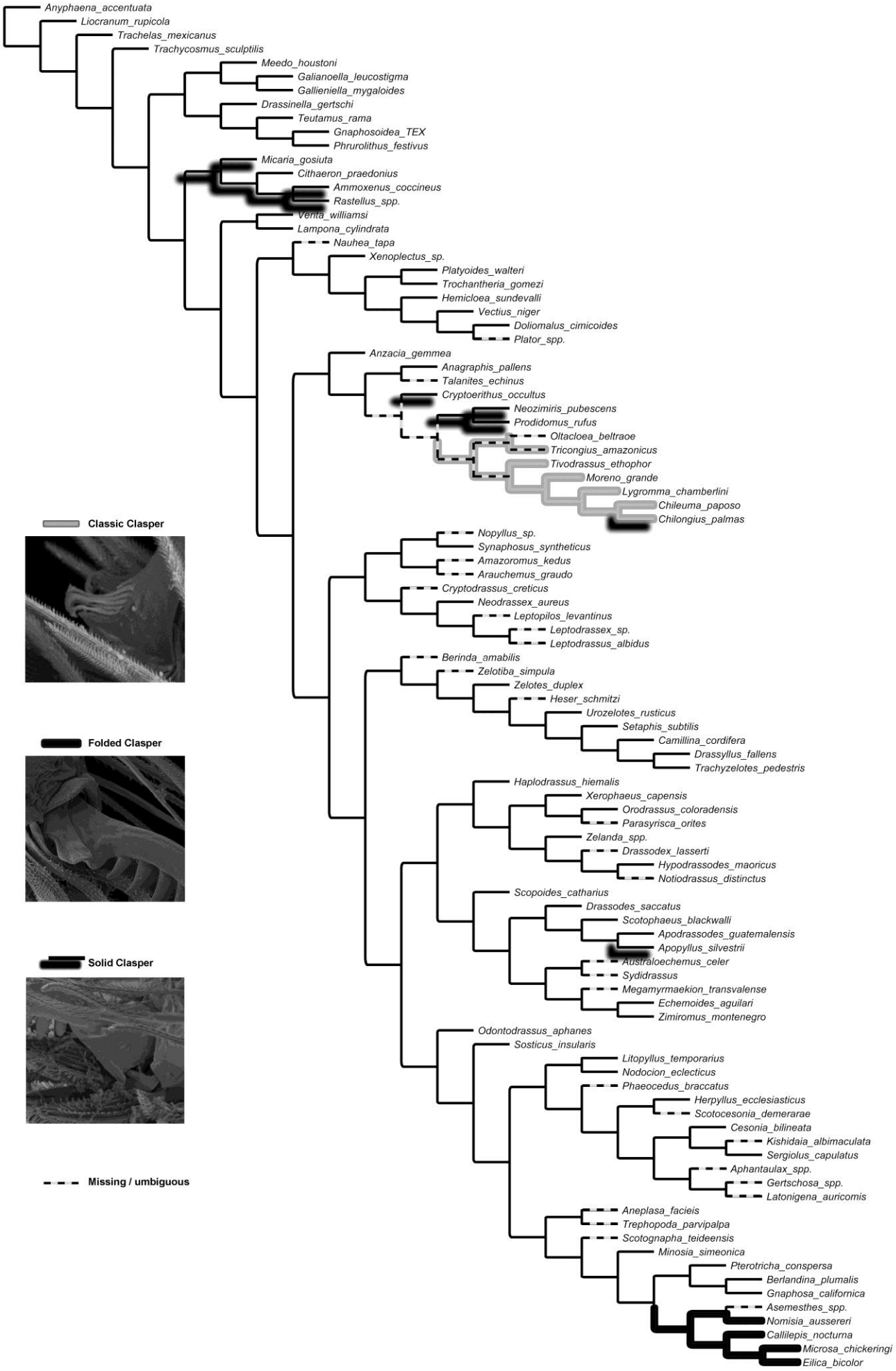

Fig. 10: The evolution of the three types of claspers, classic clasper (char.134), folded clasper (char. 135) and solid clasper (char. 136), on the preferred tree (concavity function k=15). Optimized according to accelerated transformation series (ACTRAN) criteria.

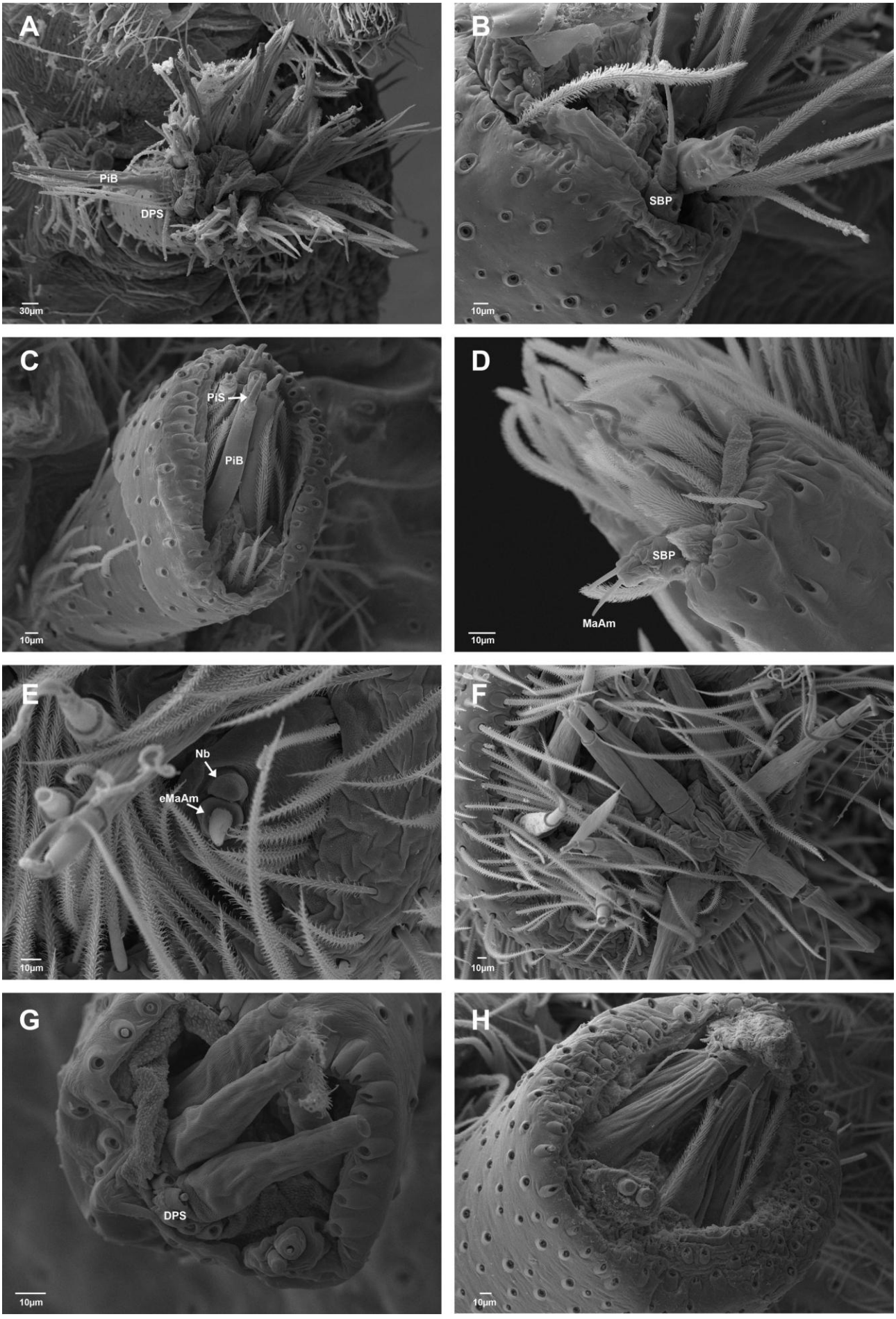

Fig. 11: Female anterior lateral spinnerets. A) *Chileuma paposo*. B) *Chileuma paposo*, detail. C) *Chilongius palmas*. D) *Moreno grande*. E-F) *Hypodrassodes maoricus*. G) *Tivodrassus etaphor*. H) *Zelanda erebus*. DPS: Distal article, patches of associated setae around spigots; eMaAm: Ectal major ampullate spigot; MaAm: Major Ampullate spigots; Nb: Spigot nubbin; Pi: Piriform spigots; PiB: Piriform spigot base; PiS: Piriform spigot shaft; SBP: Setae bearing projection.

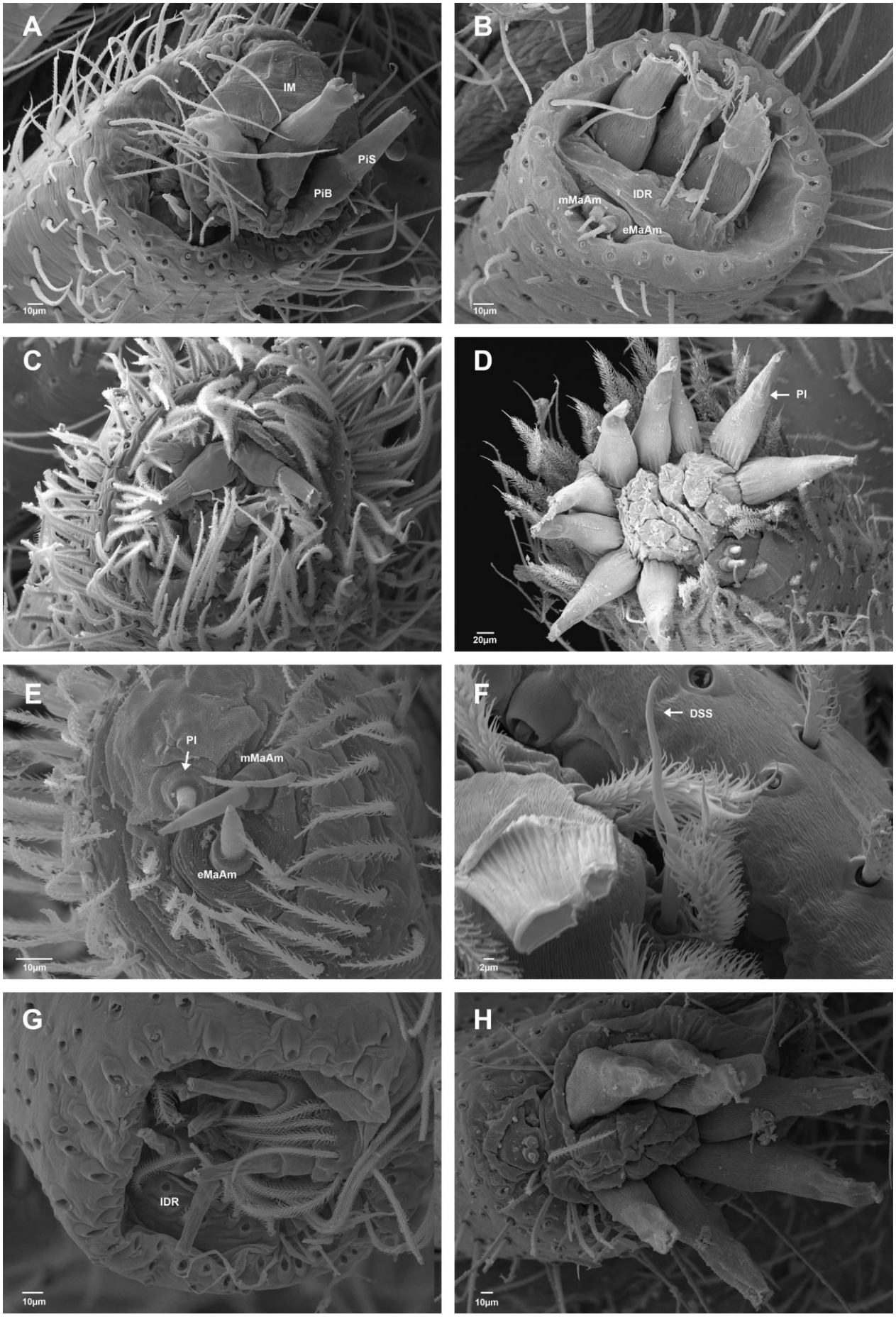

Fig. 12: Female anterior lateral spinnerets. A) *Callilepis nocturna*. B) *Camillina cordifera*. C) *Drassodes sacatus*. D) *Herpyllus ecclesiasticus*. E) *Micaria gosiuta.* F) *Nodocion eclecticus.* G) *Talanites echinus*. H) *Urozelotes ruticus*. DSS: Distal article sensory seta; eMaAm: Ectal major ampullate spigot; IDA: Incomplete distal article; IM: Inflatable membrane; mMaAm: Mesal major ampullate spigot; Pi: Piriform spigots; PiB: Piriform spigot base; PiS: Piriform spigot shaft.

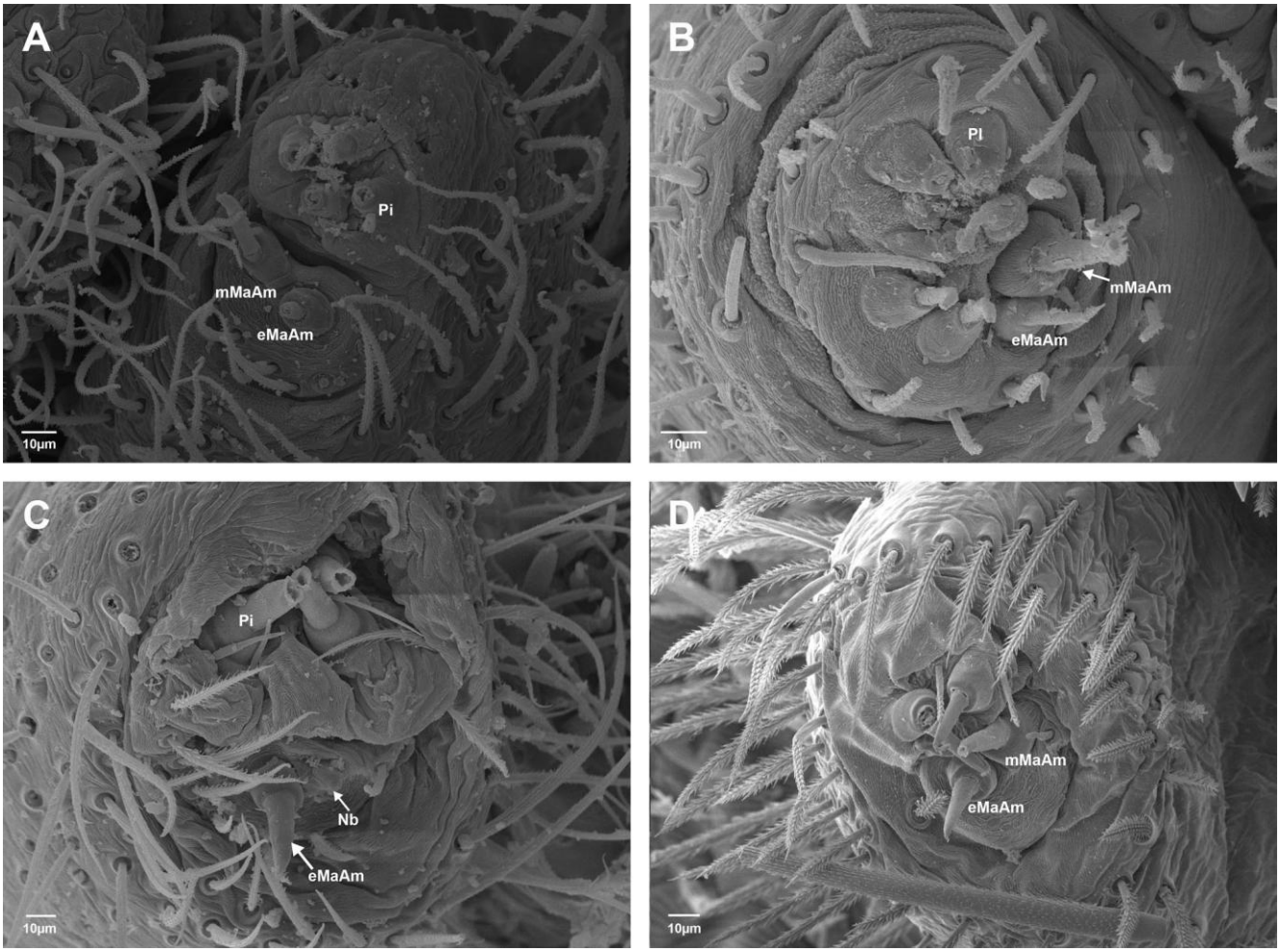

Fig. 13: Female anterior lateral spinnerets. A) *Cithaeron praedonius*. B) *Gallieniella mygaloides*. C) *Hemicloea sundevalli*. D) *Trochanteria gomezi*. eMaAm: Ectal major ampullate spigot; mMaAm: Mesal major ampullate spigot; Nb: Spigot nubbin; Pi: Piriform spigots.

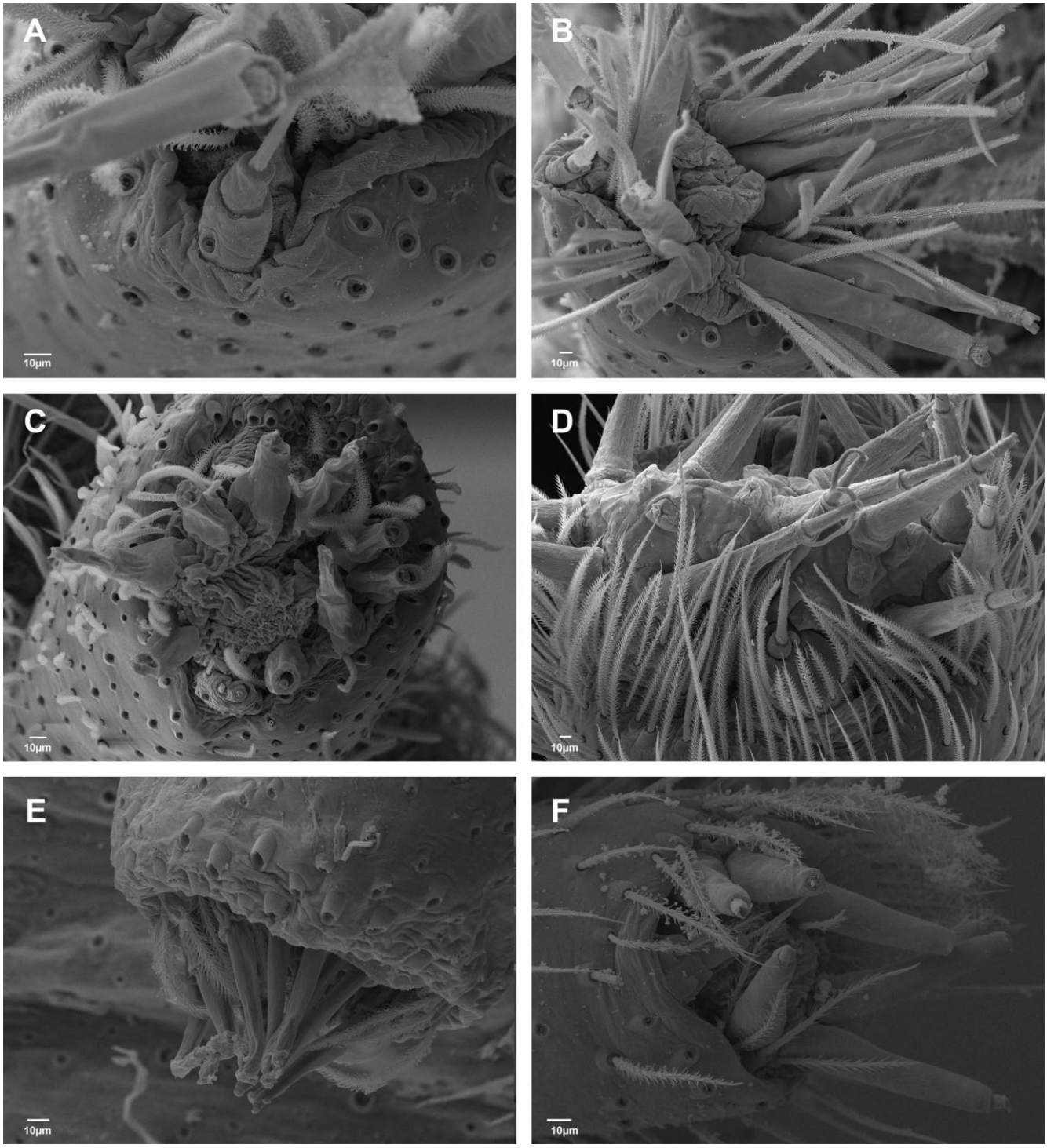

Fig. 14: Male anterior lateral spinnerets. A) *Anagraphis pallens*. B) *Chileuma paposo*. C) *Chileuma paposo*. D) *Hypodrassodes maoricus*. E) *Talanites echinus* F) *Tivodrassus etaphor*.

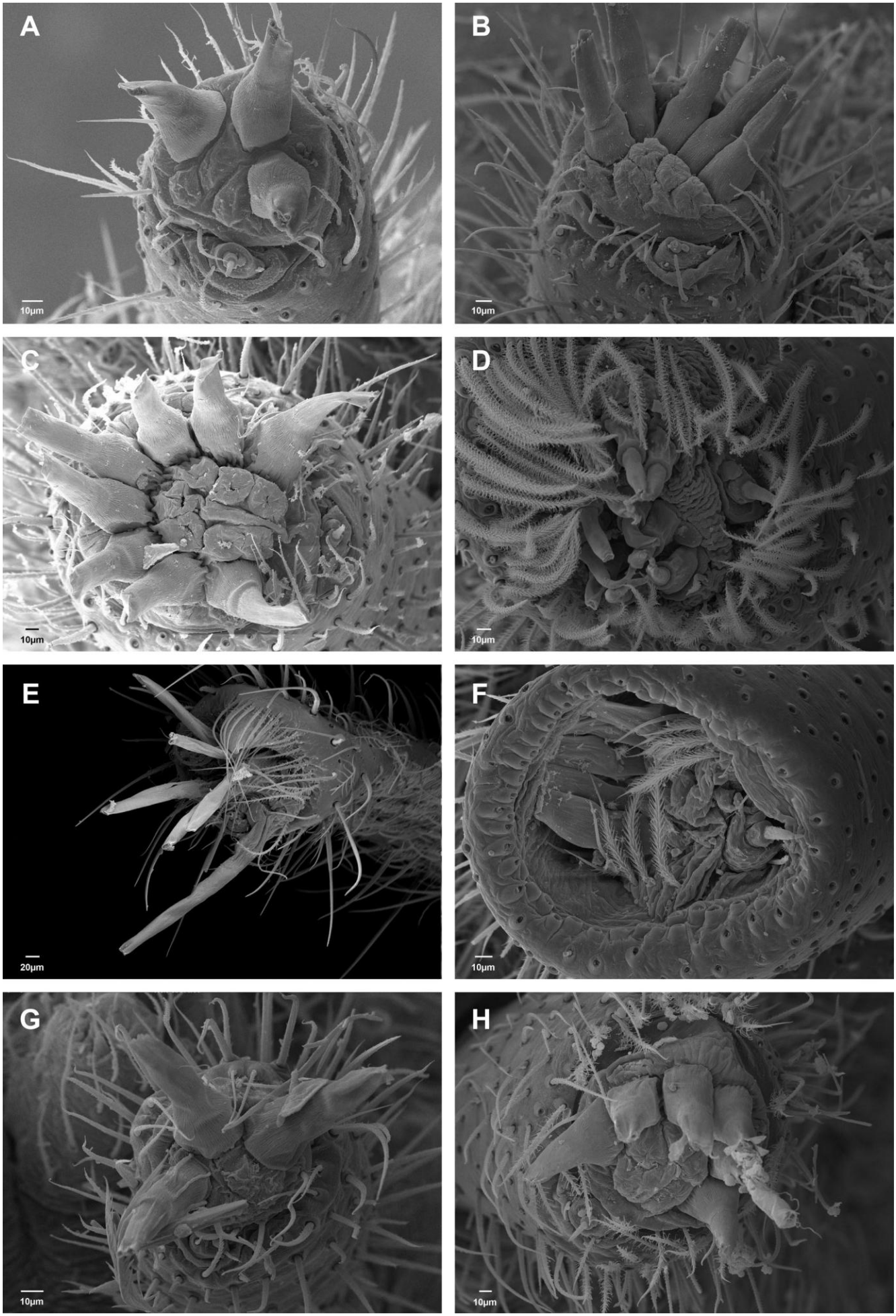

Fig. 15: Male anterior lateral spinnerets. A) *Camillina cordifera*. B) *Drassyllus fallens*. C) *Gnaphosa californica*. D) *Orodrassus coloradensis*. E) *Pterotricha conspersa*. F) *Sergiolus capulatus*. G) *Setaphis subtilis*. H) *Zelotes duplex*.

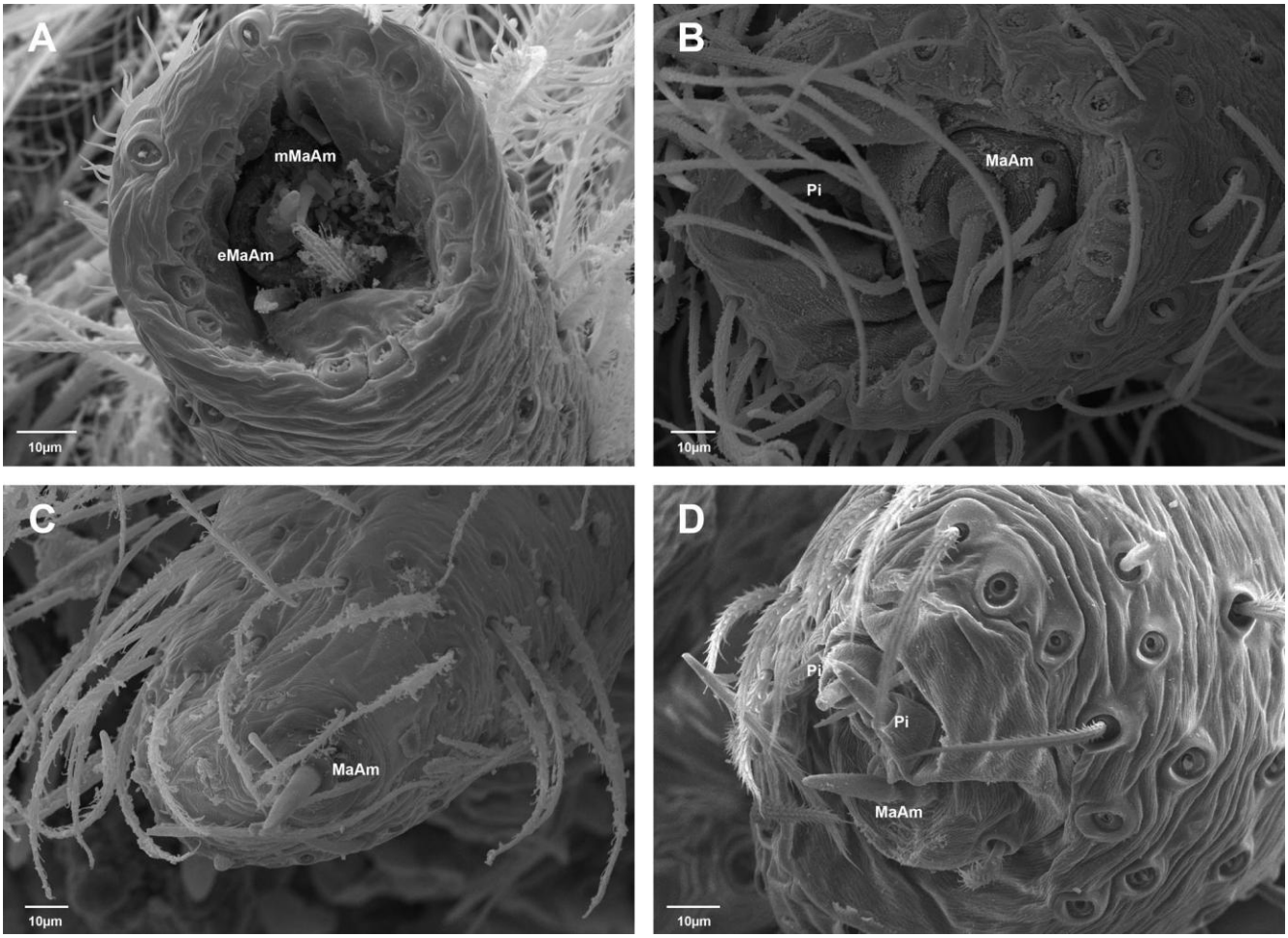

Fig. 16: Male anterior lateral spinnerets. A) *Ammoxenus cocineus*. B) *Cithaeron praedonius*. C) *Micaria gosiuta*. D) *Trochanteria gomezi*. eMaAm: Ectal major ampullate spigot; MaAm: Major Ampullate spigots; mMaAm: Mesal major ampullate spigot; Pi: Piriform spigots.

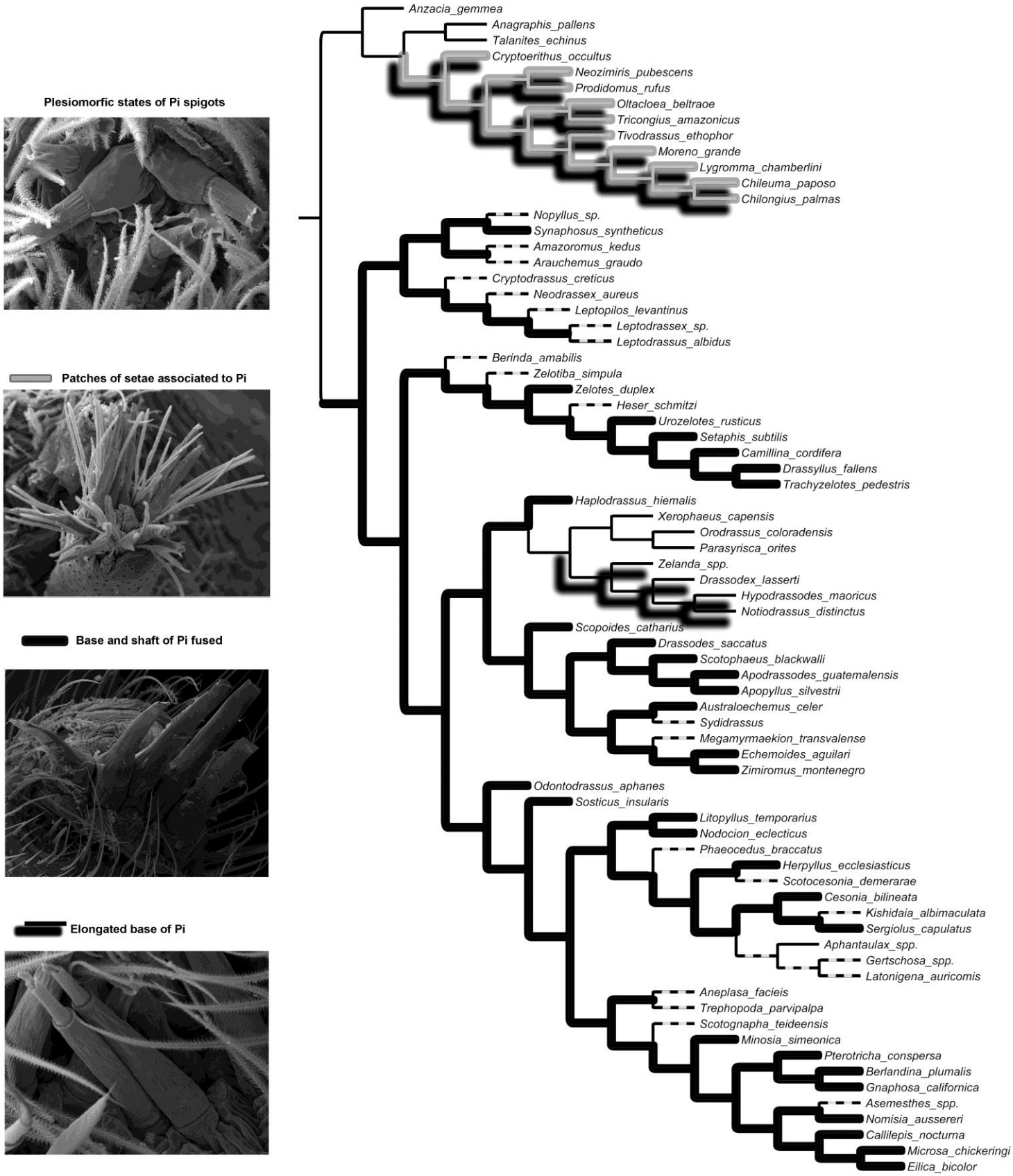

Fig. 17: The evolution of incomplete ring type (char. 284), of piriform spigot base length relative to shaft (char. 294) and of the fusion of base and shaft of piriform spigots (char. 298) on the Enlarged Piriform Spigots Clade. The plesiomorphic states for this character in this clade are: the incomplete ring as a semi-circle on the anterior margin of ALS (char. 284, sate 0), base of Pi shorter or about the same as shaft (char. 294, state 0) and base of Pi not fused to base (char. 298, state 0). Optimized according to accelerated transformation series (ACTRAN) criteria.

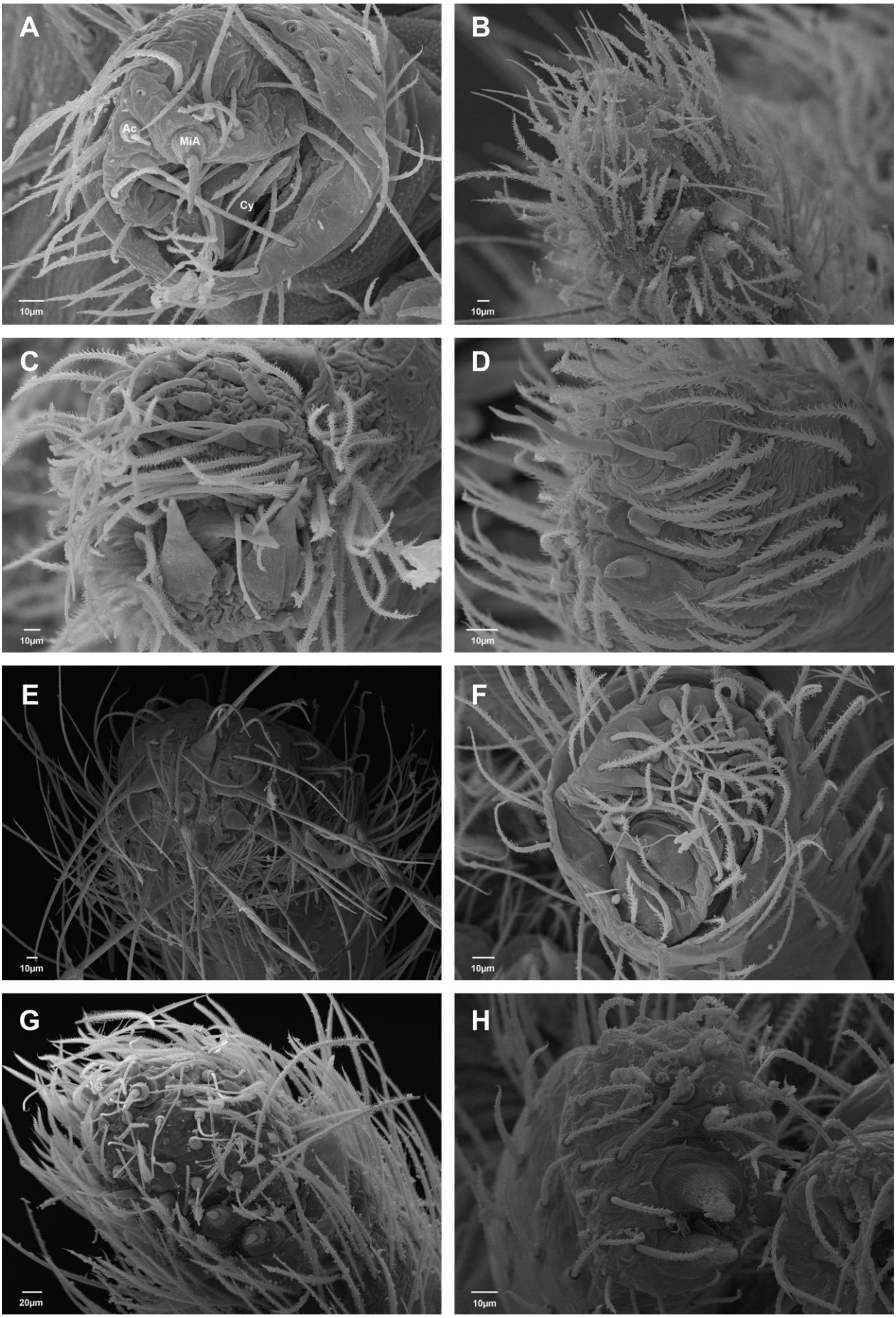

Fig. 18: Female posterior lateral spinnerets. A) *Camillina cordifera*. B) *Cesonia bilineata*. C) *Echemoides aguilari*. D) *Micaria gosiuta*. E) *Minosia simeonica.* F) *Odontodrassus aphanes*. G) *Scotophaeus blackwalli*. H) *Setaphis subtilis*. Ac: Aciniform gland spigots; Cyb: Cylindrical gland spigots; MiAm: Minor ampullate gland spigots.

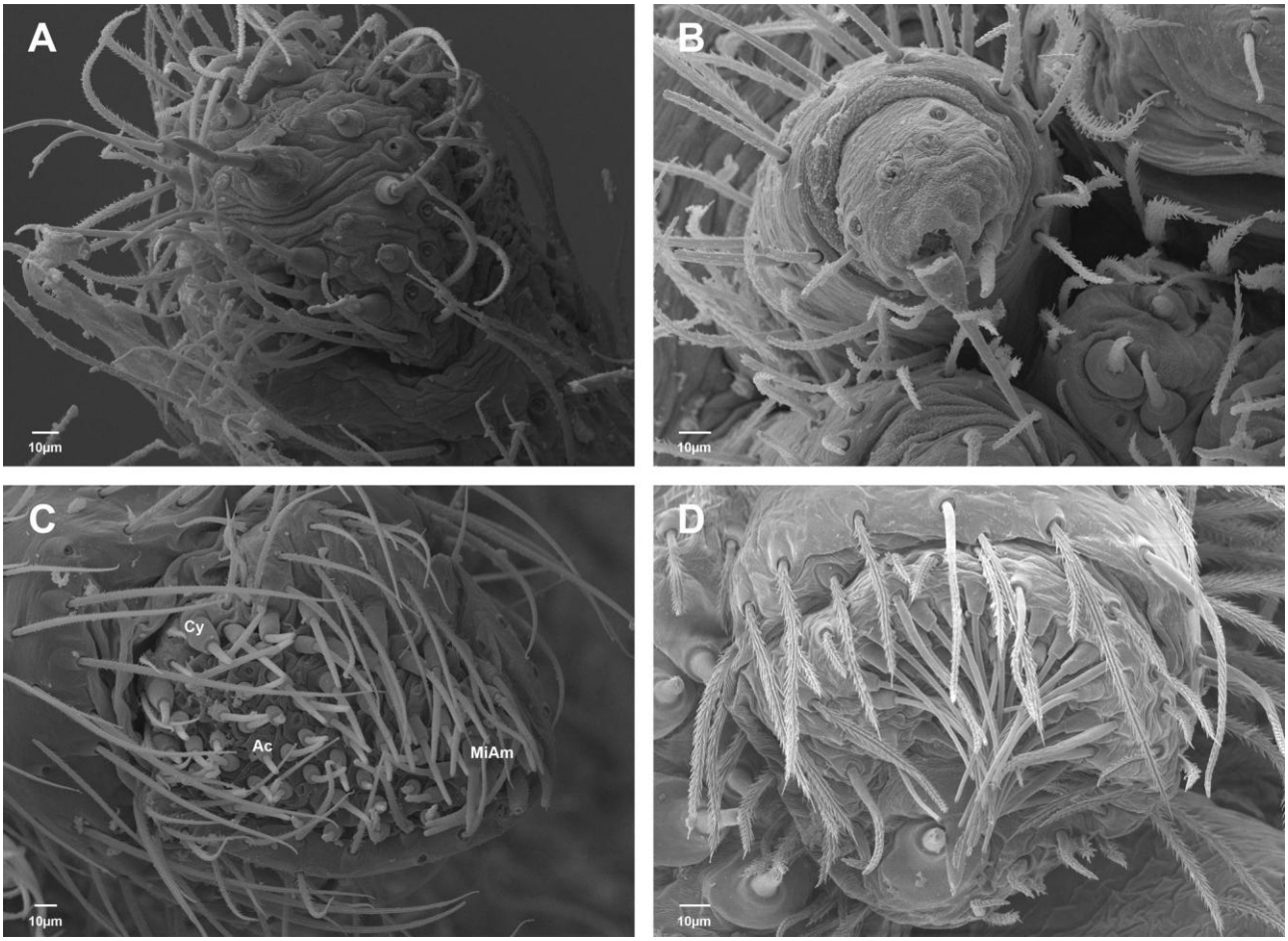

Fig. 19: Female posterior lateral spinnerets. A) *Cithaeron praedonius*. B) *Gallieniella mygaloides*. C) *Hemicloea sundevalli*. D) *Trochanteria ranucula*. Ac: Aciniform gland spigots; Cyb: Cylindrical gland spigots; MiAm: Minor ampullate gland spigots.

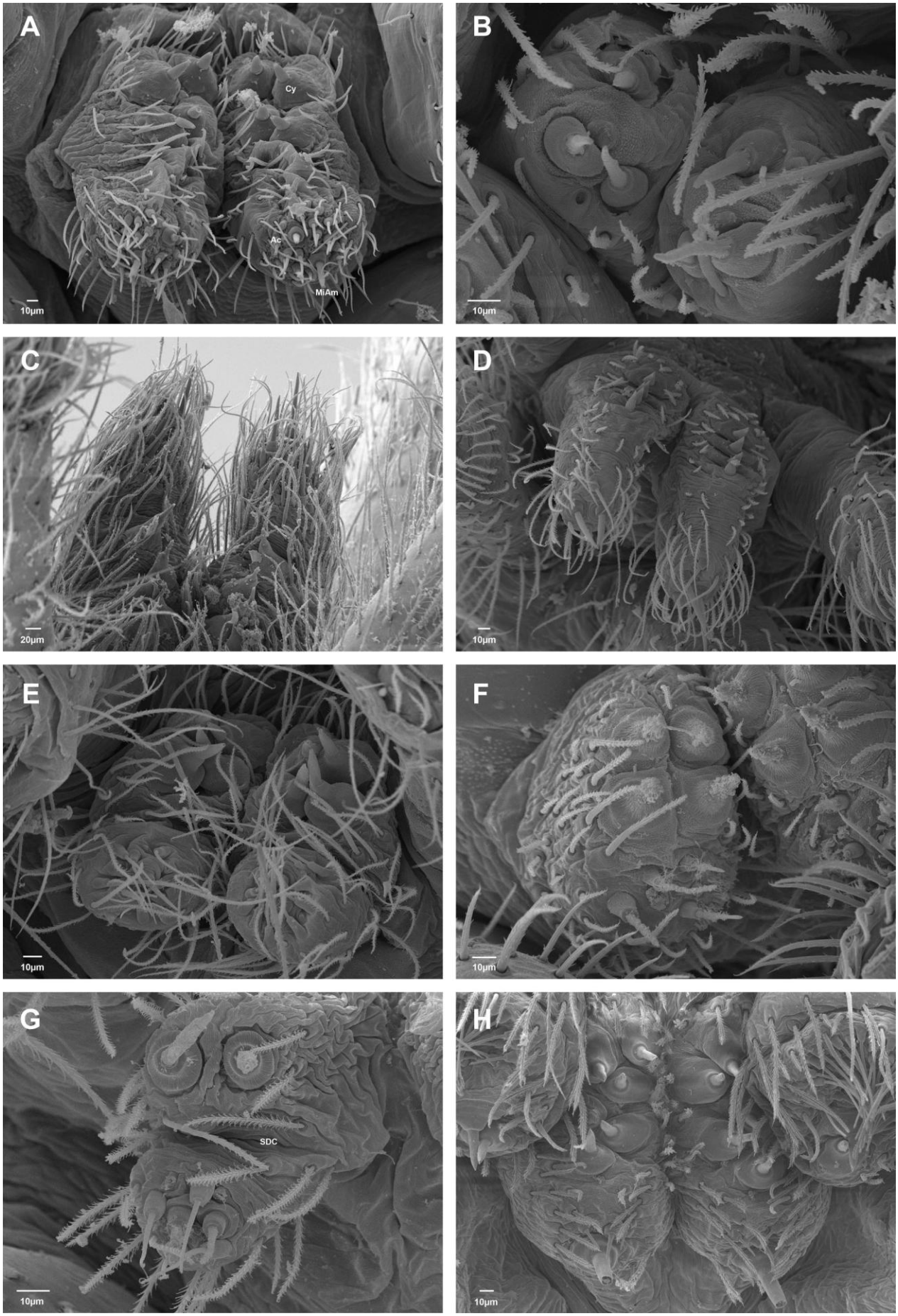

Fig. 20: Female posterior median spinnerets. A) *Eilica bicolor*. B) *Gallieniella mygaloides.* C) *Herpyllus ecclesiasticus*. D) *Micaria gosiuta*. E) *Odontodrassus aphanes.* F) *Setaphis subtilis*. G) *Synaphosus syntheticus*. H) *Trochanteria gomezi*. Ac: Aciniform gland spigots; Cyb: Cylindrical gland spigots; MiAm: Minor ampullate gland spigots; SDC: Spinning field deep constriction.

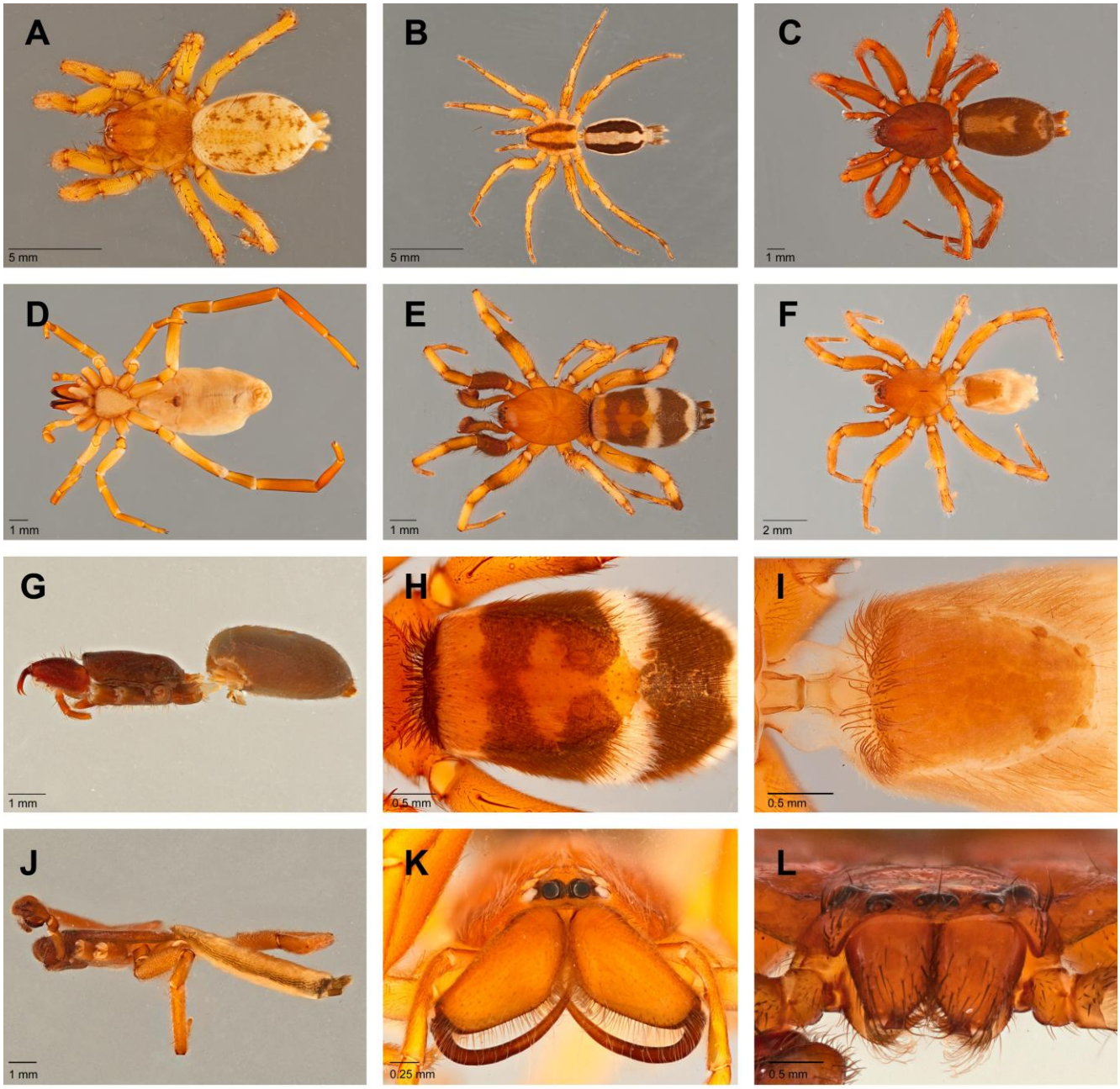

Fig. 21: A) *Berlandina plumalis*, habitus dorsal. B) *Cesonia bilineata*, habitus dorsal. C) *Herpyllus ecclesiasticus*, habitus dorsal. D) *Meedo houstoni*, habitus ventral. E) *Sergiolus capulatus*, habitus dorsal. F) *Litopyllus temporarius*, habitus dorsal. G) *Gallieniella mygaloides* habitus lateral. H) *S. capulatus*, opisthosoma, dorsal. I) *L. temporarius*, opisthosoma dorsal. J) *Hemicloea sundevalli*, habitus lateral. K) *Prodidomus rufus*, frontal. L) *Vectius nigeri*, frontal.

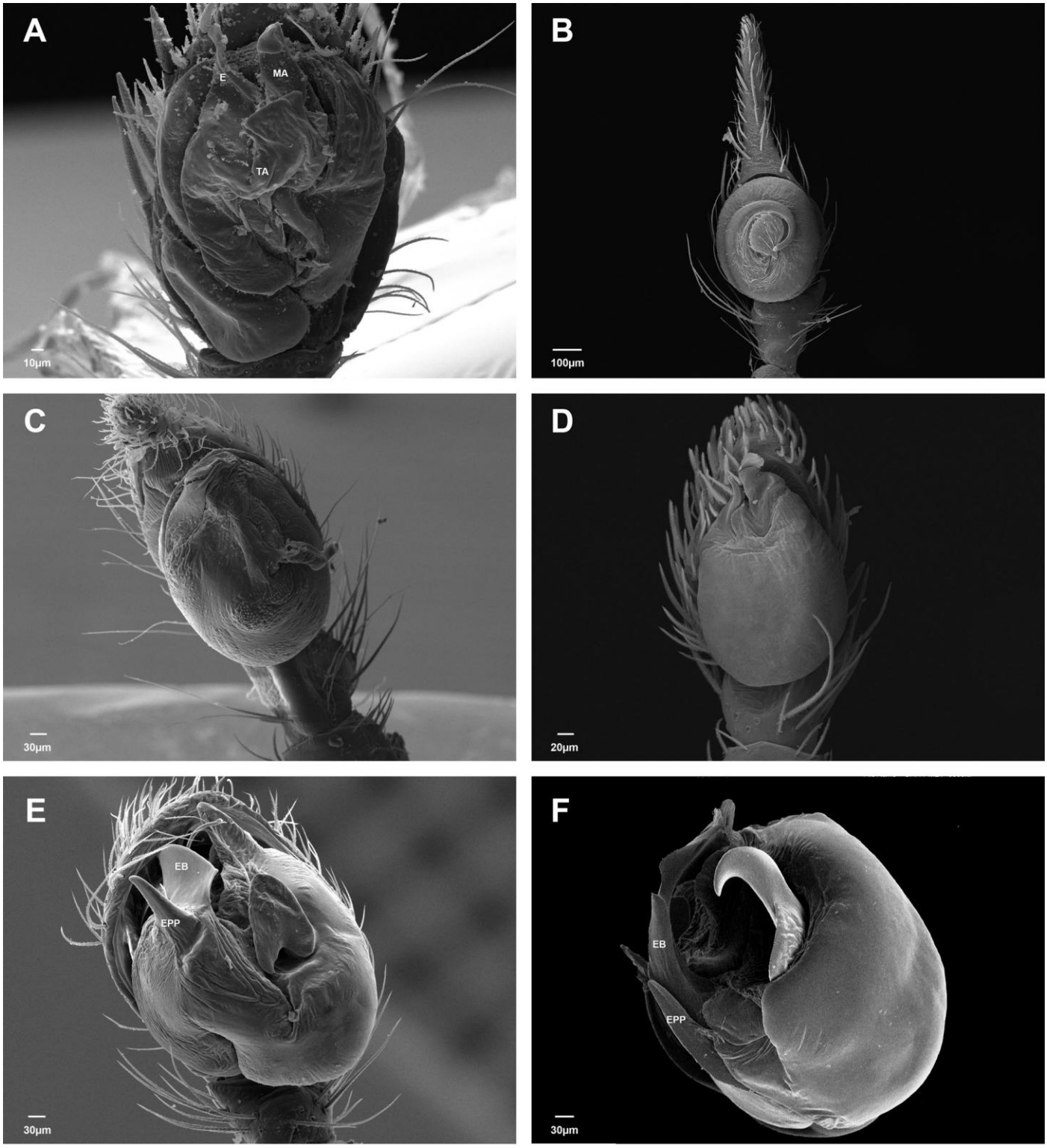

Fig. 22: Right male palps. A) *Ammoxenus coccineus*. B) *Cithaeron praedonius*. C) *Micaria gosiuta*. D) *Moreno grande*. E) *Trochanteria gomezi.* F) *Vectius niger*. E: Embolus; EB: Embolar base; EPP: Embolar base proximal projection; MA: Median apophysis; TA: Terminal apophysis.

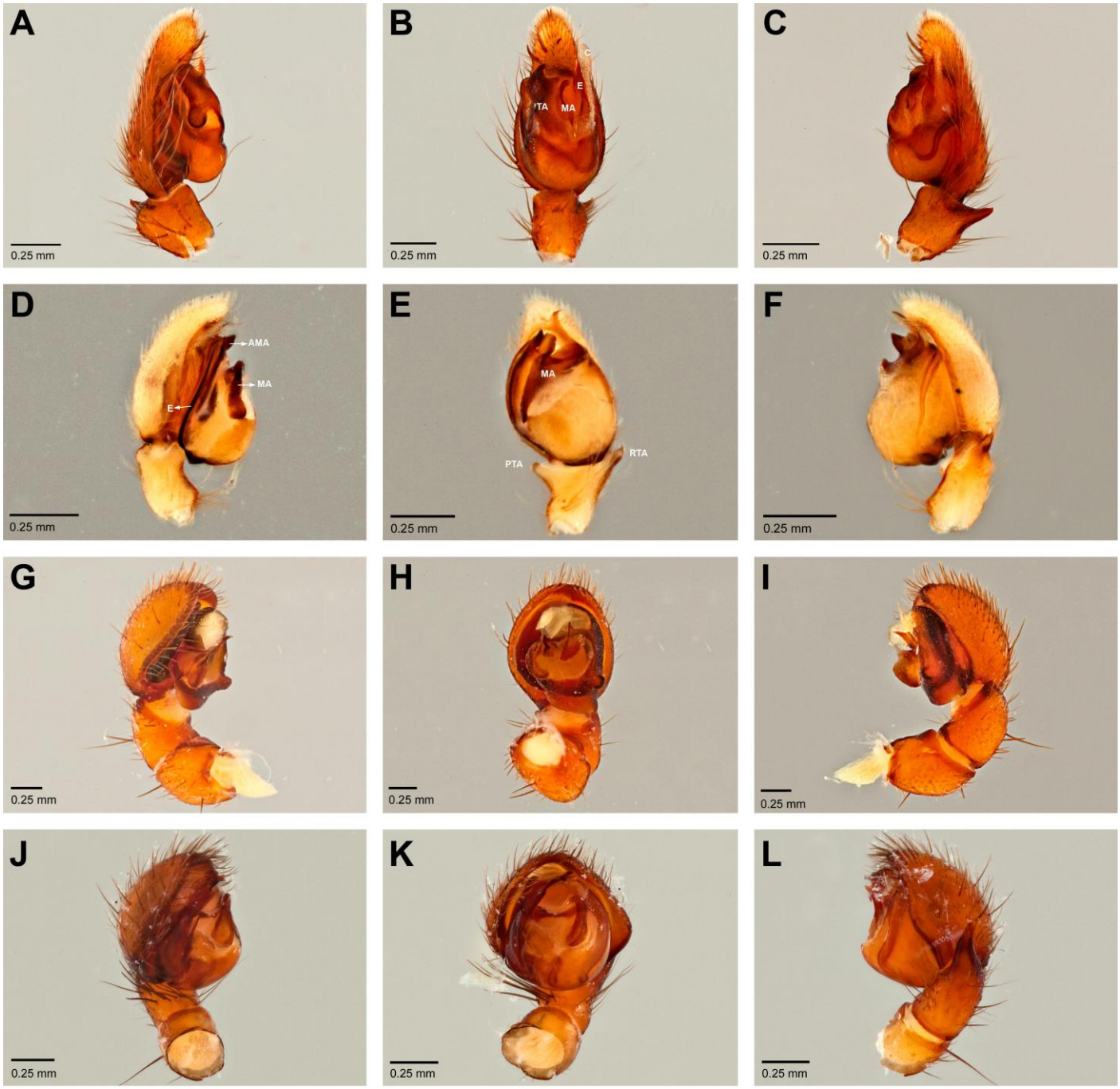

Fig. 23: Right male palps, prolateral (A, D, G, J), ventral (B, E, H, J) and retrolateral (C, F, I, L). A–C) *Anzacia gemmea*. D–F) *Neodrassex aureus*. G–I) *Plator sp*. J–L) *Vectius niger*. AMA: Acessory median apophysis; C: Conductor; E: Embolus; MA: Median apophysis; PTA: Prolateral tibial apophysis; RTA: Retrolateral tibial apophysis; TA: Terminal apophysis.

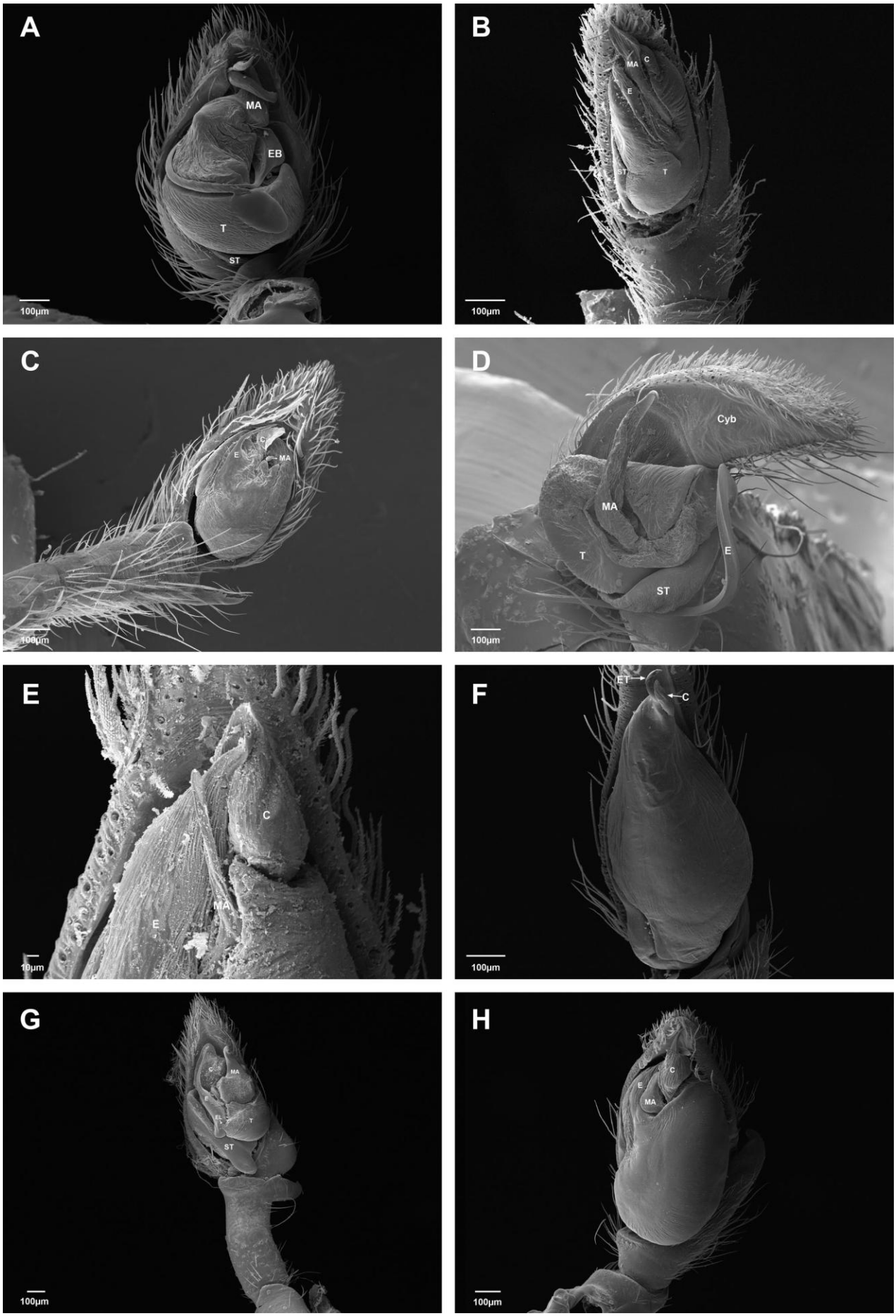

Fig. 24: Right male palps. A) *Callilepis gosoga*. B) *Cesonia bilineata*. C) *Drassodes saccatus*. D) *Gnaphosa californica*. E) *Herpyllus ecclesiasticus.* F) *Litopyllus temporarius*. G) *Pterotricha conspersa*. H) *Sergiolus capulatus*. C: Conductor; Cyb: Cymbium; E: Embolus; EB: Embolus base; EL: Embolar locking lobe; ET: Embolus tip.; MA: Median apophysis; ST: Subtegulum; T: Tegulum.

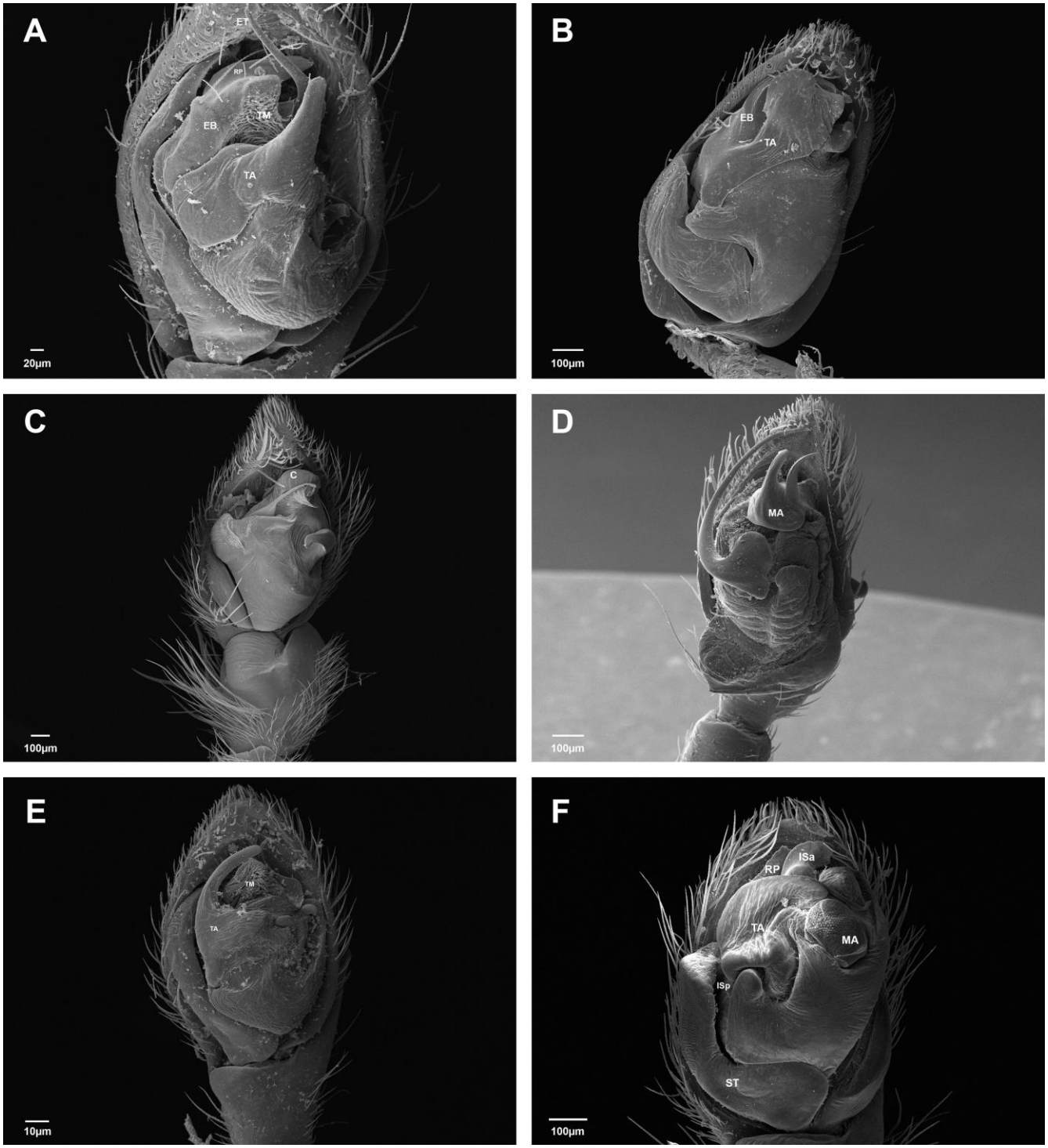

Fig. 25: Right male palps. A) *Drassyllus fallens*. B) *Haplodrassus hiemalis*. C) *Hypodrassodes maoricus*. D) *Sosticus insularis*. E) *Trachyzelotes pedestris.* F) *Zelotes duplex*. C: Conductor; EB: Embolus base; ET: Embolus tip.; Isa: Intercalary sclerite, apical part; ISp: Intercalary sclerite, proximal part; MA: Median apophysis; RP: Radix dorsal projection; ST: Subtegulum; TA: Terminal apophysis; TM: Terminal membrane.

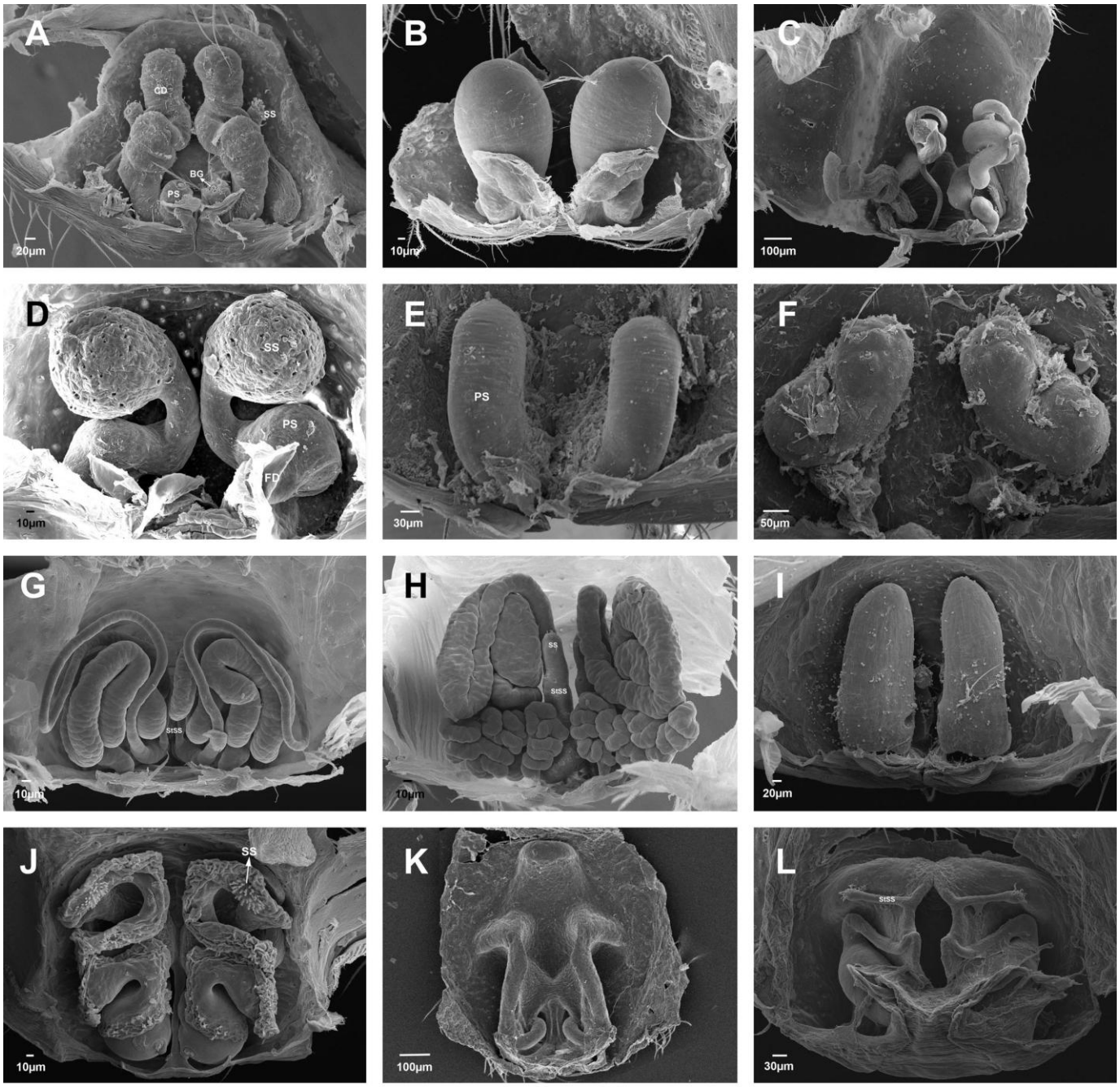

Fig. 26: Female internal genitalia, dorsal view. A) *Callilepis nocturna*. B) *Cesonia bilineata*. C) *Cithaeron praedonius*. D) *Drassodes saccatus*. E) *Herpyllus ecclesiasticus.* F) *Hypodrassodes maoricus*. G) *Lygromma chamberlini*. H) *Moreno grande*. I) *Nodocion eclecticus*. J) *Setaphis subtilis*. K) *Vectius niger*. L) *Zelanda erebus*. BG: Bennett"s Gland; CD: Copulatory duct; FD: Fertilization duct; PS: Primary spermathecae; SS: Secondary spermatheca; StSS: Stalk of secondary spermatheca;

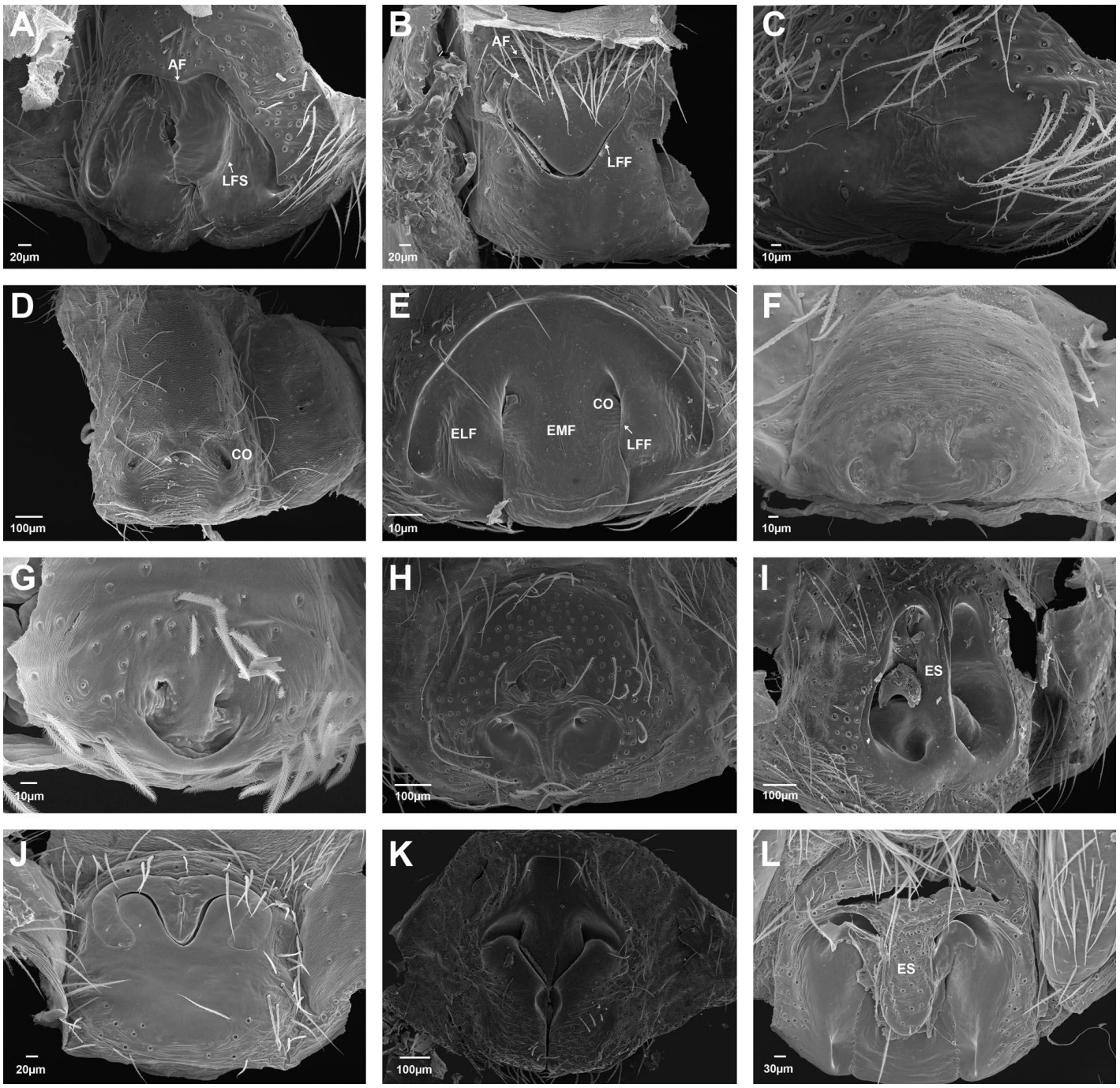

Fig. 27: Female genitalia, ventral view. A) *Callilepis nocturna*. B) *Camillina cordifera*. C) *Cesonia bilineata*. D) *Cithaeron praedonius*. E) *Hypodrassodes maoricus.* F) *Lygromma chamberlini*. G) *Moreno grande*. H) *Nodocion eclecticus.* I) *Nomisia aussereri.* J) *Setaphis subtilis.* K) *Vectius niger*. L) *Zelanda erebus*. AF: Anterior fold; CO: Copulatory opening; ELF: Epigynal lateral field; EMF: Epigynal midian field; ES: Epigynal scape; LFF: Lateral fold furrow; LFS: Lateral fold suture.

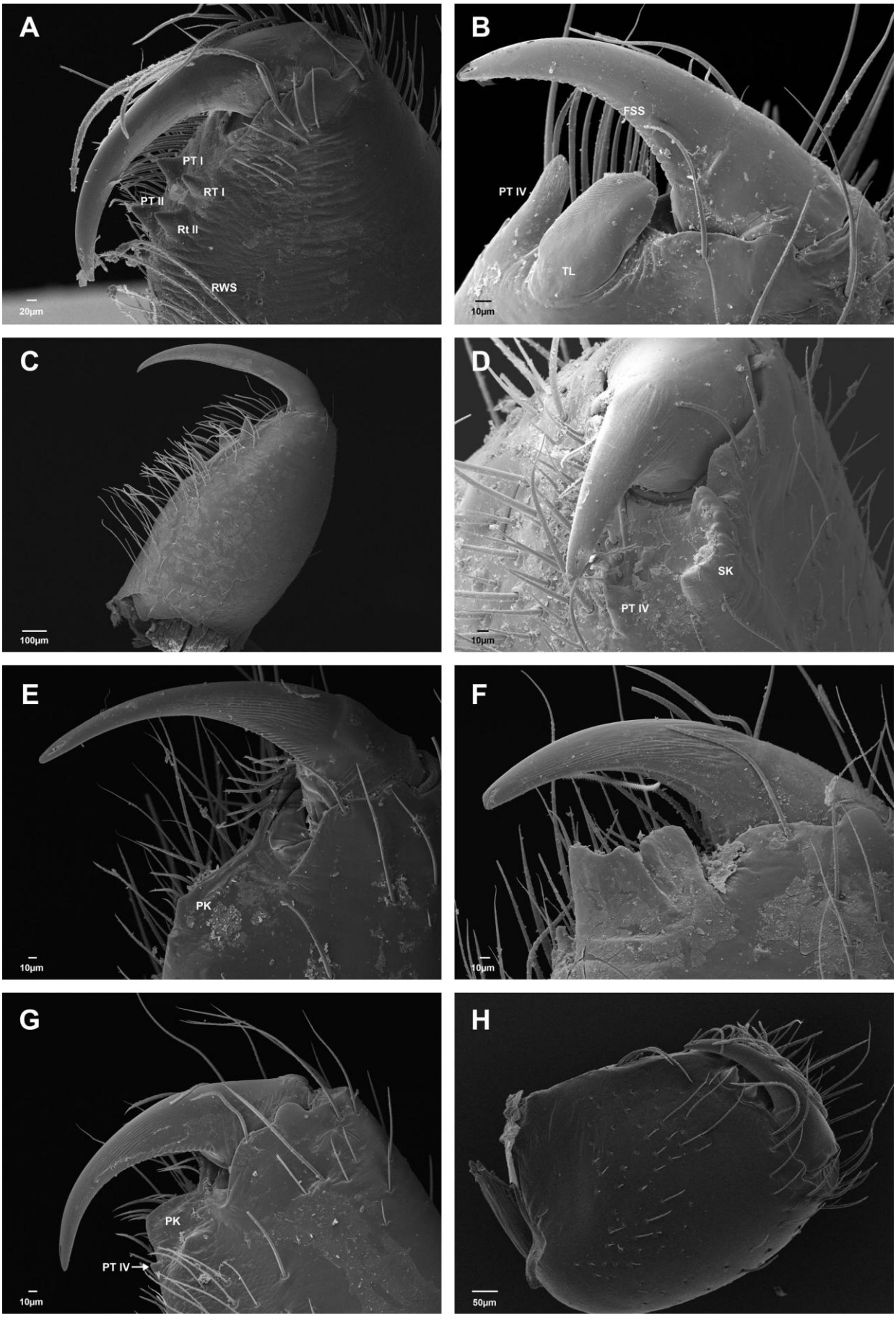

Fig. 28: Female **c**helicerae, ventral view A) *Anagraphis pallens*. B) *Callilepis gosoga*. C) *Gallieniella mygaloides*. D) *Gnaphosa californica*. E) *Nodocion eclecticus.* F) *Pterotricha conspersa*. G) *Sergiolus capulatus*. H) *Vectius niger*. FSS: Fang shaft serula; PK: Prolateral keel; PT I: Prolateral tooth I; PT II: Prolateral tooth II; PT IV: Prolateral tooth IV; RT I: Retrolateral tooth I; RT II: Retrolateral tooth II; RWS: Retrolateral whisker setae; SK: Serrated keel.

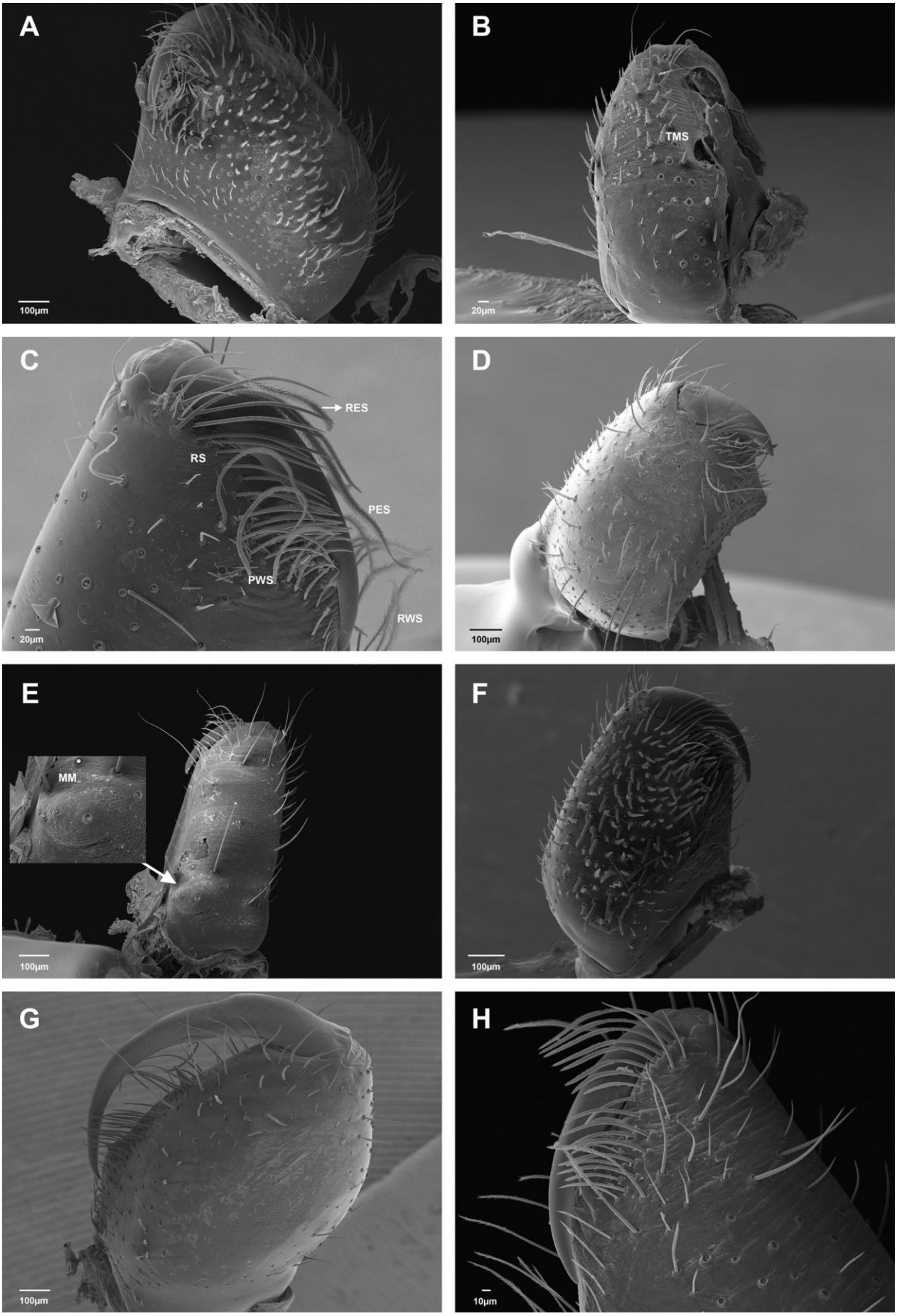

Fig. 29: Female (except E) chelicerae, dorsal view. A) *Berlandina plumalis*. B) *Callilepis nocturna*. C) *Chilongius palmas*. D) *Gnaphosa californica*. E) *Micaria gosiuta* (male). F) *Trachyzelotes pedestris*. G) *Trochanteria gomezi*. H) *Xerophaeus capensis*. PES: Prolateral escort seta; PWS: Prolateral whisker setae; RES: Retrolateral escort seta; RS: Rake setae; RWS: Retrolateral whisker setae; TMS: Thick macrosetae.

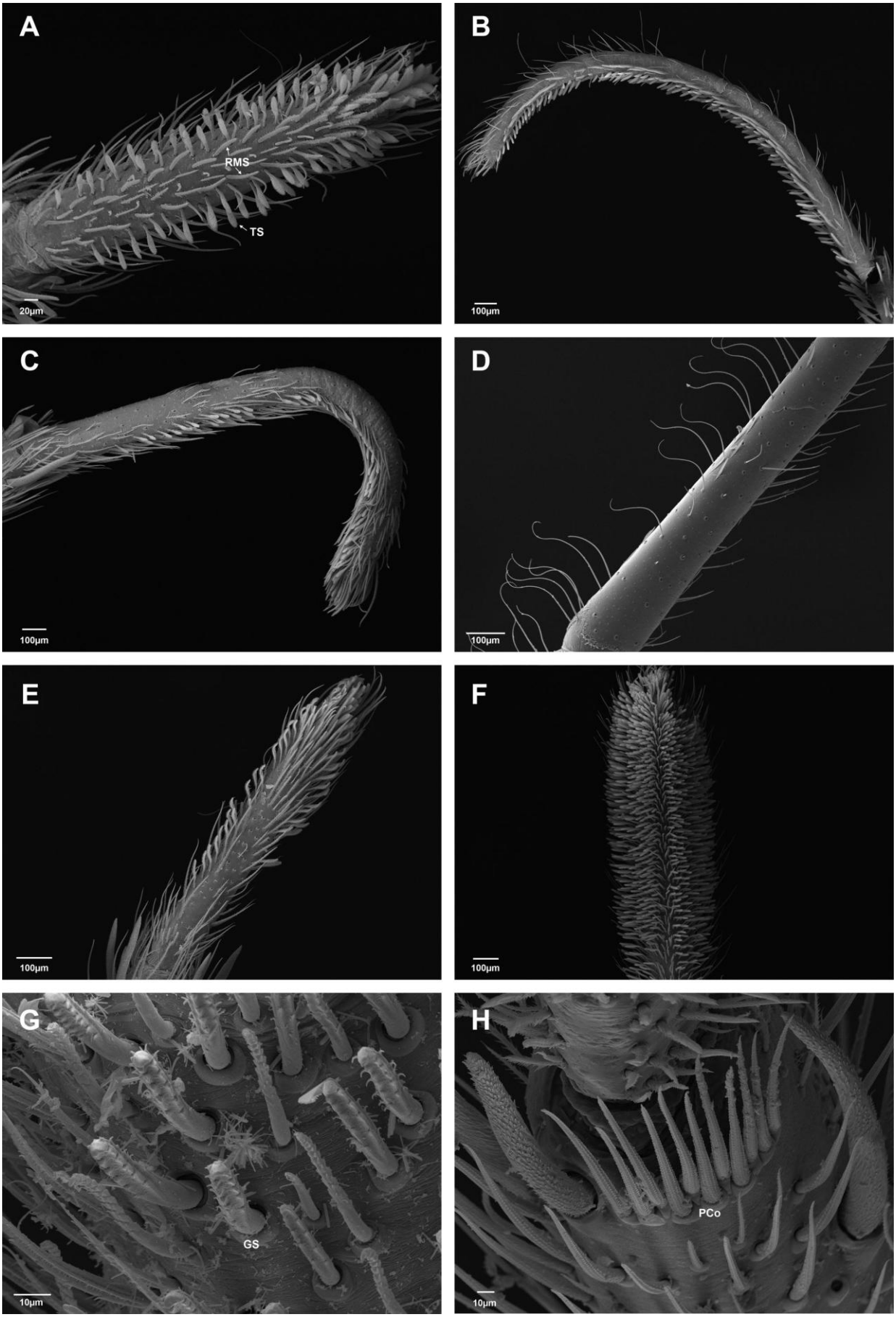

Fig. 30: Female right legs (except D). A) *Callilepis nocturna*, tarsus I, ventral. B) *Cithaeron praedonius*, leg IV, prolateral. C) *Echemoides aguilari*, leg IV, retrolateral. D) *Micaria gosiuta*, male tibia I, retrolateral, showing long, curved, sensory ventral setae. E) *Nodocion eclecticus*, tarsus IV, ventral. F) *Orodrassus coloradensis*, leg I, ventral. G) *Trachyzelotes pedestris*, tarsus I, ventral. H) *Zelotes duplex*, distal part of metatarsus IV, ventral. GS: Grasping setae; PCo: Preening comb; RMS: Row of ventral macrosetae; TS: Tenent setae.

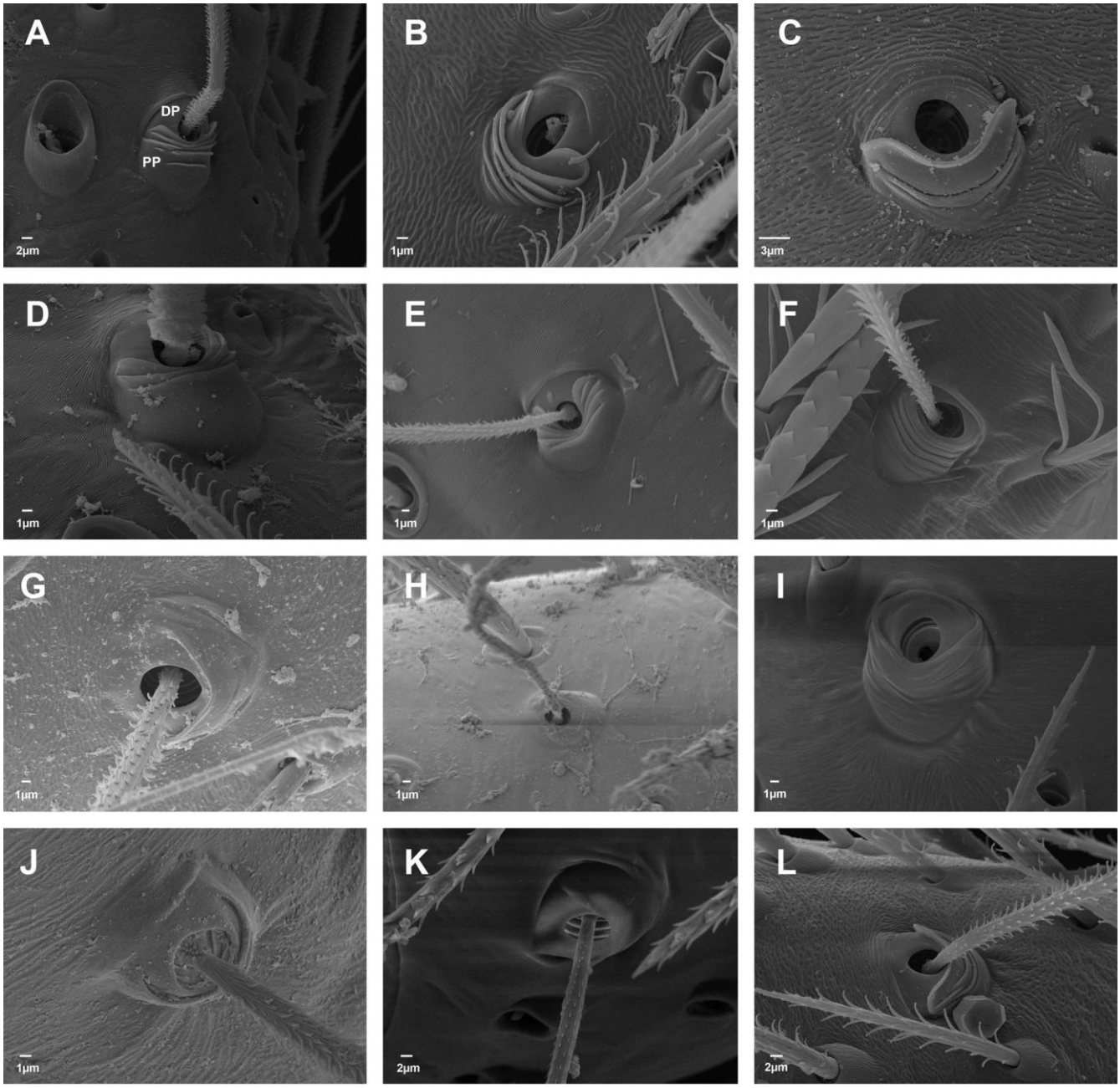

Fig. 31: Trichobothria. A) *Anagraphis pallens*. B) *Apopyllus silvestrii*. C) *Camillina cordifera*. D) *Chileuma paposo*. E) *Chilongius palmas.* F) *Cryptoeritus occultus.* G) *Gnaphosa californica*. H) *Micaria gosiuta*. I) *Minosia simeonica*. J) *Trochanteria gomezi*. K) *Vectius niger*. L) *Zelanda erebus*. DP: Distal plate; PP: Proximal plate.

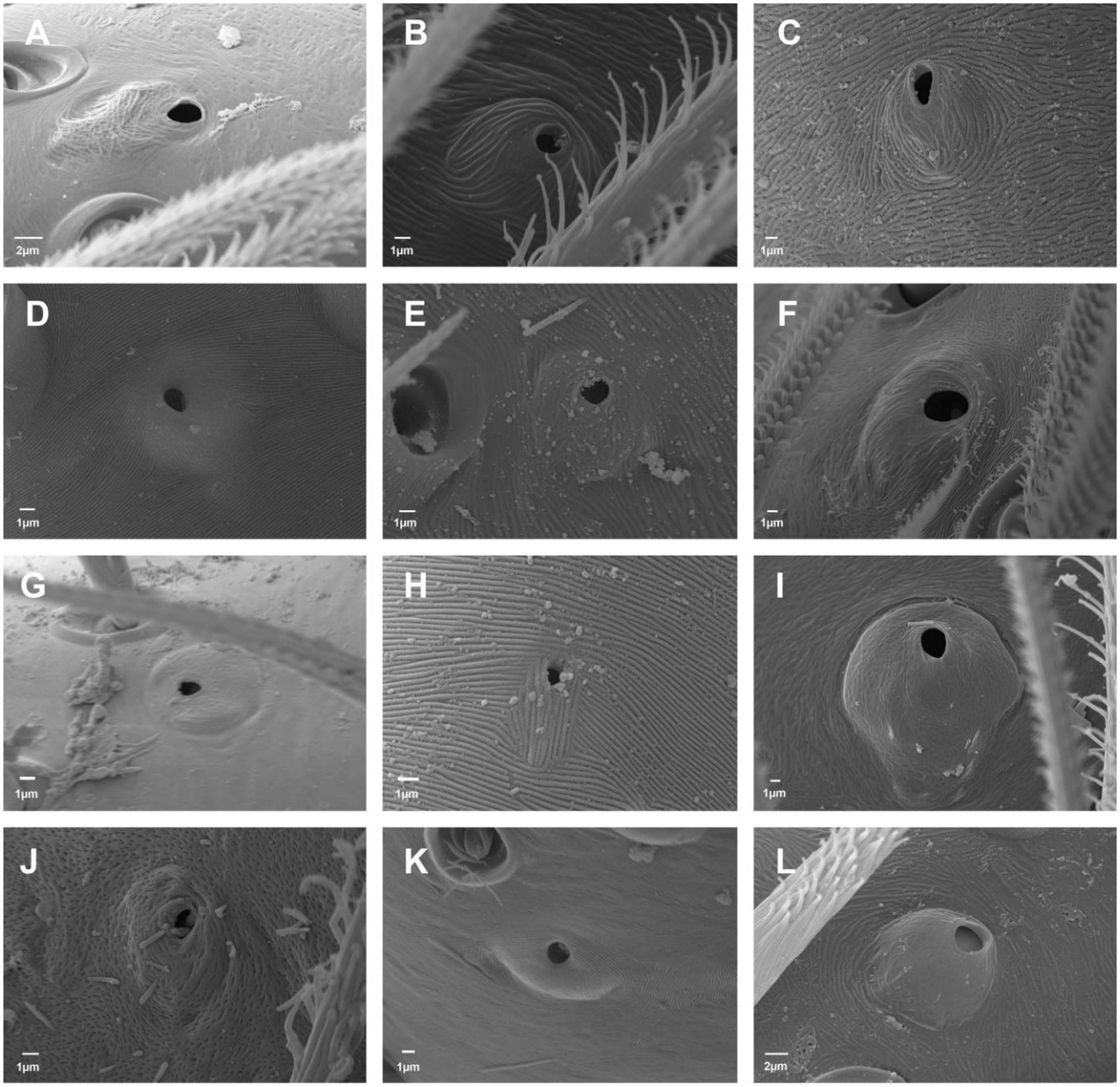

Fig. 32: Tarsal organs. A) *Anzacia gemmea*. B) *Apopyllus silvestrii*. C) *Camillina cordifera*. D) *Chilongius palmas*. E) *Hemicloea sundevalli.* F) *Hypodrassodes maoricus.* G) *Micaria gosiuta*. H) *Moreno grande*. I) *Orodrassus coloradensis*. J) *Sergiolus capulatus*. K) *Talanites equinus*. L) *Xerophaeus capensis*.

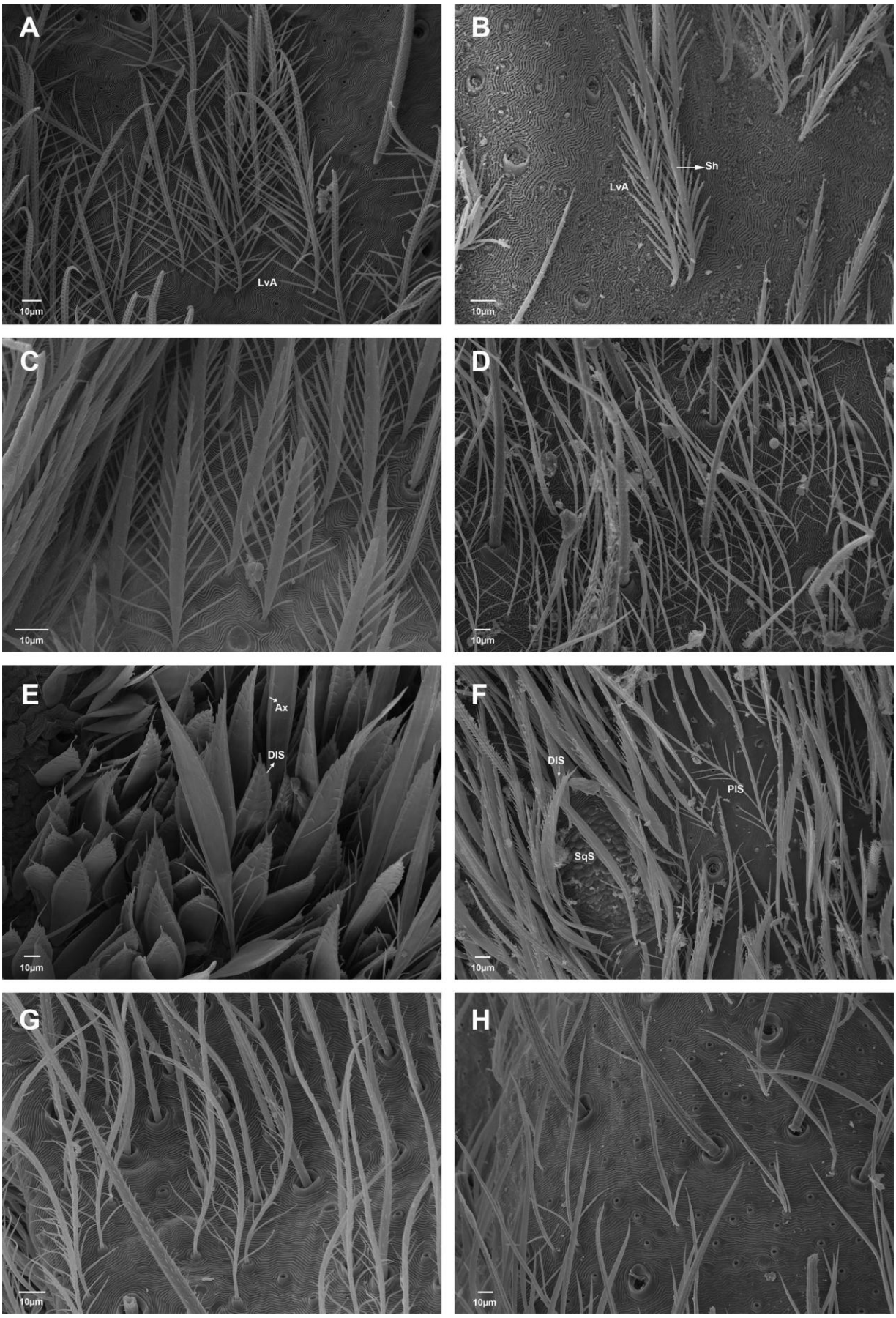

Fig. 33: Squamose (A, C, E, F) and plumose (B, D, F, H) setae. A) *Anagraphis pallens*. B) *Callilepis nocturna*. C) *Cryptoeritus occultus*. D) *Haplodrassus hiemalis*. E) *Hypodrassodes maoricus.* F) *Litopyllus temporarius*. G) *Sergiolus capulatus*. H) *Sosticus insularis*. Ax: Axis; DlS: Dorso-lateral spines; LvA: Later-ventral appendages; PlS: Plumose setae; Sh: Shaft; SqS: Squamose setae.

Appendices

Appendix 1. Character list. Characters marked with "(F)" were scored for females and with "(M)" for males, since they might show sexual dimorphism.

Abdomen

0. Abdomen, antero-dorsal, tuft of setae: absent = 0; present = 1. (Bosselaers & Jocqué, 2002: char. 101; Ramírez, 2014: char. 213)

1. Abdomen, dorsal, black and white color pattern: absent = 0; present = 1.

2. Abdomen, dorsal, dark chevrons: absent = 0; present = 1.

3. Abdomen, ventral, genital segment, sclerotization: not sclerotized = 0; sclerotized = 1.

4. Abdomen, lateral border, thick macrosetae: absent = 0; present = 1.

5. Abdomen, pedicel, dorsal and ventral, sclerites, fusion: absent = 0; present = 1. (Platnick, 2000: chars. 6 and 19)

6. Abdomen, pedicel, ventral, anterior margin, shape: pointed = 0; truncated = 1. (Ramírez, 2014, char. 199)

7. Abdomen, pedicel, ventral, sclerite, articulation with sternum: free = 0; fused = 1. (Ramírez, 2014, char. 198). *Ammoxenus coccineus* scored 0, against Ramírez (2014) for *A. amphalodes*.

8. Abdomen, surface, plumose setae: absent = 0; present = 1. The plumose setae are scales (covering setae) with cylindrical shaft (at least the proximal third; Fig. 33).

9. Abdomen, surface, plumose setae, appendages (brachia) disposition: only in proximal part = 0; reaching terminal half = 1.

10. Abdomen, surface, plumose setae, tip shape: cylindrical = 0; flattened = 1.

11. Abdomen, surface, squamose setae: absent = 0; present = 1 (Fig. 33). Squamose setae are flattened scales. Used in a broader sense than Zakharov & Ovtsharenko (2015). These authors described different types of flattened covering setae. Herein, the structures composing each type were considered different characters (see above) that could be present on a flattened scale. *Anzacia gemmea* scored based on Zakharov & Ovtsharenko (2015).

12. Abdomen, surface, squamose setae, lateroventral appendages: absent = 0; present = 1 (Fig. 33).

13. Abdomen, surface, squamose setae, dorsolateral spines: absent = 0; present = 1 (Fig. 33).

14. Abdomen, surface, squamose setae, dorsolateral spines, type: short and contiguous = 0; long and separated = 1 (Fig. 33).

15. Abdomen, surface, squamose setae, dorsolateral spines, disposition: on both sides = 0; only on one side = 1.

16. Abdomen, surface, squamose setae, number of axes: zero = 0; one = 1; two = 2 (Fig. 33).

17. Abdomen, surface, squamose setae, ventral projections: absent = 0; present = 1 (Fig. 33).

18. Abdomen, ventral, internally invaginated postepigastric sclerites: absent = 0; present = 1 (Platnick, 2000: char. 11. Platnick, 2002: char. 7)

19. Abdomen (F), dorsal, scutum: absent = 0; present = 1.

20. Abdomen (F), dorsal, scutum, size: only on the anterior face of abdomen = 0; passing first apodeme = 1. Adapted from Platnick (2000).

21. Abdomen (M), dorsal, scutum: absent = 0; present = 1. *Notiodrassus distinctus* scored 1, against Murphy (2007). *Teutamus rama* scored based on Ramírez (2014).

22. Abdomen (M), dorsal, scutum, size: not reaching the first apodeme = 0; surpassing first apodeme = 1.

23. Abdomen (M), ventral, epiandrum, epiandrous spigots: absent = 0; present = 1. *Xenoplectus* sp. scored 1, there seems to be two spigots (against Ramírez, 2014).

24. Abdomen (M), ventral, epiandrum, epiandrous spigots, disposition: sparse =0; two groups in separated cavities = 1; two groups in one unique cavity = 2. *Drassinella*, *Liocranum* and *Trachelas*: the spigots are not inserted in a whole on cuticular surface but they are in groups (scored 1). No taxon in this dataset was scored 0, but the state was kept since it show variation on Dionycha spiders and might be useful for further analyses.

Cephalothorax

25. Cephalothorax, carapace, surface, plumose setae: absent = 0; present = 1.

26. Cephalothorax, carapace, surface, plumose setae, appendages (brachia) disposition: only on proximal part = 0; reaching terminal half = 1.

27. Cephalothorax, carapace, surface, plumose setae, tip shape: cylindrical = 0; flattened = 1.

28. Cephalothorax, carapace, surface, squamose setae: absent = 0; present = 1.

29. Cephalothorax, carapace, surface, squamose setae, lateroventral appendages: absent = 0; present = 1.

30. Cephalothorax, carapace, surface, squamose setae, dorsolateral spines: absent = 0; present = 1.

31. Cephalothorax, carapace, surface, squamose setae, dorsolateral spines, type: short and contiguous = 0; long and separated = 1.

32. Cephalothorax, carapace, surface, squamose setae, dorsolateral spines, disposition: on both sides = 0; only on one side = 1. All terminals have state 0, but the character was kept in the matrix as it could be useful in future studies..

33. Cephalothorax, carapace, surface, squamose setae, number of axes: zero = 0; one = 1; two = 2.

34. Cephalothorax, carapace, surface, squamose setae, ventral projections: absent = 0; present = 1.

35. Cephalothorax, carapace, anterior, chilum: absent = 0; present = 1. *Vectius niger* scored 0 (against Ramírez, 2014).

36. Cephalothorax, carapace, anterior, chilum, configuration: single sclerite = 0; paired sclerites = 1.

37. Cephalothorax, carapace, anterior, clypeus, margin profile in anterior view: straight or slightly curved = 0; produced in a median lobe anteriorlly = 1; very curved, forming an arc = 2.

38. Cephalothorax, carapace, cephalic area, anterior lateral eyes tapetum symmetry axis: vertical to oblique = 0; horizontal = 1 (Ramírez, 2014: char. 23).

39. Cephalothorax, carapace, cephalic area, anterior median eyes, black surrounds: absent = 0; present = 1. It was considered present when the black surrounds of the two eyes are connected. (Murphy, 2007)

40. Cephalothorax, carapace, cephalic area, anterior median eyes, size relative to others: smaller = 0; about same size = 1; larger = 2.

41. Cephalothorax, carapace, cephalic area, posterior lateral and median eyes tapeta axes: parallel = 0; orthogonal = 1 (Ramírez, 2014: char. 28).

42. Cephalothorax, carapace, cephalic area, posterior median eyes, lens limits: raised from surrounding cuticule = 0; not raised = 1 (Ramírez, 2014: char. 20).

43. Cephalothorax, carapace, cephalic area, posterior median eyes, lens ridges: absent = 0; present = 1.

44. Cephalothorax, carapace, cephalic area, posterior median eyes, tapeta, symmetry axes: parallel to each other = 0; orthogonal to each other = 1 (Ramírez, 2014: char. 23). *Tricongius* and *Oltacloea:* it looks slightly oblique, but not orthogonal (scored 0).

45. Cephalothorax, carapace, cephalic area, posterior median eyes, tapeta, symmetry axes orthogonal, direction of the 45 degree angle: anterior = 0; posterior = 1. Although the shape of lens might be in different arrangement between genera, the tapeta angle is always directed anteriorly.

46. Cephalothorax, carapace, dorsal, cephalic area, eye row tubercle: absent = 0; present = 1.

47. Cephalothorax, carapace, dorsal, cephalic area, posterior median eyes, lens: domed = 0; flattened = 1 (Platnick, 2000: char. 9; Platnick, 2002: char. 1).

48. Cephalothorax, carapace, dorsal, cephalic area, posterior median eyes, position in relation to each other: separated = 0; close, almost touching = 1.

49. Cephalothorax, carapace, dorsal, cephalic area, posterior median eyes, size relative to laterals: smaller = 0; same size = 1; larger = 2.

50. Cephalothorax, carapace, dorsal, color pattern: plain colored = 0; colored stripes = 1.

51. Cephalothorax, carapace, dorsal, fovea: absent = 0; present = 1.

52. Cephalothorax, carapace, flatness: domed = 0; extremely flat = 1.

53. Cephalothorax, carapace, thoracic area, height relative to cephalon: lower = 0; about as high = 1; higher = 2.

54. Cephalothorax, lateral, epimeric sclerites, type: not fused = 0; fused = 1.

55. Cephalothorax, ventral, intercoxal extensions: absent = 0; present = 1 (Platnick 2000: chars. 24, 25; Platnick, 2002: char.5; Ramírez 2014: char. 96.). Ramírez (2014) used the character "Detached intercoxal sternum extensions" with the states "0. Absent or fused to sternum" and "1. Present". Here it was separated into a neomorphic (present/absent) and a transformational character (fused/not fused). *Platyoides walteri* scored 0 (against Ramírez, 2014).

56. Cephalothorax, ventral, intercoxal extensions, fusion to sternum: not fused = 0; fused = 1.

57. Cephalothorax, ventral, precoxal sclerites: absent = 0; present = 1 (Silva Davila, 2003; Ramírez, 2014: char. 95). Ramírez (2014) used as a three state character: absent, fused and not fused. Here it was separated into a neomorphic and a trasformational character with two states each.

58. Cephalothorax, ventral, precoxal sclerites, fusion to sternum: not fused (free) = 0; fused = 1.

Chelicerae

59. Chelicerae, fang, shaft serrula: absent = 0; present = 1.

60. Chelicerae, fang, shaft, tubercle in males: absent = 0; present = 1. Males *Gallieniella mygaloides* have a small tubercle on the concave side of chelicerae.

61. Chelicerae, fang, length: normal = 0; elongated, with tip almost reaching paturon base = 1 (Fig. 29G).

62. Chelicerae, paturon, anterior surface, proximal, mesal mounds in male: absent = 0; present = 1. Male of *Micaria gosiuta* have a small mound with some setae (Fig. 29E).

63. Chelicerae, paturon, anterior surface, thick spines: absent = 0; present = 1. (Ramírez, 2014: fig. 25B, D)

64. Chelicerae, paturon, anterior surface, tuft of macrosetae: absent = 0; present = 1. (Fig. 29A, B, F)

65. Chelicerae, paturon, anterior surface, tuft of macrosetae, length: smaller than half the fang length = 0; at least half the fang size = 1.

66. Chelicerae, paturon, anterior surface, tuft of macrosetae, density: sparse = 0; dense = 1 (Fig. 29F).

67. Chelicerae, paturon, basal, posterior membranous mound: absent = 0; present = 1 (Ramírez, 2014: char. 35). *Rastellus*: scored based on Ramírez (2014).

68. Chelicerae, paturon, ectal, boss: absent = 0; present = 1. *Ammoxenus coccineus*: scored 0, against Ramírez (2014) for *A. amphalodes*

69. Chelicerae, paturon, ectal, boss type: smal, weakly pronounced = 0; very pronounced = 1.

70. Chelicerae, paturon, posterior, fang furrow, teeth: absent = 0; present = 1.

71. Chelicerae, paturon, promargin, rake setae: absent = 0; present = 1. *Ammoxenus*, *Doliomalus* and *Neozimiris*: There is a row of setae but it is not flattened with aligned barbs (scored 0).

72. Chelicerae, paturon, promargin, whisker setae: absent = 0; present = 1.

73. Chelicerae, paturon, promargin, escort setae: absent = 0; present = 1. Only considered escort setae when it is different from the whisker setae. There might be different types of escort setae, but it was not coded here since homology establishment is difficult.

74. Chelicerae, paturon, promargin, keel: absent = 0; present = 1. The promargin is elevated in a smooth (not serrated) keel (Fig. 28E, G). Not considered homologous to teeth because keel and teeth IV can co-occur (e.g: *Sergiolus*). *Herpyllus:* base of teeth is elevated and contiguous (scored 1). *Latonigena:* scored 1, against Ott et al. (2012). It is said that *Latonigena* differs from *Sergioulus* by having teeth instead of the carina (Ott *et al.*, 2012), but the structure on the promargin is like the one in *Sergioulus*, looking like two teeth fused. *Nodocion*: not very pronounced (scored 1). *Scotocesonia*: similar to *Latonigena* (scored 1).

75. Chelicerae, paturon, promargin, tooth II: absent = 0; present = 1. Teeth were separated into serial homologous structures according to the distance to the paturon-fang articulation, being the tooth I the closest. In a few cases, there were more than five teeth, so they all were lumped into one character “tooth extras” (Fig. 28).

76. Chelicerae, paturon, promargin, tooth II: absent = 0; present = 1.

77. Chelicerae, paturon, promargin, tooth III: absent = 0; present = 1.

78. Chelicerae, paturon, promargin, tooth IV: absent = 0; present = 1. *Callilepis* and *Eilica*: laminar and rounded (scored 1). *Latonigena, Litopyllus, Scotocesonia* and S*ergiolus*: small and it might be part of the keel (scored 1).

79. Chelicerae, paturon, promargin, tooth V: absent = 0; present = 1.

80. Chelicerae, paturon, promargin, tooth extras: absent = 0; present = 1.

81. Chelicerae, paturon, proximal region, deep constriction: absent = 0; present = 1 (Platnick, 2002: char. 21.).

82. Chelicerae, paturon, retromargin, projections (lamina, keel or teeth): absent = 0; present = 1. All kinds of projections of the cuticle retromargin were considered homologous, including normal teeth, the gnaphosines serrated keels and laroniines lamina. However, they were considered as different modifications of this cuticular projection and a transformational character (char. 83) was created to accommodate these different states (Fig. 28).

83. Chelicerae, paturon, retromargin, projections type: teeth = 0; serrated keel = 1 (Fig. 28D); translucent lamina = 2. (Fig. 28B). *Litopillus levantinus:* It looks like an intermediate between an angular lamina and teeth. Since not having lamina is one of the diagnostic characters of the genus, it was considered a teeth, but it might indicate that the genus is paraphyletic or that this species is misplaced.

84. Chelicerae, paturon, retromargin, rake setae: absent = 0; present = 1.

85. Chelicerae, paturon, retromargin, escort setae: absent = 0; present = 1. Only considered escort setae when it is different from the whisker setae. There might be different types of escort setae, but it was not coded here since homology establishment is difficult.

86. Chelicerae, paturon, retromargin, whisker setae: absent = 0; present = 1.

87. Chelicerae, paturon, retromargin, tooth I: absent = 0; present = 1. Not applicable when the projection type is a serrated keel or translucent lamina (Char. 83).

88. Chelicerae, paturon, retromargin, tooth II: absent = 0; present = 1. Not applicable when the projection type is a serrated keel or translucent lamina (Char. 83).

89. Chelicerae, paturon, retromargin, tooth III: absent = 0; present = 1. Not applicable when the projection type is a serrated keel or translucent lamina (Char. 83).

90. Chelicerae, paturon, retromargin, tooth IV: absent = 0; present = 1. Not applicable when the projection type is a serrated keel or translucent lamina (Char. 83).

91. Chelicerae, paturon, retromargin, tooth extras: absent = 0; present = 1. Not applicable when the projection type is a serrated keel or translucent lamina (Char. 83).

92. Chelicerae, paturon, retromargin, translucent lamina number: one = 0; two = 1. Only applicable when projection type is a translucent lamina.

93. Chelicerae, paturon, retromargin, translucent lamina type: rounded = 0; angular = 1. Only applicable when projection type is a translucent lamina. Murphy (2007) proposed this character to differentiate the lamina present in *Laronius* group (rounded) from the ones in *Leptodrassus* group (angular). The angular type resembles more a long, laminar teeth, with pointed edges, while the rounded lamina looks more modified.

94. Chelicerae, paturon, retromargin and furrow, sclerotization: sclerotized = 0; unsclerotized posterior patch just distal from cheliceral gland area = 1; completely unsclerotized = 2 (Ramírez, 2014: char. 44).

95. Chelicerae, paturon, shape: conical, longer than wide = 0; rounded, about as long as wide = 1. (Fig. 28).

96. Chelicerae, projection: ventrally = 0; anteriorly = 1 (Fig. 21 D, G, K).

97. Chelicerae, disposition: plagiognathous = 0; orthognathous = 1 (Fig. 21 D).

Female Genitalia

98. Epigynum, anterior fold: absent = 0; present = 1. The anterior fold is a transversal furrow on the anterior part of the epigynum, separating the anterior field from the middle fild (Fig. 27).

99. Epigynum, anterior fold, posterior extension forming a secondary lateral fold: absent = 0; present = 1. The lateral tips of the furrow might be extended towards posterior part forming a longitudinal furrow (Fig. 27). This longitudinal furrow differs from the lateral fold because the latter is associated to the internal copulatory ducts and openings.

100. Epigynum, anterior fold, hood: absent = 0; present = 1. The furrow covers part of the epigynal plate (Fig. 27).

101. Epigynum, anterior fold, scape: absent = 0; present = 1. The scape is a median projection of the anterior fold, not connected to the epigynal plate (Fig. 27).

102. Epigynum, lateral folds: absent, epigynum is an undivided plate = 0; present = 1 (Fig. 27). Lateral folds are longitudinal furrows or sutures that divide the epyginum and are usually associated with the copulatory ducts (Sierwald, 1989).

103. Epigynum, lateral folds, type: suture = 0; furrow = 1 (Fig. 27).

104. Epigynum, lateral folds, forming small paramedian epigynal pockets: absent = 0; present = 1. Present in *Apopyllus* and *Synaphosus* (see Chapter 3 of this thesis)

105. Epigynum, median field, septum: absent = 0; present = 1. The septum is a medial longitudinal keel on the median field.

106. Epigynum, median field, plate surface, atrium: absent, the median field is on same plane as lateral field = 0; present, there is an excavation on median field = 1.

107. Epigynum, vulva, copulatory ducts, extension relative to copulatory opening: extending anteriorly = 0; not extending anteriorly = 1.

108. Epigynum, vulva, copulatory ducts, shape: highly convoluted = 0; spiral = 1; curved or with a few curls = 2.

109. Epigynum, vulva, copulatory ducts, sclerotization: completely sclerotized = 0; only proximal part = 1; only terminal part = 2.

110. Epigynum, vulva, cuticular glands: absent = 0; present = 1.

111. Epigynum, vulva, fertilization duct, direction: ventrally directed = 0; posteriorly directed = 1.

112. Epigynum, vulva, fertilization duct, position: posterior = 0; anterior = 1.

113. Epigynum, vulva, massive midpiece: absent = 0; present = 1 (Platnick, 1983).

114. Epigynum, vulva, primary spermatheca: absent = 0; present = 1. The primary spermathecae is a dilatation of copulatory duct and connected with the fertilization duct (base of spermatheca in Sierwald, 1989). It might bear the Bennett's gland. The state 0 means that it cannot be clearly differentiated from ducts (Fig. 26C, G, H).

115. Epigynum, vulva, primary spermatheca, position: paramedian, close to each other = 0; lateral, apart from each other = 1.

116. Epigynum, vulva, primary spermatheca, Bennett's gland, insertion: depressed = 0; superficial = 1.

117. Epigynum, vulva, secondary spermatheca: absent = 0; present = 1 (Fig. 26). Secondary spermatheca is a blind sac with large pores (Ramírez, 2014).

118. Epigynum, vulva, secondary spermatheca, location: copulatory duct = 0; spermatheca = 1. There is no (or very small) duct between secondary and primary spermathecae. Equivalent to char. 377 in Ramírez (2014).

119. Epigynum, vulva, secondary spermatheca, size relative to primary spermatheca: smaller = 0; about as large = 1; at least 1.5 larger = 2.

120. Epigynum, vulva, secondary spermatheca, well defined lumen: absent = 0, there is a patch of pores on the copulatory ducts or in the primary spermatheca (Fig. 26J); present = 1.

121. Epigynum, vulva, secondary spermatheca, long duct (stalk, at least two times the head): absent = 0; present = 1 (Fig. 26G, H, L).

122. Epigynum, vulva primary spermatheca, shape: rounded = 0; elongated = 1; reniform = 2.

Legs and Female Palp

123. Legs, surface, plumose setae: absent = 0; present = 1.

124. Legs, surface, plumose setae, appendages (brachia) disposition: only on proximal part = 0; reaching terminal half = 1.

125. Legs, surface, plumose setae, tip shape: cylindrical = 0; flattened = 1.

126. Legs, surface, squamose setae: absent = 0; present = 1.

127. Legs, surface, squamose setae, lateroventral appendages: absent = 0; present = 1.

128. Legs, surface, squamose setae, dorsolateral spines: absent = 0; present = 1.

129. Legs, surface, squamose setae, dorsolateral spines, type: short and contiguous = 0; long and separated = 1.

130. Legs, surface, squamose setae, dorsolateral spines, disposition: on both sides = 0; on one side = 1.

131. Legs, surface, squamose setae, number of axes (shafts): zero = 0; one = 1; two = 2.

132. Legs, surface, squamose setae, ventral projections: absent = 0; present = 1. Only state 1 was observed, but the character was kept in the matrix as it could be useful for future studies.

133. Legs, orientation: prograde = 0; laterigrade = 1.

134. Legs, tarsi, apical, claw-claw tuft clasping mechanism of teeth appressed together (classic clasper): absent = 0; present = 1 (Fig. 8B, C, G, H). See text for discussion about claspers homology.

135. Legs, tarsi, apical, claw-claw tuft clasping mechanism formed by a developed basal fold (folded clasper): absent = 0; present = 1 (Fig. 8A, E).

136. Legs, tarsi, apical, claw-claw tuft clasping mechanism formed by solid projection of basal fold (solid projection clasper): absent = 0; present = 1 (Fig. 8C, D, F).

137. Legs, tarsi, apical, claw-claw tuft clasping mechanism, structure: teeth appressed together = 0; solid = 1. Alternative coding considering the claspers as different states of same character as in Ramírez (2014). This character was inactive during search and was kept in dataset for comparisons purpose and test the effect of alternative coding. See text for discussion about claspers homology.

138. Legs, tarsi, apical, claws, denticles (teeth): absent = 0; present = 1.

139. Legs, tarsi, apical, claws, denticles (teeth), size: reduced = 0 (Fig. 9E, F); normal = 1.

140. Legs, tarsi, apical, claws, teeth insertion line: ectal = 0; median = 1 (Fig. 9); mesal = 2 (Fig. 8A).

141. Legs, tarsi, apical, claws, dorsal scales (velvety texture): absent = 0; present = 1. (Fig. 8B, D, G)

142. Legs, tarsi, apical, claw tufts: absent = 0; present = 1.

143. Legs, tarsi, apical, two-three pairs of pseudotenent seta with spaced barbs only on leg IV: absent = 0; present = 1 (Fig. 9B).

144. Legs, tarsi, apical, claw tuft, insertion: continuous with lateral cuticle (or slightly separated by sutures) = 0; well delimited plate = 1 (Ramírez, 2014: char. 173).

145. Legs, tarsi, apical, claw tuft, seta, basal rectangular blocks: absent = 0; present = 1 (Ramírez, 2014: char. 167).

146. Legs, tarsi, apical, claw tuft, seta, basal section, shape: almost cylindrical = 0; with folds or ribs = 1 (Ramírez, 2014: char. 164).

147. Legs, tarsi, apical, claw tuft, seta, base, packing: in individual sockets = 0; together = 1; base fused = 2 (Ramírez, 2014: char. 166).

148. Legs, tarsi, apical, claw tuft, seta, tenant surface, orientation: facing ventrally = 0; facing mesally = 1.

149. Legs, tarsi, apical, claw tuft, seta, type: pseudotenant setae = 0; tenant setae = 1.

150. Legs, tarsi, apical, modified setae with long apical tube: absent = 0; present = 1 (Ramírez, 2014: char. 175).

151. Legs, tarsi, distal, ventral, claw slit suture: absent = 0; present = 1 (Fig. 9A, F; Ramírez, 2014).

152. Legs, tarsi, distal, claw slit suture complete, forming onychium: absent = 0; present = 1 (Fig. 9A).

153. Legs, tarsi, cuticle, texture: smooth to rugose = 0; fingerprint = 1 (Fig. 32D, H).

154. Legs, tarsi, tarsal organ, capsule elevation: absent = 0; present = 1 (Fig. 32).

155. Legs, tarsi, tarsal organ, capsule, marginal sulci: absent = 0; present = 1 (Fig. 32).

156. Legs, tarsi, tarsal organ, capsule, texture: same as surrounding cuticle = 0; different = 1.

157. Legs, tarsi, tarsal organ, opening, rim, type: depressed = 0; elevated = 1 (Fig. 32).

158. Legs, tarsi, tarsal organ, opening, shape: round to oval = 0; tear-drop = 1.

159. Legs, tarsi, tarsal organ on leg IV: absent = 0; present = 1.

160. Legs, tarsi, trichobothria, plates, differentiation: absent, distal and proximal are similar = 0; present = 1 (Fig. 31).

161. Legs, tarsi, trichobothria, distal plate, transversal ridges: absent = 0; present = 1 (Fig. 31).

162. Legs, tarsi, trichobothria, proximal plate, distal margin, medial limit differentiation: absent = 0; present = 1 (Ramírez, 2014: char. 177).

163. Legs, tarsi, trichobothria, proximal plate, transversal ridges: absent = 0; present = 1.

164. Legs, whorled setae: absent = 0; present = 1.

165. Legs I, coxa, retrolateral hymen: absent = 0; present = 1. Ramírez (2014: char. 102) used one character with four states: "0. absent", "1. present in leg I", "2. present on legs I-II", and "3. present on legs I-III". Since the states are not mutually exclusive, this character was divided into three neomorphic characters, one for each leg.

166. Legs I and II, metatarsi, ventral, scopulae of tenent setae: absent = 0; present = 1.

167. Legs I and II, metatarsi, ventral, scopulae of tenent setae, density: sparse = 0; dense = 1.

168. Legs I and II, metatarsi, ventral, scopulae of tenent setae, longitudinal extension: restricted to distal part = 0; reaching proximal third = 1.

169. Legs I and II, metatarsi, ventral, scopulae of tenent setae, scopulae type: continuous = 0; divided = 1; only on prolateral side = 2.

170. Legs I and II, metatarsi and tarsi, ventral, scopulae of tenent setae, setae socket, indentation: absent = 0; present = 1.

171. Legs I and II, metatarsi and tarsi, ventral, scopulae of tenent setae, setae type: tenent = 0; pseudotenent (filiform end) = 1.

172. Legs I and II, patellae, indentation: absent = 0; present = 1. *Platyoides*: It seems to be weakly sclerotized, but without a clear indentation (scored 0, against Ramírez 2014).

173. Legs I and II, tarsi, ventral, paired row of spines between scopulae: absent = 0; present = 1.

174. Legs I and II, tarsi, ventral, grasping setae: absent = 0; present = 1. Grasping setae are thick setae with short and spaced barbs (Fig. 30G).

175. Legs I and II, tarsi, ventral, scopulae of tenent setae: absent = 0; present = 1.

176. Legs I and II, tarsi, ventral, scopulae of tenent setae, density: sparse = 0 (Fig. 30A, E); dense = 1 (Fig. 30F).

177. Legs I and II, tarsi, ventral, scopulae of tenent setae, scopulae type: continuous = 0 (Fig. 30F); divided = 1 (Fig. 30A, E).

178. Legs I and II, trochanters, distal rim: straight = 0; shallow indentation = 1; notched = 2.

179. Legs I and II, tarsi, pseudosegmenation: absent = 0; present = 1 (Fig. 30B, C).

180. Legs III, tarsus, pseudosegmentation: absent = 0; present = 1.

181. Legs IV (F), tarsi, pseudosegmentation: absent = 0; present = 1.

182. Legs IV (M), tarsi, pseudosegmentation: absent = 0; present = 1.

183. Legs, tarsi, pseudosegmentation, dorsal extension: absent, pseudosegmentation restricted to ventral part = 0; present = 1.

184. Legs, tarsi, pseudosegmentation, longitudinal extension: only in terminal = 0; reaching proximal = 1.

185. Legs, tarsi, pseudosegmentation, type: rings = 0 (Fig. 30B); cracked = 1 (Fig. 30C).

186. Legs I and II, tibia and metatarsi, ventral, parallel row of strong spines: absent = 0; present = 1.

187. Legs III and IV, metatarsi, distal, preening bush: absent = 0; present = 1. Preening bush is a dense concentration of normal tactile setae on the distal part of metatarsi III and IV. Sometimes it might be difficult to determine if it is really present. It was considered present when there was a clear difference of setae concentration on that area.

188. Legs III and IV, metatarsi, distal, preening comb: absent = 0; present = 1 (Fig. 30H). Preening comb is an organized row of strong setae on the distal part of metatarsi.

189. Legs III, metatarsi, ventral, scopulae of tenant setae: absent = 0; present = 1.

190. Legs III, metatarsi, ventral, scopulae of tenent setae, density: sparse = 0; dense = 1.

191. Legs III, metatarsi, ventral, scopulae of tenent setae, longitudinal extension: restricted to distal part = 0; reaching proximal part = 1.

192. Legs III, metatarsi, ventral, scopulae of tenent setae, scopulae type: continuous = 0; divided = 1; only on prolateral side = 2.

193. Legs III, tarsi, ventral, paired row of macrosetae: absent = 0; present = 1.

194. Legs III, tarsi, ventral, scopulae of tenent setae: absent = 0; present = 1.

195. Legs III, tarsi, ventral, scopulae of tenent setae, density: sparse = 0; dense = 1.

196. Legs III, tarsi, ventral, scopulae of tenent setae, scopulae type: continuous = 0; divided = 1.

197. Legs III and IV, trochanter, distal rim: normal = 0; shallow indentation = 1; notched = 2.

198. Legs IV, metatarsi, ventral, scopulae of tenant setae: absent = 0; present = 1.

199. Legs IV, metatarsi, ventral, scopulae of tenent setae, density: sparse = 0; dense = 1.

200. Legs IV, metatarsi, ventral, scopulae of tenent setae, longitudinal extension: restricted to distal part = 0; reaching proximal part = 1.

201. Legs IV, metatarsi, ventral, scopulae of tenent setae, scopulae type: continuous = 0; divided = 1; only on prolateral side = 2.

202. Legs IV, tarsi, ventral, paired row of macrosetae: absent = 0; present = 1.

203. Legs IV, tarsi, ventral, trident setae: absent = 0; present = 1.

204. Legs IV, tarsi, ventral, scopulae of tenent setae: absent = 0; present = 1.

205. Legs IV, tarsi, ventral, scopulae of tenent setae, density: sparse = 0; dense = 1.

206. Legs IV, tarsi, ventral, scopulae of tenent setae, scopulae type: continuous = 0; divided = 1.

207. Legs IV, tarsus, claw, distal teeth elongated compared to others teeth: absent = 0; present = 1 (Fig. 9E).

208. Legs IV, trochanter, length relative to trochanter III: about the same size = 0; at least 1.5 times longer = 1 (Platnick, 2002).

209. Palp, endite, distal, macrosetae: absent = 0; present = 1 (Ramírez, 2015: char. 71).

210. Palp, endite, dorsal, setae, branched setae: absent = 0; present = 1 (Ramirez, 2015: char. 73). Not observed on the terminals used here.

211. Palp, endite, prolateral edge, longitudinal groove: absent = 0; present = 1 (Platnick, 2000: char. 21)

212. Palp, endite, serrula: absent = 0; present = 1.

213. Palp, endite, ventral surface, oblique depression: absent = 0; present = 1. *Phrurolithus festivus* and *Trachelas mexicanus:* scored 1, against Ramírez (2014). *Trachycosmus:* looking at the images, it seems that it is present, but restricted to the median edge, which agrees with Platnick (2002) and disagrees with Ramírez (2014).

214. Palp (F), femur, lateroventral, row of 7–9 long, strong spines: absent = 0; present = 1. Found in *Wesmaldra* and *Wydundra* (Platnick & Baehr, 2006: char. 10). Not observed in this dataset.

215. Palp (F), tarsus, dorsal, chemosensory patch, position: on dorso-apical surface = 0; on apical truncation = 1 (Ramírez, 2014: char. 84).

216. Palp (F), tarsus, dorsal, chemosensory setae, distribution: scattered = 0; in a defined patch = 1 (Ramírez, 2014: char. 83).

217. Palp (F), tarsus, whorled setae: absent = 0; present = 1.

218. Palp (F), tarsus, terminal, claw: absent = 0; present = 1.

219. Palp (F), tarsus, terminal, claw, teeth: absent = 0; present = 1.

220. Palp (F), tarsus, terminal, claw, type: normal = 0; reduced to a nubbin = 1.

Male Genitalia

221. Palp, copulatory bulb, median apophysis, shape: elongate = 0 (Fig. 24D); rounded, or irregularry shaped, but approximately as long as wide = 1 (Fig. 24C). The median apophysis is a projection that arises from the membranous median area of tegulum, on the concave side of the sperm duct.

222. Palp, copulatory bulb, conductor: absent = 0; present = 1 (Fig. 24B). The conductor is an outgrowth of the proximal part of tegular wall associated to the embolus tip (Zakharov & Ovtcharenko, 2011). *Amazoromu*s: Althought it was described as not having conductor, there is a small projection, with lightly sclerotized base and translucid tip, proximal on the tegulum. It can be seen in Brescovit & Höfer (1994: fig. 1b). It is more easily seen on expanded bulb. *Gallieniellidae*: it looks more terminally situated. It might be a tegular membranous projection (scored 0). *Oltacloea beltraoe*: not described as having a conductor, but it can be seen, on expanded palp, a long sclerotized sclerite arising from proximal part of the tegulum and folowing the embolus (scored 1). *Phrurolithus festivus*: There is a proximal projection on tegulum, interpreted as a sclrerotized conductor due to its position (scored 1). *Sergiolus capulatus*: the membranous projection is not connected to the embolus, but to proximal part of the tegulum, thus it could be called a conductor (against Zakharov & Ovtcharenko 2013), in agreement with Platnick (1981). *Zelotes duplex*: there is a membranous area proximal in tegulum that holds the embolus, but it is not a clear outgrowth (scored 0, against Platnick & Shadab 1983).

223. Palp, copulatory bulb, conductor, sclerotization: translucid = 0; sclerotized = 1.

224. Palp, copulatory bulb, conductor, shape: rounded lobe = 0; elongated = 1. *Anzacia gemmea*: according to Zakharov & Ovtcharenko (2011) the conductor should be a clover leaf, but, according to criteria applied herein, what they called conductor is a terminal apophysis (in agreement with Ovtsharenko & Platnick 1995) an the conductor is an elongated membranous projection.

225. Palp, copulatory bulb, embolus distal tubular membrane (articulation): absent, embolus fused to tegulum = 0 (Fig. 24B); present, embolus articulated = 1 (Fig. 25D; Zakharov & Ovtcharenko, 2011)

226. Palp, copulatory bulb, embolar base distal projection: absent = 0; present = 1 (Senglet, 2004).

227. Palp, copulatory bulb, embolar base, proximal projection: absent = 0; present = 1 (Fig. 22E, F). Some trochanteriids have a ventral projection on proximal part of embolus base.

228. Palp, copulatory bulb, embolar locking lobe: absent = 0; present = 1 (Fig. 24G). The embolus has a lobe that fits a corresponding lobe on the tegulum. It is not a homologue to the tegular locking lobes on embolus base described by Griswold et al. (2005: char. 116 state 1), since herein the character refers to a more ventral positioned structure that interacts with the tegulun, not a dorsolateral projection that interacts with the subtegulum.

229. Palp, copulatory bulb, embolus, embolar base, dilatation: absent = 0; present, the transition between the proximal part of embolus to the distal is abrubt = 1.

230. Palp, copulatory bulb, embolus, embolar radix projection: absent = 0; present = 1. The radix projection is a dorsal projection on the embolar base. The radix here is defined, following Senglet (2004), as the dorsal part of the embolar base that connects the embolus to the proximal part of the tegulum. It is not homologous to the araneiods radix (Fig. 25A, F).

231. Palp, copulatory bulb, embolus, embolar escort esclerite: absent = 0; present = 1. There is a projection from the dorsal base that escorts the embolus and it is attached to it by a membrane. In this dataset it was found in *Berlandina plumalis* and in *Zelanda* e*rebus*. Zakharov & Ovtcharenko (2011) called this sclerite, in *Zelanda,* subterminal apophysis and the membrane was called *pars pendula*.

232. Palp, copulatory bulb, embolus, insertion in tegulum on unexpanded bulb: retrolateral = 0; prolateral = 1.

233. Palp, copulatory bulb, embolus, length relative to tegulum: about half = 0; about the same = 1; longer, with loops around it = 2.

234. Palp, copulatory bulb, embolus, pars pendula: absent = 0; present = 1. *Pars pendula* is a membrane on concave side of embolus (Zakharov & Ovtcharenko, 2011).

235. Palp, copulatory bulb, embolus, shape: laminar = 0; tubular = 1.

236. Palp, copulatory bulb, embolus, tubular embolus type: filiform, or conical = 0; wide, massive, with rounded tip = 1.

237. Palp, copulatory bulb, embolus, terminal membrane: absent = 0; present = 1. The terminal membrane is an inflatable membrane located on terminal part of the embolus (Zakharov & Ovtcharenko, 2011). It is equivalent to the terminal haematodocha described for Zelotinae by Senglet (2004).

238. Palp, copulatory bulb, embolus, embolar granulation: absent = 0; present = 1.

239. Palp, copulatory bulb, fulcrum: absent = 0; present = 1. The fulcrum is a movable small sclerite on embolus tip (Zakharov & Ovtcharenko, 2011).

240. Palp, copulatory bulb, intercalary sclerite: absent = 0; present = 1 (Fig. 25F). The intercalary sclerite is a sclerotized structure that connects the embolus base, or base of the terminal apophysis, to the terminal part of tegulum. It is situated more dorsally in relation to embolus (Platnick & Shadab, 1983; Senglet, 2004; Zakharov & Ovtcharenko, 2013). *Berlandina plumalis*: it might be part of the subtegulum (scored 1). *Heser schmitzi*: according to Tuneva (2004) the genus does not have terminal apophysis neither intercalary sclerite. *Heser schmitzi* was trasfered from *Zelotes* by Senglet (2012), who called the intercalary

sclerite an "embolar base". However, it is a separate sclerite, located between the tegulum and terminal apophysis. *Hemicloea, Trochanteria* and *Vectius*: there is a small sclerite seen on expanded bulb (scored 1).

241. Palp, copulatory bulb, median apophysis: absent = 0; present = 1 (Figs 24, 25). The median apophysis is a projection that arises from a membranous median area on the tegulum, near the concave side of the sperm duct. *Cithaeron*: it may act like a conductor, but its position suggests it is a median apophysis (scored 1).

242. Palp, copulatory bulb, median apophysis, proximal, numerous small spines (granulation): absent = 0; present = 1.

243. Palp, copulatory bulb, median apophysis, sclerotization: completely sclerotized = 0; partially sclerotized = 1; not sclerotized = 2.

244. Palp, copulatory bulb, median apophysis, terminal hook: absent = 0; present = 1.

245. Palp, copulatory bulb, accessory median apophysis: absent = 0; present = 1. The accessory median apophysis is a sclerite on the terminal part of the tegulum, distal in relation to median apophysis and associated to the embolus, probably functioning as a conductor. *Anyphaena accentuata*: not clear if it belongs to terminal or median division of bulbus but, according to criteria herein, it is most likely an accessory median apophysis (scored 0; see Ramírez, 1995 and references therein for discussion of terms used for this structure). *Neodrassex aureus*: the structure Ott (2012) called embolus is actually an apophysis terminal on tegulum that acts like a conductor (scored 1; Fig. 23D–F).

246. Palp, copulatory bulb, membranous tegular extension: absent = 0; present = 1. It is a membrane distally situated on tegulum (see chapter 3 of this thesis). *Apodrassodes guatemalensis:* it is not clear if the membranous area is really terminal on tegulum (score 1).

247. Palp, copulatory bulb, membranous tegular extension, type: long, with sulci to support the embolus = 0; short = 1.

248. Palp, copulatory bulb, petiole: absent = 0; present = 1. Smal sclerite on the alveolus of the cymbium, which connects the cymbium to the subtegulum.

249. Palp, copulatory bulb, subtegulum, locking lobe: absent = 0; present = 1. The subtegulum has a lobe that fits a corresponding lobe on the tegulum (Griswold et al. 2005: char. 115).

250. Palp, copulatory bulb, subtegulum, proximal projection: absent = 0; present = 1. It is a projection near the fundus.

251. Palp, copulatory bulb, tegulum, distal tegular projection: absent = 0; present = 1.

252. Palp, copulatory bulb, tegulum, distal tegular spine-like process: absent = 0; present = 1. This projection is located on the terminal part of the tegulum, near the embolus base, and is found in *Cryptoeritus occultus*.

253. Palp, copulatory bulb, tegulum, proximal part: uncovered = 0; covered by the subtegulum = 1.

254. Palp, copulatory bulb, terminal apophysis: absent = 0; present = 1. The terminal apophysis is a sclerite on the terminal division of bulbus, proximally and ventrally positioned in relation to embolus and connected (fused or not) to embolar base (Fig. 25). *Heser schmitzi*: according to Senglet (2012) there is no terminal apophysis, but there is a terminal sclerite, ventral to embolus and connectet to it (scored 1). *Zelotibia simpula*: there is a small lightly sclerotized terminal structure on the tegulum, but it is uncertain if it could be considered a terminal apophysis (scored 0).

255. Palp, copulatory bulb, terminal apophysis, distal part, shape: simple, undivided = 0; bifid = 1. Present in *Camillina* (Platnick & Shadab, 1982a).

256. Palp, copulatory bulb, terminal apophysis, sheet shaped sclerite surrounding the embolus: absent = 0; present = 1. *Echemoides* and *Zimiromus* have a long membranous sclerite that surrounds the embolus. Based on the trajectory of the spermatic duct, it seems to belong to the terminal division of bulbus, since it is distal to the beginning of the ejaculatory duct and closely associated to the embolus. Also, in *Echemoides aguilari* this sclerite is distal to an accessory median apophysis. So, given its topology, it was considered a terminal apophysis. However, it might not be a homologue to the terminal apophysis of Zelotinae, since it is not detached from the tegulum and is morphologically very different. This character was then, created to accommodate this difference.

257. Palp, cymbium, dorsal, terminal, chemosensory patch: absent = 0; present = 1 (Ramírez, 2014: char. 324).

258. Palp, cymbium, dorsal, trichobothria: absent = 0; present = 1. *Lampona cylindrata*: scored 1 (against Ramírez 2014).

259. Palp, cymbium, retrolateral, median process (projection): absent = 0; present = 1. The incision in *Apopyllus* is considered a median process, forming a conductor-like structure.

260. Palp, cymbium, retrolateral, median process, type: without incision = 0; with incision, forming a conductor-like canal = 1 (cymbial incision in see chapter 3 of this thesis).

261. Palp, cymbium, retrolateral, proximal process: absent = 0; present = 1. Present in *Nopyllus* (Ott, 2014).

262. Palp, cymbium, ventral, apex, size: short = 0; long = 1.

263. Palp, cymbium, ventral, terminal, bunch of thick setae: absent = 0; present = 1 (Ramírez, 2014: char. 326).

264. Palp, femur, distal, dorsal process: absent = 0; present = 1.

265. Palp, femur, distal, prolateral, process: absent = 0; present = 1.

266. Palp, femur, median, ventral, process: absent = 0; present = 1 (Ramírez, 2014: char. 306).

267. Palp, tibia, retrolateral tibial apophysis: absent = 0; present = 1. *Zelotibia simpula*: very small projection. The structure identified as a RTA by Nzigidahera & Jocqué (2009) is here called Proximal Retrolateral Tibial Apophysis.

268. Palp, tibia, retrolateral tibial apophysis, position: retrolateral = 0; shifted dorsally = 1.

269. Palp, tibia, retrolateral tibial apophysis, type: laminar = 0; almost conical or spine-like = 1.

270. Palp, tibia, retrolateral tibial apophysis, elaborated folds: absent = 0; present = 1. Applicable only if the RTA is laminar, as seen in *Apopyllus* (see chapter 3 of this thesis).

271. Palp, tibia, retrolateral tibial apophysis, ventral lobe: absent = 0; present = 1.

272. Palp, tibia, ventral tibial apophysis: absent = 0; present = 1.

273. Palp, tibia, ventral tibial apophysis, type: singular = 0; bifid = 1.

274. Palp, tibia, dorsal tibial apophysis: absent = 0; present = 1.

275. Palp, tibia, prolateral tibial apophysis: absent = 0; present = 1.

276. Palp, patellae, retrolateral apophysis: absent = 0; present = 1.

277. Palp, tibia, proximal retrolateral tibial apophysis: absent = 0; present = 1.

Morphometrics-defined characters

278. Cephalothorax, dorsal, carapace, overall shape: longer than wide = 0; wider than long = 1. See Supplementary Material.

279. Cephalothorax, dorsal, carapace, anterior margin shape: with a cephalic moderate constriction and convex anterior margin = 0; without a cephalic constriction and straight to concave anterior margin = 1. See Supplementary Material.

280. Cephalothorax, ventral, sternum, overall shape: longer than wide = 0; wider than long = 1.

281. Cephalothorax, carapace, dorsal, cephalic area, posterior eye row, shape: procurved = 0; straight to recurved = 1. See Supplementary Material.

Spinnerets

282. Abdomen, anterior lateral spinnerets, basal article, whorled setae: absent = 0; present = 1.

283. Abdomen, anterior lateral spinnerets, distal article: complete sclerotized ring = 0 (Fig. 13A, B); incomplete ring = 1 (Figs 11, 12, 14, 15; Platnick 2000: char. 15; Platnick, 2002: char. 3; Ramírez, 2014: char. 247).

284. Abdomen, anterior lateral spinnerets, distal article, incomplete ring, type: semi-circle in the anterior margin = 0 (Figs 11E, F, H; 12); patches of setae on the base of spigots = 1 (Fig. 11A–D, G).

285. Abdomen, anterior lateral spinnerets, distal article, sensory seta near piriform gland spigot: absent = 0; present = 1 (Fig. 12F).

286. Abdomen, anterior lateral spinnerets, distal article, setae, elevated base: absent = 0; present = 1.

287. Abdomen, anterior lateral spinnerets, distance between them in relation to their diameter: slightly separated = 0; separated about one ALS diameter or more = 1.

288. Abdomen, anterior lateral spinnerets, length in relation to abdomen: more than 25%= 0; less than 25%= 1 (Platnick & Baehr, 2006: char. 5.)

289. Abdomen, anterior lateral spinnerets, position: next to other two pairs = 0; anteriorly placed = 1.

290. Abdomen, anterior lateral spinnerets, sclerotization: light = 0; heavy = 1.

291. Abdomen, anterior lateral spinnerets, shape: conical = 0; cylindrical = 1; compressed laterally = 2.

292. Abdomen, anterior lateral spinnerets, spinning field, inflatable membrane: absent = 0 (Fig. 13A, B); present = 1 (Fig. 12A).

293. Abdomen, anterior lateral spinnerets, major ampullate gland spigot field, conical setae bearing projection: absent = 0; present = 1 (Figs 11B, D; 14A).

294. Abdomen, anterior lateral spinnerets, piriform gland spigots, base length relative to shaft: shorter or as short as = 0 (Figs 12; 13; 15); longer = 1 (Fig. 11). Platnick (2000, 2002) assumed dependence between plumose setae and elongated base of spigots, and coded both as a single character. However they are independent and each one should be considered a different character.

295. Abdomen, anterior lateral spinnerets, piriform gland spigots, base width in relation to MaAm: about the same = 0 (Fig. 13); greatly widened = 1 (Figs 11; 12A–D, F–H; 14; 15).

296. Abdomen, anterior lateral spinnerets, piriform gland spigots, length relative to the major ampullate gland spigots: shorter or about as long as = 0 (Figs 12E; 13); longer = 1 (Figs 11; 12 A–D, F–H; 14; 15).

297. Abdomen, anterior lateral spinnerets, piriform gland spigots, plumose setae base (with barbs): absent = 0; present = 1 (Ramírez, 2014: char. 270).

298. Abdomen, anterior lateral spinnerets, piriform gland spigots, shaft fused to base: absent = 0 (Fig. 12C, E, G); present = 1 (Fig 12A, B, D, H).

299. Abdomen, anterior lateral spinnerets, piriform gland spigots, shaft width relative to base: narrower = 0 (Fig. 13B, D); as wide as base, with broad openings = 1 (Figs 12; 13C).

300. Abdomen, posterior lateral spinnerets, distal, long spigots on a flat non-distensible pad: absent = 0; present = 1 (Fig. 19C).

301. Abdomen, posterior median and lateral spinnerets, modified interdigitate setae: absent = 0; present = 1 (Platnick, 1990). Same as claviform setae in Ramírez (2014: char. 292).

302. Abdomen, posterior median spinnerets, minor ampullate gland spigot, shaft: about the same size as the aciniform = 0; reduced to needlelike extension = 1.

303. Abdomen, posterior median spinnerets, position: posterior to ALS = 0; anteriorly advanced, in same line as ALS = 1.

304. Abdomen (F), anterior lateral spinnerets, anterior (ectal) major ampullate gland spigots, shaft and base, thickness relative to posterior (mesal): anterior (ectal) thinner = 0; same size = 1; anterior thicker = 2.

305. Abdomen (F), anterior lateral spinnerets, major ampullate gland spigots, ectal spigots: absent = 0 (Fig. 11B); present, functional or as a nubbin = 1 (Figs 11E; 12B).

306. Abdomen (F), anterior lateral spinnerets, major ampullate gland spigots, mesal spigots: absent = 0; present = 1.

307. Abdomen (F), anterior lateral spinnerets, major ampullate gland spigots, mesal spigots, type: normal = 0 (Fig. 12B); nubbin = 1 (Fig. 11E).

308. Abdomen (M), anterior lateral spinnerets, major ampullate gland spigots, ectal spigots: abset = 0; present = 1.

309. Abdomen (M), anterior lateral spinnerets, major ampullate gland spigots, mesal spigots: absent = 0; present = 1.

310. Abdomen (M), anterior lateral spinnerets, major ampullate gland spigots, mesal spigots, type: normal = 0; nubbin = 1.

311. Abdomen, anterior lateral spinnerets, major ampullate gland spigots, position: touching basal article border = 0 (Fig. 11B, D, G); far from the border = 1 (Fig. 11E, H).

312. Abdomen (F), anterior lateral spinnerets, piriform gland spigots: absent = 0; present = 1.

313. Abdomen (M), anterior lateral spinnerets, piriform gland spigots: absent = 0; present = 1 (Fig. 16A, C).

314. Abdomen (F), anterior lateral spinnerets, piriform gland spigots position: only on the edge = 0 (Fig. 12A, B, D, H); at the edge and in the middle of spinnerets = 1 (Fig. 12C, E, G).

315. Abdomen (F), anterior lateral spinnerets, spinning field, furrow between major ampullate and piriform gland spigots: absent = 0; present = 1. Adapted from Ramírez (2014: char. 264).

316. Abdomen (M), anterior lateral spinnerets, spinning field, furrow between major ampullate and piriform gland spigots: absent = 0; present = 1. Adapted from Ramírez (2014: char. 264).

317. Abdomen (F), posterior lateral spinnerets, aciniform gland spigots: absent = 0; present = 1.

318. Abdomen (M), posterior lateral spinnerets, aciniform gland spigots: absent = 0; present = 1.

319. Abdomen (F), posterior lateral spinnerets, cylindrical gland spigots: absent = 0; present = 1.

320. Abdomen (F), posterior lateral spinnerets, minor ampullate gland spigots: absent = 0; present = 1 (Fig. 18). Same as "Modified Spigots" in Griswold *et al.* (2005: char. 96) and Ramírez (2014: char. 296).

321. Abdomen (M), posterior lateral spinnerets, minor ampullate gland spigots: absent = 0; present = 1.

322. Abdomen (F), posterior median spinnerets, aciniform gland spigots: absent = 0; present = 1.

323. Abdomen (M), posterior median spinnerets, aciniform gland spigots: absent = 0; present = 1.

324. Abdomen (F), posterior median spinnerets, cylindrical gland spigots: absent = 0; present = 1.

325. Abdomen (F), posterior median spinnerets, cylindrical gland spigots in parallel rows: absent = 0; present = 1.

326. Abdomen (F), posterior median spinnerets, cylindrical gland spigots, separated field: absent = 0; present, the Cy are not mixed with other spigots = 1 (Ramírez, 2014).

327. Abdomen (F), posterior median spinnerets, spinning field, deep constriction: absent = 0; present = 1 (Fig. 20G; Murphy, 2007).

328. Abdomen (F), posterior median spinnerets, minor ampullate gland spigots: absent = 0; present = 1.

329. Abdomen (M), posterior median spinnerets, minor ampullate gland spigots: absent = 0; present = 1.

330. Abdomen (F), posterior median spinnerets, minor ampullate gland spigots, number: two = 0; one plus nubbin = 1; one = 2.

331. Abdomen (M), posterior median spinnerets, minor ampullate gland spigots, number: two = 0; one plus nubbin = 1; one = 2.

332. Abdomen, spinnerets, major ampullate and aciniform gland spigots, shaft, shape: cylindrical or tapering = 0; clavate = 1 (Ramírez, 2014: char. 250).

333. Abdomen, spinnerets, spigot, insertion articulation, type: simple = 0; annulate, flexible = 1 (Ramírez, 2014: char. 238).

334. Abdomen, ventral, posterior, colulus: absent = 0; present = 1.

335. Abdomen, ventral, posterior, colulus type: plate with few hairs = 0; well defined lobe =1. Only state 0 was observed in this dataset.

Inactive characters

The following characters show some variation and were tentatively scored. However, they could not be clearly separated into discrete states and, therefore, were treated as inactive during search. They were kept in matrix for documentation, since they could be useful for further studies.

336. Abdomen, anterior lateral spinnerets, major ampullate gland spigots, location: mesal margin = 0; anterior margin = 1; intermediate = 2. Inactive: Not clear the difference between mesal and anterior.

337. Abdomen, anterior lateral spinnerets, basal article, distal rim, plumose setae: absent = 0; present = 1. Inactive: Homology between seta is hard to determine.

338. Abdomen, anterior lateral spinnerets, distal article, setae kind: plumose = 0; minutely plumose = 1; aculeate = 2. Inactive: Homology between seta is hard to determine.

339. Abdomen, anterior lateral spinnerets, piriform gland spigots, shaft sclerotization: lightly = 0; heavily = 1. Inactive: level of sclerotization is har to distinguish.

340. Abdomen, antero-dorsal, tuft of setae, type: Aculeate = 0; minutely plumose = 1. Inactive: Homology between seta is hard to determine.

341. Abdomen, dorsal, anal tubercle, setae: Plumose = 0; minutely plumose = 1; Aculeate = 2. Inactive: Homology between seta is hard to determine.

342. Cephalothorax, carapace, dorsal, posterior margin, shape: not reflected anteriorly = 0; reflected anteriorly with narrow rim = 1; reflected anteriorly with broad rim = 2. Inactive: geometric morphometrics shows that there is no continuous variation between reflected anteriorly and not reflected. The difference in shape is represented by two characters defined by GM: overall shape and anterior margin shape (Platnick, 2002: char. 13.).

343. Cephalothorax, sternum, posterior edge: projected between coxae IV = 0; not projected between coxae IV = 1. Inactive: morphometrics shows that there is continuous variation between projected and not projected between coxa, but there is a discrete difference between elongated and almost rounded sterna.

344. Cephalothorax, carapace, frontal, cephalic area, anterior eye row, shape: procurved = 0; straight = 1. Inactive: geometric morphometrics shows that it is a continuum of variation.

345. Chelicerae, paturon, anterior surface, weakly sclerotized oval area: absent = 0; present = 1. Inactive: several taxa seem to have a little more unsclerotized area. It is harder to determinie, especially in taxa with pale cuticle (Platnick, 2000: char. 17.).

Appendix 2. Material examined.

Ammoxenidae

Ammoxenus coccineus

CAS 9051663: 2 M, 1 F. Namibia, Erongo, Gobabeb. 2/VI/1979. Wharton

CAS 9051664: 1 F. Namibia, Aasvölnes. 16/VI/1991. V.Roth & B. Roth

Rastellus africanus

AMNH: 3 M, 3 F. Botswana, Okavango Delta. Mopane woodland. 3/X/1975.

Anyphaenidae

Anyphaena acentuata

AMNH: 2 M, 2 F.

Cithaeronidae

Cithaeron praedonius

AMNH: 1 F. Libya, Wadi Kuf. 24/I/1960. JALC

AMNH: 1 M, 1 F. U.S.A, Florida, Passo, Port Richey. 20/VI/2011. J.T. stiles

UFMG 14503: 1 M, 1 F. Brazil, Piauí, Teresina, Bairro Morada do Sol. I/2014. L.S. Carvalho

Gallieniellidae

Galianoella leucostigma

AMNH: 1 F. Argentina, Salta, Chuscha, 6km NW Cafayate. 20/XI/1995. P. Goloboff

CHNUFPI 161: 1 M. Brazil, Piauí, Guaribas, Parque Nacional da Serra das Confusões. 9-15/XII/2010. L. S. Carvalho et. al.

Gallieniella mygaloides

AMNH: 1 F. Madagascar, Anjavidilava, massif de l'Andringitra. 15/I/1971. J.M. Betsch

AMNH: 2 M, 1 F. Madagascar, Tananarive:col du Tsiafajavona, massif de 18 Ankaratra. II/1967. R. legendrene & J.M. Betsch

CAS 9051641: 1 F, 8 J. Madagascar, Fianarantsoa, Res. Andringitra, 8.5km SE Antanitotsy. 6/III/1997. B.L. Fisher

CAS 9064158: 1 M. Madagascar, Sofia Region, Anjiamangirana, 45km S Antsohihy, Analagnambe, Analagnambe Gallery forest, 5Km W Anjiamangirana. 25-2/IV-V/2013. M. Irwin & H. Rinha

Meedo hustoni

CAS 9051640: 1 F. Australia, Western Australia, Milly Milly. 6/X/1962.

Gnaphosidae

"Megamyrmaekion" nr. transvaalicus

MNRJ 6661: 1 F. África do Sul, Gauteng, Pretoria, Groenkloof Nature Reserve. 29/X/2002. A. Kury

Amazoromus kedus

AMNH: 1 M. , Amazonas, Manaus, Reserva Ducke. 14/X/1991.

INPA 114: 1 F. Brazil, Amazonas, Manaus, Reserva Ducke. 17/VIII/1992. Hofer & Gasnier

INPA 28: 1 M. Brazil, Amazonas, Manaus, Reserva Ducke. 30/XI/1991.

Anagraphis pallens

MCZ 69794: 1 M, 1 F. Israel, Sede Boqer, Hatira Ridge. 5/VII/1993. Y. Lubin

MCZ 69795: 1 M, 1 F. Israel, Wad I Mashash. 23/VII/1992. Y. Lubin

Aneplasa facieis

CAS 9058646: 1 F, 1 J. South Africa, Cape Province, Oudtshoorn. 29/X/1949. Malkin

Anzacia gemmea

CAS 9051590: 1 M. New Zeland, South Island, Arthur's Pass, outside youth hostel. 21/III/1995. J. Boutin

CAS 9051644: 1 F. New Zeland, South Island, Queen Charlotte Sound. III-IV/1993. J. Boutin

CAS 9051645: 1 F. New Zeland, South Island, Mosgiel, Outram Bridge Taieri River. 28/III/1995. J. Boutin

Aphantaulax cincta

MCZ 33036: 1 F. Not in Phylogeny.

Aphantaulax sp.

CAS 9064210: 1 M. Madagascar, Andrefana Region, District of Horombe, Vohibasia National Park. 15-22/VIII/2011. M. Irwin & H. Rinha

CAS 9064211: 1 F. Madagascar, Andrefana Region, District of Horombe, Vohibasia National Park. 10-17/VI/2011. M. Irwin & H. Rinha

Apodrassodes guatemalensis

MCN 29246: 2 M. Brazil, Rio Grande do Sul, Bom Jesus. 28-30/III/1998. A. B. Bonaldo

MCTP 460: 2 M, 16 F, 13 J. Brazil, Quillota, Rio Grande do Sul. 24-28/V/1991. A.A. Lise

Apopyllus silvestrii

CAS 9051658: 1 M. Bolivia, Potosi. 22/II/1951.

CAS 9051659: 1 F. Argentina, Chubut, Shaman. 19/XI/1966. E.I. Schingler & M.E. Irwin

CAS 9051660: 1 F. Bolivia, Potosi. 23/II/1951.

Arauchemus graudo

MCN 47666: 2 M. Brazil, Rio Grande do Sul, São Francisco de Paula. 14/IV/2002. R. Ott

MCN 47673: 1 F, 1 J. Brazil, Rio Grande do Sul, São Francisco de Paula. 11/X/2001. R. Ott

Arauchemus miudo

MCN 47700: 4 F. Brazil, Rio Grande do Sul, São Francisco de Paula, Porteiro Velho. 13/XI/2001. R. Ott

Asemesthes albovittatus

CAS 9058616: 1 F.

Asemesthes montanus

USNM : 1 M. South Africa, Free State, Brandford, Florisbad. 21/X/1985. L.N. Lotz

Australoehemus celer

CAS 9067682: 1 M. Curaçao, , Carmabi Institute. 7/X/2004.

CAS 9067686: 1 F. Bonaire, , DROB. 6/XII/2004. G. van Hoorn

Berinda amabilis

DUT 859: 1 M, 1 F. Greece. 17-22/V-VII/1998.

Berlandina plumalis

MCZ 33661: 1 M, 1 F. Israel, Sede Boqer, Halukim Ridge. 5/VII/1993. Y. Lubin

MCZ 33695: 1 M, 1 F. Israel, Sede Boqer, Halukim Ridge. 5/VII/1993. Y. Lubin

Callilepis gosoga

CAS 9048349: 9 M, 2 F. U.S.A, California, Riverside, Whitewater Cyn. R.L. Aalbu

CAS 9051227: 1 F. U.S.A, California, Stabislaus, PG&E Plant Site; 5 miles n Turlock Lake. 26/V/1976. J.Colins

CAS 9051304: 1 M. U.S.A, California, Santa Clara. 30/V/1971.

CAS 9051363: 1 M. U.S.A, California, Inyo, Birchum Springs. 30/V/1997. G. Pratt et al.

CAS 9051416: 1 F. U.S.A, California, Inyo, Coso Village. 30/V/1997. G. Pratt et al.

Callilepis nocturna

AMNH: 2 M, 2 F. Austria, Innsbruck-Umgebung Fallen. V-VII/1964.

Camillina cordifera

AMNH: 3 M, 4 F. Botswana, Maxwee.

AMNH: 4 M, 3 F. South Africa, Transvaal, Pretoria. 4-28/I/1980. J. Peck

Cesonia bilineata

CAS 9051599: 1 M. U.S.A, Arkansas, Mississippi. 16-23/VI/1966.

CAS 9058792: 1 M. U.S.A, Arkansas, Washington, Cove Creek. 3/V/1963. O. & M. Hite

CAS 9058793: 1 F. . 26/VII/1964.

CAS 9151600: 1 F. U.S.A, Arkansas, Bradley. VI-VII/1963. Leslie

Cryptodrassus creticus

MariaGrecia 8432: 3 M, 1 F. Greece, Astypalaia, Agia Kyriaki isl. 25-11/IV-VI/2005.

Drassodes lapidosus

MCN 23585: 4 M, 2 F. Germany, Albshausen, Witzenhausen. 15/V/1993. A. D. Brescovit

Drassodes saccatus

CAS 9051356: 1 F. U.S.A, California, Stanilaus, Frank Raines Park. 4/IV/1970. S.C. Williams

CAS 9051587: 1 F. U.S.A, Washington, Vantage. 28/IV/1936. M.H. Hatch

CAS 9051587: 1 M, 1 F. U.S.A, Washington, Vantage. 26/IV/1936.

CAS 9051589: 2 M. U.S.A, Kansas, Riley. 16/V/1964.

CAS 9051649: 1 M. U.S.A, Nevada, Sheldon Wildlife Refuge. VIII/1947. J.C. Exline

Drassodex lesserti

MZSP 13751: 1 M, 1 F. Germany.

Drassyllus fallens

MCZ 33506: 1 M, 1 F, 1 J. U.S.A, Michigan, Calhoum, Albium. 18/V/1935. A.M. Chickering

MCZ 33515: 3 F. U.S.A, Pennsylvania, Gettysburg. 20/VI/1960. R.D. Barnes

Echemoides aguilari

CAS 9058763: 1 M, 2 F.

MUSM 504986: 1 M, 1 F, 4 J. Peru, Ica, Paracas. 19-20/VI/1999.

Eilica bicolor

AMNH: 1 F. U.S.A, Florida, Sebring. 1/III/1960.

AMNH: 1 M. U.S.A, Florida, Monroe, Cudjoekey. 29-14/VIII-XIII?/1986. S. & J. Peck

Gertschosa amphiloga

CAS 9058796: 1 F. Mexico, Colima. XII/1929. S.F. Light

Gertschosa concinna

CAS 9051602: 1 M. Mexico, Islas Tres Marias, M.M. Zóre. 13-23/V/1925. H.H. Keifer

Gnaphosa californica

CAS 9049342: 1 F. U.S.A, California, Modocco, 5 mi w Canby. 30/VI/1974. C. Griswold

CAS 9049584: 2 M. U.S.A, California, Alameda, Grizzly Peak Bvd.. 10/VI/1962. P.R. Craig et al.

CAS 9051585: 6 F, J. U.S.A, Oregon, Carvallis. J. Kincaid

CAS 9051586: 1 M, 1 J. U.S.A, Washington, Wenatchee. 14/V/1932.

Gnaphosa clara

CAS 9051666: 4 F. U.S.A, New Mexico, Socorro. 18/VI/1949. Wheeler Exline

CAS 9051667: 1 M. U.S.A, Nevada, Washoe, 3 miles N. of Nixon. 21/VI/1960. D.C. Rentz

Haplodrassus chamberlini

CAS 9051592: 1 M. U.S.A, Colorado, Fremont, Wet mountains. 7/V/1964. B.H. Bbanta

CAS 9051593: 1 M. U.S.A, Colorado, El Paso, Peyton Road. 2/V/1964. B.H. Banta

Haplodrassus hiemalis

MCZ 33035: 1 F. Canada, Ontario, Thunder Bay Dist, Klotz Lake, 25 miles east of Longlac. Summer/1960. D. Windle

MCZ 33675: 1 M. U.S.A, Massachusetts, Essex, Ipswich River, Topsfield. 15/V/1915. J.H. Emerton Collection

MCZ 33689: 1 M. U.S.A, Massachusetts, Worcester, Grafton. J.H. Emerton Collection

Herpyllus eclesiasticus

CAS 9051591: 1 M. U.S.A, Arkansas, Mississippi. 9 -15/VI/1966.

CAS 9051646: 1 M. U.S.A, Missouri, Rolla. 29/V/1949. H.E.F.

CAS 9051647: 2 F. U.S.A, Missouri, Johnson, Portle Springs. 5/VIII/1961. W. Peck

CAS 9051648: 1 M. U.S.A, Texas, Austin. 1-10/VIII/1945. H.E.F.

Heser schmitzi

CAS 9029973: 1 M, 1 F. U.S.A, California, Marin, San Rafael, 8 Park Ridge Rod. 8-14/VIII/2014. Jere Schweikert

Hypodrassodes maoricus

CAS 9058742: 1 M, 2 J. New Zeland, South Island, Greymouth. 20/III/1993. J. Boutin

CAS 9058743: 2 F. New Zeland, North Island, Wellington, Town belt, Hay Street. I-II/1995. J. Boutin

Kishidaia albomaculata

CAS 9051629: 1 F, 1 J. Russia, Siberia, Moneron Island, SSE shore, Usovo Creek. 24/VIII/2001. Y.M. Marusik

Latonigena auricomis

MCN 13406: 1 F. Brazil, Rio Grande do Sul, Porto Alegre. 7/IX/1985. A. D. Brescovit

MCN 16582: 1 M. Brazil, Rio Grande do Sul, Rio Grande. 4/XII/1986. E. H. Buckup

MCN 21955: 1 M. Brazil, Rio Grande do Sul, Porto Alegre. 18/I/1992. M. A. L. Marques

MCN 43575: 1 F. Brazil, Rio Grande do Sul, Porto Alegre. 23/IX/2007. M. C. Pairet Jr

Leptodrassex sp.

CAS 9058718: 1 F. Kenya, Nairobi, Magadi Road, 33mi N Magadi. 24/XI/1957.

Leptodrassus albidus

DUT 476: 117 F. Greece. 20-26/V-VII/1999.

Leptopilos levantinus

DUT : 1 F. Greece.

DUT 894: 1 M. Greece. 30-01/VI-IX/1998.

Litopyllus temporarius

CAS 9058744: 1 M. U.S.A, Missouri, Johnson, Wsrrensburg. 6/V/1964. W. Peck

CAS 9058745: 1 F. U.S.A, Missouri, Johnson, Wsrrensburg. 1/VI/1963. W. Peck

Micaria gosiuta

CAS 9048287: 1 F. U.S.A, California, Inyo, Big Pine. 6/X/1986. D. Giuliani

CAS 9048499: 3 M, 1 F. U.S.A, California, Mono. 2-IX-1980 a 22-IV-1981. D. Giuliani

CAS 9051596: 1 M. U.S.A, Nevada, Lincon, Dry Lake Valley. III-XI/1986. D. Giuliani

CAS 9051654: 1 M, 2 F. U.S.A, Nevada, Lincon, Meadow Valley Range, Oak Springs Summit.

Microsa chickeringi

MCZ 60749: 4 F. U.S.A, Virgin Islands, St. Thomas. VIII/1966. A.M. Chickering

Minosia simeonica

MCZ 60750: 8 M. Israel, , Sede Boqer, Sede Zin. 2/X/1992. Y.D. Lubin

MCZ 60751: 2 F. Israel, , Ma'ale Ramon. 2/XI/1992. Y.D. Lubin

Nauhea tapa

CAS 9058802: 1 M. New Zeland, Otago, Blue Mountains, tussock grasslands. 27/III/1995. J. Boutin

Neodrassex aureus

MCN 17305: 3 F. Brazil, Paraná, Curitiba. 2/XI/1987. A. D. Brescovit

MCN 21574: 1 M. Brazil, Amazonas, Manaus. 16/X/1985. B. C. Klein

Nodocion ecclecticus

CAS 9048447: 1 M, 1 J. U.S.A, California, Napa, N. side Howell Mt. 3km NNE of Angwin. 8/VIII/1984. H.B. Leech

CAS 9058750: 1 F. México, Baja California, Sur Isla Santa Catalina. 21/V/1970. S.C. Willians & V.F. Lee

Nomisia ausseri

CAS 9058749: 4 M, 7 F. Kazakhstan, Almaty, Kapcagay. 26/VIII/1992. Masusik, Logunov, Eskov

Nopyllus sp.

IBSP 149352: 1 M. Brazil, Paraná, Foz do Iguaçu, Parque Nacional do Iguaçu. 3-12/III/2002. Eq. Biota

IBSP 149353: 1 M. Brazil, Paraná, Foz do Iguaçu, Parque Nacional do Iguaçu. 3-12/III/2002. Eq. Biota

Notiodrassus distinctus

CMNZ 2015.4.1: 1 F. New Zeland, Otago, Dunedin, 47 Hunt St. Anderson Bay. 19/V/2014.

CMNZ 2015.4.1: 1 F. New Zeland, Otago, Dunedin, Nichols Falls. 22/V/2014.

UFMG tombar: 1 M. New Zeland, Otago, Dunedin, 47 Hunt St.. 7/X/2015.

Odontodrasus aphanes

MCZ 60710: 4 F, 1 J. Jamaica, St. Andrew, Liguanea. 15/X/1957. Chickering

MCZ 60711: 2 M. Jamaica, St. Andrew, Liguanea. 15/X/1957. Chickering

MCZ 60713: 3 M, 2 F. Jamaica, Middlesex, St. Catherine, 1.5 mi S-w of Spanish town. 10/X/1957. Chickering

Orodrassus coloradensis

MCZ 33485: 2 M, 3 F. U.S.A, Utah, Summit, Chalk Creek. 1917. R.V. Chamberlin

Parasyrisca orites

CAS 9058769: 1 F. U.S.A, Washington, Paradise Park, Mt. Rainier.

Phaeocedus braccatus

USNM : 1 F. Russia, Maritime provence, Lazovski Res. Korpad' Camp.. 6-9/VIII/1998. Y.M. Marusik

Pterotricha conspersa

MCZ 60755: 1 M, 2 F. Israel, , Machtesh Ramon. 19/IV/1993. Y. Lubin

Scopoides catharius

AMNH: 1 M. U.S.A, California, San Diego, Mt. Palomar. 30/VI/1956. W. Gertsch

CAS 9048199: 1 F. U.S.A, California, Inyo, Quens Valley, 3 miles n.n.w. of Lone Pine. 31/XII/1980. Derham Giuliani

Scotocesonia dermerarae

MZLS 196: 1 F. Guyana.

Scotognapha teideensis

AMNH: 1 F. Canary Island, Tenerife, Las Cañadas. 7/X/1995. N. Zurita

AMNH: 1 M. Canary Island, Tenerife, Las Cañadas. 29/VI/1995. N. Zurita

Scotophaeus blckwalli

CAS 9044775: 1 M. U.S.A, California, San Francisco, in bldg.. 6/X/1994. C. Griswold

CAS 9044781: 1 F. U.S.A, California, Contra Costa, Concord, in hause. 18/VII/1994. J. Goutier

Sergiolus capulatus

CAS 9051665: 1 M. U.S.A, Missouri, Johnson, Wsrrensburg. 1/VI/1963. W. Peck

CAS 9058747: 1 F. U.S.A, Missouri, Johnson, Wsrrensburg. 2/VI/1961. W. Peck

CAS 9058748: 1 M. U.S.A, Arkansas, Bradley, Sumpter Comm.. 18/V/1963. Leslie

Setaphis subtilis

AMNH: 4 M, 2 F. Cote D'Ivoire, Bafing, Touba. 23/VII/1994.

AMNH: 3 M, 4 F. Ethiopia, , Awash National Park. 22/VI/1988.

Sidydrassus shumakovi

PSU 3723: 1 M, 1 F. . 11/VI/2003.

Sosticus insularis

CAS 9058751: 1 F. U.S.A, Missouri, Johnson, Wsrrensburg. 22-25/VI/1962. W. Peck

MCZ 33495: 1 M. U.S.A, Michigan, N.W. Marquette co. - N.E. Baraga co.. 13/VII/1948. Chickering

Synaphosus syntheticus

CAS 9051613: 1 M, 1 J. U.S.A, Georgia, Ashburn. 9/V/1968. J.A. Payne

CAS 9051628: 1 F. Mexico, Baja California, Beach at Palm Wells. 25-27/VI/1921.

CAS 9058752: 1 M. Mexico, Baja California, Isla Raza. 21/IV/1921. J.C Chammberlin

MCZ 60637: 1 M, 3 F. U.S.A, Texas, Brewster, Big Bend Nat. Park. 24-25/V/1967. E. Sabath

Talanites echinus

CAS 9051655: 1 F. U.S.A, Arkansas, Washington, Cove Creek. 25/III/1961.

CAS 9051656: 1 F. U.S.A, Arkansas, Washington. 25/IV/1961.

CAS 9051657: 6 M. U.S.A, Arkansas, Washington, Cove Creek. 12/V/1963.

Trachyzelotes pedestris

MCZ 60605: 1 M, 1 F. France.

Trephopoda parvipalpa

CAS 9058766: 1 M. South Africa, Cape Province, Oudtshoorn. 29/X/1949. B. Malkfu

Urozelotes rusticus

CAS 9044653: 1 M. U.S.A, California, Tulare, Ash Moutain, Kaweah Power Station #3. 29/III/1982. R.D. Haines

CAS 9049245: 1 F. U.S.A, California, Orange, La Habra. 17/IX/2001.

CAS 9049399: 1 F. U.S.A, California, Alameda, Redwood Regional Park, Roberts recreational Area.. 17/VI/1964. P.R. & D.L. Craig

CAS 9051339: 1 M. U.S.A, California, Fresno, 11 mi S Nendota, nr Cantua Ck.. 11-14/VI/1989. P. Sherrill

Xerophaeus capensis

NCA 2005/555: 1 M. South Africa, Western Cape, Potberg, De Loop Nature Reserve. 6/IV/2004. C. Haddad

NCA 2008/410: 2 M. South Africa, Western Cape, Jakobsbaii. 2/X/2001. C. Haddad & R. Lyle

Zelanda erebus

CAS 9051618: 1 F. New Zeland, South Island, Otago, Dunedin. 14-18/IX/1995. J. Boutin

CAS 9058754: 1 F. New Zeland, South Island, Otago, Dunedin. 12/IV/1993. J. Boutin

Zelanda kaituna

CAS 9058753: 1 M. New Zeland, South Island, Central Otago, Blue Mountain, tussok grasslands. 27/III/1995. J. Boutin

Zelotes duplex

CAS 9051594: 1 M. U.S.A, Arkansas, Nashiville. 25/V/1962.

CAS 9051595: 1 M. U.S.A.

CAS 9051650: 1 F. U.S.A, Missouri, Dent, Montauk Park. 21/VI/1961. H.E.F.

CAS 9051651: 2 M. U.S.A, Arkansas, Bradley. 11/V/1963. Leslie

CAS 9051652: 2 F. U.S.A, Arkansas, Bradley. 10/VIII/1963. Leslie

CAS 9051653: 14 M, 7 F. U.S.A, Arkansas, Bradley. VI-VII/1964.

Zelotibia simpula

CAS 9064176: 1 M, 1 F. Uganda, Western Uganda, Kabarole, Kibale National Park, Kanyawara Biological Station. 26-15/VII-VIII/2012. B. Fisher et al.

Zimiromus montenegro

MCN 32003: 2 M. Brazil, Rio Grande do Sul, Estrela Velha. 27/X/1999. A. F. Franceschini

MCN 40104: 2 F. Brazil, Rio Grande do Sul, Triunfo. 7/XII/2005. R. Ott & A. Barcellos

Lamponidae

Lampona cylindrata

QSM 26748: 2 M. Australia, Victoria, Snake gully, Monash University. VI/1975. V. Salanitri

Liocranidae

Liocranum rupicola

AMNH: 1 F. England, Purbeck Coast, Dorset, Seacombe. 26/V/1974.

AMNH: 1 M. Wales, Gower, Swansea, Nicholaston Burrows. 6/IV/1966.

Teutamus serrulatus

AMNH: 1 F. Malaysia, Pahang, 4mi NE Cameron. 25/IV/1977. L.E. Watrous

Xenoplectus sp.

MCTP 16001: 2 F. Brazil, Rio Grande do Sul, São Francisco de Paula, Porteiro Velho. XII/2001. L.A. Bertonello et al.

MCTP 23303: 2 M. Brazil, Rio Grande do Sul, São Francisco de Paula, Porteiro Velho. 12-15/X/1999.

Phrurolithidae

Drassinella gertschi

CAS 9058794: 1 M. U.S.A, California, Inyo, Alabama Hills, 2 mi w. of lone Pine. XII-III/1980-1981. D. Giuliani

CAS 9058795: 3 F. U.S.A, California, San Bernardino, Ft. Irwin Avawatz Mts. (spring). 26/V/1997. G. Pratt, W. Savary & D. Ubick

Phrurolithus festivus

CAS 9051630: 7 F. Russia, Siberia, Sakhalin Island, SE part Belaya River, middle fork near Skol Field Station. 16-21/VII-VIII/2001. Y.M. Marusik

CAS 9051636: 1 M. Russia, Siberia, Maritime provence, Lazovsky Reserve, Kordon Korpad'. 7/V/1999. Y. Sundukov

Prodidomidae

Chileuma paposo

AMNH: 4 M, 5 F. Chile, Antofagasta, 6 Km E Paposo. 12/X/1992. N. Platnick, K. Catley and P. Goloboff

Chilongius palmas

AMNH: 1 F. Chile, Quillota, Palmas de Ocoa, Parque Nacional La Campana, umburned sit, pitfall #13. 19/VII/1985. R. Calderón G.

AMNH: 1 M. Chile, Quillota, Palmas de Ocoa, Parque Nacional La Campana, umburned sit, pitfall #1. 30/XI/1984. R. Calderón G.

AMNH: 1 M, 1 F. Chile, Quillota, Palmas de Ocoa, Parque Nacional La Campana. 21/XII/1984. R. Calderón

Cryptoeritus occultus

WAM T44975: 2 M. Australia, Western Cape, Mardathuna Station. 14-24/I-IV/1995. A.Sampey

WAM T44980: 1 F. Australia, Weastern Australia, Nerren Nerren Station. 15-11/X-I/1994-1995. N.Mackenzie & J. Rolfe

Lygromma chamberlini

MCZ 78848: M, F, J. Panama, , Canal Zone, Barro Colorado Island. VI-VII/1943-1944. A.M. Chickering

MCZ 78854: 1 M, 1 F. Panama, , Canal Zone, Barro Colorado Island. VI-VIII/1949. A.M. Chickering

Moreno Grande

AMNH: 1 M, 1 F. Chile, Elqui, beach 6km S Cruz Grande. 7/X/1992. N. Platncik, P. Goloboff, K. Catley

AMNH: 2 M, 1 F. Chile, Elqui, 20Km N La Serena. 8/II/1994. N.Platnick, K. Catley, R. Calderón, R.T. Allen

Oltacloea beltraoe

UFMG 9309: 1 F. Brazil, Minas Gerais, Itacarambi, Parque Nacional Cavernas do Peruaçu. 17-22/X/2010. G.F.B.P. Ferreira et al.

Oltacloea sp.

IBSP 67175: 1 M. Brazil, Paraíba, Areia, Reserva Mata de Pau de Ferro. 26-29/IX/1999. A.D. Brescivit et al.

Prodidomus rufus

CAS 9036861: 1 F. U.S.A, California, Orange. 20/X/2002. I. Beck

CAS 9058764: 1 F. U.S.A, California, Inyo, 5.7 mi N Shoshone. 8/I/1981. V. Roth

MCZ 70333: 1 M. U.S.A, Texas, Denton. 4/XII/1946. S. Jones

MCZ 70334: 1 F. U.S.A, Texas, Dallas, Bluff View. 16/V/1935. S. Jones

Tivodrassus etaphor

AMNH: 1 F. Mexico, Hidalgo. 23/VII/1966.

MCZ 78843: 2 M, 1 F. Mexico, Oaxaca, Oaxaca. 7/VI/1971. S.B. Peck

Tricongius amazonicus

INPA 38: 1 M. Brazil, Amazonas, Manaus, Igapó Trumã Mirím. 3/X/1987. Hofer

INPA 39: 1 F. Brazil, Amazonas, Manaus, Igapó Trumã Mirím. 3/X/1987. Hofer

Zimiris doriai

MPEG 21962: 1 F. Brazil, Pará, Belém, Bairro Batista Campos. 13/II/2002. Barreiros, J.A.P.

Trochanteriidae

Doliomalus cimicoides

AMNH: 1 M.

CAS 9025484: 3 F.

Hemicloea sundevalli

QSM s36573: 1 M, 3 F. , , Boggomoss #7 (BS8). 13/VI/1996.

Plator indicus

MCZ 33623: 3 F. India, Uttarakhand, Mussoorie. IV-XII/1934.

Plator sp.

CAS 9025486: 2 M. Pakistan, , 2 Mi W of Cherat. 20/XII/1961.

Trochanteria gomezi

CHNUFPI 1307: 2 M, 6 F, 9 J. Brazil, Roraima, Boa Vista, Campus de Cauamé, Universidade Federal de Roraima. 22/VII/2014. L.S. Carvalho & M.C. Schneider

CHNUFPI 1571: 1 M. Brazil, Roraima, Boa Vista, Campus de Cauamé, Universidade Federal de Roraima. 22/VII/2014. L.S. Carvalho & M.C. Schneider

Vectius niger

CAS 9051661: 1 M. Paraguai, Guaira, Sierra San Cervacia. 6/VI/1988. V.D & B. Roth

CAS 9051662: 2 F, 5 J. Argentina, Salta. 14/II/1951.

Undertemined

Gnaphosoidea-TEX

CAS 9058805: 2 M. U.S.A, Texas, Brewster, Big Sandy. 11-28/VIII/2010. N.V. Horner

CAS 9058806: 1 F. U.S.A, Texas, Brewster, Big Sandy. 29-13/VIII-IX/2010. N.V. Horner

Supplementary Material for Cladistic analysis of the worldwide family Gnaphosidae

Geometric Morphometrics Analysis

Supplementary Material and Methods

Shape of structures is frequently used as discrete characters to reconstruct spider phylogeny or to diagnose taxa. The reliability of such separation into discrete states are rarely discussed, even though it has been show that carapace shape might not be efficient as a phylogenetic character for Mygalomorphae (Bond & Beamer, 2006). Here, Geometric Morphometrics (Rohlf, 1990; Adams et al., 2004; Zelditch et al., 2004; Slice, 2007) techniques were applied to evaluate if the shape of some structures could be used as discrete states characters in the phylogeny.

Geometric Morphometrics requires the establishment of homologous points known as landmarks. Sometimes, when some landmarks cannot be established with confidence, outlined-based technics (e.g.: semi-landmarks) might be used together with landmarks-based describe shape (Bookstein, 1997; Zelditch et al., 2004; Slice, 2007). However, structures with very variable shapes or with complex tri-dimensionality might offer impediments for shape analysis in two dimensions, since it might not be possible to determine landmarks and semi-landmarks with confidence. Based on this, five structures suitable for 2D morphometrics with landmarks and semi-landmarks were chosen: dorsal shape of carapace, ventral labium shape, ventral sternum shape, and the anterior and posterior eye rows. Images from digital camera and from scanning electronic microscopy were used to obtain the coordinates of landmarks and semi-landmarks for each structure (Figs. S1A-E) using tpsDig v.2.17 (Rohlf, 2013). The structures were analyzed separately, 84 species were sampled for cephalothorax analyses, 65 for posterior eye row, and 86 for the sternum. Landmarks and semi-landmarks were aligned using Procrustes superimposition and semi-landmarks were aligned using Minimum Procrustes Distance. A Relative Warp Analysis (RWA) with $\alpha = 0$, which is equivalent to a Principal Component Analysis of shape variables (Adams et al., 2004; Zelditch et al., 2004), was applied to data aligned for each one of the five structures using tpsRelw v. 1.54 (Rohlf, 2014). The graphical output of the analysis was used to search for evidence of discrete morphological changes.

Supplementary Results

The first RWA axis for the carapace is related with the widening/straightening of the carapace (Fig. S2A). Two genera are well separated from the remaining points along this axis: *Vectius* and *Doliomalus*. These genera have the carapace wider than long. The other clouds with smaller values along the first axis have the carapace longer than wide. The first axis, therefore, contributed with one character with two discrete states (char. 278). There is one genera with intermediate shape between these two, *Hemicloea*, which the state of character could not determined (scored 0&1 in the matrix).

The second axis is correlated with the shape of the anterior part of cephalic area (Fig. S2A). Specimens with higher scores in this axis have a cephalic area better delimited by a constriction of carapace, and the anterior margin is straight to convex, while the opposite is observed for the smaller scores. Two discrete groups can be well established based on this axis, and it a character with two states were created to accommodate this variation (char. 279). The remaining axes of RWA were not able to reveal discrete shape differences.

The first axis of RWA of the sternum show two taxa, *Vectius* and *Doliomalus*, with the sternum wider than long, while the remaining genera have the sternum longer than wide (Fig. S3A). This two sates were used in the character 280 of the cladistic analysis. The remaining axes did not show clear discrete variation of shape.

The posterior yes row is usually characterized as procurved, straight or recurved. In Gnaphosidae, these characters are used to differentiate genera and groups of genera. The first axis of RWA show that the posterior eye row disposition can be divided in only two discrete states: procurved or straight to recurved (Fig. S3A). These states were used as part of the character 281 in the cladistics analysis.

The analyses of the anterior eye row and the labium show that these structures could not be separated in clear-cut, discrete characters representing their shapes (Fig. S3B, C). Therefore, they were not used to estimate the phylogenetic relationships.

Supplementary References

Adams D., Rohlf F. & Slice D.E. (2004) Geometric morphometrics: ten years of progress following the “revolution.” *Italian Journal of Zoology*, **71**, 5–16.

Bond J.E. & Beamer D.A. (2006) A morphometric analysis of mygalomorph spider carapace shape and its efficacy as a phylogenetic character (Araneae). *Invertebrate Systematics*, **20**, 1–7.

Bookstein F.L. (1997) Landmark methods for forms without landmarks: morphometrics of group differences in outline shape. *Medical Image Analysis*, **1**, 225–243.
Rohlf F.J. (1990) Morphometrics. *Annual Review of Ecology and Systematics*, **21**, 299–316.
Rohlf F.J. (2013) *The tpsDig program, ver. 2.17*. The Stony Book University, NY, USA.
Rohlf F.J. (2014) *tpsRelw, relative warps analysis, version 1.54.* Department of Ecology and Evolution, State University of New York at Stony Brook. Software available at: http://life. bio. sunysb. edu/morph/soft-tps. html.
Slice D.E. (2007) Geometric Morphometrics. *Annual Review of Anthropology*, **36**, 261–281.
Zelditch M.L., Swiderski D.L., Sheets H.D. & Fink W.L. (2004) *Geometric morphometrics for biologists: a primer*. Elsevier Academic Press, London.

Supplementary Figures

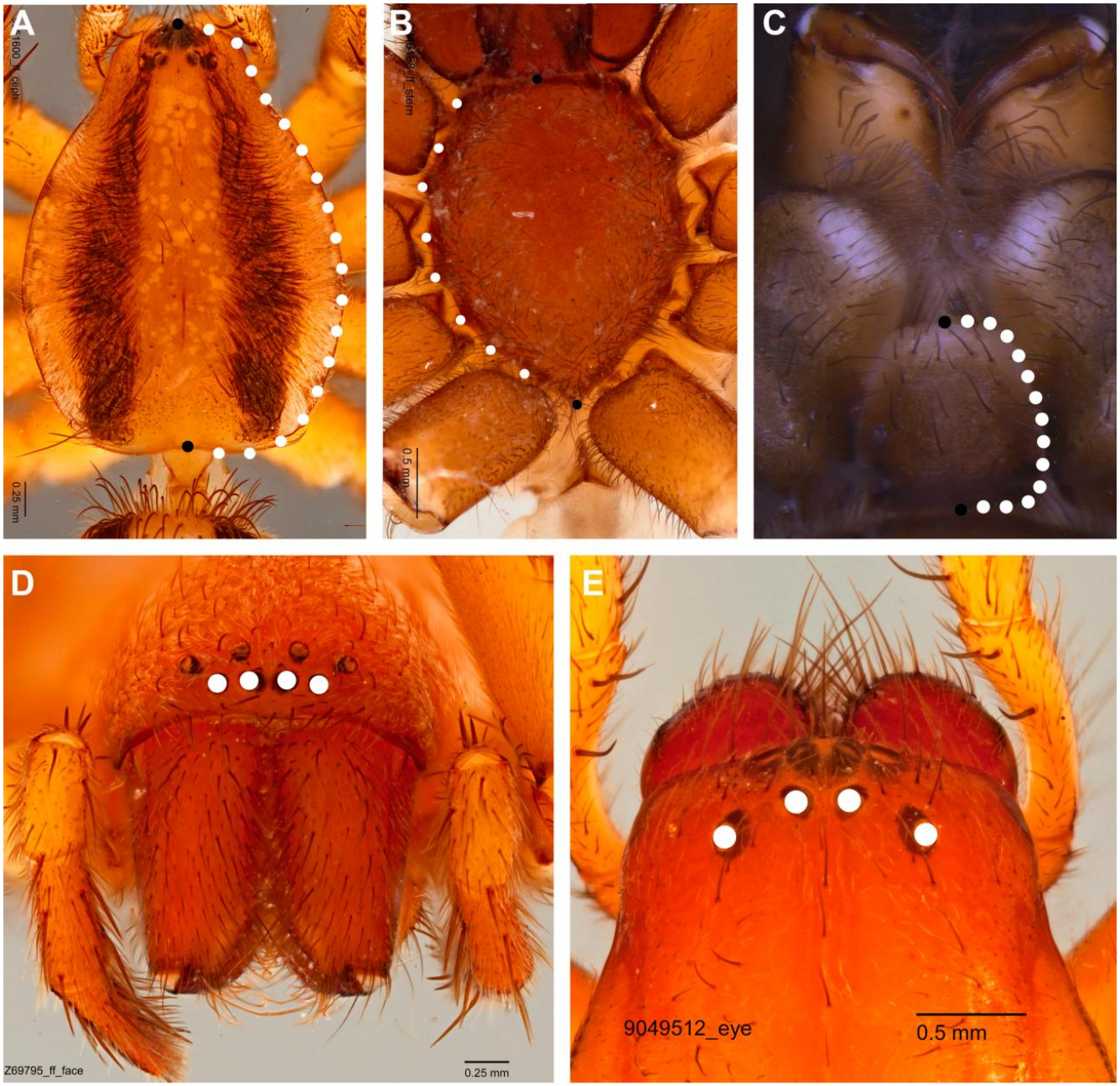

Figure S1: Landmarks (white dots) and semi-landmarks (black dots) established for the structures. **A)** *Cesonia bilineata* cephalothorax. Landmarks are the mid-point of the anterior and posterior edges. Semi-landmarks are points evenly spaced between landmarks. **B)** *Haplodrassus hiemalis* sternum. Landmarks are the mid-point of the anterior and posterior edges. Semi-landmarks are based on the pre and intercoxal sclerites, or the perpendicular line in the middle of the coxae and between coxae when the sclerites are absent. **C)** *Apopyllus silvestrii* labium. Landmarks are the mid-point of the anterior and posterior edges. Semi-landmarks are points evenly spaced between landmarks. **D)** *Anagraphis pallens* frontal view. Landmarks are the eyes itself. **D)** *Gnaphosa californica* cephalic area, dorsal view. Landmarks are the eyes itself.

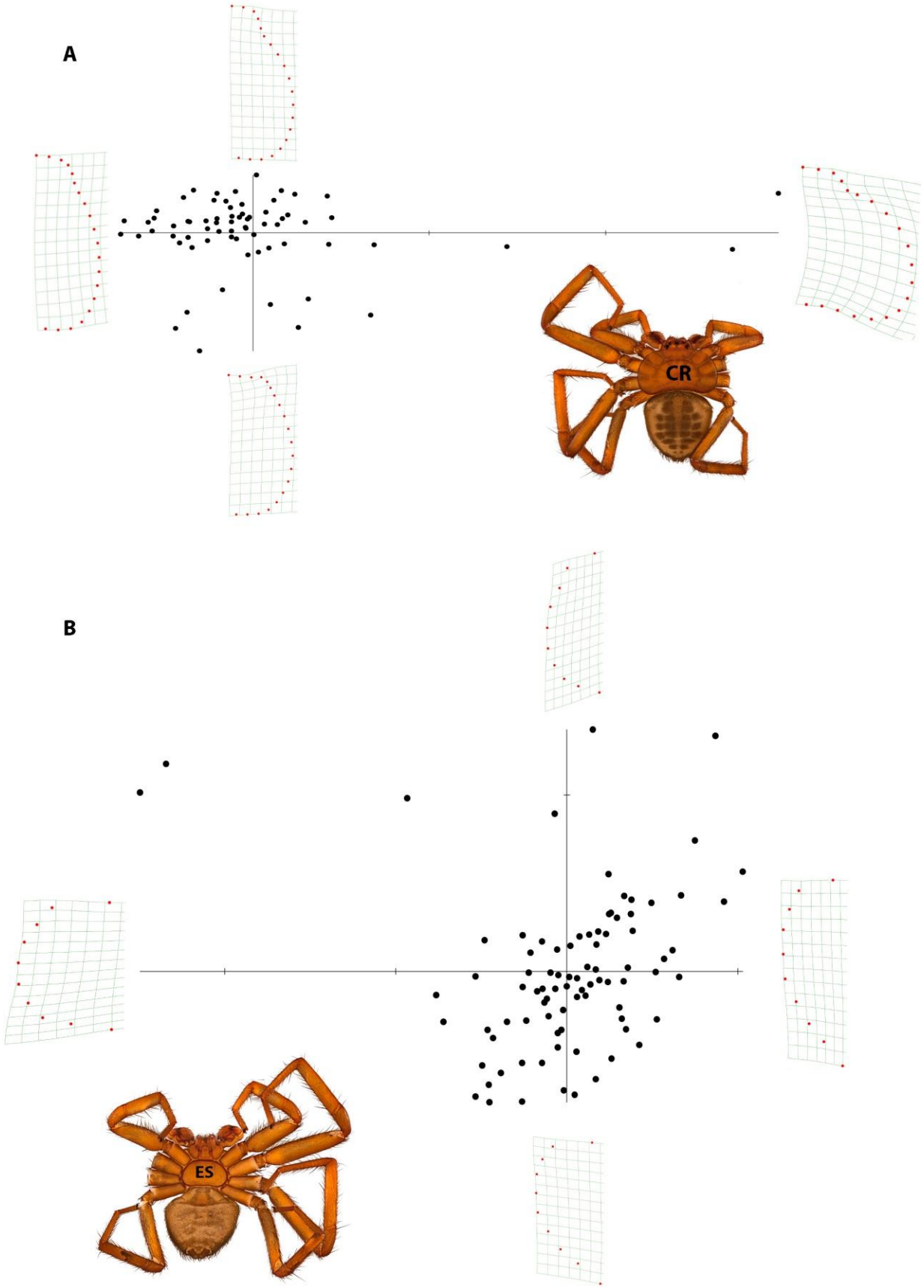

Figure S2: Relative Warps Analysis for the cephalothorax (A) and sternum (B). Figures on extremity of each axis are thin-plate splines showing shape deformation in that direction along axes and an example of spider with that kind of shape.

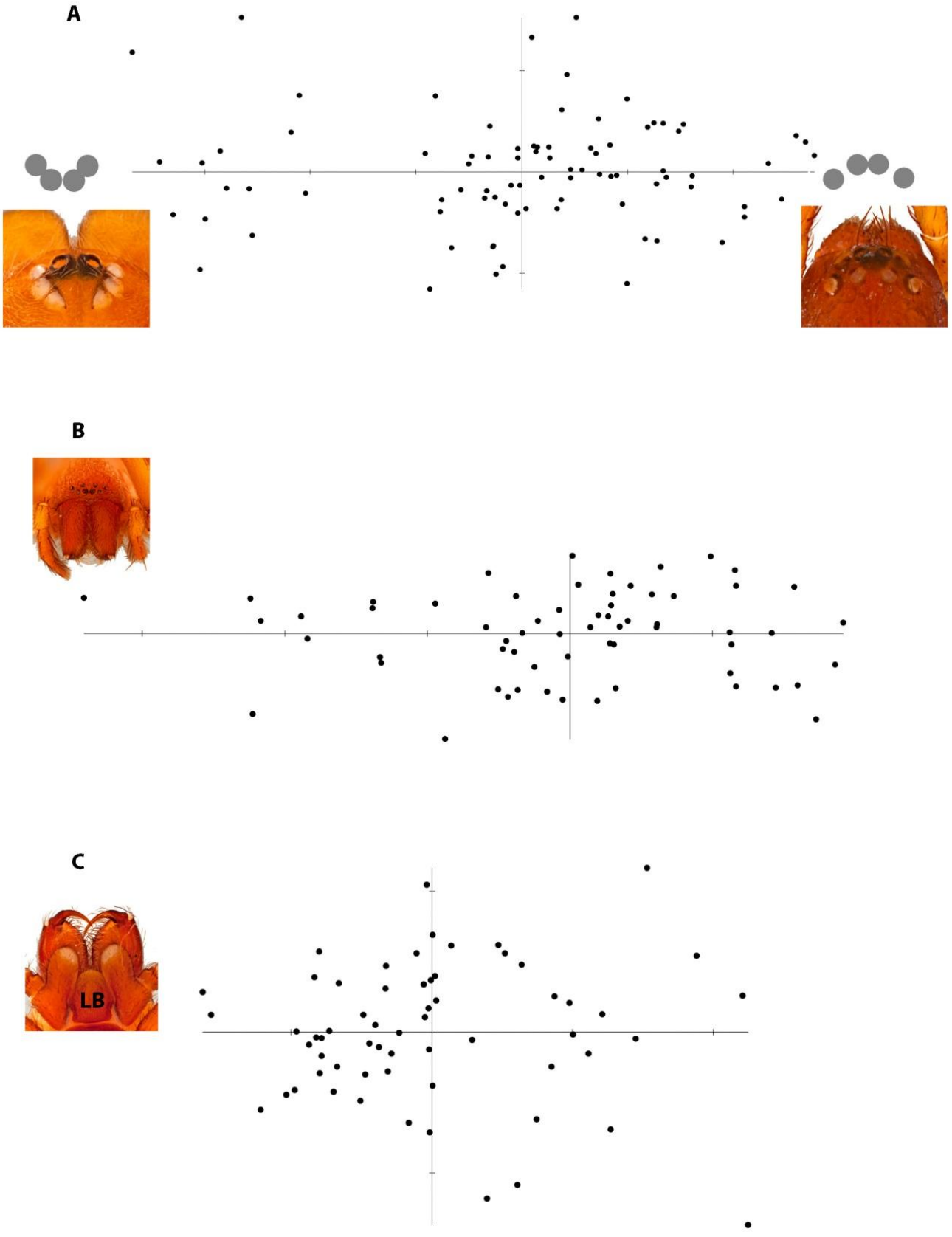

Figure S3: Relative Warp Analysis for the posterior eye row (A), anterior eye row (B) and labium (C). Figures on extremity of each axis show shape deformation in that direction along axes and an example of spider with that kind of shape.

CAPÍTULO II

WHAT DO FEMALES WANT: COMPLICATED OR SIMPLIFIED SEX? THE EVOLUTION OF GENITALIA IN GROUND SPIDERS (ARANEAE, DIONYCHA, GNAPHOSIDAE)

What do females want: complicated or simplified sex? The evolution of genitalia in ground spiders (Araneae, Dionycha, Gnaphosidae)

GUILHERME H.F. AZEVEDO[1, 2], CHARLES E. GRISWOLD[3] & ADALBERTO J. SANTOS[1]

[1]*Departamento de Zoologia, Instituto de Ciências Biológicas, Universidade Federal de Minas Gerais. Av. Antônio Carlos, 6627, 31270-901, Belo Horizonte, MG, Brasil. E- mail: ghfazevedo@gmail.com*

[1]*Pós-graduação em Zoologia, Universidade Federal de Minas Gerais.*

[3]*California Academy of Sciences, 55 Music Concourse Drive, San Francisco, CA 94118, United States.*

Abstract

Spiders may be good models for studying genitalia diversity and evolution given their peculiar copulatory mechanism, with male external copulatory apparatus located in palps. Gnaphosidae can be particularly interesting for this kind of study, as it holds in a same monophyletic group a remarkable structural diversity in male copulatory apparatus. The family contains species with simple, bipartite palps, with tripartite palps and a few elements, and species with several structures on tripartite palp. Some palpal homology studies suggest intermediate palp complexity as the ancestral condition for the family, from which both more complex and simpler palp would have evolved, with a trend to sclerite fusion. However, this hypothesis was never tested on a phylogenetic background, since no Gnaphosidae phylogeny was available until recently. Regarding female genitalia, both the epigynum and vulva range from simple to complex, but there is no information on its evolution. Thus, despite the great diversity of Gnaphosidae, patterns of genital evolution and mechanisms involved in copulatory organ diversification in the family are barely known. The aim of this study was to contribute to the understanding of genital evolution through the exploration of macroevolutionary patterns related to copulatory organ diversity in Gnaphosidae. More specifically, the evolutionary trend in complexity and predictions about genital evolution were tested using phylogenetic comparative methods. A phylogenetic tree inferred with morphological data was used hypothesis for the comparative method. We sampled 35 female and 57 male characters to explore genital evolution, based on phylogenetic trees obtained. A bipartite palp with intermediate complexity was found to be the plesiomorphic condition, but there was no trend toward simplification or increasing complexity. The same intermediate complexity with no trend was found for females. Additionally, we discovered that complexity of female and male copulatory organs did not coevolve, suggesting no support for sexual antagonistic conflict hypothesis. Homology and evolution of some structures are discussed. Additional information on copulatory behavior of gnaphosids might contribute to the understanding of genital evolution.

Introduction

Copulatory organs are widespread in several animal lineages, present impressive variety of forms and are thought to evolve relatively faster than other traits (Huber, 2003; Eberhard, 2010a). Many evolutionary hypotheses have been proposed to explain this great diversity of genitalia including (1) pleiotropy, which postulates that genitalia are neutral and evolve with other genetically correlated traits, (2) natural selection, according to which the genitalia would evolve to avoid hybrid formation through a species-specific lock–and–key mechanism, and (3) sexual selection, which predicts that some traits would be favored by some post copulatory mechanisms, such as cryptic female choice, sperm competition or sexually antagonistic coevolution (Arnqvist, 1997; Hosken & Stockley, 2004; Eberhard, 2010b,a, 2015).

Sexual selection by cryptic female choice has usually been indicated as the main general mechanism to explain genital diversity in spiders (Eberhard, 2010a, 2015; Eberhard & Huber, 2010). Nevertheless, few studies test specific hypotheses about the genitalia evolution based on phylogenetic comparative methods and some of them indicate alternative explanations for genital diversity within the group (Kuntner, Coddington, & Schneider, 2009). In fact, studies on arthropod genitalia suggest that genital evolution might be more complex, not explained by single mechanism, (Simmons, 2014), indicating that much effort is still necessary to make progress on the understanding of genital evolution.

Spiders may be good models for studding genitalia diversity and evolution (Eberhard, 2004a). In Araneae, the sperm transference evolved in a unique manner among arachnids through the modification of male palps into a peculiar copulatory apparatus. The copulatory bulb is a compound of sclerotized structures with reduced sensorial and muscular organs that need to fit precisely to the female genitalia (Eberhard & Huber, 2010; but see Lipke, Hammel, & Michalik, 2015, for evidence of neurons on copulatory bulb). Spider species-level systematics is based mainly on the morphology of male and female copulatory organs. Therefore, the number of described species is a good proxy of genitalia diversity in the order and suggests the existence of 45.942 different forms of copulatory organs (World Spider Catalog, 2016). Even though the importance of copulatory structures might have been overestimated in systematics (Jocqué, 2002; Huber, 2004), the great diversity of forms and elements in spider genitalia perceived by arachnologists are indubitable and begs for an explanation.

The putative plesiomorphic male palp bulb in spiders is a tripartite structure, with proximal (subtegulum), median (tegulum) and terminal (embolus) divisions (Platnick & Gertsch, 1976; Kraus, 1978; Coddington, 1990; Sierwald, 1990). This basic ground plan

might have evolved in different directions among great lineages, resulting in relatively simple copulatory bulbs with fused elements, as in some Mygalomorphae (Bertani, 2000) and Haplogynae spiders (Platnick & Dupérré, 2009), or more complex organs, with additional elements and variable shape, as in most araneoid spiders (Coddington, 1990). There is less information about the evolution of female genitalia, but it is suggested that it might have evolved from a simple system of glandular sperm storage with no external structure to a more complex system with additional ducts and receptaculae and with external sclerotized structures with folds and projections (Forster, 1980; Sierwald, 1989).

Gnaphosidae spiders, besides the great diversity – it is the sixth most species-rich spider family (World Spider Catalog, 2016), are remarkable in having species with simple palps, with bipartite bulb and few elements (e.g. *Litopyllus* Chamberlin, 1922; Platnick & Shadab, 1980a), species with intermediate conditions, with tripartite palp and few elements (e.g. *Gnaphosa* Latreille, 1804; Platnick & Shadab, 1975), and species with several additional structures on a tripartite palp (e.g. *Zelotes* Gistel, 1848; Senglet, 2004). Some studies on palpal structure homology among gnaphosids suggest that an intermediate complexity palp might be the ancestral condition for the family, from which the more complex and more simple palps would evolve, but with a major evolutionary trend to fusion of sclerites (Zakharov & Ovtcharenko, 2011, 2013). However, those hypotheses were never tested on a phylogenetic background, since no Gnaphosidae phylogeny was available at time, and the studies were limited to few taxa.

Regarding female genitalia, gnaphosids are considered entelegyne spiders, which means that the internal genitalia (vulva) have two pairs of openings to exterior, one that leads to the copulatory duct and one that arises from the fertilization duct, and have a sclerotized external structure, the epigynum (Coddington & Levi, 1991; Garrison *et al.*, 2016). Both the epigynum and the vulva range from simple structured organs, with short ducts and an undivided external plate (e.g. *Cesonia* Simon, 1893; Platnick & Shadab, 1980b), to more complex structures, with long coiled ducts and the epigynum with ventral folds and projections (e.g.: *Apopyllus* Platnick & Shadab, 1984). However, only some zelotine spiders have been explored in a more detailed comparative morphological study of female genitalia (Senglet, 2004) and little is known about the homology between their components.

Despite the great diversity of Gnaphosidae, the patterns of genital evolution and mechanisms involved on copulatory organ diversification in the family are barely known. The aim of this study was to contribute to the understanding the genital evolution through the exploration of macroevolutionary patterns and processes related to the copulatory organ

diversity in Gnaphosidae. More specifically, the evolutionary trend in complexity and some predictions of genital evolution hypothesis (cryptic choice, arms race or lock-and-key) were tested using phylogenetic comparative methods.

Material and Methods

Dataset

Our analyses were based on a phylogenetic hypothesis and genitalic characters taken from the morphological matrix of previous work on Gnaphosidae systematics (Azevedo *et al*., unpublished). Only characters that could easily indicate complexity (see below) were kept for the analyses, resulting in 48 male and 15 female characters (Appendix 1). Missing data was conservatively treated as absent character. Taxa with more than 10% of missing entries were excluded from complexity analysis (Appendix 2), although they are shown on the tree and used on the character evolution. The final dataset consists of 89 males and 93 female taxa. The tree found under concavity function with k=15 in Azevedo *et al.* (unpublished) was used as working hypothesis for comparative analysis. WinClada v. 1.00.08 (Nixon, 2002) and Mesquite v.3.04 (Maddison & Maddison, 2015) were used to optimize discrete characters and the continuous organ complexity, under maximum parsimony and squared change parsimony (Maddison, 1991), respectively.

The characters and complexity measures were optimized in the whole tree, including outgroups, to avoid ambiguous optimization on the root of the clade of interest, the Gnaphosidae S.S. clade (Azevedo *et al.*, unpublished). However, for hypothesis testing on the genitalia complexity evolution (see below), only Gnaphosidae S.S. clade was included, since including sparsely sampled outgroup families could mislead the results.

Complexity

Complexity might be hard to define and measure (McShea, 1991; Adami, Ofria, & Collier, 2000; Adami, 2002; Ramírez & Michalik, 2014). Here it was used the structural complexity concept, in which complexity is a function of number of parts in the organism and irregularity of their arrangement (McShea, 1991). Neomorphic characters, i.e. the ones that indicate an appearance or loss of a trait (Sereno, 2007), were used to count the presence of structures on male and female genitalia. Since some transformational characters, which represents modification of an existent trait (Sereno, 2007), could also be useful for individualizing structural elements, they were also used to calculate complexity (Ramírez & Michalik, 2014). For example, some species might have a very long and coiled embolus, others might have the

embolus that is approximately as long as the tegulum, while others might have the embolus shorter than half the tegulum. A value of 1, 0.5 and 0 was given to those structures respectively. Although the short embolus is coded as 0, the presence of an embolus is coded as 1, therefore contributing to the overall complexity of the palp. The same was done for sclerotization characters, coding 0, 0.5 and 1 for unsclerotized, partially and completely sclerotized, respectively. Transformational characters representing shape of structures were not used.

Trends in complexity

Generalized estimating equations (GEE) for comparative data were used to test for evolutionary trend on complexity. This method allows parameter estimation of a generalized linear model (GLM) taking into account the correlation between specimens, which is determined by phylogenetic relationships, and there is no need to estimate ancestral states (Paradis & Claude, 2002).

The effects of taxa depth (distance to root) on the complexity measurement were analyzed to test models of possible complexity evolution. If there is an evolutionary trend of increasing complexity, it is expected a better fit of the data to a normal linear regression model with positive relationship of taxa depth and complexity (positive regression coefficients). If the tendency is to simplify genitalia, the normal regression coefficients would be estimated to be negative. A quadratic function would fit the data better if the simplicity or complexity is in intermediate position on the tree, with negative and positive coefficient, respectively. If there is no relationship, the coefficients would not be statistically different from 0, and a model that estimates only the intercept would be a better explanation for the data. The model choice was based on the Quasi-likelihood Information Criterion (QIC), a modification of the tradition Akaike Information Criterion (AIC) for GEE (Pan, 2001). If the best model includes the estimation of the coefficient, it was also checked if the value is significant different from 0. Analysis were carried out using the APE package (Paradis, Claude, & Strimmer, 2004) for R! v.3.2.1 (R Core Development Team, 2015).

The taxa depths were calculated as the number of nodes that separates the terminal from the root of the tree. This is the same as considering all branch lengths equal to unity. Since the phylogeny used provides no information on branch lengths, it is necessary some transformation. Considering all branch lengths equal is equivalent of assuming a punctuational view of evolution (Pagel, 1994, 1997, 1999). In this way, changes in a trait would be proportional to the number of speciation events (nodes) estimated from the root to

the species, independent of the length of the branches. We believe this is a conservative approach, more appropriate when branch lengths are not available.

Testing genital evolution hypothesis

Sometimes it might be hard to distinguish between hypothesis of genital evolution, as they are not always mutually exclusive (Hosken & Stockley, 2004; Eberhard, 2010a, 2015). The Sexually Antagonistic Coevolution (SAC) and Lock-and-Key (LK) hypotheses predict a strong correlation between male and female genitalia morphology, but correlation might or might not be present if genitalia are evolving under the Cryptic Female Choice (CFC) mechanism (Arnqvist, 1997; Eberhard, 2010b, 2015). If females are cryptically choosing males based mainly on stimuli that male genitalia produce, the coevolution of genital morphology would not be expected under CFC. Therefore, a lack of correlation of genital morphological complexity would favor CFC over SAC and LK.

GEE for comparative data was used to test the correlation between female and male genital complexity. A model that estimates the coefficient (inclination) of a normal regression was compared to one in which the coefficient is zero (not estimated). Model choice was based on the Quasi-likelihood Information Criterion (QIC). If the best model includes the estimation of the coefficient, it was also checked if the value is significantly different from 0. Analysis were carried out using APE package.

Another expectation of sexual selection by CFC is that male copulatory organs would have a faster evolutionary rate of morphological characters than female genitalia, since morphological changes that stimulate better the female would be suffering strong positive selective pressure (Eberhard, 2010b). To test the difference in evolutionary rate, the variance of evolutionary change (*sigma* parameter of the Brownian Motion; Pagel, 1997, 1999) of male and female complexity were estimated using independent contrasts model through Bayesian methods in BayesTraits V2 (Pagel & Meade, 2014). The MCMC consisted of 1,000,000 chains with sample period of 1,000, after a *burn in* phase of 10,000 generations. The *sigma* period was considered uniform between 0 and 100. The female and male mean rates estimated on the stationary phase of the MCMC were compared with a t-test with significance level of 0.05.

Results

Ancestral state reconstruction and character evolution

The reconstruction of ancestral character states suggests that the male palp of the most recent Gnaphosidae *S.S.* ancestor would have the following structures: petiole, subtegulum, tegulum, embolus fused to tegulum, embolus about the same size or smaller (umbiguous) than copulatory bulb, conductor, a completely sclerotized median apophysis and a retrolateral tibial apophysis. These traits do not necessarly constitue synapomorphies, they are just the conditions found on the common ancestor of the clade. The conductor was lost unambiguously six times and regained five times during Gnaphosidae *S.S.* evolution. An articulation between embolus and tegulum arises four times and was lost again three times. A long (longer than tegulum) coiled embolus appears nine times and disappears two times (one time it is reversed to an embolus as long as tegulum and other it is reduced to about half the tegulum length). The median apophysis was lost seven times, with no regain. The terminal apophysis (a sclerite on the terminal division of bulbus, proximally and ventrally positioned in relation to embolus) arises four times on gnaphosids. The Figure 1 shows the optimization of the palpal characters on phylogeny.

The ancestral epyginum would have an anterior fold, laterals folds composed by furrows, completely sclerotized short (with some curls) copulatory ducts, ventrally directed fertilization ducts, primary spermathecae, and secondary spermathecae with defined lumen and short stalk. The anterior fold was lost 10 times in Gnaphosidae S.S. The furrowed lateral folds were lost at least four times and became a suture seven times, with one ambiguous reversal to furrow. A posteriorly directed fertilization duct arises one time at the ancestor of Leptodrassinae. The primary spermathecae were lost two times, one in the most recent ancestor of Prodidominae and in *Drassodex* Murphy, 2007. The secondary spermathecae disappear two times on Gnaphosidae S.S. evolution. A long copulatory duct (spiral or highly convoluted) evolved six times, with one reversion. The Figure 1 shows the optimization of the epigynum characters on phylogeny.

Complexity evolution

The palp complexity in Gnaphosidae S.S. ranges from four, in *Gertschosa* Platnick & Shadab, 1981, to 14.5 in *Zelanda* Özdikmen, 2009. The mean palp complexity of the dataset is 9.26. The ancestral complexity in Gnaphosidae S.S. is 8.5-9.5. Therefore, an intermediate complexity is the ancestral condition from which more complex and simpler palps evolved (Fig. 2). Epigynum complexity in Gnaphosidae S.S. ranges from two, in *Zelotibia* Russell-

Smith & Murphy, 2005, to 10, in *Apopyllus* Platnick & Shadab, 1984 and *Apodrassodes* Vellard, 1924. The mean epigynum complexity of the dataset is 5.96. The ancestral complexity in Gnaphosidae S.S. is 6. As for males, an epigynum with intermediate complexity should be the ancestral condition (Fig. 2). The model with best QIC shows no relationship between complexity and distance to root, neither for palp nor epigynum (Fig. 3; Table 1, 2). Therefore, there is no trend towards either increasing or decreasing complexity.

Testing genital evolution hypothesis

The best model is the one with no correlation between female and male genitalia (Fig. 2, 4). Therefore, male and female sexual organs are not coevolving regarding their complexity. The brownian variance parameter estimated in BayesTraits using MCMC shows significant difference in the evolutionary rates of palp and epigynum ($p<0.05$, $t=29.98$, $df=1998$). The palp is evolving 1.24 times faster than epigynum.

Discussion

Genitalia structure homology

Homology between male palp structures might be hard to establish, especially when number of structures may vary between species being analyzed (Ramírez, 2007). The supposed rapid evolution of genitalia might have caused several gains and losses and it is not clear which genital structures are homologous among spiders and more comparative morphology and phylogenetic studies are necessary to unravel this issue (Coddington, 1990; Sierwald, 1990). Some important studies on Gnaphosidae spiders have contributed to proposals of primary homology hypothesis among palp characters in the family (Senglet, 2004; Zakharov & Ovtcharenko, 2011, 2013). However, testing the congruence of these characters against others is an important step on the process of establishing secondary homology (de Pinna, 1991; Richter, 2005). Here, the results of a previous phylogenetic analysis, (Azevedo *et al.*, unpublished) putting into test primary homology propositions were used to explore the evolution of some genitalic characters helping to understand their homology in Gnaphosidae.

The median apophysis, a projection that arises from the membranous median area of tegulum (Azevedo *et al.*, unpublished), is homologous among all Gnaphosidae and probably has its origin more deeply in spider phylogeny. At least this dataset suggests that it would be present in the common ancestor of the OMT clade (Ramírez, 2014). However, although in Gnaphosidae this structure was lost some times with no regains –what gives little doubts about its homology – there was one reappearance of the median apohysis after a loss in the outgroup. Therefore,

broadly taxonomical sampling is needed to understand median apophysis homology on a deep context of spider evolution.

The conductor, an outgrowth of the proximal part of tegular wall associated to embolus tip (Zakharov & Ovtcharenko, 2011), is absent in about half of the gnaphosid genera. In many cases, the supposed function of this structure (to help conducting embolus during copulation) might be overtaken by other parts of palp. In some Zelotinae (Gnaphosidae), for example, the embolus passes on the backside of median apophysis during intromission phase (Senglet, 2004). In some taxa, like in Leptodrassinae, a secondary median apophysis surrounds the embolus and might act as a conductor. Regarding the taxa that have the conductor, although this structure is present in the most recent ancestor of Gnaphosidae S.S., its homology among the whole family is not supported, since several independent appearances suggest convergence in many clades.

A tripartite bulb is supposed to be the plesiomorphic condition for spiders and also for Gnaphosidae (Platnick & Gertsch, 1976; Kraus, 1978; Coddington, 1990; Sierwald, 1990; Zakharov & Ovtcharenko, 2011, 2013). However, our results suggest that a palpal bulb with tree division is a derived condition within Gnaphosidae S.S. The ancestral gnaphosid probably had no tubular distal membrane separating embolus from tegulum, resulting in a bipartite bulb. In fact, the results suggest that the fusion of tegulum and embolus might have arisen before the origin of Gnaphosidae S.S. The membrane that separates terminal and median bulb division appears four times in the family, and a return to ancestral condition occurs three times on the phylogenetic hypothesis used. Therefore, it is hard to state that there is a trend towards fusion or separation of sclerites.

Detailed studies on comparative morphology and evolution of female genitalia are rare in spiders, but it is suggested that the spermatheca are homologous among all entelegyne spiders (Forster, 1980; Sierwald, 1989). Herein it was found that the primary and secondary spermathecae are homologous among all gnaphosids and evolved much before the most recent common ancestor of the family, which might support homology in Entelegynae. The primary spermatheca has been lost at least two times in Gaphosidae S.S., becoming an undifferentiated part, usually less sclerotized, of terminal segment of copulatory duct. The lateral folds are also plesiomorphic for gnaphosids and probably arose much before the family's ancestor. However, these structures might have been completely lost or be present as sutures. It has been show that precursors of lateral folds are present in the early stage of epigynum ontogeny and that they invaginate to form the internal ducts (Sierwald, 1989). Since the plesiomorpfic feature for the family is the lateral fold present as furrows in the

epigynum, the apomorphic conditions of lateral folds as sutures or completely absence of the structure might be regarded as paedomorfic condition. In those derived taxa, the formation of the internal genitalia and sexual organs might have reached maturation before the complete development of the precursor of lateral folds. An ontogenetic study could help to elucidate this hypothesis of gnaphosids paedomorphic epigynum revealed by the phylogeny. However, the understanding of lateral folds evolution through spiders will require much more effort to study the distribution of these characters through spider phylogeny.

Complexity

The putative plesiomorphic condition for Araneae of a tripartite palp with many taxa showing an apomorphic fusion of sclerites might support the hypothesis of a trend towards simplification of male genitalia (Platnick & Gertsch, 1976; Kraus, 1978; Coddington, 1990; Sierwald, 1990). In Gnaphosid this simplification trend was also proposed as an explanation for the presence of genera with bipartite palp in the family (Zakharov & Ovtcharenko, 2013). Herein it was show that the ancestral condition is actually a palp with embolus fused to tegulum, what would suggest simple palps originating more complex ones. However, as mentioned above, an articulated palp appears and disappears a few times, without an apparent trend. Besides, the complexity is not measured only by the fusion of two sclerites, but by the number of structures in male palp. Some genera with not flexible embolus might have other sclerites, increasing complexity. The complexity measure shows no evolutionary trend on male genitalia. The plesiomorphic condition in Gnaphosidae S.S. is a palp with moderate complexity giving rise to both complex and simple palps. The complexity would be evolving in Brownian motion, in which the trait would evolve independently in each branch of a cladogenesis event in a random direction towards simplification or increasing complexity, leaving no macroevolutionary trend.

Regarding the females, the plesiomorphic condition of a spider genitalia with few structures, with possible intermediate conditions in some clades (Mygalomorphae, Haplogynae and Leptonetidae) and the presence of many taxa with genitalia bearing many structures could bring the idea of increasing complexity (Forster, 1980). However, the same pattern observed for males was found for complexity evolution of the epigynum, with plesiomorphic moderate complexity evolving in Brownian motion with no trends.

The method applied here use a simple complexity measure and assumes a punctuated way of evolution, since there is no information on branch lengths and absolute time on Gnaphosidae evolution. Some modern methods allow the use of geometric morphometrics

technics to calculate a more elaborated measure of complexity and dated phylogenies permit incorporate and test other models of trait evolution, including variation on rate among branches (Rowe & Arnqvist, 2012; Baker *et al.*, 2015). However, geometric morphometrics technics might be difficult to apply to a large gnaphosid genitalia datatset because of (1) the great variety of morphology, resulting in no correspondent structures and, consequently, precluding landmark establishment; and (2) the tridimensionality of structures with few landmarks, requiring surface analysis methods of 3D images (Adams, Rohlf, & Slice, 2004; Zelditch *et al.*, 2004). A good sample of gnaphosid genera for molecular analysis would require worldwide effort to obtain fresh material all over the world, since the family is globally distributed, or an effort to sample old museum specimens. Until those data are available, the analysis presented herein shows a good test and overview of macroevolutionary evolution of complexity in genitalia of Gnaphosidae.

Sexual selection

The analysis presented herein shows no support for SAC. In Gnaphosidae spiders, the female might be choosing males genitalia that best stimulates the sensory system during copulation, regardless (or with little influence) of the mechanical fit with epigynum. Since there is no trend in complexity, there is no general best condition of male genitalia, and the female choice towards simple or complex palps would be idiosyncratic of each species and not predicted by epigynum complexity. Many evidence suggest sexual evolution by cryptic female choice as the mechanism generating genital diversity in spiders. Some morphological and sexual behavior studies show that females might be able to control copulation and manipulate sperm storage in Araneidae, Oonopidae, Pholcidae, Tetrablemmidae, and Tetragnathidae spiders (Huber, 1999; Burger, Nentwig, & Kropf, 2003; Burger *et al.*, 2006; Welke & Schneider, 2009; Aisenberg, Barrantes, & Eberhard, 2015; Calbacho-Rosa & Peretti, 2015; Schneider, Uhl, & Herberstein, 2015). Eberhard (2004b) found no support for coevolution of male structures and respective contact area in female genitalia among several arthropod groups (including spiders), favoring CFC over SAC. However, a correlation between male and female genital complexity was demonstrated for nephilid spiders, suggesting the occurrence of SAC, possibly together with CFC (Kuntner *et al.*, 2009).

It has been argued that the bias towards the study of male genitalia could hamper the understanding of genital evolution (Ah-King, Barron, & Herberstein, 2014). Indeed, morphological and comparative studies of female genitalia are scarcer for spiders. Detailed studies of Haplogynae spiders with simple external genitalia revealed that the internal

structure might be complex (Burger *et al.*, 2003, 2006). However, the internal structures found in those studies of haplogyne female genitalia are related to sperm control, suggesting female choice.

There is also some evidence for sperm competition (SC) in spiders (Schneider *et al.*, 2000). Some Pholcidae uses palpal structures to remove sperm of rival males present in female genitalia (Calbacho-Rosa *et al.*, 2013; Calbacho-Rosa & Peretti, 2015). The presence of genital plugs may also indicates sperm competition (Uhl, Nessler, & Schneider, 2010; Eberhard, 2015). Genital plugs have been reported for gnaphosid species, but the frequency of its use, how it is formed and the ability of males to remove it is barely known. It was show that the removal of genital plug in *Arboricaria sociabilis* (Kulczyński, 1897) is rare and the plug might be an effective way of preventing sperm competition (Sentenská *et al.*, 2015). In some zelotines, there is a hectic brushing of tibial apophysis on epigynum during copulation (Senglet, 2004). Although this movement could help to remove the genital plug, the intention and consequences of this behavior are unknown. Evidence of sperm competition, nevertheless, might not exclude the occurrence of CFC, and females might have some influence on sperm competition (Eberhard, 2015). In *Arboricaria sociabilis,* males that couple genitalia faster are allowed by females to copulate longer and to complete genital plug production (Sentenská *et al.*, 2015).

The hypotheses of sexual selection are not mutually exclusive and differing processes might affect together the evolution of genital complexity (Simmons, 2014). It has been shown that different parts, or even a single structure, in the genitalia of insects might be under different selective pressures and could evolve through distinct mechanisms of sexual selection (Rowe & Arnqvist, 2012; Frazee & Masly, 2015). Some Gnaphosidae species have a very long, coiled embolus, which seems to be, at least in part, correlated with long coiled copulatory ducts in female. These two structures might have evolved in an "arms race" in order to control copulation, while other structures in genitalia might have evolved under selection by cryptic female choice. The fact that the ecological environment might influence the context of sexual selection also illustrates how complex the processes acting on genital diversity might be (Anderson & Langerhans, 2015). Herein it is provided an evidence for CFC in Gnaphosidae spiders on a macroevolutionary scale. Detailed studies of descriptive and comparative morphology, copulatory mechanisms, and sexual behavior in populations and groups of species and genera is of interest in order to contribute to a better understanding of the mechanism generating Gnaphosidae genital diversity.

References

Adami C. **2002**. What is complexity? *BioEssays* **24**: 1085–1094.

Adami C, Ofria C & Collier TC. **2000**. Evolution of biological complexity. *Proceedings of the National Academy of Sciences* **97**: 4463–4468.

Adams D, Rohlf F & Slice DE. **2004**. Geometric morphometrics: ten years of progress following the 'revolution'. *Italian Journal of Zoology* **71**: 5–16.

Ah-King M, Barron AB & Herberstein ME. **2014**. Genital Evolution: Why Are Females Still Understudied? *PLoS Biology* **12**: 1–7.

Aisenberg A, Barrantes G & Eberhard WG. **2015**. Post-copulatory sexual selection in two tropical orb-weaving leucauge spiders. In: Peretti A V, Aisenberg A, eds. *Cryptic Female Choice in Arthropods: Patterns, Mechanisms and Prospects*. Heidelberg: Springer, 79–108.

Anderson CM & Langerhans RB. **2015**. Origins of female genital diversity: Predation risk and lock-and-key explain rapid divergence during an adaptive radiation. *Evolution* **69**: 2452–2467.

Arnqvist G. **1997**. The evolution of animal genitalia: distinguishing between hypotheses by single species studies. *Evolution in Health and Disease* **60**: 365–379.

Baker J, Meade A, Pagel M, *et al.* 2015. Adaptive evolution toward larger size in mammals. *Proceedings of the National Academy of Sciences of the United States of America* **112**: 5093–5098.

Bertani R. **2000**. Male Palpal Bulbs and Homologous Features in Theraphosinae (Araneae, Theraphosidae). *Journal of Arachnology* **28**: 29–42.

Burger M, Michalik P, Graber W, *et al.* 2006. Complex genital system of a haplogyne spider (Arachnida, Araneae, Tetrablemmidae) indicates internal fertilization and full female control over transferred sperm. *Journal of Morphology* **267**: 166–186.

Burger M, Nentwig W & Kropf C. **2003**. Complex genital structures indicate cryptic female choice in a haplogyne spider (Arachnida, Araneae, Oonopidae, Gamasomorphinae). *Journal of Morphology* **255**: 80–93.

Calbacho-Rosa L, Galicia-Mendoza I, Dutto MS, *et al.* 2013. Copulatory behavior in a pholcid spider: Males use specialized genitalic movements for sperm removal and copulatory courtship. *Naturwissenschaften* **100**: 407–416.

Calbacho-Rosa L & Peretti A V. **2015**. Copulatory and post-copulatory sexual selection in haplogyne spiders, with emphasis on Pholcidae and Oonopidae. In: Peretti A V, Aisenberg A, eds. *Cryptic Female Choice in Arthropods*. Heidelberg: Springer, 109–144.

Coddington JA. **1990**. Ontogeny and homology in the male palpus of orb-weaving spiders and their relatives, with comments on phylogeny (Araneoclada: Araneoidea, Deinopoidea). *Smithsonian Contributions to Zoology* **496**: 1–52.

Coddington JA & Levi HW. **1991**. Systematics and Evolution of Spiders (Araneae). *Annual Review of Ecology and Systematics* **22**: 565–592.

Eberhard WG. **2004a**. Why study spider sex: special traits of spiders facilitate studies of sperm competition and cryptic female choice. *The Journal of Arachnology* **32**: 545–556.

Eberhard WG. **2004b**. Rapid divergent evolution of sexual morphology: comparative tests of antagonistic coevolution and traditional female choice. *Evolution* **58**: 1947–1970.

Eberhard WG. **2010a**. Evolution of genitalia: Theories, evidence, and new directions. *Genetica* **138**: 5–18.

Eberhard W. **2010b**. Rapid divergent evolution of genitalia. In: Leonard J, Córdoba-Aguilar A, eds. *The evolution of primary sexual characters in animals*. Oxford: Oxford University Press, 40–78.

Eberhard WG. **2015**. Cryptic female choice and other types of post-copulatory sexual selection. In: Peretti A V, Aisenberg A, eds. *Cryptic Female Choice in Arthropods*. Heidelberg: Springer, 1–26.

Eberhard WG & Huber BA. **2010**. Spider genitalia - precise maneuvers with a numb structure in a complex lock. In: Leonard J, Córdoba-Aguilar A, eds. *The Evolution of Primary Sexual Characters in Animals*. Oxford, 249–284.

Forster RR. **1980**. Evolution of the tarsal organ, the respiratory system and the female genitalia in spiders. *VIII Internationaler Arachnologen Kongres Viena*.

Frazee SR & Masly JP. **2015**. Multiple sexual selection pressures drive the rapid evolution of complex morphology in a male secondary genital structure. *Ecology and Evolution* **5**: 4437–4450.

Garrison NL, Rodriguez J, Agnarsson I, *et al.* 2016. Spider phylogenomics: untangling the Spider Tree of Life. *PeerJ* **4**: e1719.

Hosken DJ & Stockley P. **2004**. Sexual selection and genital evolution. *Trends in Ecology & Evolution* **19**: 87–93.

Huber BA. **1999**. Sexual selection in pholcid spiders (Araneae, Pholcidae). *Journal of Arachnology* **27**: 135–141.

Huber BA. **2003**. Rapid evolution and species-specificity of arthropod genitalia: fact or artifact? *Organisms Diversity & Evolution* **3**: 63–71.

Huber B a. 2004. The significance of copulatory structures in spider systematics. In: Schult J, ed. *Studien zur Theorie der Biologie, Band 5, Biosemiotik - Praktische Anwendung und Konsequenzen fuer die Einzeldisziplinen*. Berlin: VWB-Verlag fuer Wissenschaft und Bildung, 89–100.

Jocqué R. **2002**. Genitalic polymorphism - a challenge for taxonomy. *Journal of Arachnology* **30**: 298–306.

Kraus O. **1978**. Liphistius and the evolution of spider genitalia. *Symposia of the Zoological Society of London* **42**: 235–254.

Kuntner M, Coddington JA & Schneider JM. **2009**. Intersexual arms race? Genital coevolution in nephilid spiders (Araneae, Nephilidae). *Evolution* **63**: 1451–1463.

Lipke E, Hammel JU & Michalik P. **2015**. First evidence of neurons in the male copulatory organ of a spider. *Biology Letters* **11**: 1–4.

Maddison WP. **1991**. Squared-change parsimony reconstruction of ancestral states for continuous-valued on a phylogenetic tree. *Systematic Zoology* **40**: 304–314.

Maddison WP & Maddison DR. **2015**. Mesquite: a modular system for evolutionary analysis. Version 3.04. *Available at: mesquiteproject. org/mesquite/download/download. html*.

McShea DW. **1991**. Complexity and evolution: what everybody knows. *Biology and Philosophy* **6**: 303–324.

Nixon KC. **2002**. WinClada, version 1.00. 08. *Published by the author, Ithaca, New York*.

Pagel M. **1994**. Detecting correlated evolution on phylogenies: a general method for the comparative analysis of discrete characters. *Proceedings of the Royal Society of London B: Biological Sciences* **255**: 37–45.

Pagel M. **1997**. Inferring evolutionary processes from phylogenies. *Zoologica Scripta* **26**: 331–348.

Pagel M. **1999**. Inferring the historical patterns of biological evolution. *Nature* **401**: 877–884.

Pagel M & Meade A. **2014**. Bayes Traits V2. *Computer program and documentation. Available at: http://www. evolution. rdg. ac. uk/BayesTraits. html*.

Pan W. **2001**. Akaike' s information criterion in generalized estimating equations. *Biometrics* **57**: 120–125.

Paradis E & Claude J. **2002**. Analysis of comparative data using generalized estimating equations. *Journal of Theoretical Biology* **218**: 175–85.

Paradis E, Claude J & Strimmer K. **2004**. APE: analyses of phylogenetics and evolution in R language. *Bioinformatics* **20**: 289–290.

De Pinna MGG. **1991**. Concepts and tests of homology in the cladistic paradigm. *Cladistics* **7**: 367–394.

Platnick NI & Dupérré N. **2009**. The American Goblin Spiders of the New Genus *Escaphiella* (Araneae, Oonopidae). *Bulletin of the American Museum of Natural History* **328**: 1–151.

Platnick N & Gertsch WJ. **1976**. The suborders of spiders: a cladistic analysis (Arachnida, Araneae). *American Museum Novitatesum Novitate*: 1–15.

Platnick NI & Shadab MU. **1975**. A revision of the spider genus *Gnaphosa* (Araneae, Gnaphosidae) in America. *Bulletin of the American Museum of Natural History* **155**: 1–66.

Platnick NI & Shadab MU. **1980a**. A Revision of the North American Spider Genera Nodocion, Litopyllus, and Synaphosus (Araneae, Gnaphosidae). *American Museum Novitates*: 1–26.

Platnick NI & Shadab MU. **1980b**. A revision of the spider genus *Cesonia* (Araneae, Gnaphosidae). *Bulletin of the American Museum of Natural History* **165**: 337–385.

Platnick NI & Shadab MU. **1984**. A revision of the neotropical spiders of the genus *Apopyllus* (Araneae, Gnaphosidae). *American Museum Novitates* **2788**: 1–9.

R Core Development Team. **2015**. R: a language and environment for statistical computing, 3.2.1. *Document freely available on the internet at: http://www. r-project. org*.

Ramírez MJ. **2007**. Homology as a parsimony problem: A dynamic homology approach for morphological data. *Cladistics* **23**: 588–612.

Ramírez MJ. **2014**. The morphology and phylogeny of dionychan spiders (Araneae: Araneomorphae). *Bulletin of the American Museum of Natural History* **390**: 1–374.

Ramírez MJ & Michalik P. **2014**. Calculating structural complexity in phylogenies using ancestral ontologies. *Cladistics* **30**: 635–649.

Richter S. **2005**. Homologies in phylogenetic analyses - Concept and tests. *Theory in Biosciences* **124**: 105–120.

Rowe L & Arnqvist G. **2012**. Sexual selection and the evolution of genital shape and complexity in water striders. *Evolution* **66**: 40–54.

Schneider JM, Herberstein ME, De Crespigny FC, *et al.* 2000. Sperm competition and small size advantage for males of the golden orb-web spider Nephila edulis. *Journal of Evolutionary Biology* **13**: 939–946.

Schneider J, Uhl G & Herberstein ME. **2015**. Cryptic female choice within the genus argiope: A comparative approach. In: Peretti A V, Aisenberg A, eds. *Cryptic Female Choice in Arthropods: Patterns, Mechanisms and Prospects*. Heidelberg: Springer, 55–77.

Senglet A. **2004**. Copulatory mechanisms in Zelotes, Drasillus and Trachyzelotes (Araneae, Gnaphosidae) with additional faunistic and taxonomy data on species from Southwest Europe. *Mitteilungen der schweizerischen entomologischen Gesellschaft* **77**: 87–119.

Sentenská L, Pekár S, Lipke E, *et al.* 2015. Female control of mate plugging in a female-cannibalistic spider (Micaria sociabilis). *BMC Evolutionary Biology* **15**: 18.

Sereno PC. **2007**. Logical basis for morphological characters in phylogenetics. *Cladistics* **23**: 565–587.

Sierwald P. **1989**. Morphology and ontogeny of female copulatory organs in American Pisauridae, with special reference to homologous features (Arachnida, Araneae). *Smithsonian Contributions to Zoology*: 1–24.

Sierwald P. **1990**. Morphology and homologous features in the male palpal organ in Pisauridae and other spider families, with notes on the taxonomy of Pisauridae (Arachnidae: Araneae). *Nemouria* **35**: 1–59.

Simmons LW. **2014**. Sexual selection and genital evolution. *Austral Entomology* **53**: 1–17.

Uhl G, Nessler SH & Schneider JM. **2010**. Securing paternity in spiders? A review on occurrence and effects of mating plugs and male genital mutilation. *Genetica* **138**: 75–104.

Welke K & Schneider JM. **2009**. Inbreeding avoidance through cryptic female choice in the cannibalistic orb-web spider Argiope lobata. *Behavioral Ecology* **20**: 1056–1062.

World Spider Catalog. **2016**. World Spider Catalog. Natural History Museum Bern, online at http://wsc.nmbe.ch, version 17.0, accessed on 27.V.2016.

Zakharov BP & Ovtcharenko VI. **2011**. Morphological organization of the male palpal organ in Australian ground spiders of the genera *Anzacia*, *Intruda*, *Zelanda*, and *Encoptarthria* (Araneae: Gnaphosidae). *Journal of Arachnology* **39**: 327–336.

Zakharov B & Ovtcharenko V. **2013**. Male palp organ morphology of three species of ground spiders (Araneae, Gnaphosidae). *Arachnologische Mitteilungen* **45**: 15–20.

Zelditch ML, Swiderski DL, Sheets HD, *et al.* 2004. *Geometric morphometrics for biologists: a primer*. London: Elsevier.

Tables

Table 1. Quasi-likelihood Information Criterion (QIC), parameters estimated and t-test significance of parameters (p) of models of relationships between taxa depth and epigynum complexity. P values less than 0.05 means that parameter is significantly different from zero.

Model_EPI	QIC	Intercept	p	Coef 1	p	Coef 2	p
No relationship	190.4296	6.492165	1.79E-07	_	_	_	_
Linear	195.0208	5.313765	0.000161	0.1367172	0.136668	_	_
Quadratic	197.9252	6.296519	1.20E-06	3.126998	1.46E-01	2.719585	9.62E-02

Table 2. Quasi-likelihood Information Criterion (QIC), parameters estimated and t-test significance of parameters (p) of models of relationships between taxa depth and palp complexity. P values less than 0.05 means that parameter is significantly different from zero.

Model_PALP	QIC	Intercept	p	Coef 1	p	Coef 2	p
No relationship	374.5783	9.350303	1.95E-07	_	_	_	_
Linear	378.3865	9.035528	3.38E-05	0.03652001	0.774535	_	_
Quadratic	381.7759	9.312672	9.45E-07	0.8377897	7.79E-01	0.524473	8.14E-01

Figures

Figure 1. Optimization of genitalic characters on the phylogenetic hypothesis for Gnaphosidae S.S. Characters optimized using Acceleration transformation series (ACCTRAN) criterion. Numbers above the branches are character numbers and below are character states, according to Appendix 1. Open circles indicate homoplastic character transformations, filled squares are non-homoplastic.

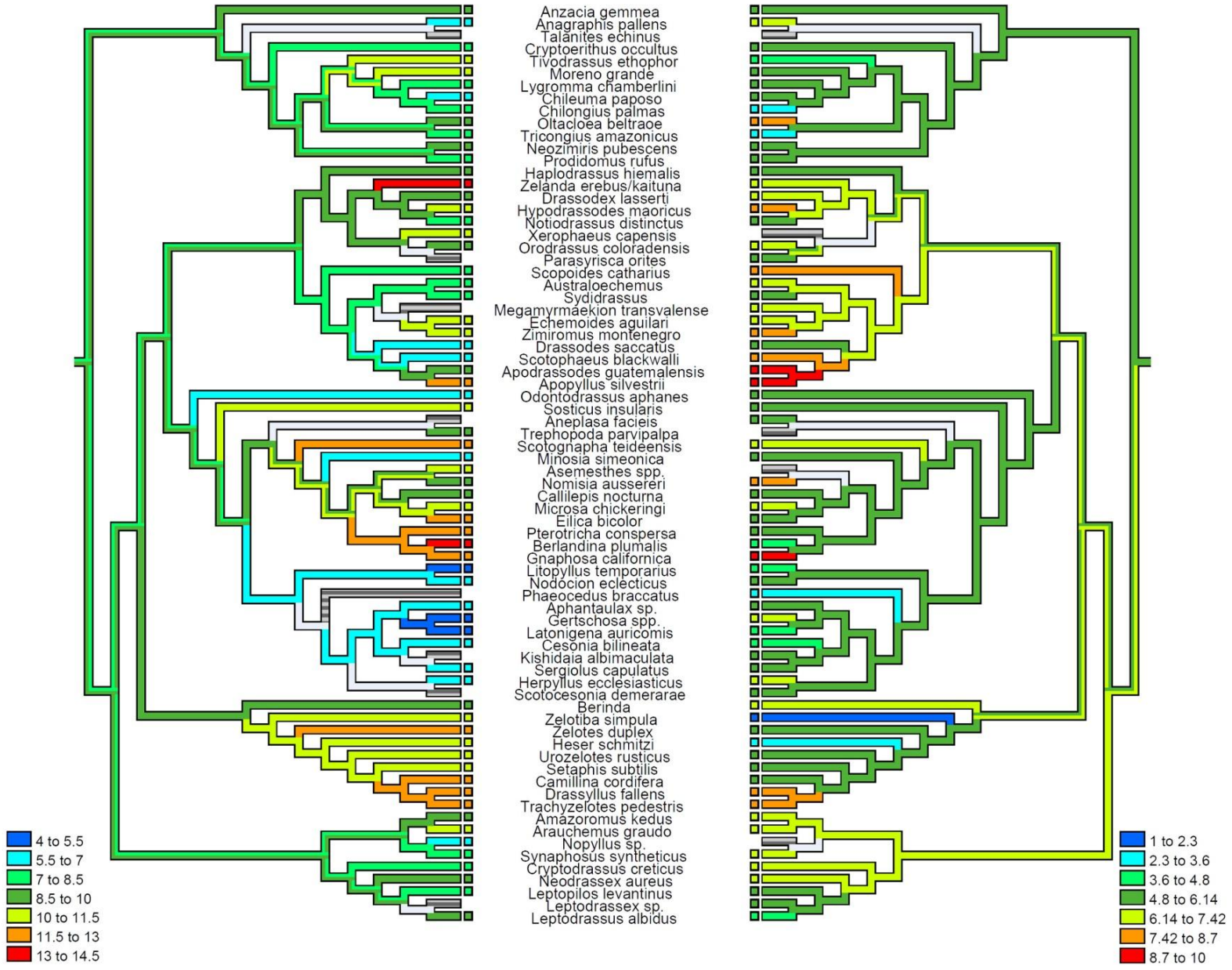

Figure 2. Optimization of palp (left) and epigynum (right) complexity on the phylogenetic hypothesis for Gnaphosidae S.S.

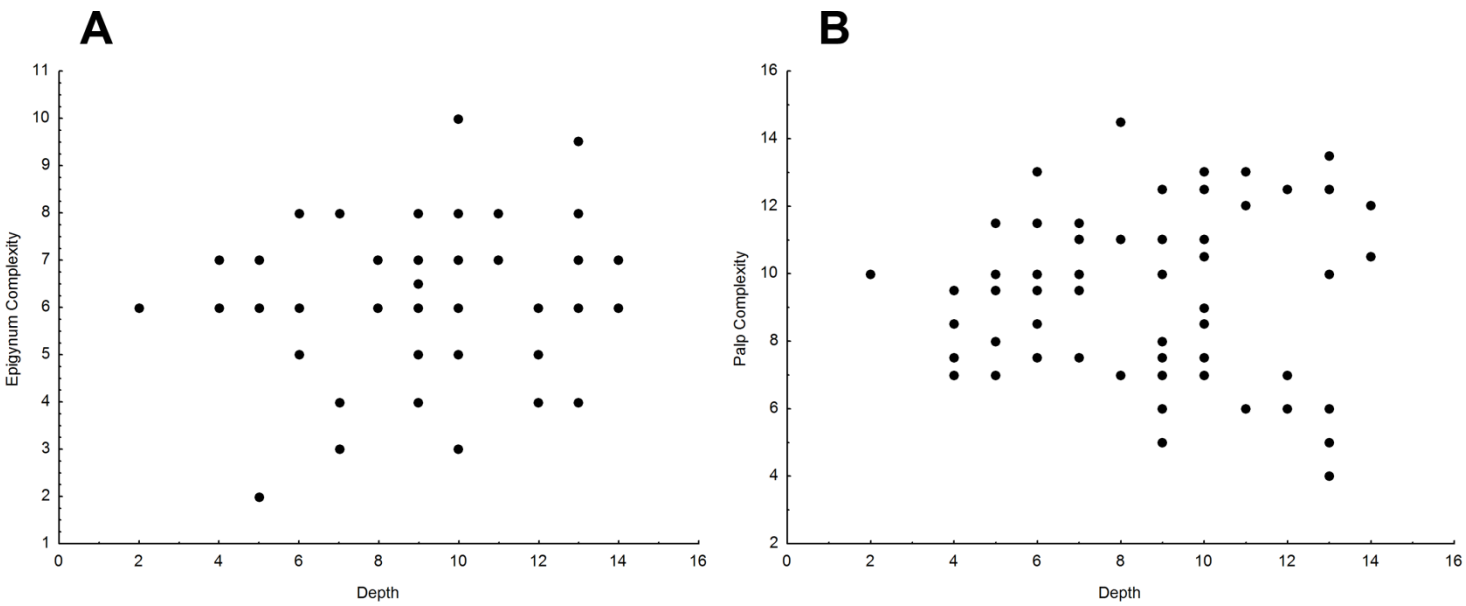

Figure 3. Regression of gnaphosid epigynum (A) and palp (B) complexity on taxa depth (distance to the root) along a family phylogeny. No significant association was found.

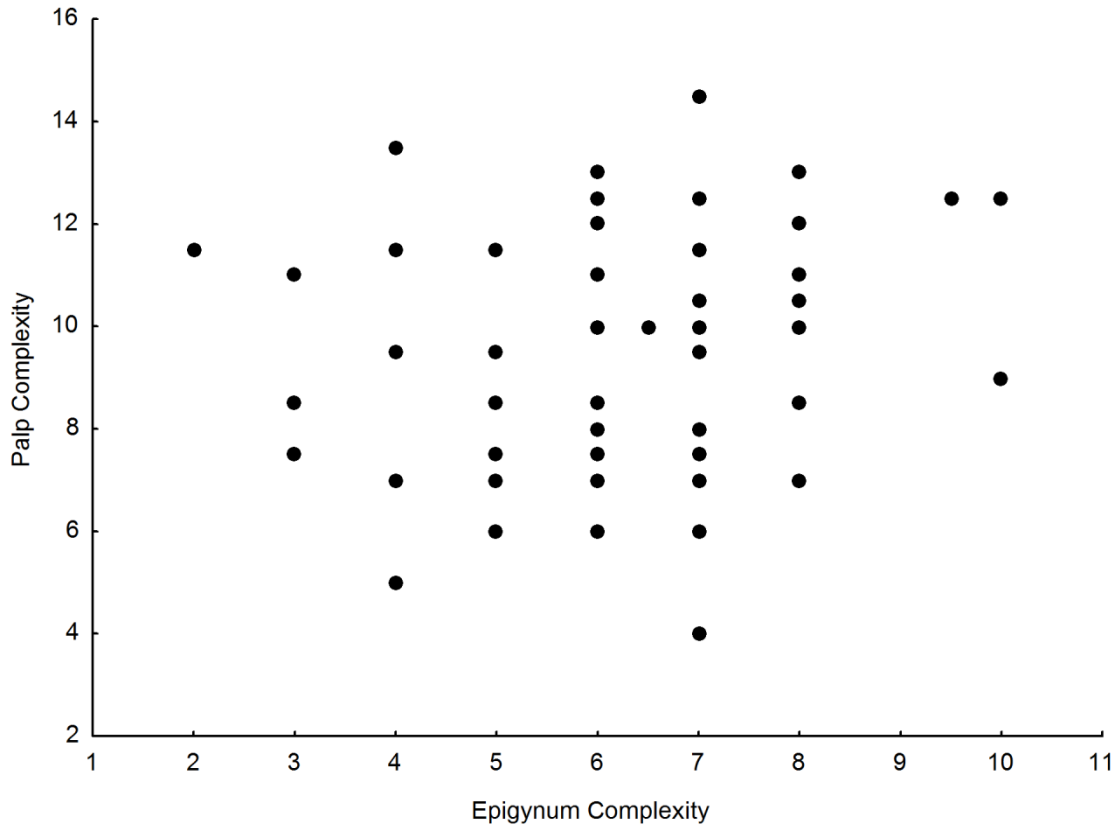

Figure 4. Regression of palp complexity on epigynum complexity among gnaphosid spiders. No significant association was found

Appendices

Appendix 1. List of genitalic characters used in analyses.

0. Epigynum, anterior fold: absent = 0; present = 1.
1. Epigynum, anterior fold, posterior extension forming a secondary lateral fold: absent = 0; present = 1.
2. Epigynum, anterior fold, hood: absent = 0; present = 1.
3. Epigynum, anterior fold, scape: absent = 0; present = 1.
4. Epigynum, lateral folds: absent = 0; present = 1.
5. Epigynum, lateral folds, type: suture = 0; furrow = 1.
6. Epigynum, lateral folds, forming small paramedian epiginal pockets: absent = 0; present = 1.
7. Epigynum, median field, septum: absent = 0; present = 1.
8. Epigynum, midian field, plate surface, atrium: absent, same plane as lateral field = 0; present = 1; unnamed state = 2. [nonadditive].
9. Epigynum, vulva, copulatory ducts, shape: highly convoluted = 0; spiral = 1; curved or with some curls = 2. [nonadditive].
10. Epigynum, vulva, massive midpiece: absent = 0; present = 1.
11. Epigynum, vulva, primary spermathecae: absent = 0; present = 1.
12. Epigynum, vulva, secondary spermatheca: absent = 0; present = 1.
13. Epigynum, vulva, secondary spermatheca, well defined lumen: absent = 0; present = 1.
14. Epigynum, vulva, secondary spermatheca, long duct (at least two imes the head): absent = 0; present = 1.
15. Palp, copulatory bulb, conductor: absent = 0; present = 1.
16. Palp, copulatory bulb, conductor, sclerotization: translucid = 0; sclerotized = 1.
17. Palp, copulatory bulb, embolus distal tubular membrane (articulation): absent = 0; present = 1.
18. Palp, copulatory bulb, embolar base distal projection: absent = 0; present = 1.
19. Palp, copulatory bulb, embolar base proximal projection: absent = 0; present = 1.

20. Palp, copulatory bulb, embolar locking lobe: absent = 0; present = 1.
21. Palp, copulatory bulb, embolus, embolar base, dilatation: absent = 0;
present = 1.
22. Palp, copulatory bulb, embolus, embolar radix projection: absent = 0;
present = 1.
23. Palp, copulatory bulb, embolus, embolar escort sclerite: absent = 0;
present = 1.
24. Palp, copulatory bulb, embolus, length relative to tegulun: about half = 0;
about the same = 1; longer, with loops around it = 2. [nonadditive].
25. Palp, copulatory bulb, embolus, pars pendula: absent = 0; present = 1.
26. Palp, copulatory bulb, embolus, terminal membrane: absent = 0; present = 1.
27. Palp, copulatory bulb, embolus, embolar granulation: absent = 0;
present = 1.
28. Palp, copulatory bulb, fulcrum: absent = 0; present = 1.
29. Palp, copulatory bulb, intercalary scletrite: absent = 0; present = 1.
30. Palp, copulatory bulb, median apophysis: absent = 0; present = 1.
31. Palp, copulatory bulb, median apophysis, proximal, numerous small spines
(granulation?):
absent = 0; present = 1.
32. Palp, copulatory bulb, median apophysis, sclerotization:
completely sclerotized = 0; partially sclerotized = 1; not sclerotized = 2.
[nonadditive].
33. Palp, copulatory bulb, median apophysis, terminal hook: absent = 0;
present = 1.
34. Palp, copulatory bulb, acessory median apophysis: absent = 0; present = 1.
35. Palp, copulatory bulb, membranous tegular extension: absent = 0;
present = 1.
36. Palp, copulatory bulb, membranous tegular extension, type:
long, with sulci to support the embolus = 0; short = 1.
37. Palp, copulatory bulb, petioles: absent = 0; present = 1.
38. Palp, copulatory bulb, subtegulum, locking lobe: absent = 0; present = 1.
39. Palp, copulatory bulb, subtegulum, proximal projection: absent = 0;
present = 1.
40. Palp, copulatory bulb, tegulum, distal tegular projection: absent = 0;

present = 1.

41. Palp, copulatory bulb, tegulum, distal tegular spine-like process: abesnt = 0; present = 1.
42. Palp, copulatory bulb, tegulum, proximal part, covered by subtegulum: absent = 0; present = 1.
43. Palp, copulatory bulb, terminal apophysis: absent = 0; present = 1.
44. Palp, copulatory bulb, terminal apophysis, distal part, bifid: absent = 0; present = 1. .
45. Palp, cymbium, dorsal, terminal, chemosensory patch: absent = 0; present = 1.
46. Palp, cymbium, dorsal, trichobothria: absent = 0; present = 1.
47. Palp, cymbium, retrolateral, median process: absent = 0; present = 1.
48. Palp, cymbium, retrolateral, median process, type: without incision = 0; with incision, forming a conductor-like canal = 1.
49. Palp, cymbium, retrolateral, proximal process: absent = 0; present = 1.
50. Palp, cymbium, ventral, terminal, bunch of thick setae: absent = 0; present = 1.
51. Palp, femur, distal, dorsal, process: absent = 0; present = 1.
52. Palp, femur, distal, prolateral, process: absent = 0; present = 1.
53. Palp, femur, medial, ventral, process: absent = 0; present = 1.
54. Palp, tibia, retrolateral tibial apophysis: absent = 0; present = 1.
55. Palp, tibia, retrolateral tibial apophysis, elaboreted folds: absent = 0; present = 1.
56. Palp, tibia, retrolateral tibial apophysis, ventral lobe: absent = 0; present = 1.
57. Palp, tibia, ventral tibial apophysis: absent = 0; present = 1.
58. Palp, tibia, ventral tibial apophysis, type: singular = 0; bifid = 1.
59. Palp, tibia, dorsal tibial apophysis: absent = 0; present = 1.
60. Palp, tibia, prolateral tibial apophysis: absent = 0; present = 1.
61. Palp, patelae, retrolateral apophysis: absent = 0; present = 1.
62. Palp, tibia, proximal retrolateral tibial apophysis: absent = 0; present = 1.

Appendix 2. Complexity values and proportion of missing data for taxa on phylogenetic tree.

TAXA	Epigynum Complexity	Missing Data (%)	Palp Complexity	Missing Data (%)
Amazoromus kedus	7	0%	10	2%
Ammoxenus coccineus	9	0%	9	2%
Anagraphis pallens	7	0%	7	0%
Aneplasa facieis	5	0%	_	96%
Anyphaena accentuata	8	0%	7.5	2%
Anzacia gemmea	6	0%	10	0%
Aphantaulax sp.	5	4%	6	0%
Apodrassodes guatemalensis	10	0%	9	0%
Apopyllus silvestrii	10	0%	12.5	0%
Arauchemus graudo	7	0%	11.5	0%
Asemesthes spp.	_	31%	11	0%
Australoechemus	7	6%	8	0%
Berinda sp.	7	0%	9.5	0%
Berlandina plumalis	4	0%	13.5	0%
Callilepis nocturna	6	0%	10	0%
Camillina cordifera	6	0%	13	0%
Cesonia bilineata	4	0%	7	0%
Chileuma paposo	5	2%	7	2%
Chilongius palmas	3	2%	8.5	0%
Cithaeron praedonius	5	0%	6	0%
Cryptodrassus creticus	7	0%	7.5	0%
Cryptoerithus occultus	6	2%	8.5	2%
Doliomalus cimicoides	8.5	0%	9	0%
Drassinella sp.	3	0%	7	0%
Drassodes saccatus	6	0%	7	0%
Drassodex lesserti	6.5	0%	10	0%
Drassyllus fallens	8	0%	12	0%
Echemoides aguilari	7	0%	10.5	2%
Eilica bicolor	6	0%	12	0%
Galianoella leucostigma	6	0%	9.5	0%
Gallieniella mygaloides	5.5	0%	12.5	0%
Gertschosa sp.	7	0%	4	0%
Gnaphosa californica	9.5	0%	12.5	0%
Gnaphosoidea TEX	1	4%	11.5	0%
Haplodrassus hiemalis	6	0%	10	10%
Hemicloea sundevalli	6	0%	13	0%
Herpyllus ecclesiasticus	7	0%	6	0%
Heser schmitzi	3	6%	11	0%

Appendix 2. Continuation.

TAXA	Epigynum Complexity	Missing Data (%)	Palp Complexity	Missing Data (%)
Hypodrassodes maoricus	8	0%	11	2%
Kishidaia albimaculata	5	4%	_	96%
Lampona cylindrata	8	0%	6	0%
Latonigena auricomis	4	0%	5	0%
Leptodrassex sp.	6	0%	_	96%
Leptodrassus albidus	4	4%	9.5	0%
Leptopilos levantinus	5	0%	8.5	0%
Liocranum	7	0%	9.5	0%
Litopyllus temporarius	4	2%	5	0%
Lygromma chamberlini	6	0%	8	2%
Meedo houstoni	5	0%	5.5	10%
Megamyrmaekion transvalense	7	0%	_	100%
Micaria gosiuta	6	0%	8	0%
Microsa chickeringi	7	0%	10.5	2%
Minosia simeonica	6	0%	7	0%
Moreno grande	6	0%	11	0%
Nauhea tapa	_	31%	6	2%
Neodrassex aureus	7	4%	9.5	0%
Neozimiris pubescens	5	2%	9.5	2%
Nodocion eclecticus	6	0%	6	0%
Nomisia aussereri	8	0%	10	0%
Nopyllus sp.	_	31%	6	0%
Notiodrassus distinctus	6	0%	7.5	0%
Odontodrassus aphanes	6	0%	7	0%
Oltacloea beltraoe	8	0%	10	0%
Orodrassus coloradensis	7	0%	10	0%
Parasyrisca orites	5	6%	_	96%
Phaeocedus braccatus	3	4%	_	96%
Phrurulithus festivus	3	0%	9	0%
Plator sp.	6	0%	9	0%
Platyoides walteri	8	0%	9.5	0%
Prodidomus rufus	6	4%	7.5	0%
Pterotricha conspersa	6	0%	12.5	0%
Rastellus spp.	3	0%	8	2%
Scopoides catharius	8	0%	8.5	0%
Scotocesonia demerarae	6	0%	_	98%
Scotognapha teideensis	7	0%	12.5	0%
Scotophaeus blackwalli	8	0%	7	2%
Sergiolus capulatus	6	0%	6	0%

Appendix 2. Continued.

TAXA	Epigynum Complexity	Missing Data (%)	Palp Complexity	Missing Data (%)
Setaphis subtilis	6	0%	11	0%
Sosticus insularis	5	0%	11.5	4%
Sydidrassus sp.	5	0%	7.5	0%
Synaphosus syntheticus	7	0%	8	0%
Talanites echinus	_	29%	_	71%
Teutamus rama	3	0%	8.5	2%
Tivodrassus ethophor	4	0%	11.5	0%
Trachelas mexicanus	3.5	0%	5	4%
Trachycosmus sculptilis	8	0%	_	35%
Trachyzelotes pedestris	8	0%	13	2%
Trephopoda parvipalpa	_	31%	9.5	0%
Tricongius amazonicus	3	6%	7.5	6%
Trochantheria gomezi	6	0%	12.5	0%
Urozelotes rusticus	6	0%	11	0%
Vectius niger	5	0%	12.5	0%
Verita sp.	6	2%	_	31%
Xenoplectus sp.	4	0%	11	2%
Xerophaeus capensis	_	29%	10.5	0%
Zelanda erebus/kaituna	7	0%	14.5	0%
Zelotes duplex	6	0%	13	2%
Zelotiba simpula	2	0%	11.5	0%
Zimiromus montenegro	8	0%	10.5	0%

CAPÍTULO III

A TAXONOMIC REVISION OF THE GROUND SPIDERS OF THE GENUS *APOPYLLUS* (ARANEAE: GNAPHOSIDAE)

A taxonomic revision of the ground spiders of the genus *Apopyllus* (Araneae: Gnaphosidae)

(27 pages)

GUILHERME H.F. AZEVEDO[1, 2], RICARDO OTT[3], CHARLES E. GRISWOLD[4] & ADALBERTO J. SANTOS[1]

[1]*Departamento de Zoologia, Instituto de Ciências Biológicas, Universidade Federal de Minas Gerais. Av. Antônio Carlos, 6627, 31270-901, Belo Horizonte, MG, Brasil. E-mail: ghfazevedo@gmail.com*

[2]*Pós-graduação em Zoologia, Universidade Federal de Minas Gerais.*

[3]*Museu de Ciências Naturais, Fundação Zoobotânica do Rio Grande do Sul. Rua Dr. Salvador França, 1427, 90690-000 Porto Alegre, RS, Brazil.*

[4]*California Academy of Sciences, 55 Music Concourse Drive, San Francisco, CA 94118, United States.*

Abstract

The Neotropical gnaphosid genus *Apopyllus* is found from southern Mexico to southern Argentina. It can be diagnosed by the complex shape of RTA, by the membranous tegular extension, the long coiled embolus, the retrolateral incision on the cymbium, the long convoluted copulatory duct extending anteriorly to the copulatory openings and by the presence of paramedian epigynal pockets and of an anterior ridge on the epigynum. The RTA characters are important in species taxonomy and the complex shape and variation of the RTA hampers identification, especially regarding the two most common described species. In this paper the genus is revised, the genital morphology is described and homology between its components and those of other genera is discussed. *Apopyllus paupe*r is considered a senior synonym of *A. iheringi*. Four new species are described from Brazil: *A. aeolicus*, *A. atlanticus*, *A. centralis* and *A. gandarela*.

Keywords: Drassodinae, spider genitalia, *Apopyllus iheringi*, *Apopyllus silvestrii*

Introduction

The spider genus *Apopyllus* was described by Platnick & Shadab (1984) to include eight Neotropical species, distributed from southern Mexico to southern Argentina. Species

of the genus have characteristic genitalic features: the presence of paramedian epigynal openings and highly convoluted copulatory ducts in females (Fig. 1A, B). Males were included in the genus based on the folded retrolateral tibial apophysis, an elongated coiled embolus, an incised cymbium and membranous bifid tegular extension (Fig. 1C, D). Since the proposal of *Apopyllus*, only one species was added to the genus, *Apopyllus isabelae* Brescovit & Lise, 1993; which later turned out to be member of a different genus, *Nopyllus* Ott, 2014 (Brescovit & Lise 1993; Ott 2014).

Despite the peculiar genitalia, species of *Apopyllus* show some characters that indicate possible relationships with other Gnaphosidae genera. The genus is considered closely related to *Apodrassodes* Vellard, 1924 and *Nopyllus*, based on the long embolus supported by a tegular extension (Ott 2014; Platnick & Shadab 1984). However, the homology between palpal sclerites in those genera is still controversial (see Ott 2014). Notwithstanding, there are no clear characters in the *Apopyllus* female genitalia that could indicate close relationship with other described South American genera. The convoluted female copulatory ducts in particular, despite intra and interspecific variation, might have some features comparable between species and genera. A detailed description of *Apopyllus* genitalia is thus essential to facilitate comparison with other genera, in order to obtain reliable primary homology hypotheses and, consequently, better understand their evolutionary relationships.

Despite the homology uncertainties expressed above, the retrolateral tibial apophysis (RTA) is a good putative synapomorphy for the genus. This structure is very complex in shape, unlike other gnaphosid genera (see Murphy 2007), and it is used to distinguish *Apopyllus* species. The two most common species of *Apopyllus*, *A. silvestrii* (Simon, 1905) and *A. iheringi* (Mello-Leitão, 1943), can be sympatric in some localities. Although female specimens can be easily attributed to one of the two species, identifying the males may be a confusing task. The difference between the two species relies on the careful observation of RTA in retrolateral view (Platnick & Shadab 1984), and any slight change in position of the palp being examined might change the perception of its shape. Also, during a survey of gnaphosid material in collections, we found great intraspecific variation in *Apopyllus* RTA morphology, which hampers species identification and suggests that the diversity of the genus could be higher than known nowadays. In this work we describe the genital morphology and the diversity within *Apopyllus* in a taxonomic revision of this Neotropical ground spider genus.

Material and Methods

Specimens were examined immersed in 75% ethanol under a Motic K series stereoscopic microscope. Female genitalia were dissected and soft tissues were cleaned using a pancreatin solution (Álvarez-Padilla & Hormiga 2007). To see better the trajectories of the ducts, epigyna were temporarily cleared using clove oil or methyl salicylate solution (Holm 1979; Levi 1965). Male palpi were expanded using lactic acid heated in double boiler for a few minutes (Levi 1965). Drawings and photographs were made using a Leica M205C, Leica MZ12 and Nikon SMZ800 stereoscopic microscopes and Zeiss Axiostar compound microscope equipped with *camera lucida* and digital cameras. Multifocal images were mounted using the softwares Leica Application Suite and Helicon Focus (Helicon Soft Ltd). Specimens were prepared for Scanning Electronic Microscopy (SEM) using critical point drying, sputter coated with 10 nm of gold and photographed with a Quanta 2000 SEM at the Centro de Microscopia da UFMG and with a LEO 1450vp SEM at the Entomology Department of California Academy of Sciences. Specimens without information about geographic coordinates were georeferenced using geoLoc tool of speciesLink (http://splink.cria.org.br/geoloc) for Brazilian localities, and Google Earth for other countries. Maps were made using ArcMap 10.3 (Esri Inc.).

The format of description follows Platnick & Shadab (1975) with the following modifications: the measurement reported is for the type specimens (holotype and allotype), and the variation are reported separated as the maximum and minimum total and carapace length of sampled specimens. The following abbreviations for the eyes are used: AME, anterior median eyes; ALE, anterior lateral eyes; PLE, posterior lateral eyes; PME, posterior median eyes; MOQ, median ocular quadrangle. Material examined sections were prepared using AUTOMATEX (Brown 2013).

The material used for this study are deposited in the following collections (abbreviations and curators in parentheses): American Museum of Natural History, New York, USA (AMNH, N.I. Platnick); California Academy of Sciences (CASENT, Lauren Esposito and Darrell Ubick); Centro de Coleções Taxonômicas, Universidade Federal de Minas Gerais (UFMG, Adalberto J. Santos); Coleção de História Natural da Universidade Federal do Piauí, Floriano, PI (CHNUFPI, Leonardo S. Carvalho); Laboratório Especial de Coleções Zoológicas, Instituto Butantan, São Paulo, (IBSP, Antonio D. Brescovit); Museo Argentino de Ciencias Naturales Bernadino Rivadavia, Buenos Aires (MACN, Martín J. Ramirez); Museo de La Plata, La Plata (MLP, Luís A.

Pereira); Museu de Ciências Naturais, Fundação Zoobotânica do Rio Grande do Sul, Porto Alegre (MCN, Ricardo Ott); Museu de Ciências e Tecnologia, Pontifícia Universidade Católica do Rio Grande do Sul, Porto Alegre (MCTP, Arno A. Lise); Museu Nacional, Rio de Janeiro (MNRJ, Adriano B. Kury); Museu Paraense Emílio Goeldi, Belém (MPEG, Alexandre B. Bonaldo); Museum of Comparative Zoology, Havard University, Cambridge, USA (MCZ, Gonzalo Giribet); National Museum of Natural History, Smithsonian Institution, Washington D.C. (USNM, Jonathan A. Coddington).

Taxonomy

Family Gnaphosidae Pocock, 1898

Genus *Apopyllus* Platnick & Shadab, 1984

Type species: *Zelotes silvestrii* (Simon, 1905)

Diagnosis. Females of *Apopyllus* can be recognized by the long, convoluted copulatory ducts extending anteriorly to the copulatory openings, and by the presence of paramedian epigynal pockets and of an anterior ridge in the epigynum (Figs 1A–B, 2A–B). Males can be distinguished from other gnaphosid genera by the shape of RTA, which is folded in an elaborated structure, by the long bifid membranous tegular extension (MTE) that supports the long coiled embolus, by a retrolateral incision on the cymbium, and by the presence of median apophysis on tegulum (Figs 1C–D, 2C).

Description. As in Platnick & Shadab (1984), except for the male and female genitalia, which are described below, and for the presence of terminal pseudosegmentation of metatarsi IV in both sexes (Fig. 2D). The female internal genitalia (vulva) of *Apopyllus* are composed of a pair of highly convoluted copulatory ducts, a pair of secondary spermathecae (blind end receptacles with large glandular pores), a pair of primary spermathecae (receptacles with small pores) that are connected to a pair of fertilization ducts (Figs. 1A–B, 2B). The copulatory ducts, though variable between and within species, have a basic structure that can be observed in all species (Figs. 1A–B). The copulatory opening leads to the proximal part of the copulatory duct (PPD) that is ventrally located and has a "U" shape. It curves dorsally and goes towards the posterior part of epigynum, forming the paramedian descendent duct (PDD). The PDD curves towards the anterior part, forming the lateral ascendant duct (LAD). It extends anteriorly to the copulatory opening forming the anterior curled duct (ACD). The ACD

leads to a ventral duct that goes posteriorly, called lateral descendent duct (LDD). It curves forming the lateral loop (LL) and then the paramedian ascendant duct (PAD). The PAD curves dorsally leading to the terminal part of the copulatory duct (TPD), which ends at the primary spermatheca. The secondary spermatheca is a rounded blind sac of variable size that arises from the lateral loop.

Male genitalia have a small subtegulum that can be seen in ventral view on unexpanded palp (Fig. 1C). The tegulum is rounded to oval, with an elongated, partially sclerotized, hook shaped median apophysis (Figs. 1C, 2C), and with a long bifid membranous tegular extension (MTE) that supports a long coiled embolus (Figs. 1C–D, 2C). The embolus articulates with the tegulum by a long distal tubular membrane (DTM) (Fig. 2C). The RTA is folded in an elaborated structure, with ventral, dorsal and apical serrated keels (Figs. 2C). The cymbium has a retrolateral projection ventrally incised (Figs. 1C–D, 2C).

Distribution. Neotropical, from southern South America to southern Mexico.

Natural History. Species of *Apopyllus* can be found in areas with rocky ground and might be active during daylight (GHFA personal observation).

Identification key to *Apopyllus* species

Males

1 Cymbial incision proximally situated, cymbial projection evident and positioned proximally (Figs. 3A–C, 3E–G, 4A–C, 4E–G, 5A–C, 5E–G, 6A–C, 6E–G, 7A–C, 7E–G, 8A–C, 8E–G) … 2

- Cymbial incision distally situated (Figs. 3D, 4D, 5D, 6D), cymbial projection small and distally positioned (Figs. 7D, 8D), RTA as in figures 3D, 4D, 5D, 6D, 7D and 8D *A. ivieorum*

2 Cymbial projection shorter than RTA in dorsal and ventral view (Figs. 3C, 4C, 7C, 8C), retrolateral loop of the embolus and MTE short, not extending as far as the proximal part of the cymbium (Figs. 5C, 6C), RTA robust (Figs 5C, 6C, 7C, 8C) … *A. now*

- Cymbial projection longer or as long as RTA in dorsal and ventral view (Fig. 3A, 3B, 3E, 3F, 4A, 4B, 4E, 4F, 7A, 7B, 7E, 7F, 8E, 8F), embolus and MTE long, extending as far to the proximal part of the cymbium (Figs. 5A, B, E-F and 6E-F), RTA otherwise… 3

3 RTA with a dorsal process (Figs. 5F, 6F, see arrow)… *A. centralis* **new sp.**

- RTA without dorsal process (Figs. 5A–E, G, 6A–E, G)… 4

4 RTA with a proximal spine on the apical keel (Fig 5E, 6E, see arrow)… *A. aeolicus* **new sp.**

- RTA without a proximal spine on the apical keel (Fig. 5A–C, F, G, 6A–C, F, G)… 5

5 RTA with truncated tip (Figs. 7A, 8A, 9A–B), dorsal keel of RTA rounded and curved in retrobasal view (Fig. 9B), apical keel of RTA sinuous in apical view (Fig. 9A)… *A. silvestrii*

- RTA with pointed tip (Figs. 7B, G, 8B, G, 9C–F), dorsal keel of RTA more or less rhomboidal in retrobasal view (Figs. 9D, 9F), apical keel of RTA gently curved in apical view (Figs. 9C, 9E) … 6

6 RTA very pointed in dorsal and retrobasal view (Figs. 7G, 8G, 9E–F), shape of RTA in retrobasal view as in figure 9F… *A. atlanticus* **new sp.**

- RTA blunt in dorsal, apical and retrobasal view (Figs. 7B, 8B, 9C–D), shape of RTA as in figure 9D… *A. pauper*

Females

1 Anterior ridge completely sclerotized (Figs. 10A–F, 11A–F)… 2

- Anterior ridge less sclerotized in the middle, conferring an incomplete appearance (Fig 10G, 11G)… *A. centralis* **new sp.**

2 Anterior ridge thin (Figs. 10D, 11D)… 3

- Anterior ridge thick (Figs. 10A–C, E, F, H, 11A–C, E, F, H)… 4

3 PDD and LAD extended posteriorly beyond the anterior edge of primary spermathecae (See Platnick & Shadab 1984: fig. 18)… *A. suavis*

- PDD and LAD not extended posteriorly beyond the secondary spermathecae (Figs. 10D, 11D)… *A. huanuco*

4 Diameter of secondary spermathecae at least two thirds the diameter of primary spermathecae (Figs. 12B, 12F, 12H, 13B, 13F, 13H)… 5
- Diameter of secondary spermathecae less than two thirds the diameter of primary spermathecae (Figs. 12A, 12C-E, 12G, 13A, 13C–E, 13G)… 7

5 Anterior ridge sinuous (Figs. 10F, 11F)… *A. gandarela* **new sp.**
- Anterior ridge otherwise (Figs. 10A, 10B, 10E, 11G, 11H, 11A, 11B, 11E, 11GH) … 6

6 Epigynal pockets bell-shaped, with the angle between them directed posteriorly (Figs. 10B, 11B)… *A. pauper*
- Epigynal pockets elongated, with the angle between them directed anteriorly (Fig. 10H, 11H)… *A. atlanticus* **new sp.**

7 Anterior ridge sinuous (Figs. 10C, 11C), ACD single-coiled (Figs. 12C, 13C)… *A. malleco*
- Anterior ridge otherwise (Figs. 10A, 10B, 10E, 11G, 11H, 11A, 11B, 11E, 11GH)…8

8 PDD and LAD parallel (Figs. 12A, 13A), anterior ridge not arched (Figs. 10A, 11A)… *A. silvestrii*
- PDD and LAD not parallel (Fig 12E, 13E), anterior ridge arched (Fig. 10E, 11E)… *A. now*

***Apopyllus silvestrii* (Simon, 1905)**
Figures 2A–D, 3A, 4A, 5A, 6A, 7A, 8A, 9A–B, 10A, 11A, 12A, 13A, 14A

Melanophora silvestrii Simon, 1905: 4. Male and female syntypes from Missioneros, Río Santa Cruz, Santa Cruz, Argentina. Deposited in MNHN (not examined).
Zelotes silvestrii: Petrunkevitch, 1911: 151.
Zelotes melanophorus Mello-Leitao, 1941: 169, fig. 59. Male and female syntypes from Colalao, Tucuman, Argentina (31º14’3”S, 64º15’40”W). Deposited in MLP 14895 (examined through photographs). Synonym by Platnick & Shadab (1984).

Gytha argentina Mello-Leitão, 1944: 351, fig. 42. Male holotype from La Plata, Buenos Aires, Argentina (34º55'16"S, 57º57'15"W). Deposited in MLP 16080 (examined through photographs). Synonym by Platnick & Shadab (1984).
Apopyllus silvestrii: Platnick & Shadab, 1984: 3, figs. 1–4.

Diagnosis. Males can be distinguished by truncated terminal tip of RTA in dorsal view (Figs 7A, 8A), a sinuous apical keel of RTA (Fig. 9A) and dorsal keel of RTA rounded and curved in retrobasal view (Fig. 9B). Females can be distinguished by the parallel PDD and LAD and by the secondary spermatheca much smaller than the primary spermatheca (Figs. 12A, 13A).
Description. See Platnick & Shadab (1984). In addition, the RTA has a small basal retrolateral tubercle (Fig. 2C).
Variation. Male carapace length (N=18) 1.84–3.32. Female carapace length (N=15) 2.28-3.32.
Material Examined. Material examined. **ARGENTINA: Chubut:** Epuyén (labeled as Epuylu), 42º14'3"S, 71º21'3"W, 6m# 3f# 1 juvenile, 12/VI/1962, A. Kovacs coll. (AMNH), 1m# 1f#, 2/VIII/1962, A. Kovacs coll. (AMNH), Esquel, Road to La Hoya, 42º54'S, 71º19'W, 2f#, 16/XI/1988, V. & B. Roth coll. (CASENT 9066946); **Córdoba:** Pampa de Achala, El Cóndor, 31º36'31"S, 64º45'44"W, 2152.2m, 1f#, 8/XII/1997, A. Kury coll. (MNRJ 6664). **BOLÍVIA: Huatajata:** La Paz, Lake Titicaca, 16º13'37"S, 68º41'37"W, 2m# 1f#, 8/VIII/1993, H. Höfer & A.D. Brescovit coll. (MCN 23741). **BRAZIL: Minas Gerais:** Belo Horizonte, Campus da UFMG, 19º51'41"S, 43º57'48"W, 1m#, 6/V/2001, E.O. Machado coll. (UFMG 686), Belo Horizonte, Estação Ecológica da UFMG, 19º52'38"S, 43º58'16"W, 845m, 1f#, I/2001 (UFMG 8330), 1f#, III/2001 (UFMG 8323); **Rio Grande do Sul:** Bagé, 1m#, 30/X/2003, L. Almeida coll. (MCTP 16977), 1f#, 30/XII/2003, L. Almeida coll. (MCTP 16976), Carlos Barbosa, 29º18'0"S, 51º30'0"W, 1m#, 28/X/1989, A.A. Lise coll. (MCN 18964), Eldorado do Sul, 1m#, 25-30/XI/1996, G. Carvalho & R. Silva coll. (MCTP 12551), Itaara, 29º45'18"S, 53º59'31"W, 1m#, 24/VIII/2009, R. Alves coll. (MCTP 26289), 29º45'18"S, 57º5'16"W, 3m# 1f#, X/2009, R. Alves coll. (MCTP 26292, 26293), Morrinhos do Sul, Pixirica, 2f#, 02/XI/2006, A. Gonçalves coll. (MCN 52302), 1m, 1f#, 1-16/VI/2006, A. Gonçalves coll. (MCN 52300), Porto Alegre, 1m#, 10/V/2000, A. Braul coll. (MCTP 11216), Morrinhos do Sul, Três Passos, 1f#, 01/XI/2006, A. Gonçalves coll. (MCN 52301), Porto Alegre, Vila Nova, 29º59'29"S, 51º13'16"W, 2m#

1f#, 21/XI/2006, E.L.C. Silva coll. (MCTP 19720), Santana do Livramento, Rincão Bonito do Ibirapuitã, 30º37'49"S, 55º32'26"W, 1m#, 13/XI/2012, Equipe PELD/MCN coll. (MCN 52296), São Francisco de Paula, Potreiro Velho, Pró Mata, 1f#, 20/VII/1999, A. A. Lise coll. (MCTP 12671), 1m#, 21-24/X/1999, A. A. Lise coll. (MCTP 16028), Uruguaiana, Imbaa, 1m#, 24/VI/2009, R. Alves coll. (MCTP 26288), 2f#, 2m#, I/2009, R. Alves coll. (MCTP 26282, 26283, 26285, 26286), 1f#, II/2009, R. Alves coll. (MCTP 26284), 1m#, IX/2009, R. Alves coll. (MCTP 26290), 1m#, X/2009, R. Alves coll. (MCTP 26291), Minas do Leão, 1m#, 12/VI/2008, L. R. Podgaiski coll. (MCN 44393), Viamão, Parque Estadual Itapuã, 2m#, 2f#, 18/IV–06/V.2007, R. Moraes coll. (MCTP 29996), ; **Santa Catarina:** Chapecó, 27º6'1"S, 52º35'59"W, 1m#, 23/IX/2008, R.C. Francisco coll. (MCTP 29641), Florianópolis, 27º34'60"S, 48º33'59"W, 1f#, 24/X/1988, V. & B. Roth coll. (CASENT 9066937), 1m#, 23/V/2003, C. E. Santo coll. (MCTP 19765). **PERU: Puna:** Lake Titicaca, 15º50'28"S, 70º1'31"W, 3900m, 1f#, VI/1947, W. Weyrauch coll. (AMNH); **Puno:** 60km N Puno, 15º50'24"S, 70º1'18"W, 1m# 1f# 2 juveniles#, 21/II/1951, Ross & Michelbacher coll. (CASENT 9048498). **URUGUAY: Lavalleja:** Arequita, Cerro Arequita, 34º17'11"S, 55º16'5"W, 1f#, 5/XII/1997, A.D. Brescovit coll. (IBSP 14468).

Distribution. Southern Chile and Argentina to Southern Peru and Central- Western Brazil (Fig. 14A).

***Apopyllus pauper* (Mello-Leitão, 1942)**

Figures 3B, 4B, 5B, 6B, 7B, 8B, 9C–D, 10B, 11B, 12B, 13B, 14B

Zelotes pauper Mello-Leitão, 1942: 413, fig. 39. Female holotype from General Capdevila, Chaco, Argentina (27º25’18”S, 61º28’37”W). Deposited in MLP 15500 (examined through photographs).

Zelotes iheringi Mello-Leitão, 1943: 262. Female holotype from Paraiba do Norte, Paraíba, Brazil (36º30’S, 75º15’W). Deposited in MNRJ 58361 (examined). **New synonymy.**

Apopyllus pauper: Platnick & Shadab, 1984: 4, figs. 5, 6.

Apopyllus iheringi: Platnick & Shadab, 1984: 5, figs. 11–14. **New synonymy.**

Diagnosis. Females can be distinguished by the secondary spermatheca with diameter at least two thirds as long as the primary spermatheca, by the TPD curved dorsally, by the

curved PDD (Figs 12B, 13B) and by the short bell-like paramedian epigynal pockets (Figs 10B, 11B). Males can be distinguished by the moderately pointed terminal part of RTA in dorsal and retrobasal view (Figs. 7B, 8B, 9D), by the gently curved dorsal keel of RTA in apical view (Fig. 9C) and by the rhomboidal shape of RTA in retrobasal view (Fig. 9D).

Synonymy. *Apopyllus pauper* was described as having the PAD "expanded anteriorly into bulbous form" (Platnick & Shadab 1984: p. 5, figs. 5–6). This description matches the aspect of the holotype genitalia when examined ventrally, without any preparation. However, the expanded ducts are not visible when the genitalia are examined under clove oil or methyl salicilate (Fig. 15A–B), and the duct aspect does not seem to be different from that described for *Apopyllus iheringi* (Platnick & Shadab 1984: p. 5). Other aspects of the morphology of the *A. pauper* holotype also seem to be within the variation observed in the *A. iheringi*. Thus, we do not see evidence that could indicate that *A. iheringi* and *A. pauper* are different species.

Description. For the female see description of *Apopyllus pauper* in Platnick & Shadab (1984), which is like in the diagnosis reported here except for the description of female genitalia. For the males, see *Apopyllus iheringi* in Platnick & Shadab (1984).

Variation. The anterior ridge of the epigynum varies from straight to concave in the posterior and/or anterior margin. The dorsal keel of RTA might be from moderate to strongly curved. RTA simple or with a small basal retrolateral tubercle as in *A. silvestrii*. Some specimens might be dark brown to black with a white or silver gray dorsal longitudinal stripe in the opisthosoma and carapace, or with carapace entirely silver gray. Male carapace length (N=18) 1.28-3.4. Female carapace length (N=16) 1.96-3.40.

Material Examined. ARGENTINA: Catamarca: Villavil, 8km E. of Andalgala, 27º36'16"S, 66º17'16"W, 3f#, 30/XII/1974, F.A. Enders coll. (USNM); **Córdoba:** Los Molinos, 31º50'46"S, 64º22'59"W, 1f# 1 juvenile#, 7/XII/1997, A. Kury coll. (MNRJ 6663); **La Pampa:** Cuaracó, RN 152, 56 km from Casa de Piedra, 38º8'40"S, 66º29'33"W, 295m, 2m# 2 juveniles#, 11/X/2014, A.D. Brescovit *et al.* coll. (IBSP 167048, MACN 34838), Lihue Calel, PN Lihue Calel, cerro Fortaleza, 38º1'15"S, 65º35'32"W, 419m, 3m# 3 juveniles#, 11/X/2014, A.D. Brescovit *et al.* coll. (IBSP 167047, MACN 34843), Linhue, 1m# 1 juvenile# (IBSP 167049); **La Rioja:** Mazan, 29º25'15"S, 66º51'0"W, 1f#, 8/XII/1974, F.A. Enders coll. (USNM); **Río Negro:** El Cuy, RP 6, 88 km SW from General Roca, 39º42'28"S, 68º9'19"W, 617 m, 1m#,

12/X/2014, A.D. Brescovit *et al.* coll. (MACN 34844), General Roca, Cinco Saltos, camino a Lago Pellegrini, 38º48'42"S, 68º3'7"W, 270m, 1f#, 16/X/2014, A.D. Brescovit *et al.* coll. (IBSP 167054), General Roca, Paso Córdoba, 39º7'37"S, 67º40'6"W, 266m, 1m#, 15/X/2014, A.D. Brescovit *et al.* coll. (MACN 34839), Valcheta, 1f# (IBSP 167050), Valcheta, RN 23, 36 km SE from Valcheta, 40º51'37"S, 65º48'44"W, 208m, 2m# 3f# 1 juvenile, 13/X/2014, A.D. Brescovit *et al.* coll. (MACN 34841). **BRAZIL: Bahia:** Feira de Santana, Chácara Promenade, 1f#, 4-6/I/2003, T. V. Aguzzoli coll. (MCN 35061); **Goiás:** Catalão, Barragem para Aproveitamento Hidrelétrico Serra do Facão, 17º31'56.09"S, 47º33'36"W, 754m, 1f#, VII/2010, R.B. Martines & R.M.C. Silveira coll. (UFMG 4565), 17º52'20.39"S, 47º37'34.89"W, 739m, 1f#, VII/2010, R.B. Martines & R.M.C. Silveira coll. (UFMG 4584), 17º36'26.07"S, 47º37'13.57"W, 811m, 2m#, VII/2010, R.B. Martines & R.M.C. Silveira coll. (UFMG 4566); **Maranhão:** Caxias, Reserva Ecológica Inhamum, 4º49'60"S, 43º20'69"W, 5f#, 2–5/X/2007, J.F.B. Lima-Lobato & F. Limeira de Oliveira coll. (IBSP 129017, 129022, 129023), 1m# 4f#, 26–29/IX/2007, J.F.B. Lima-Lobato & F. Limeira de Oliveira coll. (IBSP 129015, 129024); **Mato Grosso:** Chapada dos Guimarães, 2m#, 20-29/VII/2000, C. Strussmann coll. (MCTP 11310), 2m#, 23-30/VIII/2000, C. Strussmann coll. (MCTP 11327); **Piauí:** Piracuruca, Parque Nacional Sete Cidades, 4º05'56.2"S, 41º43'12.9"W, 1m#, no data, no col. (MPEG 7904); **Mato Grosso do Sul:** Três Lagoas, Horto Barra do Moeda, 20º57'0"S, 51º47'0"W, 1m# 1f#, 8/VIII/2007, M. Uehara-Prado coll. (UFMG 5073); **Minas Gerais:** Belo Horizonte, Estação Ecológica da UFMG, 19º52'38"S, 43º58'16"W, 845m, 1m#, 2003 (UFMG 8328), Belo Horizonte, Parque Municipal das Mangabeiras, 19º56'38.98"S, 43º54'1.07"W, 1f#, 5–12/XII/2008, H.H. Santos *et al.* coll. (UFMG 7886), Cardeal Mota, Serra do Cipó, 19º20'15.84"S, 43º38'18.72"W, 805m, 2f#, 17/VII/2012, P.H. Martins *et al.* coll. (UFMG 12326, 12327), Catas Altas, RPPN Santuário do Caraça, Cachoeira da Bocaina, 20º7'25"S, 43º27'56"W, 1f#, 12/IX/2015, G.H.F. Azevedo coll. (UFMG 18861), Leme do Prado, Reserva Estadual de Acauã, 17º7'94.2"S, 42º43'98.1"W, 887m, 2m# 2f#, 18–28/II/2013, P.H. Martins coll. (UFMG 12837), 17º9'3.6"S, 42º46'24.1"W, 856m, 4f#, 18–28/II/2013, P.H. Martins coll. (UFMG 12982), Manga, Parque Estadual da Mata Seca, 14º50'54"S, 43º59'17"W, 1f#, IX/2010, 14º50'58"S, 44º0'28"W, 2m#, IX/2011, 14º50'54"S, 43º59'17"W, 2m#, IX/2011, R.N.S.L. Garro *et al.* coll. (UFMG 14775–14777), Santo Antônio do Itambé, Parque Estadual do Pico de Itambé, 18º27'58"S, 43º18'27"W, 757m, 1f#, 16–17/II/2013, P.H. Martins coll. (UFMG 12981), São

Gonçalo do Rio Abaixo, Estação de Preservação e Desenvolvimento Ambiental de Peti, 19º58'23"S, 43º29'57"W, 820m, 1f#, 8–9/XII/2012, G.H.F. Azevedo *et al.* coll. (UFMG 12653); **Pernambuco:** Serra Talhada, Fazenda Saco, Mata da Pimenteira, 7º53'S, 38º18'W, 1f#, 17/X/2010, M. Carvalho coll. (UFMG 4492); **Rio Grande do Sul:** Santana do Livramento, Faz. Bela Vista do Ibirapuitã, 1m#, 14/XI/2012, Equipe PELD/MCN coll. (MCN 52297); Santana do Livramento, APA do Ibirapuitã, Faz. D. Laura, Rincão Bonito, 1f#, 12/XI/2012; R. Ott coll. (MCN 52309), APA do Ibirapuitã Faz. Bela Vista, 1f, 14/XI/2012; Eq. PELD/MCN coll (MCN 52310). **Roraima:** Amajari, Vila Tepequém, prox. Da Pousada PSJ, 3º47'10.4"N, 61º43'15.3"W, 640m, 1m#, 17/VII/2014, L.S. Carvalho *et al.* coll. (UFMG 17107); **Tocantins:** Santa Fé do Araguaia, 6º43'41.6"S, 48º48'8"W, 1m#, 19/IV/2009, U. Oliveira & M.D. Miranda coll. (UFMG 5736). **PERU: Apurimac:** Chincherros, 13º31'3"S, 73º42'24"W, 2m# 3f# 1 juvenile, 12/XII/1980, C. Gold coll. (CASENT 9057334).

Distribution. Northern Argentina to southern Peru and to northern and northeastern Brazil (Fig. 14B).

***Apopyllus malleco* Platnick & Shadab, 1984**

Figs. 1A–B, 10C, 11C, 12C, 13C, 14B

Apopyllus malleco Platnick & Shadab, 1984: 6, figs. 7–8. Female holotype from 10 km. west of Collipulli, Malleco, Chile (38º21’33”S, 72º38’20”W), 4/I/1961, J. K. Greer coll., deposited in AMNH (examined).

Diagnosis. Females **c**an be distinguished by the sinuous anterior ridge of the epigynum and ACD with a single coil (Figs. 10C, 11C, 12C, 13C).

Description. See Platnick & Shadab (1984).

Material examined. Only the holotype.

Distribution. Known only from the type locality, Malleco, Chile (Fig. 14B).

***Apopyllus huanuco* Platnick & Shadab, 1984**

Figs. 10D, 11D, 12D, 13D, 14C

Apopyllus huanuco Platnick & Shadab, 1984: 6, figs. 9–10. Female holotype from Acomayo, Huanuco, Peru (13º55'26"S, 71º41'35"W, 2100m), VII/1946, F. Woytkowski coll. Deposited in AMNH (examined).

Diagnosis. Females can be distinguished by the very arched and thin anterior ridge in the epigynum, by the short PDD and LAD not overlapping the secondary spermathecae. (Figs. 10D, 11D, 12D, 13D).

Description. See Platnick & Shadab (1984).

Material examined. Huanuco, Peru, 9º27'1"S 76º16'15"W, 1f#, 27/I/1947, J.C. Pallister col. (AMNH).

Distribution. Known only from the type locality, Huanuco, Peru (Fig. 14C).

***Apopyllus now* Platnick & Shadab, 1984**

Figs. 3C, 4C, 5C, 6C, 7C, 8C, 10E, 11E, 12E, 13E, 14A

Apopyllus now Platnick & Shadab, 1984: 7, figs. 19–22. Male holotype and female paratype from the south slope of Veeris Berg, Curaçao (12º10'7"N, 68º59'25"W), 20/XII/1962, H.W. Levi coll., deposited in MCZ (examined).

Diagnosis. Females can be distinguished by the anterior ridge arched and thick on the sides (Figs. 10E, 11E) and by the dorsal longitudinal pale white stripe in the prosoma and opisthosoma. Males can be diagnosed by the retrolateral cymbial projection shorter than the RTA in dorsal and ventral view, by the shorter embolus, with a more distally situated embolus loop, and by the shape of the robust RTA (Fig. 3C, 4C, 5C, 6C, 7C, 8C).

Description. See Platnick & Shadab (1984).

Material examined. The holotype and paratype only.

Distribution. Known only from the type locality, Curaçao (Fig. 14A).

***Apopyllus ivieorum* Platnick & Shadab, 1984**

Figs. 3D, 4D, 5D, 6D, 7D, 8D, 14A

Apopyllus ivieorum Platnick & Shadab, 1984: 8, figs. 15–16. Male holotype from 8 mi. west of Tehuantepec, Oaxaca, Mexico (16º57’19”N 96º28’15”W), 29/VIII/1966. J. and W. Ivie coll., deposited in AMNH (examined).

Diagnosis. Males can be distinguished by the cymbial incision distally situated, by the absence of a cymbial retrolateral projection, and the characteristic shape of RTA (Figs 3D, 4D, 5D, 6D, 7D, 8D).
Description. See Platnick & Shadab (1984). Females unknown.
Material examined. Only the type material.
Distribution. Known only from the type locality, Oaxaca, Mexico (Fig. 14A).

***Apopyllus suavis* (Simon, 1893)**

Herpyllus suavis Simon, 1893: 455, fig. 25. Two female syntypes from Colonia Tovar, Aragua, Venezuela (10º24’19”N, 67º17’22”W), deposited in MNHN (not examined).
Apopyllus suavis: Platnick & Shadab 1984: 7, figs. 17–18.

Diagnosis. Females can be distinguished by the PDD and LAD extending beyond the anterior edge of primary spermathecae, and by the arched anterior ridge (see Platnick & Shadab, 1984, figs 17, 18).
Description. See Platnick & Shadab (1984). Males unknown.
Distribution. Known only from the type locality, Aragua, Venezuela (Fig. 14C).
Remarks. Although we have not seen the syntypes, the description and drawings in Platnick & Shadab (1984) allow us to infer that this specimen is morphologically different from the other species in the genus and might be acknowledged as a distinct species.

***Apopyllus gandarela* new species**
Figs. 10F, 11F, 12F, 13F, 14A

Type Material. Female holotype from Serra da Gandarela, Rio Acima, Minas Gerais, Brazil (20º5´31” S, 43º41’0” W, 1636m), 14/II/2015, A.J. Santos coll., deposited in UFMG 16876.

Etymology. The specific name is taken from the type locality, Serra da Gandarela, one of the many mountain ranges that contribute to the aquifer system of the region, and which is threatened by mining activities.

Diagnosis. Females can be distinguished by the sinuous anterior ridge, with the middle part projected anteriorly, by the ACD very coiled, and by the secondary spermathecae about two thirds the diameter of the primary ones (Figs. 10F, 11F, 12F, 13F).

Description. Female (holotype): Total length 7.5. Carapace 2.6 long, 1.88 wide. Femur II 1.68 long. Carapace dark brown, with black reticulations. Legs and palps brown, lighter in patellae, tibiae, metatarsi and tarsi. Femur I with a lighter area in the prolateral proximal part. Sternum and labium brown. Endites light brown with white anterior border. Opisthosoma pale gray. Eyes sizes and interdistances: AME 0.08, ALE 0.1, PME 0.07, PLE 0.08, AME–AME 0.06, AME–ALE 0.02, ALE–PLE 0.05, PME–PME 0.06, PME–PLE 0.06. MOQ 0.48 wide. Leg spination: femora: I, II d1-1-1, p0-0-1; III d1-1-1, r0-1-1, p0-1-1; patellae: III, IV p0-1-0, r0- 1-0; tibiae: I v0-0-1p; II vlr-2-0; III, IV d1-0-0, p1-1-0, v1p-2-2, r2-2-0; Metatarsi: I, II v2-0-0; II, IV p1d-2-1v, v2-2-2, r1d-1d-2.

Male: unknown.

Material examined. Only the holotype.

Distribution. Known only from the type locality, Serra da Gandarela, Rio Acima, Minas Gerais, Brazil (Fig. 14D). The type locality is an area of Canga, a mountain field vegetation typical of iron-ore plateaus (Salgado & Carmo 2015).

***Apopyllus aeolicus* new species**

Figs. 3E, 4E, 5E, 6E, 7E, 8E, 14A

Type Material. Male holotype from Parque Eólico de Guanambi, Caetité, Bahia, Brazil (14º6’41.7”S 42º36’27.7”W, 998m), 13/IV/2015, L.S. Carvalho col., deposited in CHNUFPI 1567.

Etymology. The specific name is taken from the Greek mythological character Aeolus, the god of wind, and is a reference to type locality, which is in a wind power plant.

Diagnosis. Males can be distinguished by the proximal spine on the apical keel of the RTA (Fig. 5E, 6E, arrow).

Description. Male (holotype): Total length 5.24. Carapace 2.32 long, 1.80 wide. Femur II 1.44 long. Carapace dark brown to black with a longitudinal stripe of white setae. Legs and palps dark brown, lighter on patellae, tibiae, metatarsi and tarsi. Femur I and palp with a lighter area on the prolateral part. Sternum and labium dark brown. Endites light brown with white anterior border and lighter oval area on the basal part. Opisthosoma dorsum dark gray with a longitudinal stripe of white setae and a dark brown scutum. Ventral side of opisthosoma light brown. Eyes sizes and interdistances: AME 0.08, ALE 0.1, PME 0.06, PLE 0.08, AME–AME 0.06, AME–ALE 0.02, ALE–PLE 0.04, PME–PME 0.06, PME–PLE 0.06. MOQ 0.44 wide. RTA with proximal spine on the apical keel. Leg spination: femora: I, II d1-1-1, p0-0-1; III d1-1-1, r0-1-1, p0-1-1; patellae: III, IV p0-1-0, r0-1-0; tibiae: I, II v1-0-1; III p1-1-0, v1p-2-2, r2-1d-0; IV d1-0-1, p1-0-1, v1p-2-2, r2-0-2; metatarsi: I, II v2-0-0; III p1-2-1, v1p-2-2, r1-1-2; IV p1-2-1d, v2-2-2, r1-2-2.

Female: unknown.

Material Examined. Only the holotype.

Distribution. Known only from the type locality, Parque Eólico de Guanambi, Caetité, Bahia, Brazil (Fig. 14A).

***Apopyllus centralis* new species**

Figs. 3F, 4F, 5F, 6F, 7F, 8F, 10G, 11G, 12G, 13G, 14D

Type material. Male holotype from Usina de Aproveitamento Hidrelétrico Serra do Facão, Catalão, Goiás, Brazil (17º30’9”S 47º33’32”W, 754m), I/2010, R.B. Martines & R.M.C. Silveira coll., deposited in UFMG 4395. Paratypes: one female from Usina de Aproveitamento Hidrelétrico Serra do Facão, Catalão, Goiás, Brazil (17º44”36.93”S 47º35’19.56” W, 933m), VII/2010, R.B. Martines & R.M.C. Silveira coll. (UFMG 4564); one female from Parque Nacional da Serra das Confusões, Cristino Castro, Piauí, Brazil (8º56’16.9”S 43º51’48.1”W), 9/XII/2012, L.S. Carvalho coll. (CHNUFPI 609); one male and one female from Pimenta Bueno, Rondônia, Brazil (11º38’60”S 61º12’0”W), VII/2000, M. Carvalho col. (IBSP 137001); two males and one female from Campo de Provas Brigadeiro Velloso, Serra do Cachimbo, Novo Progresso, Pará, Brazil (9º21’45.33”S 54º54’54.4”W), 7–17/IX/2003 (MPEG 22022).

Etymology. The specific name is a reference to the distribution of the species in central Brazil.

Diagnosis. Males can be distinguished by the presence of a dorsal process in the RTA (Fig. 5F, 6F [arrow], 7F, 8F). Females can be distinguished by the anterior ridge of the epigynum less sclerotized in the middle, conferring an incomplete appearance (Figs. 10G, 11G).

Description. Male (holotype): Total length 4.44. Carapace 1.84 long, 1.56 wide. Femur II 1.2 long. Carapace brown. Legs and palps brown. Coxae white on the terminal part in dorsal view. Femur I and palp with a lighter area on the prolateral part. Sternum and labium light brown. Endites light brown with white anterior border. Opisthosoma dorsum dark gray with a brown scutum. Ventral side of opisthosoma light brown. Eyes sizes and interdistances: AME 0.08, ALE 0.08, PME 0.1, PLE 0.1, AME–AME 0.02, AME–ALE 0.02, ALE–PLE 0.02, PME–PME 0.02, PME–PLE 0.05. MOQ 0.38 wide. RTA with dorsal process. Leg spination: femora: I, II d1-1-1, p0-0-1; III d1-1-1, r0-1-1, p0-1-1; patellae: III, IV p0-1-0, r0-1-0; tibiae: I v1r-2-0, II v1r-2-1p, III, IV d1-1-0, v1p-2-2; metatarsi: I, II v2-0-0, III p0-1-1-0, v2-2-2, r1-1-1; IV p0-1-1, v2-2-2, r1-0-1.

Female (UFMG 4564): Total length 4.88. Carapace 2.16 long, 1.6 wide. Femur II 1.36 long. Coloration as in male. No dorsal scutum on the opisthosoma. Eyes sizes and interdistances: AME 0.07, ALE 0.08, PME 0.06, PLE 0.08, AME–AME 0.04, AME–ALE 0.02, ALE–PLE 0.02, PME–PME 0.06, PME–PLE 0.06. MOQ 0.38 wide. Epigynum with incomplete anterior ridge and secondary spermathecae smaller than primary spermathecae. Leg spination: femora: I, II d1-1-1, p0-0-1; III d1-1-1, r0-1-1, p0-1-1; patellae: III, IV p0-1-0, r0-1-0; tibiae: I v0-0-1; II v1-0-1; III p1-1-1, v1p-2-2, r1-1-0; IV d1-1-1, p1-1-0, v1p-2-2, r1-1-0; metatarsi: I v2-0-0; II v2-1r-0; III p1-2-1, v2-2-2, r1d-1d-2; IV d0-1-1, p1d-1-1, v2-2-2, r1-1-1.

Variation. Male (N = 45) carapace length 1.51–2.01. Female (N = 20), carapace length, 1.71–2.16.

Material Examined. BRAZIL: Amapá: Macapá, 110m, 2f#, 24-28/XII/2004, R. A. Silva coll. (MCTP 16590), Mazagão, 1m#, 03/XII/2003, R. A. Silva coll. (MCTP 16537); **Goiás:** Alto Paraíso de Goiás, 14º9'43"S, 47º36'36"W, 1m#, VIII/1991, S.T. Amaranto (IBSP 98752), Catalão, Barragem para Aproveitamento Hidrelétrico Serra do Facão, 17º35'34"S, 47º37'16"W, 835m, 1f#, I/2010, 17º51'40"S, 47º37'38"W, 762m, 1m# 1f#, I/2010, 17º44'36.93"S, 47º35'19.56"W, 933m, 21f#, VII/2010, 17º36'23.9"S, 47º37'18.52"W, 835m, 1m#, VII/2010, 17º52'24.62"S, 47º37'33.3"W, 762m, 2m# 2f#, VII/2010, R.B. Martines & R.M.C. Silveira coll. (UFMG 4394, 4406, 4564, 4552, 4567); **Maranhão:** Caxias, Reserva Ecológica Inhamum, 4º49'60"S,

43º20'69"W, 1m#, 23–26/IV/2007, J.F.B. Lima-Lobato *et al.* coll. (IBSP 130925), 1m#, IX–X/2007, J.F.B. Lima-Lobato & F. Limeira de Oliveira coll. (IBSP 129026); **Mato Grosso:** Nossa Senhora do Livramento, Pantanal do Poconé - Pirizal, Fazenda Retiro Novo, 16º15'S, 56º36'W, 1f# 1m#, I/2004–III/2005, L.D. Battirola coll. (IBSP 125469), Nossa Senhora do Livramento, Pantanal do Poconé - Pirizal, Fazenda Retiro Novo, 16º22'1"S, 56º17'58"W, 125m, 2f#, F.S.F. Leite coll. (UFMG 8781); Santo Antonio do Levergere, 1m#, 09/X/1981, H. Duarte coll. (MCTP 2522); **Mato Grosso do Sul:** Brasilândia, Horto Rio Verde, 20º50'0"S, 51º40'0"W, 1m# 1 juvenile, 14/VIII/2007, M. Uehara-Prado coll. (UFMG 12496), Selvíria, Horto Matão, 20º20'0"S, 51º40'0"W, 1m#, 19/VIII/2007, M. Uehara-Prado coll. (UFMG 12495); **Minas Gerais:** Belo Horizonte, Campus da UFMG, 19º51'53"S, 48º57'58"W, 835m, 1m#, 3/VIII/2012, P.H. Martins *et al.* coll. (UFMG 11940), Leme do Prado, Reserva Estadual de Acauã, 17º7'94.2"S, 42º43'98.1", 887m, 1f#, 18–28/II/2013, P.H. Martins coll. (UFMG 19407); **Pará:** Novo Progresso, Campo de Provas Brigadeiro Velloso, Serra do Cachimbo, 9º21'45.3"S, 54º54'54.4"W, 1f#, 1m#, 16–26/III/2004 (MPEG 22028, 22029), 11m# 7f# 1 juvenile, 7–17/IX/2003 (MPEG 22007–22024), Igarapé-açu, 3f#, 7m#, 09/XII/2002, Eq. FEIGA-UFRA coll. (MPEG 21825–21833), 1f#, 1m#, 14/IX/2011, S. Ribeiro coll. (MPEG 21839), 1f#, 19/V/2011, S. Ribeiro coll. (MPEG 21836), São Geraldo do Araguaia, Serra das Andorinhas, 1f#, 27/X–07/XI/2011, A. B. Bonaldo *et al.* coll. (MPEG 21838); **Piauí:** Alvorada do Gurguéia, Fazenda Escola da UFPI, 8º22'28.6"S, 43º51'32.5"W, 1f#, 15–17/II/2012, L.S. Carvalho coll. (CHNUFPI 608), ditto, Caatinga, 8º22'28.6"S, 43º51'32.5"W, 230m, 3f#, 15–17/II/2012, I.L.F. Magalhães *et al.* coll. (IBSP 165373), Cristino Castro, Parque Nacional da Serra das Confusões, 8º56'16.9"S, 43º51'48.1"W, 1f#, 9/XII/2012, L.S. Carvalho coll. (CHNUFPI 609), Castelo do Piauí, ECB Rochas Ornamentais, 5º13'46"S, 41o41'29.9"W, 1m#, 03/XII/2005, F. M. Oliveira-Neto coll. (MPEG 7901), 1f#, 11/XI/2005, F. M. Oliveira-Neto coll. (MPEG 7903), 1m#, 19/X/2005, F. M. Oliveira-Neto coll. (MPEG 7902), 1m#, 26/X/2005, F. M. Oliveira-Neto coll. (MPEG 7900), ECB Rochas Ornamentais, Fazenda Bonito, 5º14'7"S, 41o41'16.3"W, 1m#, no date, F. M. Oliveira-Neto coll. (MPEG 21868), Piracuruca, Parque Nacional Sete Cidades, 4º05'39.9"S, 41º43'53.3"W, 1m#, 06/XII/2006, L. S. Carvalho, D. Candiani & N. F. Lo Man Hung coll. (MPEG 21871), 1m#, 13/IX/2006, L. S. Carvalho & F. M de Oliveira-Neto coll. (MPEG 9708), 1m#, 21/VI/2007, F. M. Oliveira-Neto coll. (MPEG 21877), 6m# 5f#, 24/VI/2007, Carvalho, Albuquerque & Oliveira-Neto coll. (MPEG 21878–

21884), 3m#, 3f#, 26/I/2007, L. S. Carvalho, M. T. Avelino & M. P. Albuquerque coll. (MPEG 21872–21876), 1m#, 3f#, no date, no col. (MPEG 21870, 21886); **Rondônia:** Pimenta Bueno, 11º38'60"S, 61º12'0"W, 8m# 4f#, VII/2000, M. Carvalho coll. (IBSP 137001, 137007, 137010, 137011); **São Paulo:** Botucatu, Usina São Manoel, 1m#, 01/XII/1998, Mendes coll. (MZUSP 62766), Itirapina, Estação Ecológica de Itirapina, 22º16'49"S, 48º7'10"W, 1f#, 2001, C. Bertim coll. (IBSP 126311).

Distribution. Central Brazil, mainly in Cerrado biome, with some occurrences in Caatinga (Fig. 14D).

***Apopyllus atlanticus* new species**

Figs. 3G, 4G, 5G, 6G, 7G, 8G, 9E–F, 10H, 11H, 12H, 13H, 14C

Type material. Male holotype from Mampituba, Rio Grande do Sul, Brazil, (29°12'42.22"S 49°56'9.52"W), 01/XI/2006, A. Gonçalves *et al*. coll., deposited in MCN 52307. Paratypes: two females, same data of holotype (MCN 52303).

Etymology. The specific name is a reference to the distribution of this species mainly in the Atlantic Forest of Brazil.

Diagnosis. Females can be distinguished by the elongated paramedian epigynal pockets, forming a anteriorly directed angle with each other, by the thick AR, by the secondary spermatheca with diameter at least two thirds as long as the primary spermatheca, by the TPD curved dorsally and by the curved PDD (Fig 10H, 11H, 12H, 13H). Males can be distinguished by the very pointed terminal part of RTA in dorsal and retrobasal views (Figs. 7G, 8G, 9F), by the gently curved dorsal keel of RTA in apical view (Fig. 9E) and by the rhomboidal shape of RTA in retrobasal view (Fig. 7G, 8G).

Description. Male (holotype). Total length 4.98. Carapace 2.33 long, 1.85 wide. Femur II 1.52 long. Eyes sizes and interdistances: AME 0.08, ALE 0.10, PME 0.08, PLE 0.06, AME–AME 0.06, AME–ALE 0.01, PME–PME 0.06, PME–PLE 0.03, ALE–PLE, 0.03. MOQ length 0.23, front 0.21, back 0.23. Cymbium widened at level of retrolateral incision. RTA very long, bearing a toothed keel and 2–3 distal teeth. Leg spination: femur III p0-0-1, patella III p0-0-1, tibia III v1-2-2, p1-1-1, r 1-1-1, femur IV p0-0-1, patella p0-0-1, tibia IV v1-2-2.

Female (BADIT 51). Total length 7.08. Carapace 2.49 long, 1.98 wide. Femur II 1.65 long. Eyes sizes and interdistances as in male. Female genitalia with elongated openings. Leg spination: femur III p0-1-1, r0-1-1, patella III p0-0-1, r0-0-1, tibia III d0-

0-1, v1-2-2, p1-2-1, r 1-1-1, femur IV p0-1-1, r0-0-1, patella p0-1-1, r0-0-1, tibia IV d0-0-1, v1-2-2, p1-3-1, r1-3-1.

Variation. A few specimens have epigynal pockets not so thin and elongated as in the holotype.

Material Examined. BRAZIL: Bahia: Abaíra, Distrito de Catolés, Pico da Serra do Barbado, 13º17'27"S, 41º54'6"W, 2033 m, 1m#, 3/XI/2013, L.S.Carvalho coll. (CHNUFPI 613); Porto Seguro, 16º23'21"S, 39º10'1.5"W, 126 m, 4m#, 16/V/2012, L.D. Audino coll. (UFMG 16790, 16791), 16º38'48.1"S, 39º6'0.1"W, 27 m, 1m#, 21/V/2012, L.D. Audino coll. (UFMG 16835), 16º8'27.6"S, 39º9'23.4"W, 91 m, 2m#, 29/V/2012, L.D. Audino coll. (UFMG 16828); **Mato Grosso do Sul:** Três Lagoas, Horto Barra do Moeda, 20º57'0"S, 51º47'0"W, 1m#, 16/V/2009, M. Uehara-Prado coll. (UFMG 5080), ditto, 3m#, 18/V/2009, M. Uehara-Prado coll. (UFMG 5082); **Minas Gerais:** Catas Altas, RPPN Serra do Caraça, 20º5'S, 43º29'W, 1m#, IV–V/2002, Equipe Biota coll. (IBSP 148889), Juatuba, Área de Preservação da COPASA, Serra Azul/Rio Manso, 20º8'60"S, 44º27'0", 4m# 1 juvenile#, 18–24/IV/2002, Equipe Biota coll. (IBSP 149306, 149321), Nova Lima, RPPN Mata Samuel de Paula, 20º0'S, 43º52'W, 967m, 1m#, 29/IV–1/V/2007, J.P.P. Pena-Barbosa *et al.* coll. (UFMG 2526), Ouro Preto, Parque Estadual do Itacolomi, 20º26'5.3"S, 43º30'32.6"W, 1326 m, 25m# 11f#, 11–13/IV/2008, K.P. Santos *et al.* coll. (UFMG 2361, 2435), 1m# 1f# 2–4/XI/2007, K.P. Santos *et al.* (UFMG 2065, 2066), Santa Bárbara, RPPN Santuário do Caraça, Pico do Sol, 20º4'8.17"S, 43º30'17.21"W, 1210 m, 1m#, 15/IX/2010, L.N. Perillo coll. (UFMG 6691), Santana do Riacho, Parque Nacional da Serra do Cipó, Travessão, 19º19'34"S, 43º30'21"W, 1215 m, 1m#, 10–14/II/2001, E.S.S. Álvares & E.O. Machado coll. (UFMG 488), São Gonçalo do Rio Abaixo, Estação de Preservação e Desenvolvimento Ambiental de Peti, 19º58'23"S, 43º29'57"W, 820 m, 1f#, 8–9/XII/2012, G.H.F. Azevedo *et al.* coll. (UFMG 12652); **Paraíba:** Cabaceiras, 7º29'25"S, 36º17'16"W, 1m#, 26/V/2012, R.L. Andrade coll. (CHNUFPI 1448); **Pernambuco:** Serra Talhada, Fazenda Saco, Mata da Pimenteira, 7º53'S, 38º18'W, 1m#, X/2008, M. Carvalho coll. (UFMG 4336); **Rio Grande do Sul:** Augusto Pestana, 28º31'2"S, 53º59'31"W, 1f#, 10/I/2009, L.V. Silva *et al.* coll. (MCTP 27336), 1m#, 12/XII/2008, L.V. Silva *et al.* coll. (MCTP 26610), 1f#, 24/I/2009, L.V. Silva *et al.* coll (MCTP 27337), 2f#, 24/II/2009, L.V. Silva *et al.* coll. (MCTP 27339, 27340), 1m#, 04/X/2009, L. V. Silva coll. (MCTP 32459), 5f#, 10/I/2009, L. V. Silva coll. (MCTP 27345–42736), 1f#, 12/XI/2008, L. V. Silva coll. (MCTP 26618), 1f#,

12/XII/.2008, L. V. Silva coll. (MCTP 26617), 1f#, 18/IV/2009, L. V. Silva coll. (MCTP 27347), 1f#, 24/I/2009, L. V. Silva coll. (MCTP 27338), 1m, 1f#, 25.X.2009, L. V. Silva coll. (MCTP 32511), 1f#, 27/XI/2008, L. V. Silva coll. (MCTP 26622), 1f#, 27/XI/2008, L. V. Silva coll. (MCTP 26625), 1f#, 27/XI/2008, L. V. Silva coll. (MCTP 26623), 1f#, 27/XII/2008, L. V. Silva coll. (MCTP 26626), 2f#, 27/XII/2008, L. V. Silva coll. (MCTP 26628), Cambará do Sul, 29º8'54"S, 50º4'8"W, 1m#, XII/2004, M.V. Petry *et al.* coll. (MCTP 31222), Capão do Leão, 1f#, 15/I/2008, J. L. O. Rosado coll. (MCN 46781), Horto Florestal, Erchim, 1f#, 31/III–14/IV/2012, R. Moraes coll. (MCN 52308), Itaara, 29º34'60"S, 53º46'59"W, 1m# 1f#, XI/2006, A.A. Lise coll. (MCTP 20764, 20765), 1f#, II/2007, A. A. Lise *et al.* coll. (MCTP 20770), 1f#, XI/2006, A. A. Lise *et al.* coll. (MCTP 20769); Mampituba, 1f#, 3m#, 01/XI/2006, A. Gonçalves coll. (MCN 52303), Roça da Estância, Mampituba, 1m#, 01/XI/2006, A. Gonçalves coll. (MCN 52307), 1f#, 08/V/2006, A. Gonçalves coll. (MCN 52306), Três Passos, Morrinhos do Sul, 1m#, 01/XI/2006, A. Gonçalves coll. (MCN 52304). **Santa Catarina:** Blumenau, Parque Municipal das Nascentes do Ribeirão Garcia, 27º1'S, 49º1'W, 1f#, 18/V/2005, R.C. Francisco coll. (IBSP 122688), Guatambú, 27º6'1"S, 52º45'0"W, 1f#, 04/IX/2009, R.C. Francisco coll. (MCTP 26637); **São Paulo:** Itirapina, Estação Ecológica de Itirapina, 22º16'49"S, 48º7'10"W, 31m#, 2001, C. Bertim coll. (IBSP 126285, 126288, 126300), Jundiaí, Parque Estadual da Serra do Japi, 23º17'S, 46º59'W, 822m, 1m#, XII/2007, J. Sobjack coll. (UFMG 6527).

Distribution. Southern, southeastern and northeastern Brazil, mainly in Atlantic Forest (Fig. 14C).

Discussion

The female genitalia of *Apopyllus* were first described as having a pair of paramedian openings leading to internal convoluted ducts (Platnick & Shadab 1984). However, the copulatory duct trajectory shows that the copulatory openings are actually located below the anterior ridge of the epigynum (Figs. 1A–B) and what was thought to be the copulatory openings are blind pockets. Based on their position, we suppose that these paramedian pockets might be formed by the lateral epigynal folds. During the female genitalia development, the epigynal folds invaginate to form the ducts and spermathecae (Sierwald 1989): these remain in the adults as well demarcated folds, as a suture or they may be completely absent (Ramírez 2014). We suppose the

folds migrate to a paramedian position and are reduced in the adult female *Apopyllus*, forming the pockets and a small depression on the epigynal median field (Fig. 2A).

The female epigynum of *Apopyllus* have an anterior ridge that covers the copulatory openings (Figs. 1B, 2A). This anterior ridge varies between species (and a little within species) and can be used as a taxonomic character. In gnaphosids of the *Zelotes* group (Murphy 2007), a similar anterior structure, the anterior anchoring pocket, may be found and this is used for the anchorage of male RTA during copulation (Senglet 2004). Although *Apopyllus* does not belong to this group and the anterior ridge might not be homologous to the zelotine anchoring pocket, it might also function as a fitting point to the retrolateral tibial apophysis of *Apopyllus*. In fact, genital mechanics studies have shown that the RTA can function as a "preliminary lock" mechanism, fitting to specialized structures in the female genitalia to allow pedipalpus alignment before intromission (Huber 1995, Eberhard & Huber 2010). The RTA is the most interspecificaly variable structure in the otherwise homogeneous male palp of *Apopyllus* species, and the anterior ridge is the most interspecificaly variable structure in the external female genitalia. Therefore, changes in one may select changes in the other, and their current shape variation could be a product of male-female coevolution. Given the channels formed by the keels on RTA, we could also presume that it could have an additional function of conducting the embolus.

Apopyllus is supposed to be closely related to *Apodrassodes* based on the long coiled embolus and the MTE. However, the female genitalia of these two genera are quite different. The epigynum of *Apodrassodes* does not have paramedian pockets, shows no trace of lateral folds (Fig. 15C), and has a short anterior scape, which could be considered a projection of an anterior ridge. The *Apodrassodes* vulva has a massive mid piece (Fig. 15D; Platnick 1983), which seems to be a matted copulatory duct, from which there arises an elongated secondary spermatheca (Fig. 15D) and the short curved copulatory duct leading to the primary spermatheca. The female of *Nopyllus*, another genus considered closely related to *Apopyllus*, is not known. The only described gnaphosid that seems to have an epigynum that resembles *Apopyllus* is the Old World genus *Synaphosus*, which also has a pair of paramedian pockets and long and convoluted copulatory ducts (see Murphy 2007, Ovtsharenko *et al.* 1994). There are also some undescribed South American species with paramedian pockets, long convoluted ducts and with a long embolus in male palpi (GHFA personal observation). It might be that these female characters previously thought to be synapomorphy of

Apopyllus are, actually, shared by a small group of genera. A formal phylogenetic analysis is needed to test this hypothesis.

Despite the marked differences in female genitalia, the male copulatory apparatus shows evidence of close phylogenetic affinity between *Apopyllus*, *Apodrassodes* and *Nopyllus. The* male palp of *Apopyllus* has a long embolus supported by a membranous tegular projection (Figs. 1C, D, 2C). The gnaphosid conductor is usually represented by a membranous projection that supports the embolus and is connected to the proximal (taking as reference the trajectory of the sperm duct) part of the tegulum (Zakharov & Ovtcharenko 2011). This appears to be homologous to the "Sierwald conductor" of Polotow *et al.,* (2015: 160), which may be a synapomorphy for the Dionycha (including Gnaphosidae) plus the OC (oval Calamistrum) clade (Polotow *et al.*, 2016, p. 133, character 39, fig, 4). In *Apopyllus*, this membranous projection is located distally on the tegulum and, based on its position, it cannot be considered a homologue of the conductor of other gnaphosids, hence it is here called Membranous Tegular Extension. This membranous distal projection is also found in *Apodrassodes* and *Nopyllus* (Platnick 1983; Ott 2014), although in *Apopyllus* it is long and bifid. The conductor described in *Synaphosus* (Platnick 1983; Ovtsharenko *et al.* 1994) is a distally situated bifid membrane, and could be considered a MTE (Figs. 16A-B). *Synaphosus* also share with *Apopyllus* a long distal tubular membrane (Fig. 16A). The cymbium of *Apopyllus* is also characteristic in being projected retrolaterally, with a retrolateral incision to accommodate the embolus in the unexpanded position. In *Apodrassodes* and *Nopyllus* there is also a modification of the cymbium to accommodate the long embolus, but there is no such projection. So, the long and bifid MTE and the projected cymbial retrolateral incision might be synapomorphies of *Apopyllus*.

The most singular character of *Apopyllus* is the shape of the RTA. It is a complex folded lamina with ventral, apical and dorsal keels (Figs. 1D, 2C, 9A–F). The gnaphosid RTA is usually a simple, conical or laminar projection, and a complex structure like in *Apopyllus* is not found in other genera of the family. Therefore, this might be a good putative synapomorphy for the genus. The morphology of the bulb structures is conserved within the genus but, as shown above, the morphology of the RTA is of taxonomic value to distinguish species.

It is worth noting that, in general, the morphology of male palp seems to be less variable between species than the morphology of the epigynum. *Apopyllus silvestrii* and *A. iheringi*, for example, are two species in which the palps are very similar, but the

vulvae are notably different. Usually, the female spider genitalia is less differentiated between species than the male's (e.g.: Crews 2009; Hepner & Milasowszky 2006; Milasowszky *et al.* 1997), which is expected according to the cryptic female choice hypothesis of genital evolution, which predicts that the male genitalia are under more intense sexual selection pressure (Eberhard 2010). Thus, a different process than cryptic female choice might be involved in the genital evolution of this Gnaphosidae genus. This could be elucidated through studies of the mating mechanism and intraspecific variability of genital organs of *Apopyllus*, which seems to be an interesting model to test hypotheses on the evolution of spider genitalia. Gnaphosidae, and the larger clade Dionycha to which they belong, underwent a period of accelerated diversification relative to other spiders (Garrison *et al.,* 2016): a careful study of gnaphosid genital coevolution in a phylogenetic context may allow us to elaborate the processes leading to this remarkable evolutionary result.

Acknowledgements

We thank the curators and curatorial assistants of the institutions for the loan of material. Luis A. Pereira (MLP) and Ivan L.F. Magalhães (MACN) kindly provided photographs of the types deposited in MLP. We thank Victor Smith (CAS) for the photographs of the types of *A. huanuco*, *A. ivieorum*, *A. malleco* and *A. now*. Paulo A. Garcia and Tiago L. Pezzuti (both from UFMG) kindly provided the automontage stereomicroscope for photographs. GHFA is grateful to Júlia S. Parreiras (UFMG), for the valuable help with plate construction and to Rachel Diaz-Bastin (CAS), for advice on drawing technique. We are especially grateful to Instituto Prístino (http://institutopristino.org.br/) and Flávio S. do Carmo for supporting A.J. Santos field work that resulted in the collection of *A. gandarela* type specimen. We also extend our gratitude to the technical staff of Centro de Microscopia da UFMG for help in SEM image acquisition and Kin Master Produtos Químicos for donating the pancreatin used in genitalia preparations. This work was supported by grants from the Exline-Frizzell Fund of CAS, a CAPES scholarship to GHFA and grants from CNPq (407288/2013-9, 308072/2012-0), FAPEMIG (PPM 00335-13, PPM 00651-15) and Instituto Nacional de Ciência e Tecnologia dos Hymenoptera Parasitóides da Região Sudeste Brasileira (http:/www.hympar.ufscar.br/) to AJS.

References

Álvarez-Padilla, F. & Hormiga, G. (2007) A protocol for digesting internal soft tissues and mounting spiders for scanning electron microscopy. *Journal of Arachnology*, 35, 538–542.

Brescovit, A.D. & Lise, A.A. (1993) Novas espécies e ocorrências de aranhas dos gêneros *Apodrassodes* e *Apopylus* (Araneae, Gnaphosidae). *Biociências*, 1, 101–110.

Brown, B.V. (2013) Automating the "Material examined" section of taxonomic papers to speed up species descriptions. *Zootaxa*, 3683, 297–299.

Crews, S.C. (2009) Assessment of rampant genitalic variation in the spider genus *Homalonychus* (Araneae, Homalonychidae). *Invertebrate Biology*, 128, 107–125.

Eberhard, W.G. (2010) Evolution of genitalia: theories, evidence, and new directions. *Genetica*, 138, 5–18.

Eberhard ,W.G., Huber, B.A. (2010) Spider genitalia: precise maneuvers with a numb structure in a complex lock. *In*: J. L. Leonard & A. Córdoba-Aguilar (eds.) *Evolution of primary sexual characters in animals*. Oxford University Press, Oxford, pp-249–284.

Garrison, N., Rodriguez, J., Agnarsson, I., Coddington, J., Griswold, C., Hamilton, C., Hedin, M., Kocot, K., Ledford, J. and Bond, J. (2016) Spider Phylogenomics: Untangling the Spider Tree of Life. *PeerJ* 4:e1719; DOI 10.7717/peerj.1719

Hepner, M. & Milasowszky, N. (2006) Morphological separation of the Central European *Trochosa* females (Araneae, Lycosidae). *Arachnologische Mitteilungen*, 31, 1–7.

Holm, Å. (1979) A taxonomic study of European and East African species of the genera *Pelecopsis* and *Trichopterna* (Araneae Linyphiidae) with descriptions of a new genus and two new species of *Pelecopsis* from Kenya. *Zoologica Scripta*, 8, 255–278.

Huber B.A. (1995) The retrolateral tibial apophysis in spiders - shaped by sexual selection? *Zoological Journal of the Linnean Society*, 113, 151–163.

Levi, H.W. (1965) Techniques for the study of spider genitalia. *Psyche*, 72, 152–158.

Mello-Leitão, C.F. (1941) Las Arañas de Córdoba, La Rioja, Catamarca, Tucuman, Salta y Jujuy. *Revista del Museo de la Plata (Nueva Serie), Serie Zoología*, 2, 99–198.

Mello-Leitão, C.F. (1942) Arañas del Chaco y Santiago del Estero. *Revista del Museo de la Plata (Nueva Serie), Serie Zoología*, 2, 381–426.

Mello-Leitão, C.F. (1943) Araneologica varia brasiliana. *Anais da Academia Brasileira de Ciências*, 15, 255–265.

Mello-Leitão, C.F. (1944) Arañas de la provincia de Buenos Aires. *Revista del Museo de la Plata (Nueva Seria), Sección Zoología*, 3, 311–393.

Milasowszky, N., Herberstein, M.E., Zulka, K.P. & Selden, P. (1997) Morphological separation of *Trochosa robusta* (Simon, 1876) and *Trochosa ruricola* (De Geer, 1778) females (Araneae: Lycosidae). *In*: *Proceedings of the 17th European Colloquium of Arachnology, Edinburgh*, pp. 91–96.

Murphy, J.A. (2007) *Gnaphosid Genera of the World*. British Arachnological Society.

Ott, R. (2014) *Nopyllus*, um novo gênero de Drassodinae sul-americano (Araneae, Gnaphosidae). *Iheringia. Série Zoologia*, 104, 252–261.

Ovtsharenko, V., Levy, G. & Platnick, N. (1994) A review of the ground spider genus *Synaphosus* (Araneae, Gnaphosidae). *American Museum Novitates*, 27, 1–27.

Petrunkevitch, A. (1911) A synonymic index-catalogue of spiders of north, central and south America with all adjacent islands, Greenland, Bermuda, West Indies, Tierra del Fuego, Galapagos, etc. *Bulletin of the American Museum of Natural History*, 29.

Platnick, N.I. (1983) A revision of the neotropical spider genus *Apodrassodes* (Araneae, Gnaphosidae). *American Museum Novitates*, 2763, 1–14.

Platnick, N.I. & Shadab, M.U. (1975) A revision of the spider genus *Gnaphosa* (Araneae, Gnaphosidae) in America. *Bulletin of the American Museum of Natural History*, 155, 1–66.

Platnick, N.I. & Shadab, M.U. (1984) A revision of the neotropical spiders of the genus *Apopyllus* (Araneae, Gnaphosidae). *American Museum Novitates*, 2788, 1–9.

Polotow, D., Carmichael, A. and Griswold, C. (2015) Total evidence analysis of the phylogenetic relationships of Lycosoidea spiders (Araneae, Entelegynae). *Invertebrate Systematics*. 29: 124 – 163.

Ramírez, M.J. (2014) The morphology and phylogeny of dionychan spiders (Araneae: Araneomorphae). *Bulletin of the American Museum of Natural History*, 390, 1–374.

Salgado, A. A. R., & do Carmo, F. F. (2015) 'Quadrilátero Ferrífero': A Beautiful and Neglected Landscape Between the Gold and Iron Ore Reservoirs. *In*: *Landscapes and Landforms of Brazil*. Springer, Netherlands, pp. 319–330.

Senglet, A. (2004) Copulatory mechanisms in *Zelotes*, *Drasillus* and *Trachyzelotes* (Araneae, Gnaphosidae) with additional faunistic and taxonomy data on species from Southwest Europe. *Mitteilungen der Schweizerischen Entomologischen Gesellschaft* 77, 87–119.

Sierwald, P. (1989) Morphology and ontogeny of female copulatory organs in American Pisauridae, with special reference to homologous features (Arachnida, Araneae). *Smithsonian Contributions to Zoology*, 484, 1–24.

Simon, E. (1893). Arachnides. *In*: Voyage de M. E. Simon au Venezuela (décembre 1887 - avril 1888). 21e Mémoire. Annales de la Société Entomologique de France 61, 423–462.

Simon, E. (1905) Etude sur les Arachnides recueillis en Patagonie par le Dr Filippo Silvestri. *Bollettino dei musei di zoologia ed anatomia comparata della R. Università di Torino*, 20, 1–17.

Vellard, J. (1924) Etudes de zoologie. *Archivos do Instituto Vital Brazil* 2, 121–170.

Zakharov, B.P. & Ovtcharenko, V.I. (2011) Morphological organization of the male palpal organ in Australian ground spiders of the genera *Anzacia*, *Intruda*, *Zelanda*, and *Encoptarthria* (Araneae: Gnaphosidae). *Journal of Arachnology*, 39, 327–336.

Figures

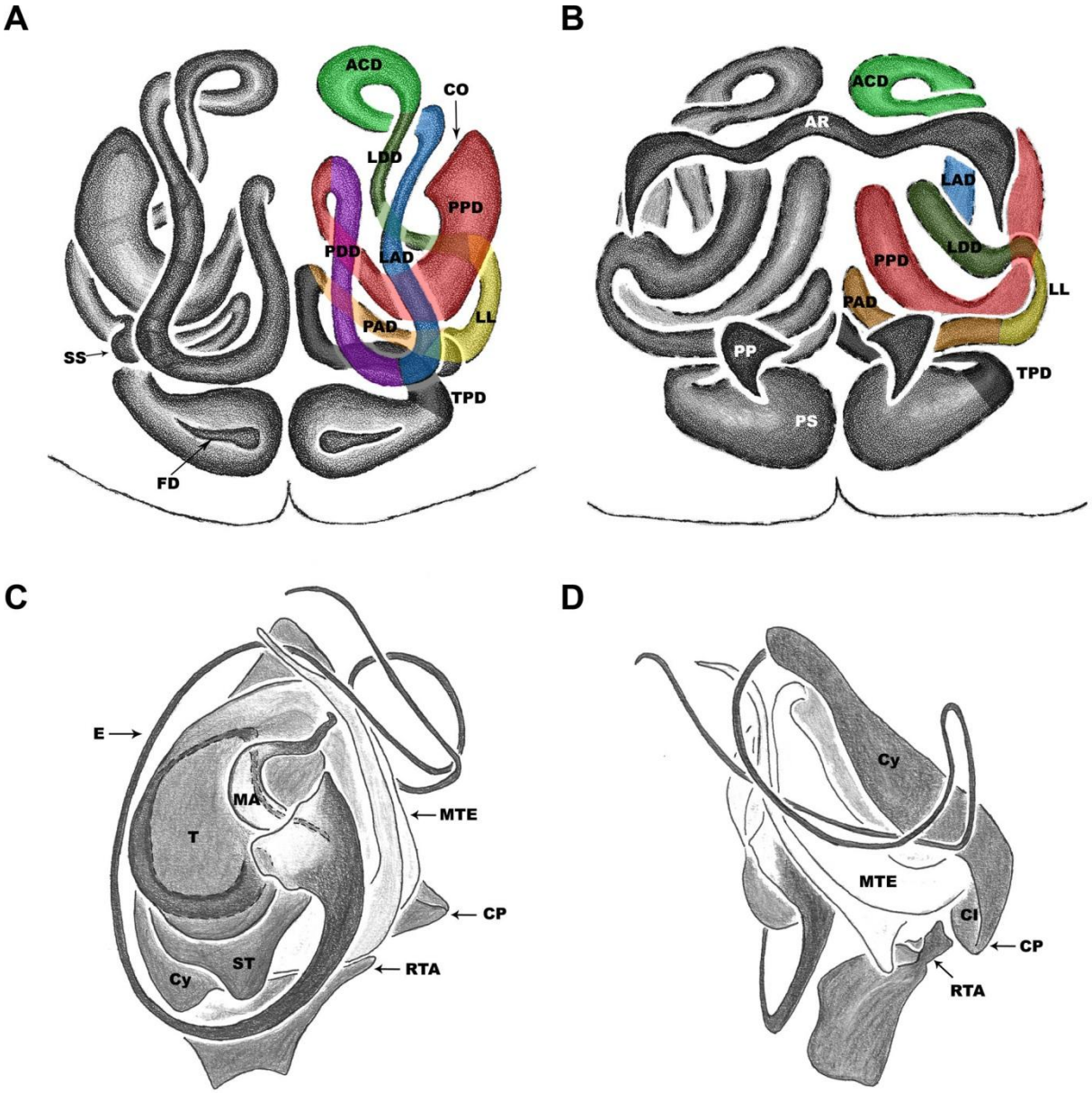

Figure 1: Genital Morphology of *Apopyllus*. A, B *A. malleco* female; C, D. *A silvestrii* male. A) Vulva, dorsal view. B) Epigynum, ventral view. Vulva can be seen by transparency. C) Male palp, ventral view. D) Male palp, retrolateral view. Abbreviations: ACD: Anterior Curled Ducts, AR: Anterior Ridge, AK: Apical Keel, CI: Cymbial Incision, CP: Cymbial Projection, Cy: Cymbium, DK: Dorsal Keel, DTM: Distal Tubular Membrane, E: Embolus, ET: Embolus Tip, FD: Fertilization Duct, LAD: Lateral Ascendant Duct, LDD: Lateral Descendant Ducts, LL: Lateral Loop, MA: Median Apophysis, MTE: Membranous Tegular Extension, PAD: Paramedian Ascendant Duct, PDD: Paramedian Descendant Duct, PP: Paramendian Pockets, PPD: Proximal Part of Copulatory Duct, PS: Primary Spermathecae, RTA: Retrolateral Tibial Apophysis, SS: Secondary Spermathecae, ST: Subtegulum, T: Tegulum, TPD: Terminal Part of Copulatory Duct, Tu: Tuberculum, VK: Ventral Keel. .

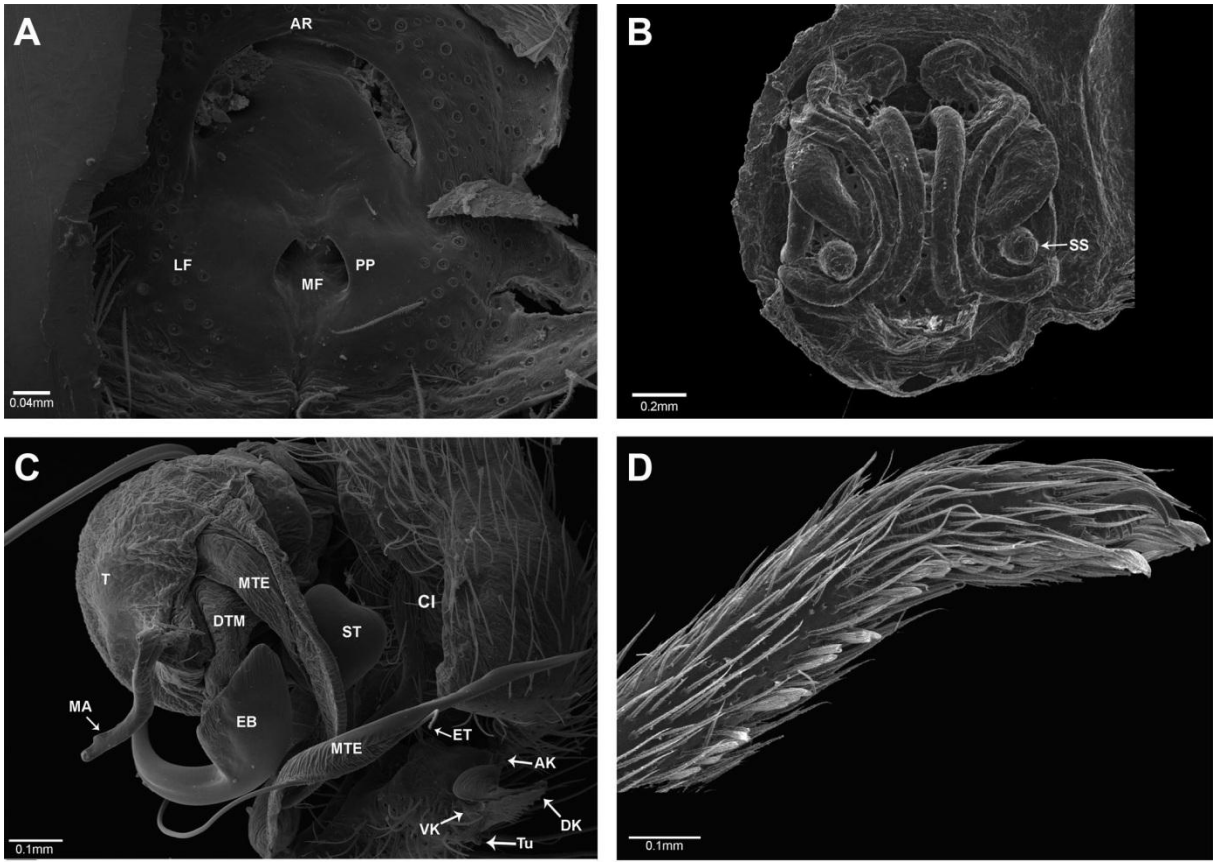

Figure 2: *Apopyllus silvestrii* (female and legs: UFMG 8323; male: CASENT 9051658): A) Epigynum, ventral view. B) Vulva, dorsal view. C) Expanded male right palp, retrolateral view. D) Tarsus of leg IV, showing pseudosegmentation. Abbreviations: AR: Anterior Ridge, AK: Apical Keel of Retrolateral Tibial Apophysis, CI: Cymbial Incision, DK: Dorsal Keel of Retrolateral Tibial Apophysis, EB: Embolus Base, ET: Embolus Tip, LF: Lateral Field, MA: Median Apophysis, MF: Median Fold, MTE: Membranous Tegular Extension, PP: Paramedian Pockets, SS: Secondary Spermathecae, ST: Subtegulum, T: Tegulum, Tu: Tubercle of Retrolateral Tibial Apophysis, VK: Ventral keel of Retrolateral Tibial Apophysis.

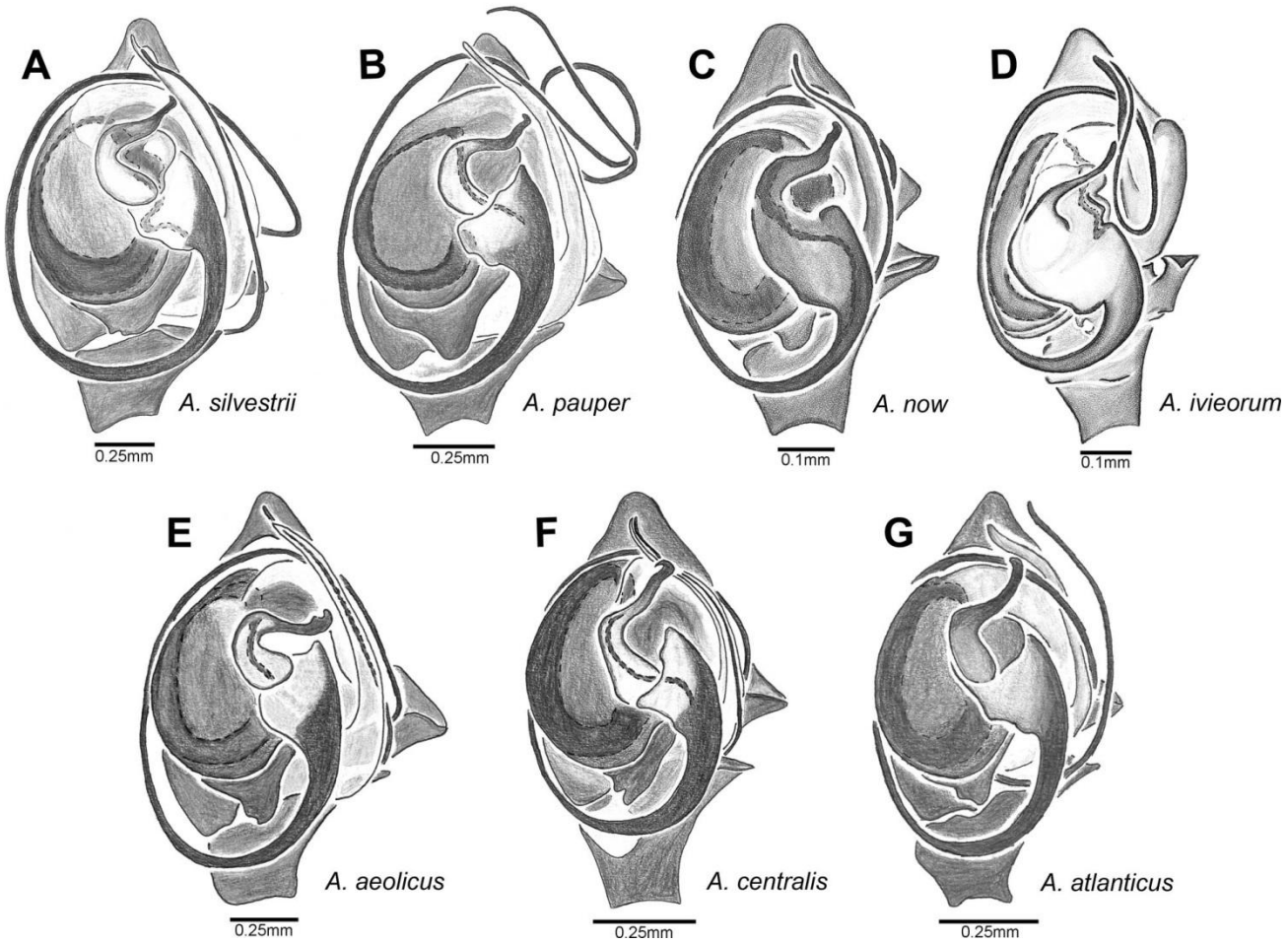

Figure 3: *Apopyllus* spp., male left palp in ventral view. **A)** *A. silvestrii* (MCTP 26293). **B)** *A. pauper* (IBSP 129024). **C)** *A. now* (MCZ 22335). **D)** *A. ivieorum* (AMNH). **E)** *A. aeolicus* **new. sp.** (CHNUFPI 1567). **F)** *A. centralis* **new sp.** (UFMG 4395). **G)** *A. atlanticus* **new sp.** (UFMG 16828).

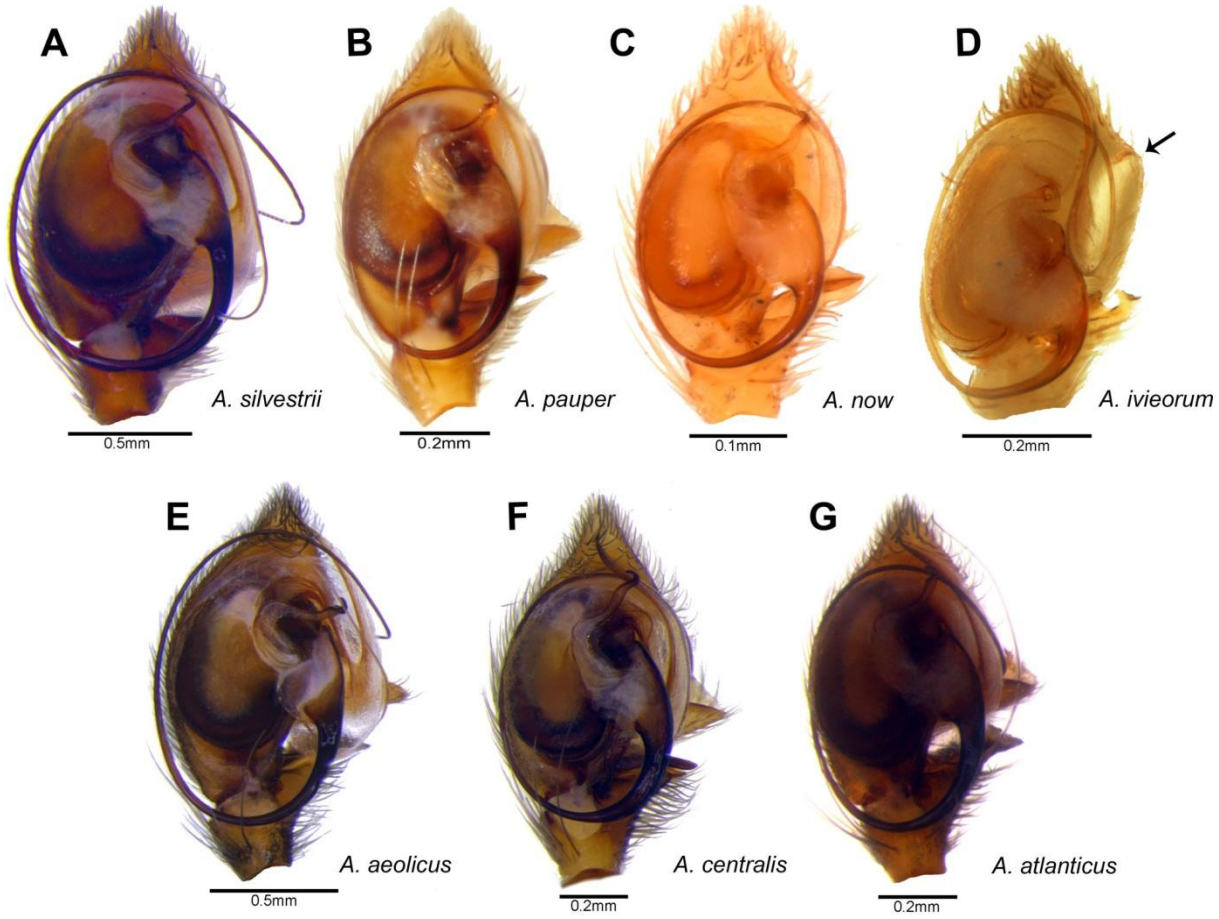

Figure 4: *Apopyllus* spp., male left palp in ventral view. **A)** *A. silvestrii* (MCTP 26293). **B)** *A. pauper* (MCTP 11327). **C)** *A. now* (MCZ 22335). **D)** *A. ivieorum* (AMNH). **E)** *A. aeolicus* **new. sp.** (CHNUFPI 1567). **F)** *A. centralis* **new sp.** (UFMG 4395). **G)** *A. atlanticus* **new sp.** (UFMG 16828).

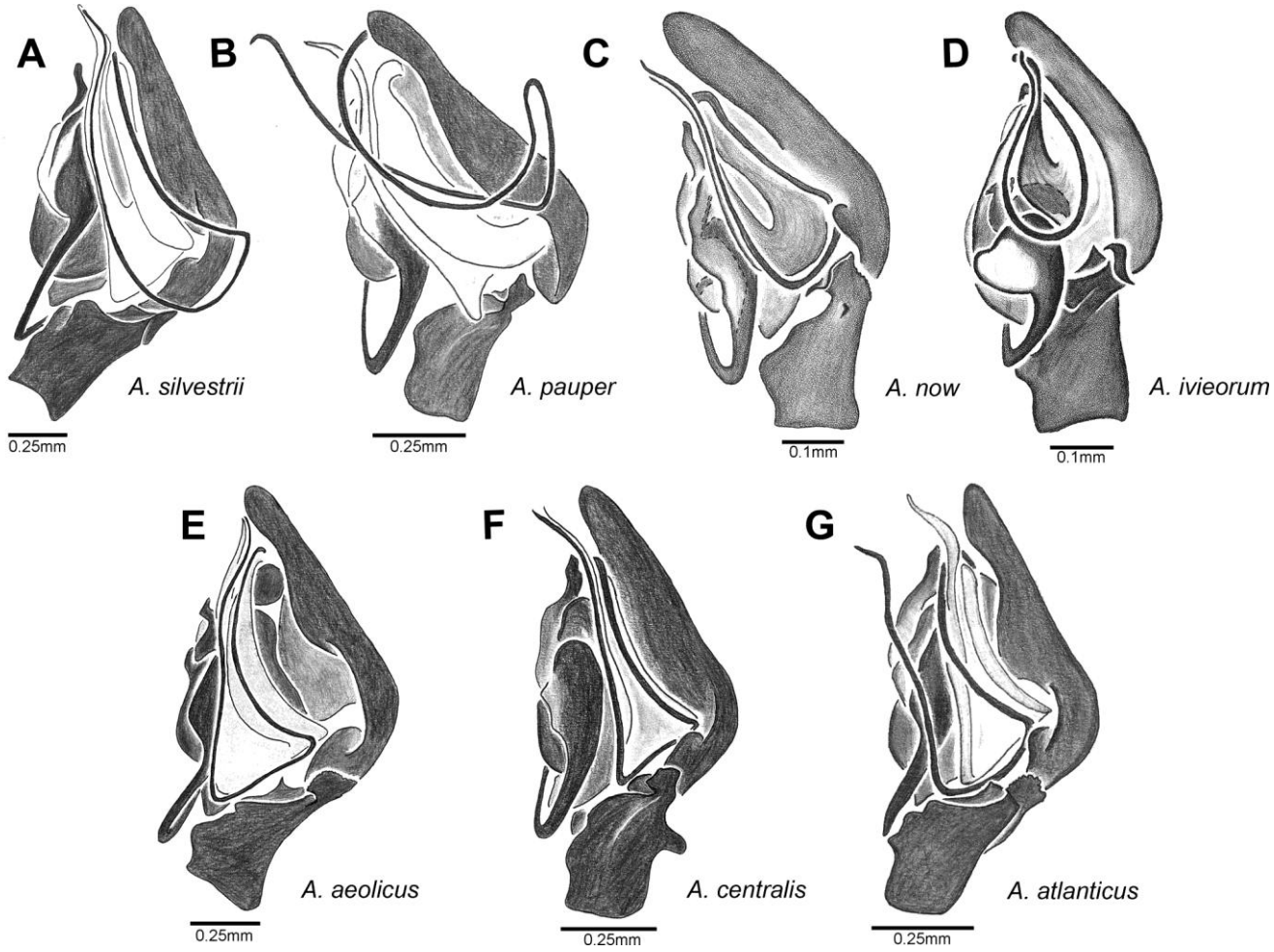

Figure 5: *Apopyllus* spp., male left palp in retrolateral view. **A)** *A. silvestrii* (MCTP 26293). **B)** *A. pauper* (IBSP 129024). **C)** *A. now* (MCZ 22335). **D)** *A. ivieorum* (AMNH). **E)** *A. aeolicus* **new. sp.** (CHNUFPI 1567). **F)** *A. centralis* **new sp.** (UFMG 4395). **G)** *A. atlanticus* **new sp.** (UFMG 16828).

Figure 6: *Apopyllus* spp., male left palp in retrolateral view. **A)** *A. silvestrii* (MCTP 26293). **B)** *A. pauper* (MCTP 11327). **C)** *A. now* (MCZ 22335). **D)** *A. ivieorum* (AMNH). **E)** *A. aeolicus* **new. sp.** (CHNUFPI 1567). **F)** *A. centralis* **new sp.** (UFMG 4395). **G)** *A. atlanticus* **new sp.** (UFMG 16828). The arrow indicates the dorsal tubercle of RTA in *A. centralis*.

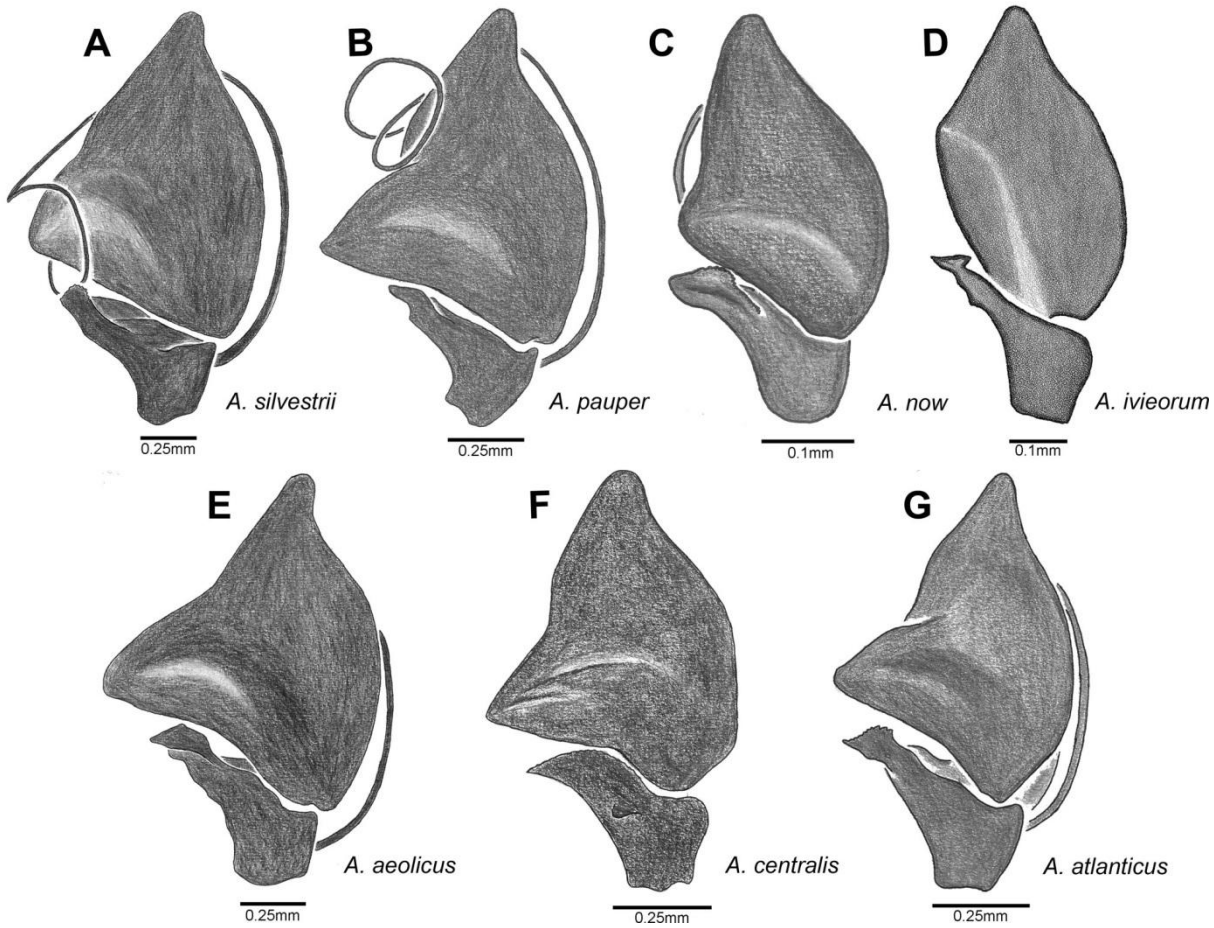

Figure 7: *Apopyllus* spp., male left palp in dorsal view. **A)** *A. silvestrii* (MCTP 26293). **B)** *A. pauper* (IBSP 129024). **C)** *A. now* (MCZ 22335). **D)** *A. ivieorum* (AMNH). **E)** *A. aeolicus* **new. sp.** (CHNUFPI 1567). **F)** *A. centralis* **new sp.** (UFMG 4395). **G)** *A. atlanticus* **new sp.** (UFMG 16828).

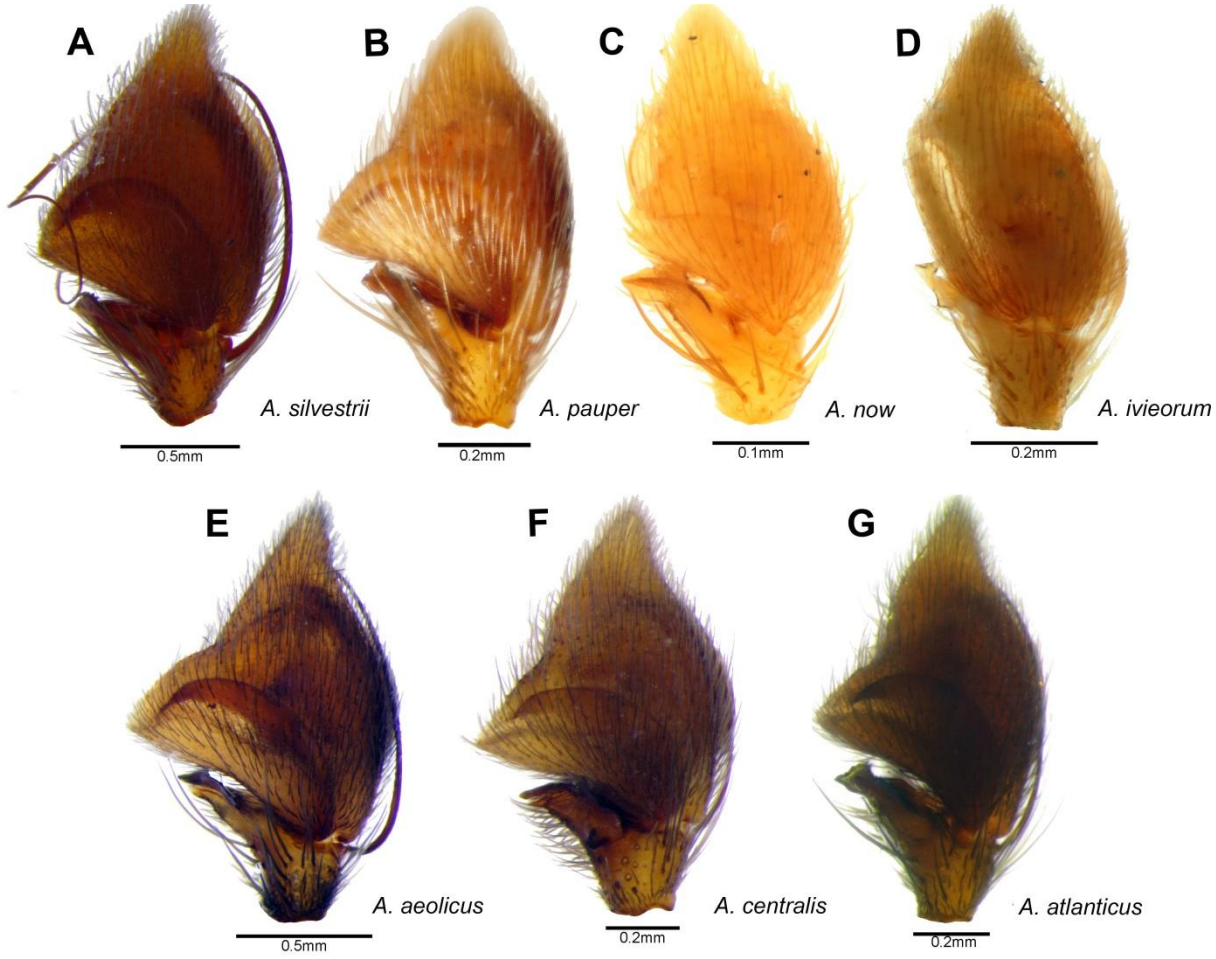

Figure 8: *Apopyllus* spp., male left palp in dorsal view. **A)** *A. silvestrii* (MCTP 26293). **B)** *A. pauper* (MCTP 11327). **C)** *A. now* (MCZ 22335). **D)** *A. ivieorum* (AMNH). **E)** *A. aeolicus* **new. sp.** (CHNUFPI 1567). **F)** *A. centralis* **new sp.** (UFMG 4395). **G)** *A. atlanticus* **new sp.** (UFMG 16828).

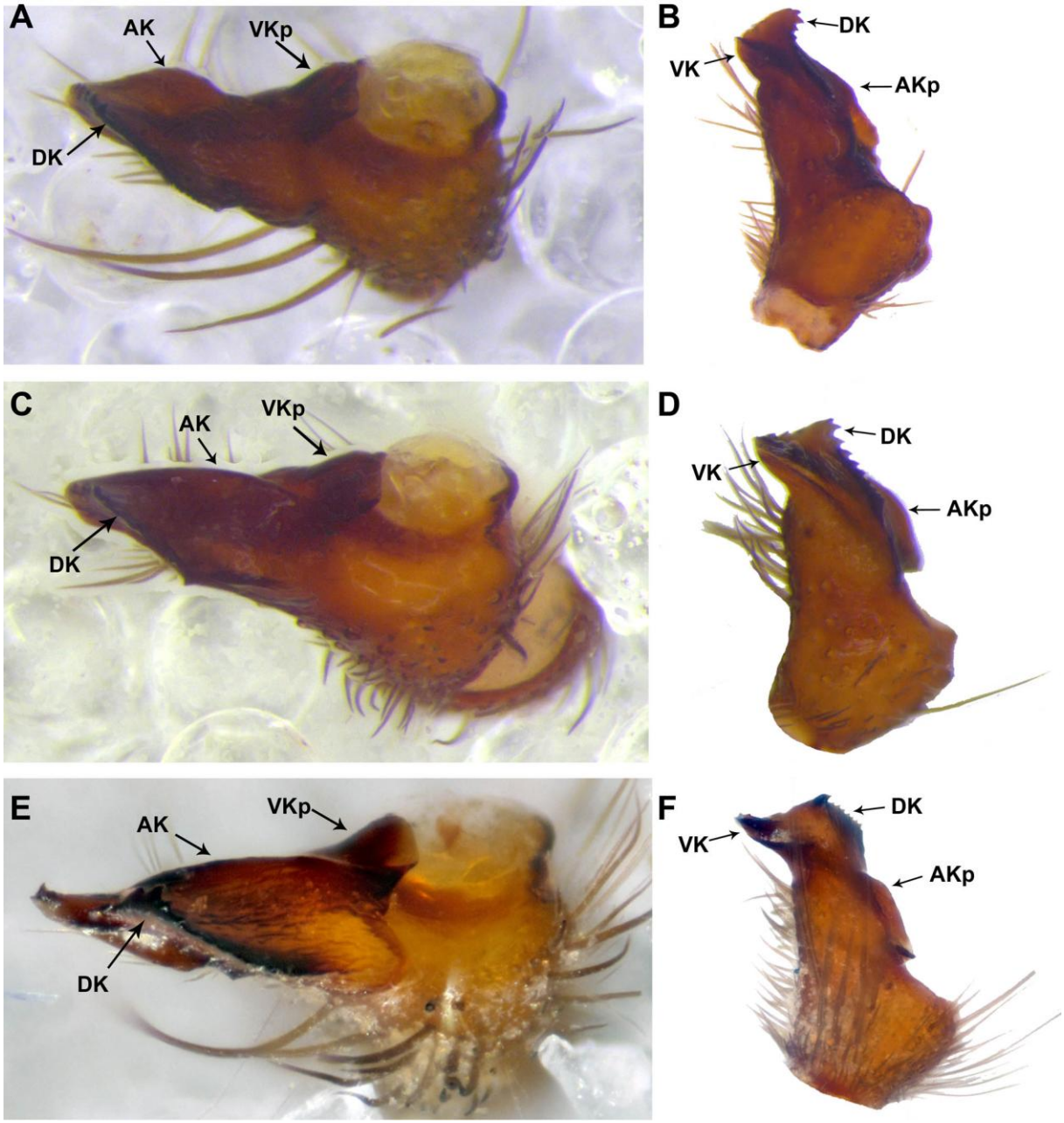

Figure 9: Right palp retrolateral tibial apophysis in apical (**A**, **C**, **E**) and retrobasal (**B**, **D**, **F**) view of *A. silvestrii* (**A**, **B**; CAS 9048498), *A. pauper* (**C**, **D**; UFMG 5736)) and *A. atlanticus* (**E**, **F**, MCN 52304). Abbreviations: AK: Apical Keel, AKp: Apical Keel proximal part, DK: Dorsal Keel, VK: Ventral Keel, VKp: Ventral Keel proximal part.

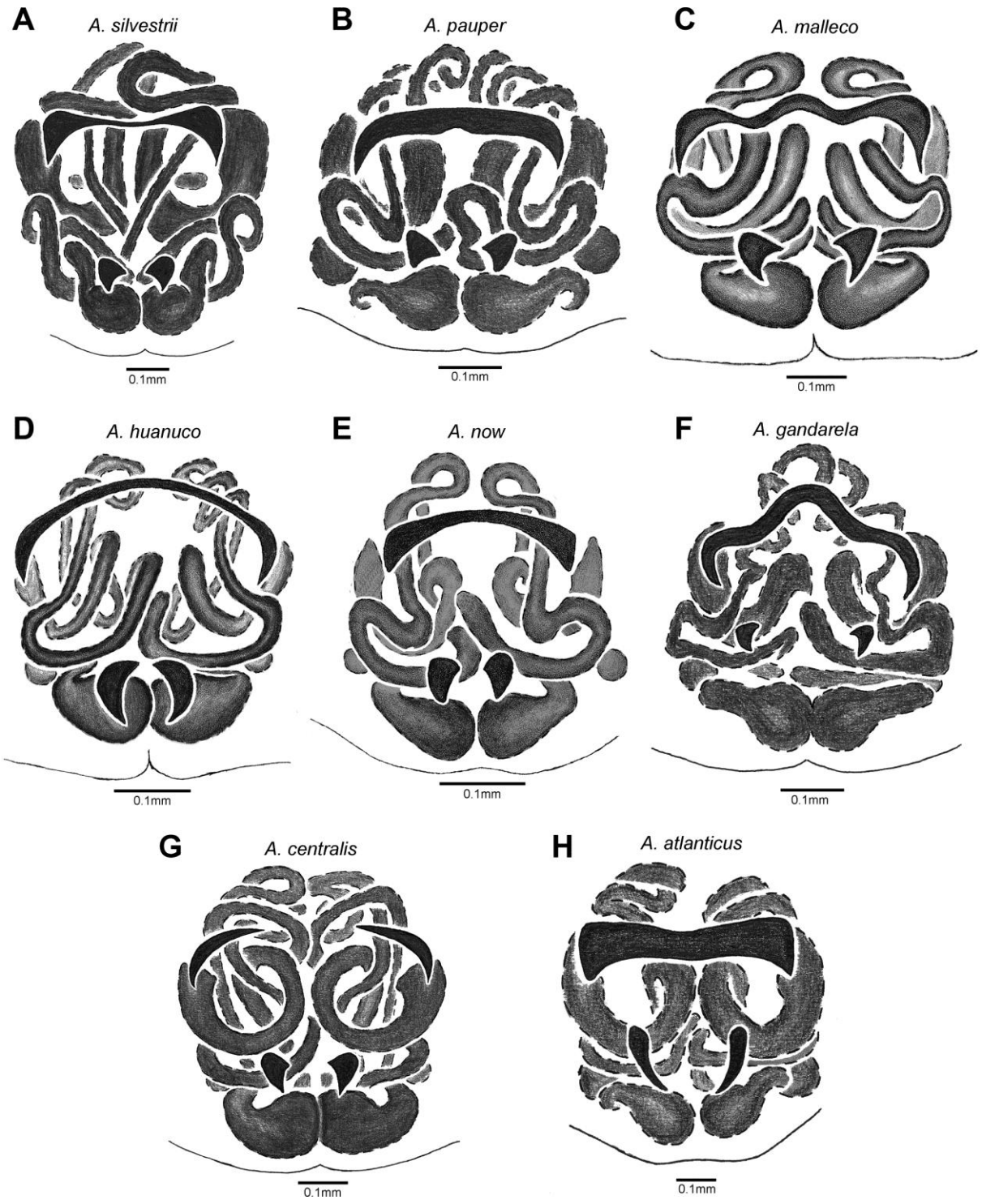

Figure 10: *Apopyllus* spp., epigynum, ventral view. Vulva can be seen by transparency. **A)** *A. silvestrii* (MCTP 26293). **B)** *A. pauper* (MNRJ58361). **C)** *A. malleco* (AMNH). **D)** *A. huanuco* (AMNH). **E)** *A. now* (MCZ 24971). **F)** *A. gandarela* **new. sp.** (UFMG 16876). **G)** *A. centralis* **new sp.** (UFMG 4564). **H)** *A. atlanticus* **new sp.** (MCTP 27338).

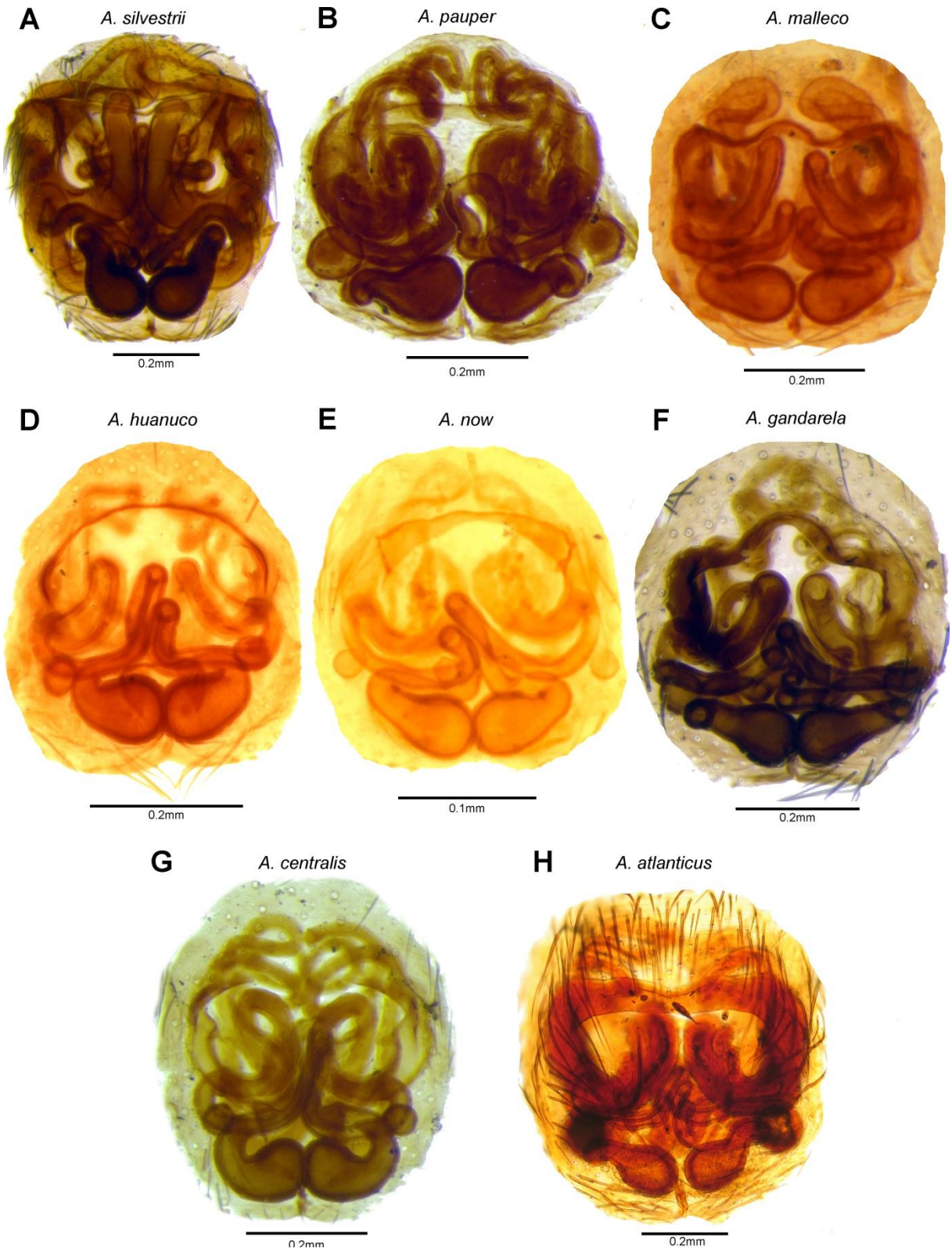

Figure 11: *Apopyllus* spp., epigynum, ventral view. Vulva can be seen by transparency. **A)** *A. silvestrii* (MCTP 26293). **B)** *A. pauper* (MNRJ58361). **C)** *A. malleco* (AMNH). **D)** *A. huanuco* (AMNH). **E)** *A. now* (MCZ 24971). **F)** *A. gandarela* **new. sp.** (UFMG 16876). **G)** *A. centralis* **new sp.** (UFMG 4564). **H)** *A. atlanticus* **new sp.** (MCTP 27338).

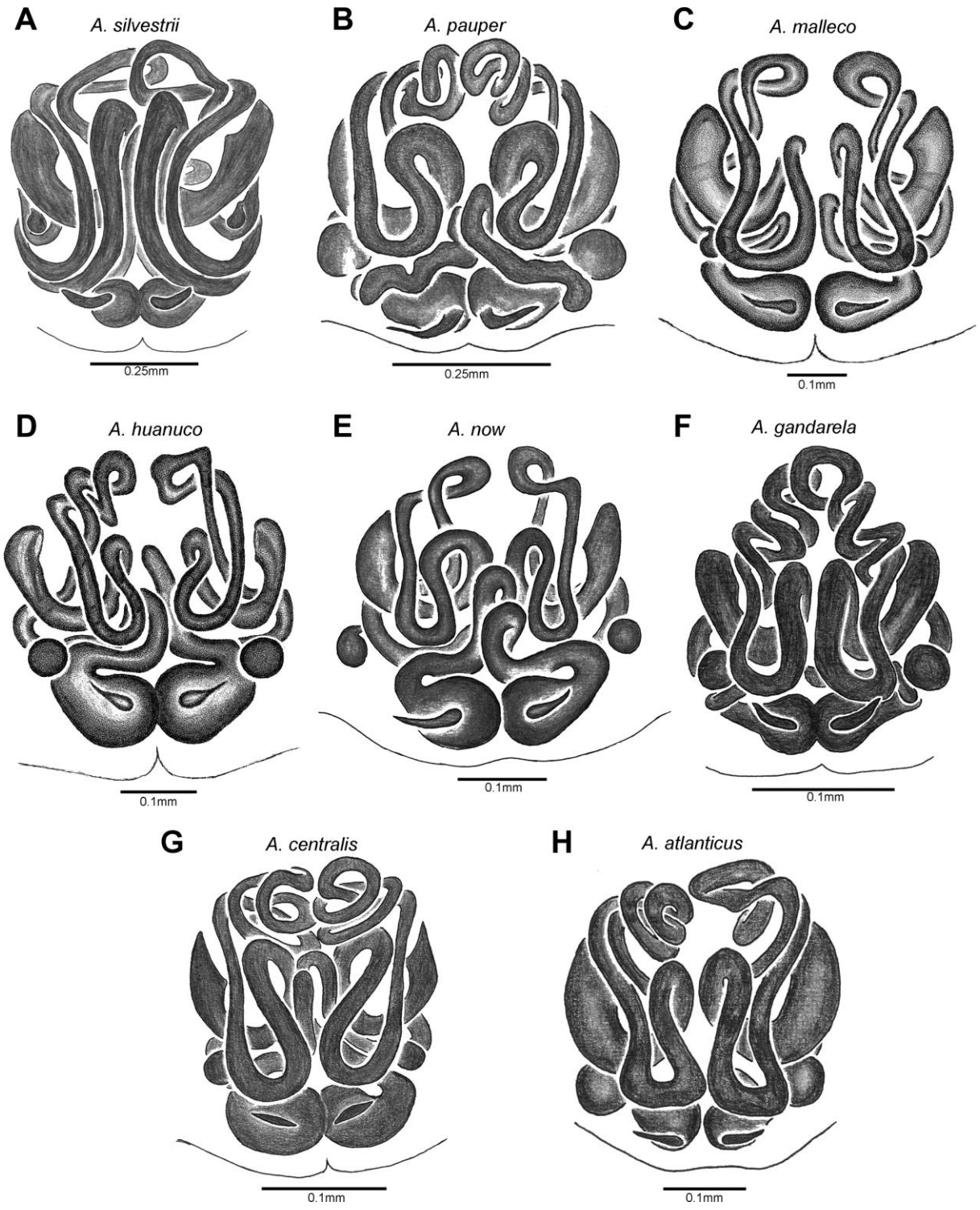

Figure 12: *Apopyllus* spp., vulva, dorsal view. **A)** *A. silvestrii* (MCTP 26293). **B)** *A. pauper* (MNRJ58361). **C)** *A. malleco* (AMNH). **D)** *A. huanuco* (AMNH). **E)** *A. now* (MCZ 24971). **F)** *A. gandarela* **new. sp.** (UFMG 16876). **G)** *A. centralis* **new sp.** (UFMG 4564). **H)** *A. atlanticus* **new sp.** (MCTP 27338).

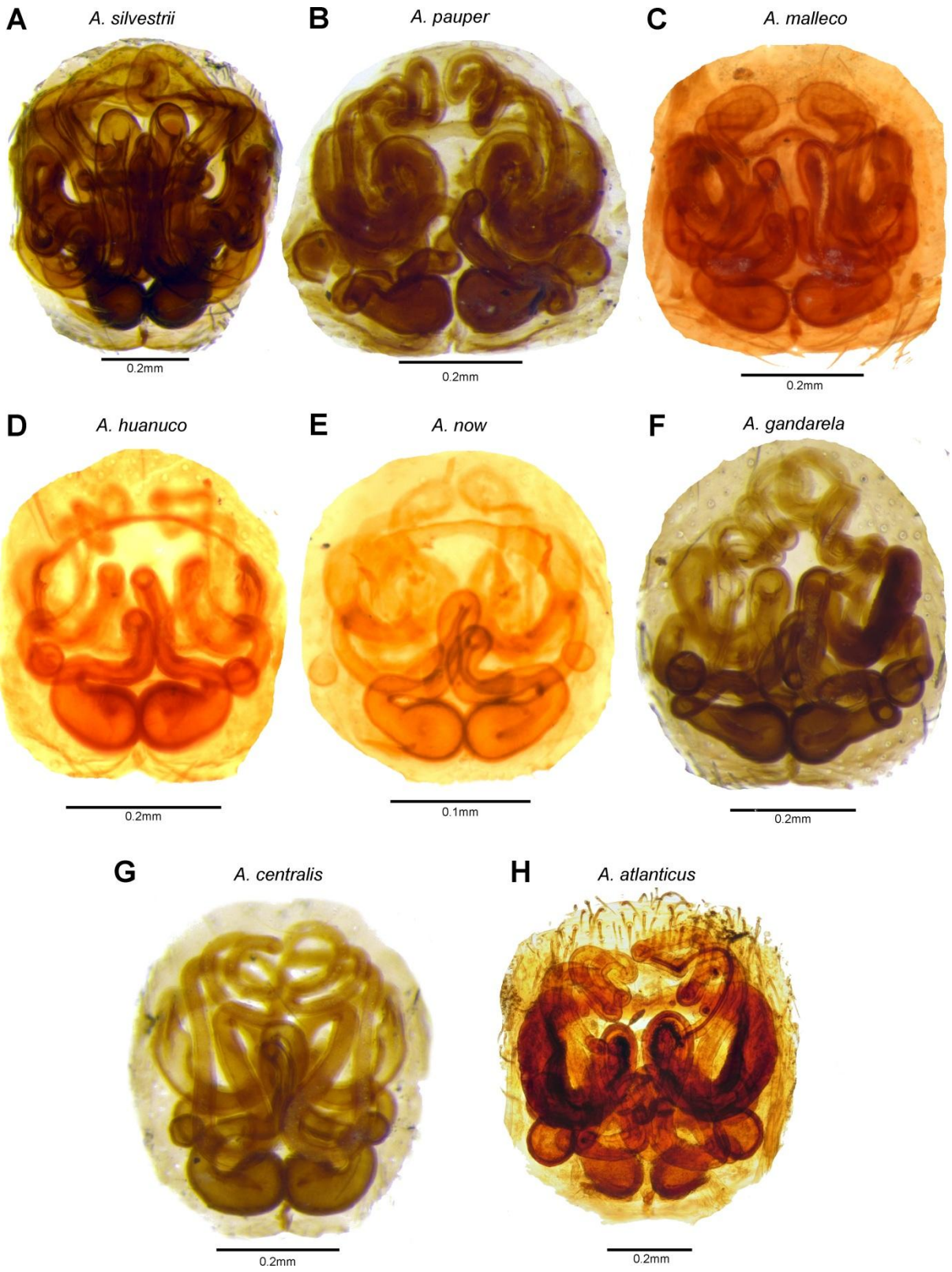

Figure 13: *Apopyllus* spp., vulva, dorsal view. **A)** *A. silvestrii* (MCTP 26293). **B)** *A. pauper* (MNRJ58361). **C)** *A. malleco* (AMNH). **D)** *A. huanuco* (AMNH). **E)** *A. now* (MCZ 24971). **F)** *A. gandarela* **new. sp.** (UFMG 16876). **G)** *A. centralis* **new sp.** (UFMG 4564). **H)** *A. atlanticus* **new sp.** (MCTP 27338).

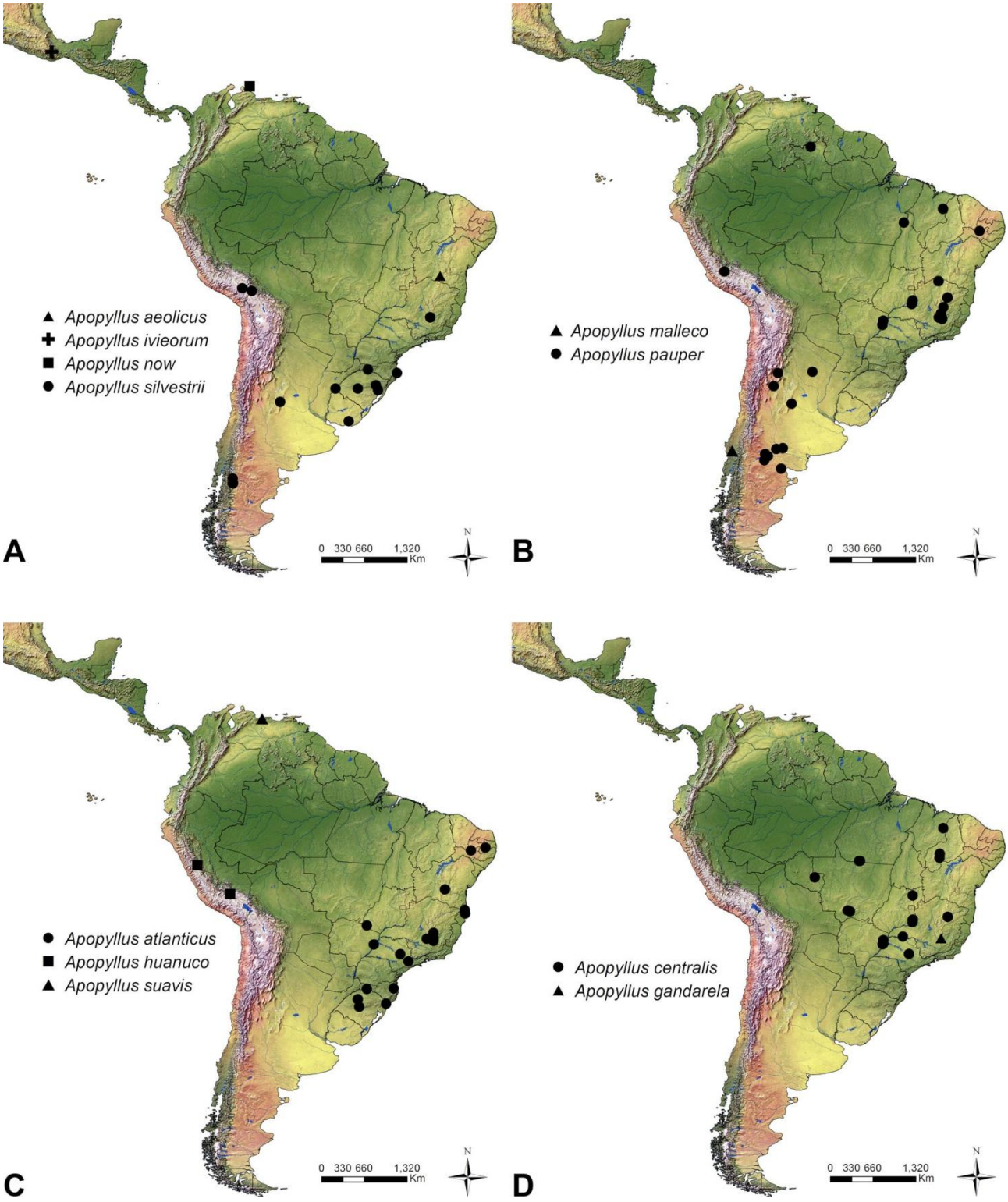

Figure 14: Geographic distribution records of *Apopyllus* species.

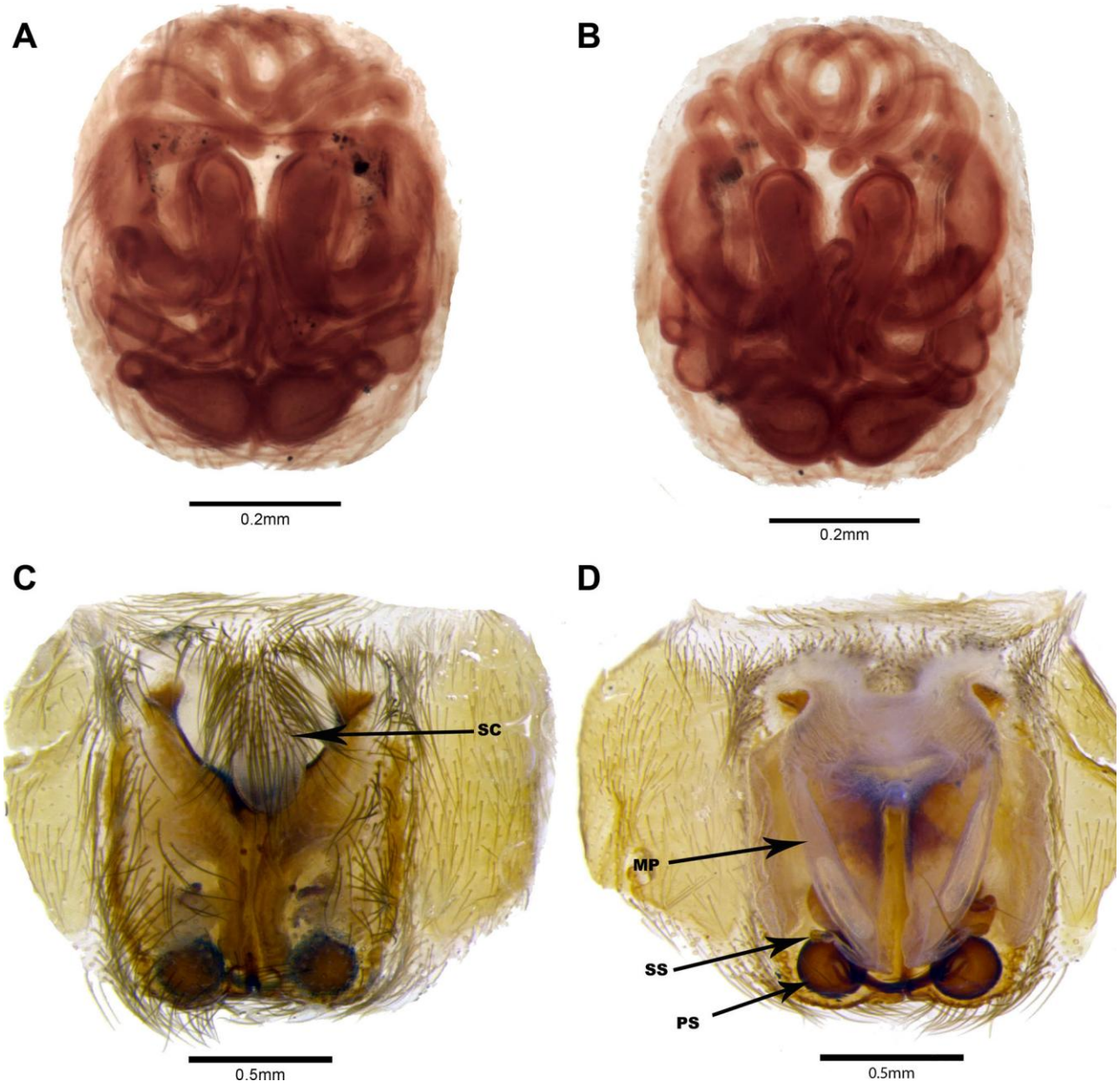

Figure 15: A) *Zelotes pauper* (= *Apopyllus pauper*), female holotype (MLP 15500), epygyne, ventral view. **B)** Ditto, vulva, dorsal view. **C)** *Apodrassodes guatemalensis* (MCN 21095), epigynum, ventral view. **D)** Ditto, vulva, dorsal view. Abbreviations: MP: Massive Midpiece, PS: Primary Spermathecae, SS: Secondary Spermathecae, SC: Scape.

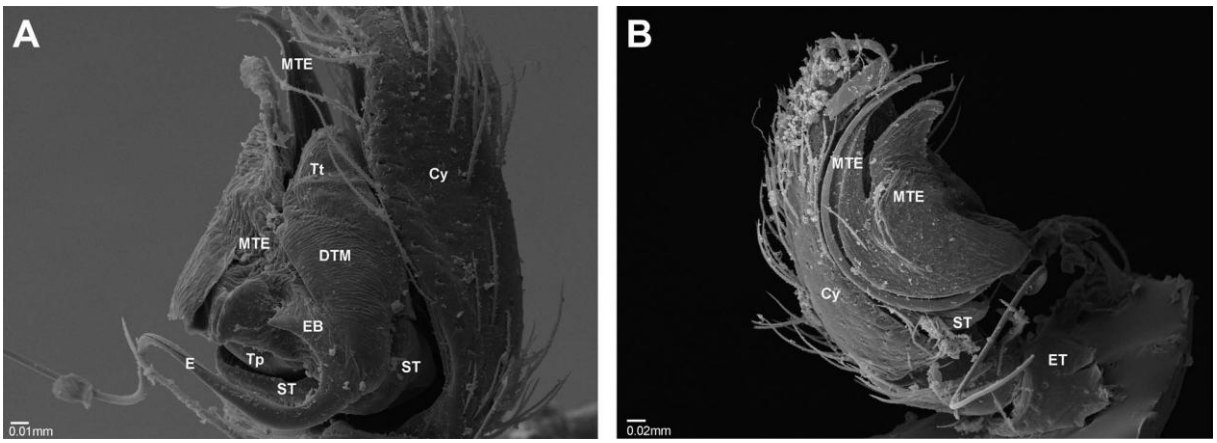

Figure 16: *Synaphosus syntheticus* right male palp. A) Retrolateral view. B) Prolateral view. Abbreviations: Cy: Cymbium, DTM: Distal Tubular Membrane, E: Embolus, EB: Embolus base, ET: Embolus Tip, MTE: Membranous Tegular Extension, ST: Subtegulum, Tp: Tegulum Proximal part, Tt: Tegulum terminal part.